UNIVERSITY OF MEDICINE AND HEALTH SCIENCES

Royal College of Surgeons in Ireland

repository@rcsi.com

The Role of HIF Hydroxylases in the Regulation of Colonic Epithelial Ion Transport

AUTHOR(S)

Joseph Bernard Jude Ward

CITATION

Ward, Joseph Bernard Jude (2011): The Role of HIF Hydroxylases in the Regulation of Colonic Epithelial Ion Transport. Royal College of Surgeons in Ireland. Thesis. https://doi.org/10.25419/rcsi.10807016.v1

DOI

10.25419/rcsi.10807016.v1

LICENCE

CC BY-NC-SA 3.0

This work is made available under the above open licence by RCSI and has been printed from https://repository.rcsi.com. For more information please contact repository@rcsi.com

URL

https://repository.rcsi.com/articles/thesis/The_Role_of_HIF_Hydroxylases_in_the_Regulation_of_Colonic_Epithelial_Ion_Transport/10807016/1

RCSI

ROYAL COLLEGE OF SURGEONS IN IRELAND

COLÁISTE RÍOGA NA MÁINLEÁ IN ÉIRINN

The Role of HIF Hydroxylases in the Regulation of Colonic Epithelial Ion Transport

A thesis presented to the
Royal College of Surgeons in Ireland
for the Degree of

Doctor of Philosophy

October 2011

Joseph Bernard Jude Ward

B.Sc. Biochemistry
M.Sc. Biochemistry
M.Sc. Environmental Science

Supervised by
Dr. Stephen J. Keely,
Molecular Medicine Laboratories,
RCSI Education and Research Centre,
Beaumont Hospital,
Dublin.

I declare that this thesis, which I submit to RCSI for examination in consideration of the award of a Ph.D. is my own personal effort. Where any of the content presented is the result of input or data from a related collaborative research programme this is duly acknowledged in the text such that it is possible to ascertain how much of the work is my own. I have not already obtained a degree in RCSI or elsewhere on the basis of this work. Furthermore, I took reasonable care to ensure that the work is original, and, to the best of my knowledge, does not breach copyright law, and has not been taken from other sources except where such work has been cited and acknowledged within the text.

Signed _____

RCSI Student Number 08500631

Date 15 March 2012

Do mo thuismitheoirí,

Bride agus Michael

Table of Contents

Dedication *3*

Table of Contents *4*

Abstract *9*

Chapter 1 General Introduction **11**

1-0 Statement of Purpose *12*

1-1 The Gastrointestinal Tract *13*

1-1.1 Introduction 13

1-1.2 Gross Anatomy 14

1-1.2.1 Mouth 15

1-1.2.2 Stomach 15

1-1.2.3 Liver 16

1-1.2.4 Gall bladder 16

1-1.2.5 Pancreas 16

1-1.2.6 Small Intestine 17

1-1.2.7 Large Intestine 18

1-1.2.8 Structure of the gastrointestinal tract 18

1-2 Intestinal Epithelium *20*

1-2.1 Introduction 20

1-2.2 Function 20

1-2.3 Structure 22

1-2.3.1 Tight junctions 22

1-3 Epithelial ion transport *25*

1-3.1 Introduction 25

1-4 Epithelial transport proteins *27*

1-4.1 ATPases 27

1-4.1.1 Na^+/K^+-ATPase 27

1-4.2 Channels 29

1-4.2.1 ENaC 29

1-4.2.2 Apical Cl^- channels 30

1-4.2.3 Basolateral K^+ channels 32

1-4.3 Exchangers 33

1-4.3.1 Cl^-/HCO_3^- exchangers 33

1-4.3.2 Na^+/H^+ exchangers 33
1-4.4 Co-transporters 34
1-4.4.1 NKCC1 34
1-4.4.2 SGLT-1 35
1-5 Hypoxia *36*
1-5.1 HIF 36
1-5.2 HIF hydroxylases 37
1-6 Hypoxic regulation of intestinal epithelial Cl^- secretion *41*
1-6.1 Introduction 41
1-6.2 Hypoxia regulates transport proteins 41
1-7 Pharmacological intervention in the treatment of diarrhoea *44*
1-8 Overall aim *45*
Chapter 2 Materials and Methods **46**
2-1 Animal studies *47*
2–1.1 Animal treatments for electrophysiological studies 47
2–1.2 Mouse model of oral allergen–induced diarrhoea 48
2-2 T_{84} cell culture *49*
2–2.1 Cell treatments 51
2-3 Electrophysiological measurements *56*
2–3.1 T_{84} colonic epithelial cells 57
2–3.1.1 Electrogenic Cl^- secretion 57
2–3.1.2 Apical Cl^- currents 59
2–3.1.3 Basolateral K^+ currents 60
2–3.1.4 Na^+/K^+-ATPase activity 61
2–3.2 Intestinal tissue 62
2–3.2.1 Colonic epithelial Cl^- secretion 62
2–3.2.2 SGLT-1 activity 63
2–3.2.3 ENaC activity 65
2-4 Preparation of protein lysates from animal tissue *66*
2-5 Preparation of protein lysates from cells *66*
2-6 Analysis of protein content *67*
2-7 Western blotting *68*
2-8 Cell surface biotinylation *72*

2-9 Co-immunoprecipitation *73*

2-10 Intracellular pH measurements *75*

2-11 RNA isolation *78*

2-12 Primer design *79*

2-13 First strand cDNA synthesis, and PCR *79*

2-14 Intracellular Ca^{2+} imaging *82*

2-15 cAMP assay *83*

2-16 Lactate dehydrogenase assay *85*

2-17 Serum alanine aminotransferase (ALT) measurement *86*

2-18 Serum creatinine measurement *87*

2-19 ATP assay *88*

2-20 Meso scale discovery (MSD) assay *89*

2-21 siRNA *90*

2-22 Crypt of Lieberkühn isolation *92*

2-23 Slide preparation with Cell-Tak™ *95*

2-24 Confocal microscopy. *96*

2-25 Statistical analysis. *100*

2-26 Materials. *100*

Chapter 3 Hydroxylases regulate intestinal epithelial ion transport **101**

3-1 Introduction *102*

3-2 Aim *104*

3-3 Results *105*

3-3.1 HIF hydroxylase inhibition increases HIF-1α expression in T_{84} cells 105

3-3.2 Hydroxylase inhibition attenuates Cl^- secretion across T_{84} cells 111

3-3.3 DMOG does not alter secretagogue-induced generation of second messengers in T_{84} cells 114

3-3.4 Hydroxylase inhibition attenuates Cl^- secretion in *ex vivo* mouse colon and ameliorates allergic diarrhoea *in vivo* 117

3-3.5 Hydroxylase inhibition attenuates ENaC activity in T_{84} cells 123

3-3.6 Hydroxylase inhibition attenuates ENaC activity in rat rectal tissue 124

3-3.7 Jejunal SGLT-1 activity is unaltered by DMOG 126

3-3.8 Hydroxylase inhibition attenuates NHE activity in T_{84} cells 128

3-4 Discussion *131*

3-5 Summary *136*

Chapter 4 Hydroxylase inhibition attenuates epithelial Na^+/K^+-ATPase activity **138**

4-1 Introduction *139*

4-2 Aim *144*

4-3 Results *145*

4.3.1 Hydroxylase inhibition attenuates CFTR expression 145

4–3.2 Hydroxylase inhibition attenuates NKCC1 expression 149

4–3.3 Hydroxylase inhibition does not affect basolateral K^+ channels, KCNN4 or KCNQ1 153

4-3.4 Hydroxylase inhibition attenuates Na^+/K^+-ATPase activity in colonic epithelial cells 158

4–3.5 Hydroxylase inhibition does not alter ATP levels in T_{84} cells 163

4–3.6 The PHD inhibitor, FG-4497, exerts anti-secretory actions in T_{84} cells and inhibits Na^+/K^+-ATPase activity 167

4–3.7 $CoCl_2$ stabilises HIF-1α protein expression and attenuates Cl^- secretion independently of Na^+/K^+-ATPase activity 170

4-3.8 EIPA reverses the inhibitory effect of DMOG on Na^+/K^+-ATPase activity 176

4-4 Discussion *177*

4-5 Summary *183*

Chapter 5 Molecular mechanisms underlying hydroxylase regulation of Na^+/K^+-ATPase activity **185**

5-1 Introduction *186*

5-2 Aim *192*

5-3 Results *193*

5-3.1 The antisecretory effects of hydroxylase inhibition are not mediated by an acutely acting soluble factor 193

5-3.2 Disruption of lipid rafts does not reverse Na^+/K^+-ATPase inhibition by hydroxylase inhibition 195

5-3.3 Post-translational modifications facilitate antisecretory actions of hydroxylase inhibition 196

5-3.4 Na^+/K^+-ATPase β_1 protein expression is significantly increased by hydroxylase inhibition 203

5-3.5 MONaKA is expressed at the plasma membrane of intestinal epithelial cells, and is increased by hydroxylase inhibition 207

5-3.6 Hydroxylase inhibition increases membrane expression of FIH-1 and its association with Na^+/K^+-ATPase α_1 219

5-4 Discussion *224*

5-5 Summary *230*

Chapter 6 General Discussion **232**

Chapter 7 Bibliography. **245**

List of Abbreviations **276**

Publications and Communications **280**

Acknowledgments **284**

Appendix I **286**

Abstract

The intestinal epithelium is a monolayer of cells that lines the entire surface of the gastrointestinal tract from mouth to anus. A key function of the intestinal epithelium is the absorption and secretion of fluids and electrolytes. The intestinal epithelium is primarily an absorptive tissue, but under normal conditions secretion also occurs. In conditions of disease the delicate balance between absorption and secretion can become dysregulated leading to the onset of diarrhoea. Chloride (Cl^-) secretion, which is the primary driving force for intestinal fluid secretion, is highly dependent on the availability of oxygen (O_2) for generation of cellular energy. Hypoxia inducible factor (HIF) hydroxylases are the primary intracellular sensors of O_2 availability. While recent studies have revealed that hydroxylases are important regulators of intestinal epithelial barrier function, there is still little known of their role in regulating epithelial fluid and electrolyte transport. This thesis set out to address this gap in our knowledge. These studies show that inhibition of hydroxylases exerts profound antisecretory effects *in vitro* and *in vivo*. The antisecretory effect of hydroxylase inhibition occurs via specific inhibition of the activity of epithelial sodium potassium adenosine triphosphatase (Na^+/K^+-ATPase) pumps, the energy-dependent step of the Cl^- secretory process. Investigations into potential mechanisms involved in the antisecretory actions of hydroxylase inhibition led to the identification of Modulator of Na^+/K^+-ATPase (MONaKA), a negative regulator of Na^+/K^+-ATPase function which, upon hydroxylase inhibition, displays increased expression at the basolateral membrane and forms part of a multimeric complex with Factor Inhibiting HIF (FIH-1) and the Na^+/K^+-ATPase itself. We propose that this complex acts as a molecular switch that, upon hydroxylase inhibition, downregulates epithelial secretory function. Our data have important implications for our understanding of how epithelial fluid and electrolyte transport can be regulated under physiological and pathophysiological conditions and suggest that by virtue of

their ability to alter epithelial transport, hydroxylases may be good targets for the development of new drugs to treat diarrhoeal diseases.

Chapter 1

General Introduction

1-0 Statement of Purpose

Intestinal disorders associated with diarrhoea are common and represent a significant social and economic problem globally. However, therapeutic options for treatment of diarrhoeal diseases are limited and new, more effective drugs for their treatment are constantly being sought. Although the epithelial transport processes that drive fluid movement in the intestine represent excellent targets for the development of new anti-diarrhoeal drugs, there are few therapeutic options that act in this way. This is largely due to our incomplete understanding of the molecular mechanisms by which epithelial fluid and electrolyte transport are regulated. This thesis sets out to address this area of research by studying the role of a family of enzymes, known as hydroxylases, in regulating epithelial transport function and the possibility that these enzymes could be targeted for treatment of diarrhoeal diseases. The following General Introduction aims to set these studies in context.

1-1 The Gastrointestinal Tract

1-1.1 Introduction

The gastrointestinal (GI) tract represents the largest mucosal membrane surface in the human body. The GI tract can also be viewed as a complex system of glands, tissues and organs that work in a concerted fashion to facilitate food intake and discharge of waste in a safe manner. It serves four main functions; namely mixing and transporting of food, secretion of digestive enzymes, electrolytes and fluids, digestion and absorption (Moffett *et al.*, 1993). Ingested food is digested by mechanical, chemical and biological means. Mechanically this involves mastication, swallowing, peristalsis and defecation (Reed and Wickham, 2009). Biochemically, the digestive process involves the breakdown of food into simple building blocks, which can then be absorbed by the epithelium. Digestion starts in the mouth where enzymes, such as α amylase, initiate the breakdown of complex to simple carbohydrates (Kaczmarek and Rosenmund, 1977). Hydrochloric acid (HCl) secretion by parietal cells of the stomach facilitates reduction of food into a broth-like material called chyme. HCl also denatures proteins and nucleic acids, transforms the inactive precursor forms of secreted enzymes into their active forms and destroys ingested bacteria. Digested food is transported mechanically through the intestine by the peristaltic motion of the muscularis and as it moves through the small intestine and colon, nutrients, electrolytes and fluids are continually absorbed and secreted across the epithelial layer. Since it is continuously exposed to a wide range of noxious substances and pathogens, the GI tract also plays an important role in immune surveillance and the intestinal immune system is the first line of host defence against mucosal microbial pathogens. Mucosal barrier function is further enhanced by a biologically active lubricant layer of mucus, composed of mucin secretions from goblet cells, which forms a crucial physiological barrier between the intestinal mucosa and the luminal contents.

1-1.2 Gross Anatomy

The anatomy of the GI tract is shown in Figure 1-1.

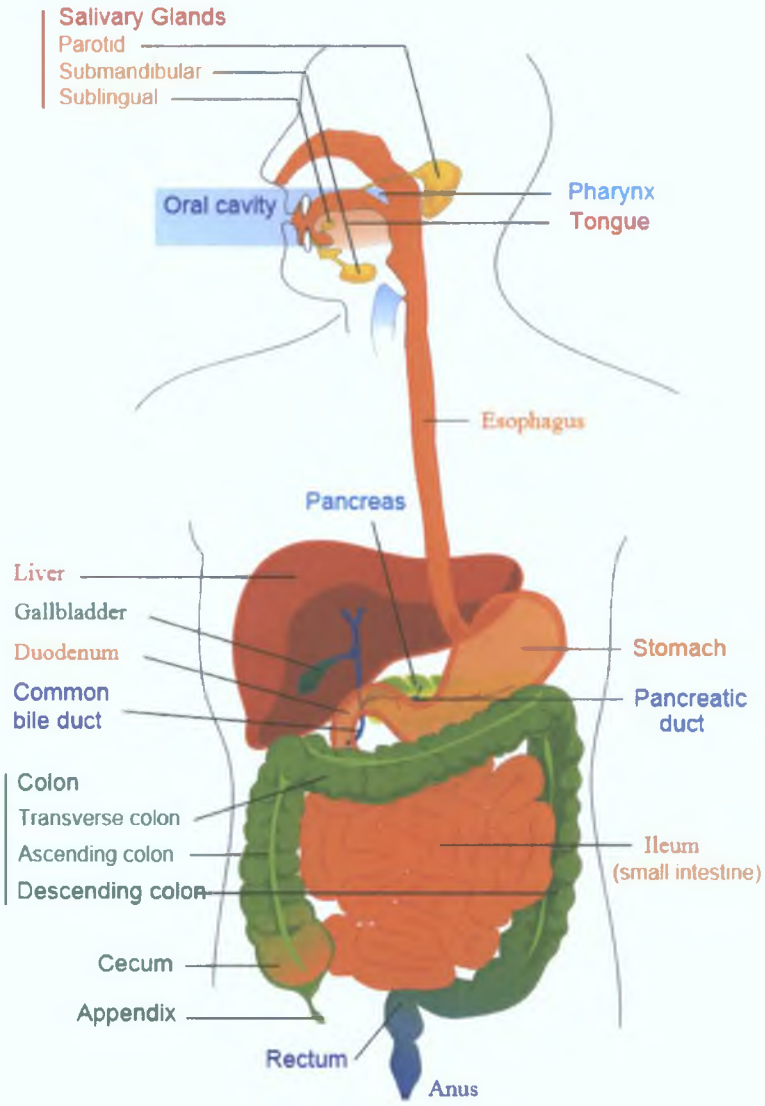

Figure 1-1 Anatomy of the gastrointestinal tract. The GI tract is comprised of the mouth, pharynx, salivary glands, oesophagus, stomach, pancreas, liver, gall bladder, small intestine, colon, rectum and the anus and intrinsic to its function is the splanchnic circulation and the enteric nervous system. This figure was downloaded from Wikimedia.org without any conditions from the author.

1-1.2.1 Mouth

The first fluid with which ingested food comes into contact is saliva. Components of saliva include enzymes for digestion, growth factors, vasoactive serine proteases and regulatory peptides, to name but a few. Salivary secretion is promoted by neurohormonal agonists, such as acetylcholine (ACh), vasoactive intestinal polypeptide (VIP), norepinephrine, substance P, neurotensin and epidermal growth factor (EGF), to name but a few (He *et al.*, 1989; Ship *et al.*, 1990; Buck and Burcher, 1985; Turner and Yu, 1991; Jaeger and Lamar, 1992). These mediators increase second messengers within the cells and activate mechanisms responsible for protein exocytosis and fluid secretion. These secretions are mixed with food and masticated in the oral cavity and are then transported to the stomach via the oesophagus (Johnson, 1994).

1-1.2.2 Stomach

The stomach lies below the diaphragm and is surrounded by several layers of smooth muscle. Goblet cells of the mucosa secrete mucus which helps form a protective layer over the mucosa, whereas parietal cells secrete HCl. Other cells, such as chief cells produce lipases which help digest dietary fats and which also require an acid environment for activity (Gargouri *et al.*, 1989). The activation of the gastric pump or parietal H^+/K^+-ATPase is regulated by gastrin, ACh and histamine. Gastrin is released by G cells in the antrum upon the presence of food and amino acids and both gastrin and ACh then stimulate the release of histamine from enterochromaffin-like (ECL) cells in the fundic wall to stimulate activation of H^+/K^+-ATPase pumps (Walsh, 1988; Berglindh, 1984; Black *et al.*, 1972). When food exits the stomach, somatostatin inhibits acid secretion by preventing histamine release from ECL cells (Prinz *et al.*, 1993). From here, the chyme is released into the duodenum via the pyloric sphincter, a structure comprised of concentrated smooth muscle.

1-1.2.3 Liver

The liver can be considered an accessory organ of the gastrointestinal tract and has numerous functions. It produces bile, it aids in metabolism and storage of nutrients, minerals and vitamins and it synthesises and deactivates clotting factors, to name but a few functions. Hepatocytes are the primary cell type of the liver and they function to secrete lipids, bile acids and cholesterol into the canaliculi and ultimately via the bile ducts, into the duodenum. The liver has 2 blood supplies; the hepatic artery which supplies O_2 for metabolism and the hepatic portal vein which transports nutrient-rich blood from the intestine (Reed and Wickham, 2009).

1-1.2.4 Gall bladder

The gallbladder is essentially a storage unit for bile, where it is kept until it is required for digestion. During overnight fasting about half of the bile produced by the liver enters the gallbladder (van Berge Henegouwen and Hofmann, 1978). The sphincter of Oddi regulates the entry and release of bile into the gallbladder and is hormonally regulated. Upon ingestion of food, bile exits the gallbladder into the duodenum. Bile drains back into the gallbladder during fasting (Johnson, 1994).

1-1.2.5 Pancreas

The pancreas is a mixed endocrine-exocrine gland, with the exocrine portion accounting for approximately 85 % of the organ. The exocrine pancreas is composed of acinar cells which produce alkaline secretions of proteins, electrolytes and fluid, which are drained by the main pancreatic duct into the duodenum (Scheele, 1980). Proteins produced in the pancreas are important for digestion, such as active enteropeptidase, which converts inactive trypsinogen to active trypsin which, in turn, activates other digestive zymogens in the lumen of the gut (Stevenson *et al.*, 1986). In fact, the pancreas produces

more protein per gram of tissue than any other organ, with up to 20 g protein and 2.5 litres of fluid being secreted in 24 hours (Johnson, 1994).

1-1.2.6 Small Intestine

The majority of digestion and absorption occurs in the small intestine. The small intestine is over 7 metres long in adults, but the surface area for absorption is greatly increased by the abundance of villi. Up to 9 litres of fluid cross the intestinal epithelium every day, with up to 78 % of this being absorbed by the small intestine (Yamada and Alpers, 2009). The small intestine is composed of the duodenum, the jejunum, and the ileum. The duodenum receives the highly acidic chyme from the stomach, and secretions from the liver and the pancreas which aid in digestion of the chyme. Approximately 10 % of the epithelial cells of the duodenum are mucus-secreting goblet cells, and similar to the stomach, the surface cells of the duodenal epithelium secrete bicarbonate (HCO_3^-) into the mucus layer to protect against the acidic chyme (Johnson, 1994). The duodenal epithelium also secretes enteropeptidase, a protein that cleaves pancreatic enzymes into active forms (Stevenson *et al.*, 1986). The jejunum which joins the duodenum at the Ligament of Treitz, is the next section of the intestine. The lumen of the jejunum has a pH of 7–9, and contains very few Peyer's patches or Brunners Glands in comparison to the duodenum and ileum, respectively. Absorption of nutrients and fluids is the primary function of the jejunum. The ileum follows the jejunum, and here the villi absorb the nutrients produced by digestion, and transport them via the hepatic portal vein to the liver. The ileum is distinguishable from the jejunum by the abundance of Peyer's patches, accumulations of lymphoid follicles. The epithelium covering the follicles consists of microfold cells (M cells), which are specialised for the uptake and transcytosis of macromolecules and microorganisms (Miller *et al.*, 2007; Corr *et al.*, 2008). Following transcytosis, antigens are presented to the underlying lymphoid aggregates (Hathaway and Kraehenbuhl, 2000). M cells have thus been exploited for the development of

vaccines, and are of great interest in diseases with an immunological component, such as Crohn's disease (Gullberg and Soderholm, 2006). The ileum ends at the ileocecal valve, which controls the entry of the small intestinal contents into the large intestine.

1-1.2.7 Large Intestine

The caecum represents the beginning of the colon and is from where the appendix protrudes. The appendix has no digestive function and consists mostly of lymphoid tissue. It is thought to be a vestigial organ, but more recent research has implicated it as being an important component of mucosal immune function that may have become defunct in industrialised societies due to better hygiene practices (McCabe, 1912; Darwin, 1871; Zahid, 2004; Laurin *et al.*, 2011). The colon can be separated into 4 separate anatomical areas namely: the ascending, the transverse, the descending, and the sigmoid colon. The main function of the colon is to absorb salt and water from the faeces, and it carries out these functions in a spatially distinct manner, displaying segmental heterogeneity in its ion transporting properties. By the time the faeces reaches the sigmoid colon it is solid, and then passes into the rectum.

1-1.2.8 Structure of the gastrointestinal tract

The intestine is composed of 4 main layers: the serosa, muscularis, submucosa, and mucosa (Figure 1–2). The serosa is the outermost layer of the GI tract and is essentially comprised of connective tissue that has a surface of mesothelium. Adjacent to the serosa is the muscularis externa. In the mouth and pharynx this layer is composed of striated muscle cells that aid in swallowing, while in the rest of the GI tract it consists of circular and longitudinal muscle layers that aid in peristalsis of food throughout the tract (Reed and Wickham, 2009). The submucosa lies inside the muscularis externa and is a connective tissue that contains blood vessels, lymphatic vessels, submucosal glands, and the Meissner's plexus. Inside the submucosa lies the mucosa, which consists of the

epithelium, the lamina propria, and the muscularis mucosa. The muscularis mucosa is a thin layer of smooth muscle that separates the mucosa from the submucosa and serves to keep the mucosal surface and underlying glands in a constant state of motion. This layer aids in the expulsion of substances from the crypts and in the absorption of nutrients from the lumen. The lamina propria is composed of connective tissue and serves several key functions, such as providing the epithelium with blood and lymphatic vessels, thereby delivering nutrients to, and transporting nutrients from, the lumen. The lamina propria is also infiltrated with lymphocytes and lymph nodules, such as the Peyer's patches. The intestinal epithelium is described in detail in the following section.

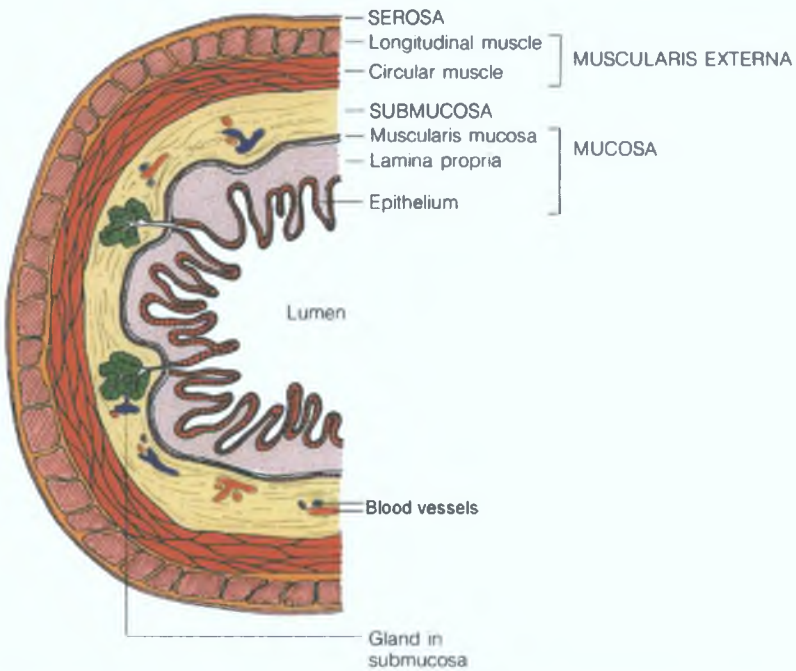

Figure 1-2 Cross section of the intestine. The intestine is composed of 4 main layers: the serosa, muscularis, submucosa, and mucosa. The innermost layer is the epithelium, which performs the barrier and transporting functions of the intestine, and which is of primary interest in this thesis.

1-2 Intestinal Epithelium

1-2.1 Introduction

Epithelial cells serve to exchange substances between the body and the external environment, or between internal body compartments. They surround organs that control fluid homeostasis and thus express a wide variety of proteins that enable the transport of nutrients, fluids and electrolytes between compartments. Epithelial cells from different parts of the intestine have different properties and can be arranged in a "leaky" or "non leaky" fashion. They are joined to one another by a dynamic arrangement of extracellular and transmembrane spanning proteins, known as the zonula occludens, or tight junctions. Epithelial cells have an added structural rigidity in the form of a basement membrane (Wills *et al.*, 1996). The epithelium exists as a monolayer of cells lining the entire surface of the gastrointestinal tract from mouth to anus. It performs several key functions, including absorption of nutrients, acting as a barrier to infection, and absorbing and secreting fluids and electrolytes. Given that the GI tract performs different functions along its length, it is not surprising that the epithelial cells in different areas can have different characteristics. Such different characteristics arise from differential expression of proteins within the cells. Another key distinguishing feature of epithelial cells is their ability to specifically target transport proteins to different poles of the cell, or in other words, to polarise. This polarisation allows epithelial cells to perform vectorial transport of ions and nutrients across the barrier to the appropriate compartment.

1-2.2 Function

The functions of the intestinal epithelium are essentially 3-fold. Firstly, absorption of nutrients is a critical function of the epithelium. In order to facilitate this, the intestinal epithelium expresses several transport proteins that

are capable of absorbing carbohydrates, amino acids, peptides and proteins, lipids, minerals, and vitamins. Carbohydrates, which account for up to 50 % of the caloric intake of Western diets are almost completely hydrolysed by the salivary and pancreatic enzyme, α amylase (Johnson, 1994). Products of α amylase are further degraded by brush border expressed glucosidases, such as glucoamylase, isomaltase, and sucrase, into monosaccharides. These molecules can then be transported across the cell by transporters, such as SGLT-1 in the case of D-glucose (Goodman, 2010). Protein breakdown into amino acids is more complicated given that there are 20 amino acids. Proteolysis begins in the stomach by pepsin, and is followed by pancreatic enzymatic digestion in the duodenum, which results in the production of approximately 40 % free amino acids and 60 % peptides (Johnson, 1994). The unprocessed peptides can be further processed by peptidases, or they can be absorbed intact as di-and tri-peptides by active transport systems, such as peptide transporter 1 (PepT1) (Daniel, 2004). However, given the widely different physicochemical properties of the 20 amino acids, and the 8000 chemically distinct combinations of tri-peptides that can be formed by protein digestion, a variety of transporters are required for their absorption.

The second function of the intestinal epithelium is to act as a barrier to prevent the entry of harmful substances and microbial infection. This is a crucial role, when one considers that there are approximately 10 times more bacteria in the healthy human gut than there are cells in the entire body (Savage, 1977). Given that up to 60 % of the dry weight of faeces is composed of bacteria (Guarner and Malagelada, 2003), it is evident that the intestinal mucosa is constantly exposed to luminal antigens. Being the first layer of defence, the epithelium must be able to sense and respond appropriately to these luminal antigens, without over-reacting.

The third main function of the intestinal epithelium is to absorb and secrete fluids and electrolytes. As already mentioned, absorption occurs primarily in

the small intestine. Fluid secretion is also a very important function of the intestinal epithelium which allows mixing and movement of the luminal contents throughout the length of the GI tract and which lubricates and protects the delicate epithelial layer. However, the finely-tuned balance between absorption and secretion can become dysregulated in disease, leading to the onset of diarrhoea, a primary symptom of several infectious and non-infectious GI disorders such as inflammatory bowel disease (IBD), irritable bowel syndrome (IBS), iatrogenic diarrhoeas and bile acid malabsorption.

1-2.3 Structure

A key feature of the intestinal epithelium is its ability to form an electrically tight monolayer, or a barrier, that is selectively permeable to molecules as small as ions and water. As already mentioned, a second key feature of epithelial cells is their ability to polarise transport protein expression. This is essential for the different functions of the epithelium throughout the GI tract. A third key feature of the structure of epithelial cells is their plasticity. These cells change their phenotype from secretory to absorptive cells as they migrate from the crypt base to surface in the colon, or the villus in the small intestine (Geibel, 2005). A fourth key structural feature of the epithelium is its ability to maintain its barrier function during the sloughing process. With the entire epithelium being replaced approximately every 7 days, a huge amount of cell loss occurs on a continuous basis. Despite this, the epithelium remains tight, and recent studies suggest that mechanisms underlying this phenomenon involve cytoskeletal rearrangements in cells adjacent to apoptotic cells that prevent luminal contents breaching the barrier (Watson *et al.*, 2009).

1-2.3.1 Tight junctions

For the epithelial barrier to remain functional the paracellular, or shunt pathway, must be tightly regulated. This is accomplished by the zonula

occludens, or tight junctions. Tight junction physiology is an area of epithelial research that is incredibly dynamic and interesting. Great advances in understanding the molecular biology of these structures have been made in the recent past and are discussed in depth in numerous reviews (Shen *et al.*, 2011; Tsukita *et al.*, 2001; Matter and Balda, 2003). Tight junction formation is a key step in the segregation of apical and basolateral compartments in cells. Once the endogenous extracellular matrix has been formed, the tight junctions become restricted to the apicolateral membrane boundary where they form an intramembranous fence to prevent the mixing of domain-specific proteins and lipids (Yeaman *et al.*, 1999). Importantly, we now know that aberrant tight junction function is implicated in numerous pathophysiological conditions, such as breast cancer (Brennan *et al.*, 2010; McSherry *et al.*, 2011) and IBD (Edelblum and Turner, 2009).

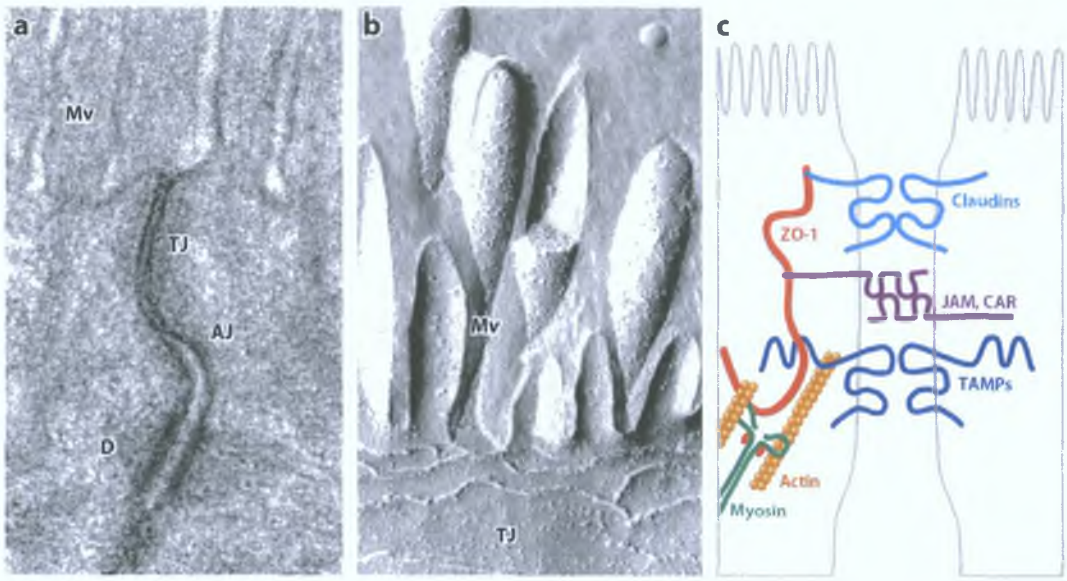

Figure 1-3 The apical junctional complex. a) Transmission electron micrograph of apical junctional complexes between two villous enterocytes. The tight junction (TJ) is just below the microvilli (Mv), with the adherens junction (AJ) located below this and the desmosomes (D) further below. **b)** Freeze-fracture electron micrograph of **a**. **c)** Schematic representation of interactions between the cytoskeleton, zona occludens-1 (ZO-1), claudins, tight junction–associated marvel proteins (TAMPs), junctional adhesion molecule (JAM), and the coxsackie adenovirus receptor (CAR). This figure is adapted from (Shen *et al.*, 2011).

As seen in Figure 1-3 tight junctions are located within apical junctional complexes. The first tight junction associated protein, zonula occludens-1 (ZO-1) was identified in 1986, with the second, cingulin, being identified the following year (Stevenson *et al.*, 1986; Citi *et al.*, 1988). However, it was the discovery of the tetraspanning protein, occludin, in 1993 that confirmed the hypothesis that integral membrane proteins are present in tight junctions (Furuse *et al.*, 1993). Somewhat surprisingly however, occludin knockout animals were found to have normal intestinal epithelial physiology, thus leading the authors to conclude that occludin is not required for the formation of tight junction strands (Saitou *et al.*, 2000). Since these early discoveries, other transmembrane spanning proteins have been discovered in tight junctions. Importantly, a large family of claudin proteins has been identified and have subsequently been associated with ion transport across the tight junction (Anderson and Van Itallie, 2009; Weber *et al.*, 2010). Research has shown that expression of different claudins change the electrical properties of epithelial monolayers, therefore, it has been suggested that claudins determine the tight junction barrier properties (Van Itallie and Anderson, 2004). Other research has more directly demonstrated that expression of specific claudin family members confers specific ion selectivity to epithelial monolayers (Van Itallie *et al.*, 2001). In summary, tight junctions are highly dynamic areas of cell-to-cell contact that maintain adhesion of epithelial cells to each other and which regulate the passage of molecules, ions and fluid across the epithelial layer.

1-3 Epithelial ion transport

1-3.1 Introduction

One of the primary functions of the intestinal epithelium is to transport electrolytes and fluids to and from the lumen. Intestinal fluid movement is driven by osmotic gradients that are, in turn, established by active ion transport across the epithelium. Fluid absorption normally predominates and is promoted by Na^+ absorption, while fluid secretion is driven predominantly by Cl^- and HCO_3^- secretion. In normal circumstances, a fine balance exists between fluid absorption and secretion which favours absorption of the 9 litres of fluid that enters the intestine every day (Yamada and Alpers, 2009). However, this balance can become disrupted in conditions of disease and can result in the clinical manifestation of diarrhoea. Chronic diarrhoea is a primary symptom of several gastrointestinal disorders, including IBD, diarrhoea-predominant IBS, iatrogenic diarrhoeas, such as those induced by chemotherapy, microscopic colitis and bile acid mal-absorption (Carter *et al.*, 2004; Maroun *et al.*, 2007; Oelkers *et al.*, 1997; Hofmann, 2009). Often, one of the main therapeutic goals of treating patients with these intestinal disorders is to treat the primary symptoms, including diarrhoea (Sohrabpour *et al.*, 2010). Ion transport in the colon is facilitated by several transport proteins that display considerable intrinsic segmental heterogeneity (Sandle *et al.*, 1986; Sandle, 1989). Transport is stimulated by multiple factors, including luminal and systemic influences, such as hormones and neuro-immune agonists, which can act as either secretagogues or absorptagogues. Secretagogues, such as ACh and VIP, typically act by binding to their cognate receptors on intestinal epithelial cells to stimulate the production of intracellular second messengers, such as Ca^{2+} and cAMP, respectively. In turn, second messenger generation drives Cl^- secretion from the cell, through the concerted action of several ion transport proteins on the cell membrane. The extracellular accumulation of Cl^- then promotes paracellular Na^+ transport and fluid movement by osmosis (Murek *et al.*, 2010).

Similarly, Na^+ absorption across the intestinal epithelium is facilitated by several transport proteins that also show considerable intrinsic segmental heterogeneity (Sandle *et al.*, 1986; Sandle, 1989). Luminal influences on epithelial ion transport processes are diverse and range from paracrine stimulation, such as the release of gastrin by G cells in the stomach causing the release of histamine from ECL cells and activation of H^+/K^+-ATPase pumps, to effects of the intestinal micro-flora and their by-products(Walsh, 1988; Berglindh, 1984; Black *et al.*, 1972). A good example of luminal factors that regulate transport are bile acids. These molecules enter the lumen of the duodenum after ingestion of food where they emulsify fats and aid in their digestion. Most bile acids are recycled from the small intestine back to the liver, but with each cycle of the enterohepatic circulation, a small percentage enters into the colon. Here, the bile acids can alter intestinal epithelial transport processes (Keating *et al.*, 2009; Keating and Keely, 2009). However, they can also be metabolised by the intestinal micro-flora, with the resulting secondary bile acids having distinct effects on ion transport (Edenharder and Knaflic, 1981; Lepercq *et al.*, 2004; Kelly *et al.*, 2009b).

The epithelial transport proteins that facilitate the movement of ions across epithelial cells comprise a diverse array of protein families. These proteins can be classified according to certain characteristics. ATPases, as their name suggests, cleave ATP to pump ions across membranes, ion channels allow passive movement of ions down electrochemical gradients, and exchangers transport ions of equal charge in opposite directions across the membrane. The diversity of ion transport proteins can be simplified by their organisation into categories, as outlined in the next section.

1-4 Epithelial transport proteins

Ion transport proteins in the intestinal epithelium perform many tasks from pH regulation, to volume regulation, to vectorial fluid absorption and secretion.

1-4.1 ATPases

ATPases are membrane-bound ion transport proteins that utilise a molecule of ATP during the transport process. There are many different forms of ATPases that have been classified as F-, V-, A-, P- and E-ATPases based on functional differences. ATPases generate membrane potentials and are thus critical for all ion transport processes across the intestinal epithelium.

1-4.1.1 Na^+/K^+-ATPase

The Na^+/K^+-ATPase is known as a P-type ATPase because it catalyses auto-Phosphorylation of a conserved aspartate residue within the pump. The importance of the Na^+/K^+-ATPase is such that it is expressed on the membrane of every mammalian cell where it creates a separation of charge across the membrane (Kaplan, 2002). The P-type ATPases all interconvert between E1 and E2 conformations, which are essentially conformations at which the pump has greater affinities for different ions (Morth *et al.*, 2011). This P-type ATPase drives both K^+ and Na^+ against their electrochemical gradients, and cleaves ATP in the process. Three Na^+ ions are extruded from the cell, while 2 K^+ ions are imported by the pump for each ATP molecule cleaved. This non-equivalent transport is electrogenic and leads to the generation of a transmembrane electrical potential of approximately -70 mV, at which point the extrusion of K^+ and the influx of Na^+ are at equal rates.

The Na^+/K^+-ATPase provides the driving force for intestinal Cl^- secretion and Na^+ absorption and is basolaterally located (Skou, 1998; Kaplan, 2002). With

respect to the Cl^- secretory pathway, the extrusion of Na^+ from the cell creates an electrochemical driving force for entry of Na^+ through the basolateral $Na^+/K^+/2Cl^-$ co-transporter (NKCC1), while in absorptive cells, the pump creates the driving force for apical Na^+ entry through ENaC and SGLT1. Na^+/K^+-ATPase pumps exist as heterodimers in the plasma membrane, with one α and one β subunit (Craig and Kyte, 1980; Horowitz *et al.,* 1990). There are several isoforms of the Na^+/K^+-ATPase which are comprised of different α and β subunits. 4 α and 3 β subunits are known to exist and in the intestine the heterodimer formed is an $\alpha_1\beta_1$ heterodimer (Morth *et al.*, 2011). Resolution of the crystal structure of the Na^+/K^+-ATPase in the recent past however, also revealed the presence of Na^+/K^+-ATPase γ subunits in renal extracts (Morth *et al.*, 2007). The catalytic α subunit contains 10 transmembrane domains that contain binding sites for ATP, Na^+, K^+, cardiac glycosides and the phosphorylation site for catalytic activity (Lutsenko and Kaplan, 1995). The β subunit has a single membrane spanning domain and interacts with the α subunit via the β ectodomain (Fambrough *et al.*, 1994). Much research over the years has shown that there are multiple mechanisms by which the pump can be regulated, for example by protein kinases, such as PKA and PKC (Beguin *et al.*, 1994; Feraille *et al.*, 2000). Its regulation under hypoxic conditions has also been well documented and is discussed in more detail in Chapter 4. Furthermore, additional studies show that Na^+/K^+-ATPase pumps can exist in a complex of multiple proteins, allowing for tissue-specific regulation (Garty and Karlish, 2006; Yoon *et al.*, 2006). Again, this is discussed in greater detail in Chapter 5. Thus, our knowledge of the structure of the Na^+/K^+-ATPase is constantly evolving, but remains incompletely understood. Na^+/K^+-ATPase regulation is multifaceted, and thus has potential to be exploited for therapeutic intervention.

1-4.2 Channels

Ion channels are pore-forming proteins that exist in the plasma membrane and help to create and maintain voltage gradients created by ATPases. Ion channels allow for the passive transport of ions down their electrochemical gradients, but they may still require ATP for functionality, or for gating. Ion channels may be voltage, ligand, or ATP-gated.

1-4.2.1 ENaC

The epithelial sodium channel (ENaC) is a hetero-multimeric protein consisting of at least 3 subunits, namely α, β and γ, which together form an active channel with a stoichiometry of $2\alpha : \beta : \gamma$ (Rossier *et al.*, 2002; Firsov *et al.*, 1998). ENaC is expressed in aldosterone-responsive epithelia and is highly expressed in the distal colon (Duc *et al.*, 1994; Bubien, 2010; Garty and Palmer, 1997). ENaC is reported to be the rate-limiting step of electrogenic Na^+ absorption and prevents Na^+ loss in the stool. The channel has heightened importance in conditions of disease, or when dietary sodium intake is low and aldosterone levels are high (Rossier *et al.*, 2002; Schultheis *et al.*, 1998; Kunzelmann and Mall, 2002; Sandle, 1998). ENaC is also important in the kidney where it plays an important role in the regulation of blood pressure and fluid homeostasis (Takahashi *et al.*, 2011; Bubien, 2010; Garty and Palmer, 1997). Some researchers have queried the role that ENaC plays in the intestine, suggesting that there is redundancy of its function due to the presence of other Na^+ absorbing proteins, such as NHEs and SGLTs (Hummler and Horisberger, 1999). The activity of ENaC is regulated in a tissue-specific manner, and in the colon it is regulated by mineralocorticoid and glucocorticoid-induced upregulation of β and γ ENaC (Epple *et al.*, 2000). Regulation of ENaC activity is complex and involves serine proteases, protein kinases, and cytokines, amongst others (Rossier and Stutts, 2009; Diakov and Korbmacher, 2004; Amasheh *et al.*, 2004). More recent research has shown the existence of a δ subunit of the human

ENaC, which when over expressed, dramatically increases ENaC activity (Haerteis *et al.*, 2009).

1-4.2.2 Apical Cl^- channels

Cl^- secretion in the colon requires the concerted activities of all the transport proteins that comprise the Cl^- secretory pathway. Cl^- enters epithelial cells through basolateral NKCC1 co-transporters, and exits to the lumen through apical Cl^- channels. There are several types of apical Cl^- channels present on the apical membrane of intestinal epithelial cells. Second messengers, such as Ca^{2+} and cAMP, can orchestrate apical Cl^- secretion through different Cl^- channels, however there does appear to be some redundancy with regard to Ca^{2+}-stimulated activation of the cAMP-regulated cystic fibrosis transmembrane conductance regulator (CFTR) (Namkung *et al.*, 2010).

CFTR

CFTR is a cAMP activated Cl^- channel and belongs to the family of ATP-binding cassette (ABC) transporters (Riordan *et al.*, 1989). While CFTR functions as an ion transport protein on the apical membrane of epithelia, it has also been proposed to play roles in vesicular trafficking and acidification of organelles (Bradbury, 1999). It is composed of five domains: two membrane-spanning domains, two nucleotide-binding domains that bind ATP and regulate gating of the channel, and a regulatory (R) domain, the phosphorylation of which determines channel activity (Sheppard and Welsh, 1999). Stimulation of CFTR by cAMP occurs by at least 2 mechanisms. Firstly, it is regulated by phosphorylation. For example, cAMP stimulates cAMP-dependent protein kinase (PKA)-mediated phosphorylation and activation of CFTR channels in the plasma membrane (Cheng *et al.*, 1991; Tabcharani *et al.*, 1991). It is also known that PKC and phosphatases can regulate channel activity, and can modulate PKA-dependent binding of the R domains (Berger *et al.*, 1993; Chappe *et al.*, 2005; Seavilleklein *et al.*, 2008). Secondly, cAMP has been shown by some

groups to stimulate trafficking of CFTR from an intracellular pool to the plasma membrane, while also inhibiting the rapid clathrin-dependent endocytosis of CFTR into endocytic pools (Lehrich *et al.*, 1998; Prince *et al.*, 1994; Lukacs *et al.*, 1997). However, the regulation of CFTR by intracellular trafficking is not a view shared by all and some studies in T_{84} cells indicate no alteration in CFTR at the apical membrane following cAMP elevation (Huflejt *et al.*, 1994).

Ca^{2+}-activated Cl^- channels (CaCC)

Ca^{2+}-activated Cl^- currents in the intestinal epithelium are short lived upon stimulation by agonists such as ACh, purines, or histamine. These agonists serve to increase intracellular Ca^{2+} by either releasing it from intracellular stores, or by causing an influx from the extracellular space (Hartzell *et al.*, 2005). Ca^{2+} may activate the CaCCs by either binding directly to the channel, or by binding to Ca^{2+}-dependent enzymes such as Ca^{2+}/calmodulin-dependent protein kinase II (CaMKII) (Worrell and Frizzell, 1991). Other second messengers, such as inositol 3,4,5,6-tetrakisphosphate (IP_4), can inhibit the activity of Ca^{2+} activated Cl^- channels (CaCC) by inhibiting activation by CaMKII (Xie *et al.*, 1996). However, the physiological relevance of these channels in the intestine has remained questionable over the years. For example, a study in 1988 showed that the intestinal tissue of patients with CF does not demonstrate secretory responses to Ca^{2+}-dependent agonists, suggesting such agonists may normally elicit their secretory effects through CFTR (Berschneider *et al.*, 1988). The identity of intestinal Ca^{2+}-activated Cl^- channels remained elusive until recent studies identified the transmembrane (TMEM) family of proteins. TMEM16A has been shown to mediate Ca^{2+}-activated Cl^- currents in neonatal mouse colon (Ousingsawat *et al.*, 2009) . However, this is in contrast to work by the Verkman group, who recently showed that Ca^{2+}-dependent Cl^- secretion also occurs via CFTR (Namkung *et al.*, 2010). Further research is required to resolve these discrepancies, although recent work by the Kunzelman group has added new weight to the potential physiological significance of TMEM16A. This study

suggested that rotavirus-induced diarrhoea is caused by activation of TMEM16A, coupled to inhibition of Na^+ absorption by SGLT-1 and ENaC (Ousingsawat *et al.*, 2011). Since it has only recently been discovered, regulation of this channel is poorly understood compared to CFTR. However, a recent study has shown that the Ca^{2+}-binding protein, calmodulin, is necessary for activation of TMEM16A (Tian *et al.*, 2011a). Finally, the precise identification of Cl^- channels that mediate responses to Ca^{2+}-dependent secretagogues is further complicated by recent findings that CFTR can interact with CaCCs, thereby modulating their activity, while Ca^{2+}-dependent agonists can also cause CFTR activation through activation of PKA (Wei *et al.*, 2001; Namkung *et al.*, 2010).

1-4.2.3 Basolateral K^+ channels

K^+ channels constitute the largest family of ion channels in humans. There are several types of K^+ channel, which are regulated by diverse stimuli, such as changes in membrane voltage, Ca^{2+}_i, phosphorylation, cAMP levels, pH, hypoxia and cell swelling, to name but a few. K^+ that enters the cell through NKCC1, the H^+/K^+-ATPase, and the Na^+/K^+-ATPase can be recycled through 2 types of basolateral K^+ channel; the cAMP-activated K^+ channel, KCNQ1, and the Ca^{2+}-activated basolateral intermediate K^+ conductance channel, KCNN4 (Schroeder *et al.*, 2000; Flores *et al.*, 2007). Basolateral K^+ transport in colonic epithelia is essential to maintain a membrane potential that sustains apical anion and fluid secretion, and it has been shown that inhibition of basolateral KCNN4 with clotrimazole (CLT) inhibits apical Ca^{2+}-dependent Cl^- secretion (Rufo *et al.*, 1997). More recent work has demonstrated that there are several isoforms of KCNN4 in the colon (Barmeyer *et al.*, 2010) and that apical KCNN4 may also be involved in anion secretion (Nanda Kumar *et al.*, 2010). KCNN4 is regulated by calmodulin, which is tightly coupled to the channel and activated by changes in intracellular Ca^{2+} levels (Fanger *et al.*, 1999). The K^+ channel that supports cAMP-activated Cl^- secretion is a complex formed by KCNQ1 and its β subunit,

KCNE3 (Kunzelmann *et al.*, 2001; Schroeder *et al.*, 2000). In the intestine both proteins co-localise in crypt epithelial cells. Interaction of KCNQ1 with its β subunit converts the voltage-dependent KCNQ1 into a voltage-independent, constitutively open, channel complex (Schroeder *et al.*, 2000).

1-4.3 Exchangers

1-4.3.1 Cl^-/HCO_3^- exchangers

Cl^-/HCO_3^- exchange in the colon acts in conjunction with NHEs to mediate NaCl absorption across the epithelium. Apical Cl^-/HCO_3^- exchangers are present in the colonic epithelium, and probably the best known of these is SLC26A3, or down regulated in adenoma (DRA), mutations of which cause congenital chloride diarrhoea (Hoglund *et al.*, 1996; Makela *et al.*, 2002; Wedenoja *et al.*, 2011; Worrell *et al.*, 2005).

1-4.3.2 Na^+/H^+ exchangers

There are 9 members in the mammalian Na^+/H^+ exchanger family (SLC9 family) which can be subdivided into 2 groups based on their cellular expression (Brett *et al.*, 2005). NHEs 1–5 are expressed in the plasma membrane, 6, 7 and 9 are expressed on intracellular organelles, whereas the expression profile of NHE8 has not yet been fully elucidated. The main NHE responsible for Na^+ absorption from the intestinal lumen is NHE3, with NHE2 being involved to a lesser degree (Ikuma *et al.*, 1999; Zachos *et al.*, 2005). NHE1 and 4 are basolaterally located where they contribute to regulation of cellular pH (Pizzonia *et al.*, 1998; Beltran *et al.*, 2008). Individual NHEs have different physiological roles and interestingly, studies show that the expression of NHE3 can be altered in intestinal diseases such as IBD (Khan and Ali, 1999; Larmonier *et al.*, 2011; Sullivan *et al.*, 2009). Regulation of NHE3 is highly complex and involves a variety of signalling proteins, including sodium hydrogen exchanger regulatory

factors (NHERF)s, ezrin, and other PDZ domain-containing proteins (Donowitz *et al.*, 2009).

1-4.4 Co-transporters

Co-transport, or secondary active transport, refers to the simultaneous movement of molecules or ions across the plasma membrane. The molecules or ions can be transported in the same (symport) or opposite (antiport) directions so long as the charge balance is equal. For this process to occur at least one of the molecules being transported must be passively travelling down its concentration gradient.

1-4.4.1 NKCC1

NKCC, of which there are 2 isoforms, facilitates the entry of Na^+, K^+, and 2 Cl^- into epithelial cells. NKCC1 has been identified as the isoform expressed in the intestinal epithelium and its function has been well characterised (Matthews *et al.*, 1992; Matthews *et al.*, 1994; D'Andrea *et al.*, 1996; Haas and Forbush, 2000; Del Castillo *et al.*, 2005; Payne *et al.*, 1995). The initial identification of the human NKCC was made in T_{84} cells by Payne *et al* in 1995 (Payne *et al.*, 1995). Following the initial identification, its localisation to the basolateral membrane of intestinal epithelial cells was characterised, and its association with the cytoskeleton was initially proposed (D'Andrea *et al.*, 1996). NKCC1 is known to be regulated by both low intracellular [Cl^-] and by cell shrinkage, indicating that the co-transporter plays an important role in maintaining cell volume. NKCC1 is also regulated by protein phosphatase 1 (PP1), PKC, Ste20-related proline-alanine-rich kinase (SPAK), PKA, and through its interaction with the cytoskeleton (Darman *et al.*, 2001; Matthews *et al.*, 1994; Piechotta *et al.*, 2003; Dowd and Forbush, 2003; Bachmann *et al.*, 2003; Haas and Forbush, 2000). More recent studies have also implicated PKC isoforms as regulators of NKCC1 trafficking to the basolateral membrane (Del Castillo *et al.*, 2005).

Secretagogue-induced regulation of NKCC1 was nicely described by Reynolds and co-workers, where they showed that Ca^{2+} -dependent agonists sequentially caused the activation, internalisation and degradation of NKCC1 (Reynolds *et al.*, 2007). This was followed by re-expression of the co-transporter several hours later, thereby completing the cycle of regulation by such agonists. The authors also showed that cAMP-dependent secretagogues caused sustained activation of the co-transporter, but that this could be curtailed by co-stimulation by Ca^{2+}-dependent agonists that activate PKC.

1-4.4.2 SGLT-1

Sugars are transported across the brush boarder membrane from the lumen by two different transporters, sodium glucose transporters (SGLTs) and glucose transporters (GLUTs). There are several SGLT isoforms expressed in human, with SGLT1 being the primary co-transporter expressed in the intestine (Wright *et al.*, 2011). SGLT-1 transports glucose or galactose from the gut lumen into epithelial cells along with Na^+, in a ratio of 1 : 2. The sugar moieties can then be transported from the cell via the basolateral transporter GLUT2, whereas Na^+ is transported basolaterally via Na^+/K^+-ATPase pumps. In order to maintain osmolarity, Cl^- and HCO_3^- are also absorbed across the epithelium, followed by water. This process forms the basis of oral rehydration therapy (ORT) (Wright *et al.*, 2011). The pathway by which water is transported across the epithelium has been the subject of much investigation and it is likely that several pathways exist including, passive diffusion across the phospholipid bilayer, solvent drag through the tight junctions and transport through water channels, such as aquaporins (Madara and Pappenheimer, 1987; Agre *et al.*, 1993). Other studies have proposed SGLT1 as a water transporter itself (Wright and Loo, 2000; Meinild *et al.*, 1998). The capacity for SGLT-1 to move water is large, with one study suggesting that 210 water molecules are transported across the epithelium with each cycle of transport activity.

1-5 Hypoxia

Hypoxia is defined as the state when cellular oxygen demand exceeds supply. This is such a common occurrence that every cell in the body is equipped to deal with it, and to mount an appropriate hypoxic response. Such is the sophistication of physiological responses to hypoxia that changes can occur from the molecular to the whole-body level. For example, reduced arterial oxygen is sensed by carotid bodies, highly vascularised organs located at bifurcations of the carotid arteries. These carotid bodies contain polarised cells that have O_2-sensitive K^+ channels located on their plasma membranes. Conditions of low O_2 inhibit the K^+ channels leading to Ca^{2+} influx, membrane depolarisation, subsequent neurotransmitter release, and changes in respiration rate and cardiac output (Peers and Kemp, 2001).

Among the most important molecular elements of hypoxic responses is hypoxia inducible factor (HIF). The identification HIF by Semenza *et al* led to the discovery of an extremely well-conserved signalling pathway that allows organisms to appropriately respond to changes in the amount of oxygen available to them (Semenza and Wang, 1992). However, the precise mechanism of how HIF itself detected oxygen eluded researchers for a further 10 years until the discovery of the HIF hydroxylases by two groups in 2001 (Epstein *et al.*, 2001; Bruick and McKnight, 2001). These proteins are the molecular 'oxygen sensors' that determine the fate of HIF.

1-5.1 HIF

HIF is a transcription factor that functionally exists as a heterodimer comprised of the constitutively expressed HIF-1β, or aryl hydrocarbon receptor translocator (ARNT), with a labile HIF-α subunit. There are 3 HIF-α subunits, with HIF-1α being the most extensively studied. HIF-α is an oxygen-dependent protein that is post-translationally regulated by HIF hydroxylases. During

conditions of normal oxygen tension, HIF-α subunits are hydroxylated at specific proline and asparagine residues by HIF hydroxylases. This proline hydroxylation targets HIF-α for ubiquitination by the von Hippel-Lindau tumour suppressor protein (pVHL) and ultimately, degradation via the proteasomal pathway. As a consequence of the action of the HIF hydroxylases, in normoxic conditions HIF-1α is turned over at a very high rate, thus keeping steady-state levels low (Huang *et al.*, 1998).

1-5.2 HIF hydroxylases

Studies published by several research groups in 2001 identified proline hydroxylation of HIF-1α as the mechanism by which HIF is recognised and targeted for destruction by an E3 ubiquitin ligase containing pVHL (Ivan *et al.*, 2001; Jaakkola *et al.*, 2001; Masson *et al.*, 2001). However, these initial studies did not identify the enzymes responsible for HIF hydroxylation until later the same year, when 2 groups independently published articles identifying an evolutionarily conserved family of proteins known as HIF prolyl hydroxylases (PHD1–3) (Epstein *et al.*, 2001; Bruick and McKnight, 2001). An asparaginyl hydroxylase of HIF-1α, factor inhibiting HIF (FIH-1), was later identified in 2002 (Lando *et al.*, 2002a). It was initially thought that the PHDs hydroxylated a consensus motif within substrate proteins, until subsequent studies demonstrated that the only obligatory residue for proline hydroxylation is the proline residue itself (Huang *et al.*, 2002). Since their discovery in 2001 there has been an increasing growth in research interest in these proteins and their roles in regulating cellular function in health and disease (Figure 1–4).

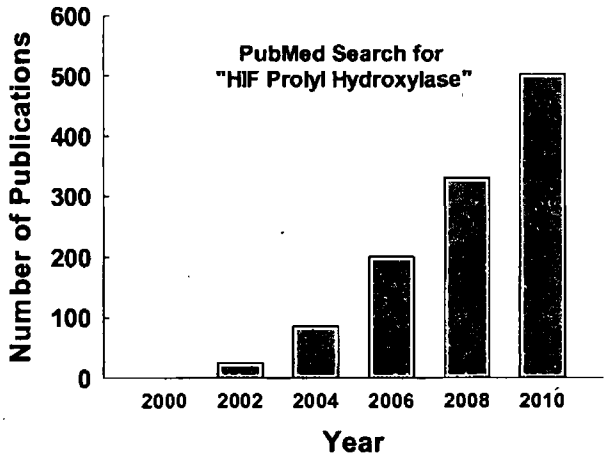

Figure 1–4 The number of published articles relating to HIF prolyl hydroxylases since 2000. More than 500 articles were found using the search term "HIF prolyl hydroxylase" since the year 2000.

The PHDs trans-4-hydroxylate Pro564 and Pro402 of HIF-1α thus targeting it for recognition by pVHL (Ivan *et al.*, 2001; Jaakkola *et al.*, 2001; Masson *et al.*, 2001). In contrast, FIH-1 β-hydroxylates asparagine 803 on HIF-1α to prevent its interaction with the co-activator p300/CBP, thereby inhibiting its transactivation domain and keeping it transcriptionally silent (Lando *et al.*, 2002a; Lando *et al.*, 2002b). The activity of PHDs is dependent on binding of α-ketoglutarate and FeII and mutational studies have identified the locations of their binding sites on the hydroxylases (McNeill *et al.*, 2002). Intracellular expression patterns of hydroxylases appear to vary greatly among different tissues, with PHD1 being present exclusively in the nucleus of osteocarcinoma cells and COS-1 monkey kidney cells, but being present in both the cytoplasm and nucleus of other cells (Metzen *et al.*, 2003; Huang *et al.*, 2002; Berchner-Pfannschmidt *et al.*, 2008). Interestingly, studies have shown that different PHDs have different preferences for the HIF-α isoform they hydroxylate, with PHD2 being more specific for HIF-1α and PHD3 preferentially hydroxylating HIF-2α (Appelhoff *et al.*, 2004). Several studies have attempted to identify the isoforms involved in particular conditions or phenomena, and reports suggest it is PHD2 that is the primary O_2 sensor involved in HIF-1α hydroxylation in normoxia (Berra *et al.*, 2003).

The great potential for modulating HIF hydroxylases in therapeutic settings did not go unnoticed, and prolyl hydroxylase inhibitors (PHIs) were rapidly adopted by pharmaceutical companies for the treatment of anaemia, and are currently in Phase 2 clinical trials (Mole *et al.*, 2003; Fraisl *et al.*, 2009; Provenzano *et al.*, 2011) (http://www.fibrogen.com/press/release/pr_1304365050).

Of the PHIs so far developed, and the most widely used for molecular biology has been dimethyloxalylglycine (DMOG) (Baader *et al.*, 1994). This is a non-selective inhibitor of HIF hydroxylases, collagen 4-hydroxylase and other α-ketoglutarate-dependent dioxygenases (Elvidge *et al.*, 2006). It was initially developed as a fibrosuppressive agent to inhibit prolyl-4 hydroxylase-regulated collagen synthesis (Baader *et al.*, 1994). Interestingly, DMOG itself is a poor inhibitor of proline hydroxylation in purified extracts, but intracellularly it is a potent inhibitor. This is thought to be due to enzymatic processing of DMOG in a manner similar to the processing of diethyl 2-4 pyridine-2,4-dicarboxylic acid (2,4-PDCA) (Tschank *et al.*, 1991). Other PHIs have been developed by biotechnology companies such as FibroGen Inc. and have been described in detail elsewhere (Salnikow *et al.*, 2004; Fraisl *et al.*, 2009; Tian *et al.*, 2011b).

The specificity of the HIF hydroxylases is not confined to HIF and it is now known that they hydroxylate residues on many other proteins, with FIH-1 being the least specific. An important non-HIF target of proline hydroxylases is IKKβ, with the consequent inhibition of NFκB under normoxic conditions (Cummins *et al.*, 2006). FIH-1 has been discovered to hydroxylate ankyrin repeat domains (Cockman *et al.*, 2006), and in fact its affinity for hydroxylation of the intracellular domain of Notch is greater than that its effects on HIF-1α (Zheng *et al.*, 2008). Given the plethora of ankyrin repeat domain-containing proteins, researchers have been keen to attribute a physiological purpose to this phenomenon. A proposed function for hydroxylation of ankyrin substrates is that they sequester FIH-1 away from HIF-1α, and thus increase HIF-1α transcriptional activity by reducing its asparagine hydroxylation (Coleman *et al.*,

2007). Other more recent studies have suggested that ankyrin hydroxylation by FIH-1 is more common than previously thought, and that it serves to stabilise ankyrin repeat domain folds, which facilitate protein-protein interactions (Kelly *et al.*, 2009a). Finally, the cytoskeletal ankyrin domain-containing family has also been shown to be hydroxylated by FIH-1 leading to alterations in protein-protein interactions (Yang *et al.*, 2011). HIF hydroxylases are not just oxygen sensors, they are also sensitive to the levels of the cofactors and substrates that they require for activity (Pan *et al.*, 2007). Thus, some researchers have also dubbed them "metabolic sensors". This feature is highlighted in FIH-1$^{-/-}$ mice, which exhibit reduced body weight, increased metabolic rate, and improved glucose and lipid homeostasis (Zhang *et al.*, 2010).

A physiological role for hydroxylases in the intestine was initially postulated in 2004 when a study revealed that HIF-1 exerted protective effects in a hapten-based murine model of colitis (Karhausen *et al.*, 2004). In this study, constitutively active HIF-1 ameliorated the onset and severity of colitis, whereas constitutive inhibition of HIF-1 led to increased disease severity. Further to this study in 2006, Cummins *et al.* published an article highlighting a non-HIF-1 target of the HIF hydroxylases, namely NFκB (Cummins *et al.*, 2006). This line of research culminated in 2008 with 2 studies being published back to back in *Gastroenterology*, both of which investigated the effects of hydroxylase inhibition in the development and progression of mouse models of colitis (Cummins *et al.*, 2008; Robinson *et al.*, 2008). These studies revealed that activation of HIF and NFκB pathways via inhibition of hydroxylase activity was protective against the onset of disease, and suggested that hydroxylases represented potential new targets for the development of therapies for IBD. Of particular relevance to this thesis, hypoxia occurs as a pathophysiological response in conditions of intestinal inflammation and can lead to alterations in several important aspects of intestinal physiology, including fluid and electrolyte transport (Eisenhut, 2006).

1-6 Hypoxic regulation of intestinal epithelial Cl^- secretion

1-6.1 Introduction

Previous sections have highlighted how epithelial transport function is dependent on cellular oxygen and energy supply, and how during conditions of hypoxia, epithelial transport can become dysregulated. Under physiological conditions the intestinal epithelium is exposed to one of the highest oxygen gradients in the body. Although the serosa is supplied by the splanchnic circulation with amply oxygenated blood, the epithelium is exposed to the harsh anoxic environment of the lumen (Taylor and Colgan, 2007). Add to this the highly dynamic nature of the splanchnic circulation, and the result is a hugely fluctuating oxygen supply to this tissue. Pathophysiological conditions, such as those underlying inflammation, can also result in hypoxia, and consequently the epithelial cells must be able to mount an appropriate response in order to survive. HIF, as already mentioned, is the master regulator of hypoxia and plays a key role in regulating metabolism, but is also known to regulate epithelial transport processes in the intestine. Some studies have shown that HIF can directly regulate the expression of epithelial ion transport proteins, while others have shown that intermediary steps, such as the generation of prosecretory second messengers can be altered in hypoxia (Ibla *et al.*, 2006; Zheng *et al.*, 2009; Taylor *et al.*, 1998).

1-6.2 Hypoxia regulates transport proteins

One of the many effects of hypoxia on the intestinal epithelial Cl^- secretory mechanism is its actions on the transport proteins themselves. This topic has received a good deal of attention, however is most well-documented with respect to hypoxic regulation of the Na^+/K^+-ATPase. While HIF itself is a transcription factor, two recent studies have demonstrated how it can act as a

transcriptional repressor of both CFTR and NKCC1. In the case of CFTR, initial studies demonstrated that hypoxia suppresses CFTR mRNA expression, not only in the intestine but also in other tissues, and subsequent investigations revealed that this occurs by a HIF-1-dependent mechanism (Guimbellot *et al.*, 2008; Zheng *et al.*, 2009). In other tissues, such as sinonasal respiratory epithelia, both CFTR and TMEM16A activity is attenuated by exposure to chronic hypoxia, an effect that is associated with decreased CFTR and TMEM16A mRNA expression (Blount *et al.*, 2011). Thus, it is clear that hypoxia has the capacity to negatively regulate Cl^- channels on the apical membranes of epithelial cells.

NKCC1 is also known to be regulated by hypoxia, and more specifically by HIF-1 which suppresses co-transporter expression at the transcriptional level (Ibla *et al.*, 2006). However, despite its importance to intestinal secretion, there is still a paucity of studies on NKCC function under conditions of hypoxia. Studies conducted by Yoo *et al.*, using a model of chemically-induced hypoxia in cultured epithelia, show that PKC ε suppresses Cl^- secretion upon activation by specific agonists (Yoo *et al.*, 2001). More recent research by the same group demonstrates that NKCC1 is rapidly internalised upon PKC activation, an event that was sensitive to PKC ε inhibition (Del Castillo *et al.*, 2005). Studies by other groups have shown PKC ε can be activated by hypoxia in cardiac myocytes (Ogbi and Johnson, 2006). Taken together these data suggest that hypoxia may activate signalling mechanisms, whereby PKC ε activation induces NKCC1 internalisation to downregulate epithelial secretion.

Na^+/K^+-ATPase pumps provide the driving force for all epithelial electrolyte transport processes, and this transporter has been demonstrated in numerous studies to be regulated under hypoxic conditions (Skou, 1998; Kaplan, 2002; Planes *et al.*, 1996; Mairbaurl *et al.*, 2002; Carpenter *et al.*, 2003; Dada *et al.*, 2003; Gusarova *et al.*, 2011). Initial studies indicated that hypoxia attenuated the activity of lung epithelial Na^+/K^+-ATPase, without altering its expression (Planes *et al.*, 1996; Carpenter *et al.*, 2003). The mechanisms involved are

complex and involve mitochondrial ROS, which is produced during hypoxia, which activate Ca^{2+}/calmodulin-dependent kinase kinase β (CaMKKβ). Activated CaMKKβ eventually results in the phosphorylation of Ser-18 on Na^+/K^+-ATPase α_1, culminating in clathrin-dependent pump endocytosis (Dada *et al.*, 2003; Chen *et al.*, 2006). This process was shown to require the ubiquitin-conjugating system and to be pVHL-dependent, but interestingly was HIF-independent (Comelias *et al.*, 2006; Dada *et al.*, 2007; Zhou *et al.*, 2008).

K^+ channels play a critical role in O_2 sensing in the carotid bodies, however there is a paucity of information on their regulation by hypoxia in the GI tract (Wyatt *et al.*, 2007; Patel and Honore, 2001; Ross *et al.*, 2011). The regulation by AMPK of KCNQ1 has been demonstrated under conditions of metabolic stress in kidney cells, and while it is possible that such effects may also occur in hypoxia, this has not been demonstrated in intestinal epithelial cells (Alzamora *et al.*, 2010). Research by other groups has shown that serum and glucocorticoid-responsive kinase-1 (SGK1) regulates KCNQ1/KCNE3 endocytosis (Seebohm *et al.*, 2007). Interestingly, SGK1 is known to be regulated by hypoxia in other systems, suggesting that KCNQ1 may be regulated under conditions of hypoxia, or by hydroxylase inhibitors, through activation of SGK1 (Aoyama *et al.*, 2005; Rusai *et al.*, 2009). Studies on the role of hypoxia in regulating Ca^{2+}-activated K^+ channels are limited to those in the carotid body (Ross *et al.*, 2011).

Thus, by virtue of their ability to regulate epithelial transport proteins through a variety of different transcriptional and post-transcriptional mechanisms, hypoxia-dependent signalling pathways represent good targets for the development of drugs to treat intestinal disorders associated with dysregulated fluid and electrolyte transport.

1-7 Pharmacological intervention in the treatment of diarrhoea

The word "diarrhoea" is derived from the Greek term "to flow through" [διά (dia, "through") + ρέω (rheō, "flow")] and is a common manifestation of gastrointestinal disease. In developing nations diarrhoea kills approximately 1.5 million children each year, and globally affects up to 2 billion people(Wardlaw *et al.*, 2010). Diarrhoeal diseases can be classified as being infectious or non-infectious, with infectious diarrhoea, e.g. rotavirus infection, accounting for up to 40 % of hospitalisations due to diarrhoea in children under 5 worldwide, including developed countries (Wardlaw *et al.*, 2010; WHO, 2008). Non-infectious chronic diarrhoea, with a duration of > 4 weeks, is a primary symptom of several gastrointestinal disorders, including IBD, diarrhoea-predominant IBS, iatrogenic diarrhoeas, such as those induced by chemotherapy, microscopic colitis and bile acid malabsorption (Carter *et al.*, 2004; Maroun *et al.*, 2007; Oelkers *et al.*, 1997; Hofmann, 2009). Together, these conditions represent a huge financial burden to Western societies in terms of healthcare and lost hours of work.

Many diarrhoeal deaths are due to dehydration, and in children with diarrhoea, rehydration and prevention of malnutrition are amongst the main therapeutic objectives. Anti-diarrhoeal drugs are not routinely used in children since this is not the primary objective, and such drugs can have sometimes fatal consequences (WHO, 1990). Dehydration caused by diarrhoea can be effectively treated by oral rehydration therapy.

For adults the primary therapeutic approaches for treating diarrhoea include adsorbents, such as cholestyramine, which bind the toxins causing the diarrhoea, or antimotility drugs, such as loperamide or codeine. These latter drugs effectively act by paralysing intestinal smooth muscle, thereby slowing motility and allowing increased time for absorption to occur (Read, 1983).

However, none of these treatments are safe for children and cannot be used in the long-term for the treatment of chronic diseases (WHO, 2005). To date, there are no therapeutic options available to clinicians that allow direct targeting of epithelial transport processes for the treatment of diarrhoea.

1-8 Overall aim

The overall aim of this thesis was to investigate the potential role that HIF-hydroxylases play in regulating intestinal epithelial Cl^- secretion and to determine the therapeutic potential of hydroxylase inhibitors in the treatment of diarrhoeal diseases.

Chapter 2

Materials and Methods

2-1 Animal studies

All animal studies were performed in compliance with Irish Department of Health and Children regulations and were approved by the Beaumont Hospital Ethics Committee.

Animal licence number:	B100/4159
Research Ethics Committee number:	628

2–1.1 Animal treatments for electrophysiological studies

Male C57BL/6 mice and male Sprague Dawley rats were bred and maintained in the environmentally controlled Biomedical Research Facility at Beaumont Hospital. Male animals were used to avoid the confounding factor oestrogen, which can alter colonic epithelial ion transport (O'Mahony *et al.*, 2007). Experiments were performed on 6–9 week old mice ranging from 20–25 g, and on 240–260 g rats of indiscriminate age. Animals were treated with either DMOG or PBS as vehicle control. DMOG was prepared in endotoxin-free PBS, and was administered by intraperitoneal (iP) injection to mice (320 mg/kg) as previously described, or to rats (40 mg/kg) as previously described (Cummins *et al.*, 2008; Zhao *et al.*, 2010). All mice were sacrificed 24 hours later by cervical dislocation, whereas rats were first anaesthetised by exposure to aerosolised isofluorane, before being sacrificed by cervical dislocation. The intestines of the animals were removed and placed in an ice-cold Ringer's solution, and were then treated as described in the relevant Methods sections. All drugs and equipment used to treat animals were sterile and endotoxin-free.

2–1.2 Mouse model of oral allergen–induced diarrhoea

These experiments were carried out in collaboration with Professor Padraic Fallon and Dr. Sylvie Amu, Trinity College Dublin, and were based on a previously published protocol (Brandt *et al.*, 2003; Perdue *et al.*, 1991). The premise behind the protocol for oral allergen-induced diarrhoea is that it is a classic clinical feature of numerous gastrointestinal allergic disorders, such as food allergies and eosinophil-associated gastrointestinal disorders. Allergic diarrhoeas are associated with significant changes in I_{sc} and Cl^- secretion, and previous research has shown that OVA-Induced diarrhoea is predominantly due to mast-cell stimulated Cl^- secretion (Harari *et al.*, 1987; Perdue *et al.*, 1991). Other researchers have corroborated this finding and have suggested that the enhanced intestinal secretion associated with allergic diarrhoea is also associated with decreased gut permeability (Wasserman *et al.*, 1988; Field, 2003; Barrett, 1991; Barrett *et al.*, 1990). Male BALB/c strain mice were sensitised twice, 2 weeks apart, with 50 μg of OVA in the presence of 1 mg of aluminium potassium sulphate adjuvant by IP injection. Two weeks following the initial sensitisation, the animals were each challenged with oral administration of 50 mg OVA in sterile saline, 3 times per week, which previous studies have shown to be the lowest dose to induce diarrhoea in this model (Brandt *et al.*, 2003). Prior to each oral challenge the animals were fasted for 4 hours to limit antigen degradation in the stomach. Mice were monitored for 1 hour following oral OVA administration, and those with profuse watery stool were diagnosed as diarrhoea-positive. Mice were treated with either DMOG (IP; 160 mg/kg), or PBS alone, 24 hours before each oral challenge with OVA.

2-2 T_{84} cell culture

The T_{84} cell line is a human colonic carcinoma cell line that was established in BALB/c nude mice. It was isolated from a lung metastasis from a patient with a colon carcinoma, and injected subcutaneously into nude mice. The resulting tumour was isolated, homogenised, and cultured in growth medium (Murakami and Masui, 1980). When grown on permeable supports, T_{84} cells form a well-differentiated, electrically tight, columnar epithelium (Madara and Dharmsathaphorn, 1985). They have the appearance of native crypt epithelial cells and retain many of their characteristics, including vectorial Cl^- secretion in a basolateral to apical direction (Dharmsathaphorn *et al.*, 1984). While T_{84} cells may lack the absorptive phenotype seen in surface cells, the simplicity of the model makes it ideal for examining molecular mechanisms that regulate intestinal epithelial Cl^- secretion. T_{84} cells were cultured, in DMEM Ham's F12 media supplemented with 5 % bovine calf serum, 1 % penicillin/streptomycin, and 1 % glutamate (Toumi *et al.*, 2011). Culture medium was replaced every second day, and on the 7th day, or when cells were approximately 90 % confluent, they were passaged by trypsinisation. For trypsinisation, cells were first washed with trypsin (0.25 %), and then incubated with trypsin for several minutes. Trypsin was deactivated by the addition of culture medium containing serum. Trypsinised cells were counted using a haemocytometer and were seeded at the densities shown in Table 2–1.

Table 2–1 T_{84} cell culture seeding conditions. T_{84} cells were trypsinised and counted using a hemacytometer. Cells were seeded at various densities ranging from 100,000 – 2,000,000 cells, depending on the area of the receptacle. MCE = mixed cellulose esters; PET = Polyethylene Terephthalate

	Hanging insert	Standing insert	Standing insert	Glass bottom petri-dish	T75
Application	Confocal	Ussing	Protein/RNA	Imaging	Culture
Porosity	1 μM	0.45 μM	0.45 μM	-	-
Material	PET	MCE	MCE	glass	Plastic
Supplier	Millipore	Millipore	Millipore	MatTek	Starstedt
Cat number	PIRP12R48	PIHA01250	PIHA03050	P35G-0-14-C	83.1813.500
Area	0.33 cm^2	0.6 cm^2	4.2 cm^2	1.54 cm^2	75 cm^2
Number of cells	1×10^5	5×10^5	2×10^6	5×10^5	2×10^6

For electrophysiological studies, T_{84} cells were cultured on 0.6 cm^2 permeable supports and were considered to be suitable for experimentation when their transepithelial resistance (R_{te}) had stabilised at ≥ 1000 Ω/cm^2, typically between 7–21 days post seeding. Cells were cultured on 4.2 cm^2 inserts for protein extraction, RNA isolation, cAMP assays, biotinylation studies, and co-immunoprecipitation studies, and were considered to be suitable for experimentation once their R_{te} had stabilised at ≥ 1000 Ω/cm^2, typically between 7–21 days post seeding. The filters used for culturing T_{84} cells were composed of MCE and had a resistance of 74.9 ± 1.4 Ω/cm^2. Time courses for the development of R_{te} across T_{84} cells grown on 0.6 and 4.2 cm^2 inserts are shown in Figure 2–1.

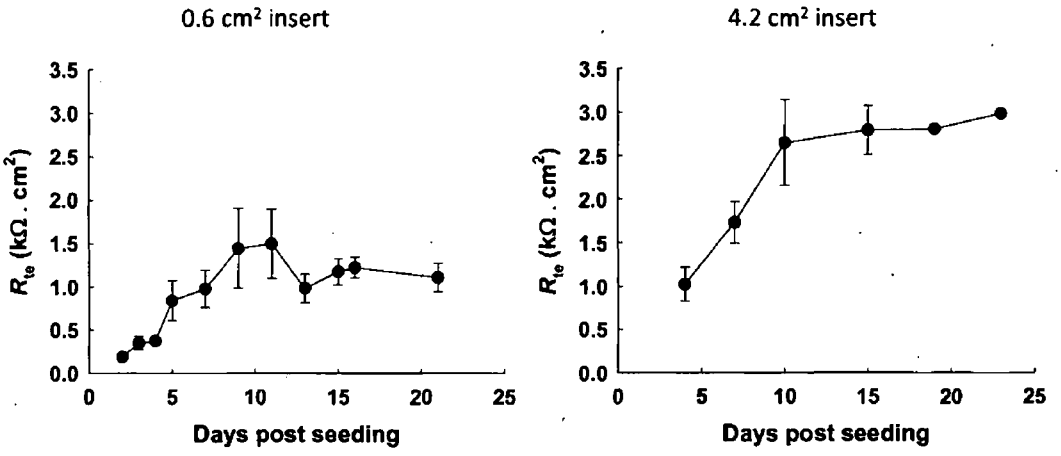

Figure 2–1 Time course of the development of R_{te} across monolayers of T_{84} cells on permeable supports. A) T_{84} cells were cultured on 0.6 cm^2 permeable supports and the R_{te} was recorded each day for several days. Data are expressed as $k\Omega.cm^2$ (n = 5–6) for each point shown. B) T_{84} cells were cultured on 4.2 cm^2 permeable supports and the R_{te} was recorded each day for several days. Data are expressed as $k\Omega.cm^2$ (n = 4 for each point shown).

2–2.1 Cell treatments

Once the R_{te} of the cells had stabilised at plateau levels, T_{84} monolayers were routinely washed once on the apical and basolateral sides with serum-free culture medium. The inserts containing the monolayers were then transferred to a new well of the culture dish, and were cultured in serum-free medium for 24 hours. This served to synchronize the cells in the quiescent G0 phase, to prevent confounding effects of serum components, and to prevent serum components from binding to and/or enzymatically cleaving the drugs that were to be used. T_{84} cell culture in serum-free medium for 24 hours caused an

increase in the basal R_{te} from 1665.4 ± 90.9 to 1970.8 ± 97.5 $\Omega.cm^2$ (*$p \leq 0.05$; n = 48). Following the 24 hour period in serum-free medium, cells were treated accordingly, with all treatment solutions being diluted in serum-free medium. When pharmacological inhibitors were used they were incubated with the cells bilaterally for a minimum of 30 minutes prior to treatment with hydroxylase inhibitors. Table 2–2 lists the inhibitors employed, their intended targets, and the concentrations at which they were used. The exception to bilateral treatment was methyl β cyclodextrin (MβCD), which was used basolaterally only. The mechanisms of action of the inhibitors used in the current studies are listed below:

- **Dimethlyoxallylglycine (DMOG)** is a non-selective inhibitor of HIF hydroxylases, collagen 4-hydroxylase and other α-ketoglutarate-dependent dioxygenases (Elvidge *et al.*, 2006; Fraisl *et al.*, 2009). DMOG was initially developed as a fibrosuppressive agent to inhibit prolyl-4 hydroxylase-regulated collagen synthesis (Baader *et al.*, 1994). Interestingly, DMOG itself is a poor inhibitor of proline hydroxylation in purified extracts, but is a potent intracellular inhibitor. This is thought to be due to enzymatic processing of DMOG in a manner similar to the processing of diethyl 2-4 pyridine-2,4-dicarboxylic acid (2,4-PDCA) (Tschank *et al.*, 1991). DMOG was the primary HIF-hydroxylase inhibitor used throughout the current studies. While cellular responses to hydroxylase inhibition by DMOG and hypoxia are known to differ, previous studies in a breast cancer cell line, MCF-7, have found there to be striking concordance between patterns of gene expression induced by hypoxia and by DMOG (Elvidge *et al.*, 2006). While many of these genes are HIF-1 or HIF-2-dependent, not all of the hypoxia or DMOG-regulated genes were targets of HIF, highlighting the importance of non-HIF targets of hydroxylases (Elvidge *et al.*, 2006).

- **FG-4497** is a proprietary compound developed by FibroGen Inc. to inhibit the activity of HIF-hydroxylases. FG4497 has been reported to inhibit HIF hydroxylases by binding to the active site of the enzymes (Fraisl *et al.*, 2009). The optimal working concentration of FG4497 was determined in these studies and it was found to be more potent than DMOG.

- **$CoCl_2$** was used to inhibit HIF-1α degradation by preventing its interaction with von Hippal Lindau protein (pVHL), thereby inhibiting its proteasomal degradation (Kanaya and Kamitani, 2003; Yuan *et al.*, 2003). More recently $CoCl_2$ was shown to deplete ascorbate in the cell, hence inhibiting the HIF hydroxylases and thereby stabilising HIF-1α (Salnikow *et al.*, 2004). The optimal working concentration of this inhibitor was determined in this study.

- **Actinomycin D (AD)** was used to inhibit gene transcription. This drug inhibits transcription in a non-specific manner by forming a stable complex with double-stranded DNA via deoxyguanosine residues at the transcription initiation complex, thereby inhibiting DNA-primed RNA synthesis (Sobell, 1985). AD also causes single-strand breaks in DNA.

- **Cycloheximide (CHX)** was used to inhibit protein translation (Schneider-Poetsch *et al.*, 2010). Recent reports show that CHX blocks the translocation step in elongation by binding to 60S ribosomal subunits in the ribosome. The optimal working concentration of this inhibitor was determined in this study.

- **H89** was used to inhibit cAMP dependent protein kinase (PKA) activity. H89 is a non-selective inhibitor of PKA that at higher concentrations is also known to inhibit other kinases, such as S6K1, MSK1, ROCK-II, PKBα, and MAPKAP-K1β (Davies *et al.*, 2000). H89 is thought to work by

competitively inhibiting the binding of ATP to the kinase, and was used in these studies at a concentration previously reported to inhibit PKA in T_{84} cells (Chijiwa *et al.*, 1990; Rudolph *et al.*, 2004).

- **BMS-345541** is a highly selective inhibitor of IκB Kinase (IKK) and thus is an inhibitor of NFκB activity. BMS-345541 binds to either the peptide binding site on IKK, or an allosteric site that changes the binding site, thus preventing peptide-binding (Burke *et al.*, 2003).

- **GF 109203X (GF)** is reported to be a specific inhibitor of PKC (Toullec *et al.*, 1991). It inhibits both classical and novel PKC isoforms via competitive inhibition with ATP (Roberts *et al.*, 2005).

- **PP2** is a potent Src family-selective tyrosine kinase inhibitor that works via competitive inhibition with ATP (Hanke *et al.*, 1996). It was used in these studies at concentrations previously shown to inhibit Src in T_{84} cells (Keely *et al.*, 2000) (20 μM).

- **Acriflavine** specifically binds to the PAS-B domain of HIF-1α and 2α. Acriflavine thus prevents HIF-α and HIF-1β dimerisation, and inhibits HIF-DNA binding and transcriptional activity (Lee *et al.*, 2009).

- **MβCD** disrupts lipid rafts by chelating cholesterol. It was used in these studies at a concentration previously reported to deplete cholesterol and disrupt lipid rafts in T_{84} cells (Wolf *et al.*, 2002). Optimal treatment times for the drug were investigated in the present studies.

- **5-(N-Ethyl-N-isopropyl)amiloride (EIPA)** inhibits NHEs with concentration-dependent specificities (Chambrey *et al.*, 1997; Beltran *et al.*, 2008). Amiloride and its derivatives are thought to bind to the

external Na^+ binding site of NHEs, thus inhibiting their activity (Masereel *et al.*, 2003).

Table 2–2 Concentrations of drugs employed and their intended cellular targets. This table summarises the inhibitors used and their concentrations employed.

Inhibitor	Target	Working Concentration
DMOG	PHDs	1 mM
FG-4497	PHDs	50 μM
$CoCl_2$	HIF-1α-pVHL interaction	500 μM
H89	PKA	30 μM
BMS-345541	NFκB	10 μM
GF	PKC	5 μM
Acriflavine	HIF-1α-HIF-1β dimerisation	5 μM
Cycloheximide	60S Ribosomal subunit	5 μM
Actinomycin D	Double-stranded DNA	250 ng/ml
EIPA	NHE	50 μM
PP2	Src	20 μM
Methyl β cyclodextrin	Lipid rafts	4 mM

2-3 Electrophysiological measurements

Electrophysiological measurements were performed using VCC MC8 Voltage clamps. All epithelial preparations, both tissues and cell cultures, were mounted in Ussing chambers (Figure 2–2), bathed in a physiological Ringer's solution(s) (see individual protocols below), aerated with a 95 % O_2, 5 % CO_2 mix, and maintained at 37°C ± 1°C. All preparations were clamped to zero potential difference (PD), and drug treatments were initiated once baseline short circuit current (I_{sc}) and R_{te} had stabilised. I_{sc} and PD were recorded for each experiment, and using Ohms Law, R_{te} and conductance were calculated. All current recordings were normalised and expressed as ΔI_{sc} ($\mu A/cm^2$).

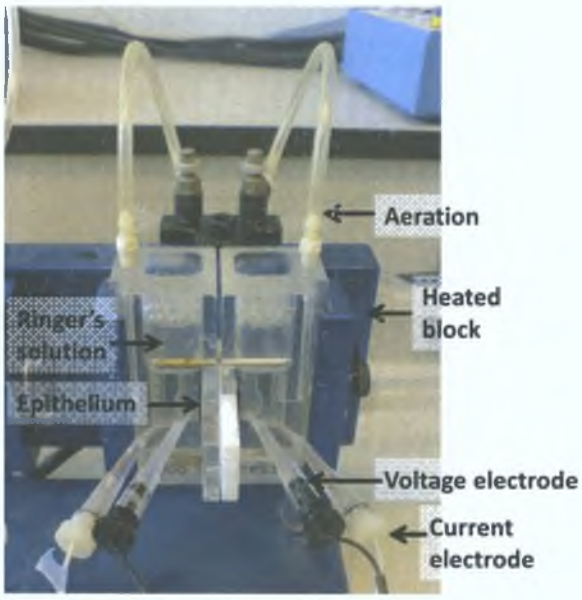

Figure 2-2 Photograph of an Ussing chamber. The Ussing chamber is composed of 2 hemi-chambers separated by an epithelial preparation. The epithelium is bathed in Ringer's solution, aerated with 95 % O_2, 5 % CO_2, and maintained at 37°C by a heating block. A voltage is applied across the epithelium, which is then clamped to zero potential difference, and the current that is applied via the current electrodes to maintain the zero potential difference is recorded as I_{sc}.

2-3.1 T_{84} colonic epithelial cells

T_{84} colonic epithelial cells were grown on 0.6 cm^2 permeable supports as described in Section 2–2. All monolayers were washed in appropriate physiological solution(s), mounted in Ussing chambers, and bathed in physiological solutions according to each individual protocol.

2-3.1.1 Electrogenic Cl^- secretion

T_{84} monolayers were mounted in Ussing chambers and bathed in Ringer's solution (**Table 2–3**) unless otherwise stated. Under such conditions, secretagogue-induced ΔI_{sc} responses across T_{84} monolayers have been shown to be wholly reflective of changes in electrogenic Cl^- secretion (Dharmsathaphorn *et al.*, 1984; Cartwright *et al.*, 1985; Dharmsathaphorn *et al.*, 1985). The prototypical secretagogues, carbachol (CCh) and forskolin (FSK), were used to stimulate Ca^{2+} and cAMP activated Cl^- secretory responses, respectively. The effects of these drugs on T_{84} cells have been well-characterised. CCh was employed at a concentration of 100 μM, and was added basolaterally, where it acts at muscarinic M3 receptors (Cuthbert *et al.*, 1987). FSK (10 μM) was added apically only since previous results from our laboratory showed that no additional increase in currents were observed upon bilateral addition of the compound.

Table 2–3 Composition of Ringer's solution. Ringer's solution is an isotonic physiological solution that contains a balance of salts and sugars to sustain animal tissue in a viable state for long periods of time. It was introduced by the physiologist Sidney Ringer in 1882 for studies of frog heart. Once prepared, Ringer's solution was aerated with a 95 % O_2, 5 % CO_2 mix to achieve a pH of 7.4 and an osmolarity of 285 ± 5 mOsms.

Component	Concentration (mM)
Na^+	140
K^+	5.2
Ca^{2+}	1.2
Mg^{2+}	0.8
Cl^-	119.8
HCO_3^-	25
$H_2PO_4^-$	2.4
D-glucose	10

Table 2–4 Composition of D-fructose Ringer's solution. D-glucose is replaced with equi-molar D-fructose in D-fructose Ringer's solution. Once prepared, D-fructose Ringer's solution was aerated with a 95 % O_2, 5 % CO_2 mix to achieve a pH of 7.4 and an osmolarity of 285 ± 5 mOsms.

Component	Concentration (mM)
Na^+	140
K^+	5.2
Ca^{2+}	1.2
Mg^{2+}	0.8
Cl^-	119.8
HCO_3^-	25
$H_2PO_4^-$	2.4
D-fructose	10

2-3.1.2 Apical Cl^- currents

Apical CFTR currents were measured by modifying previously published protocols (Rochwerger *et al.*, 1994; Bijvelds *et al.*, 2009; DuVall *et al.*, 1998). After mounting in Ussing chambers, an apical to basolateral Cl^- gradient (119.8–4.8 mM) was imposed across the epithelium. Normal Ringer's solution was applied to the apical reservoir (Table 2–3), whereas low Cl^- Ringer's solution was added basolaterally (Table 2–5). While this gradient is opposite to the physiological direction of intestinal epithelial Cl^- secretion, experiments were conducted in this way in order to remove any influence of basolateral transporters from the current and to prevent cell swelling. T_{84} monolayers were allowed to equilibrate for 15 minutes and were then basolaterally permeabilised by the ionophore, nystatin (100 μg/ml), to allow the passage of monovalent anions. After a further 35 minutes, when the basal I_{sc} had re-stabilised, cells were stimulated with apical FSK (10 μM). Under these conditions changes in I_{sc} wholly reflect changes in apical Cl^- currents through CFTR. This was confirmed in the current studies by the use of $CFTR_{inh172}$ (10μM), which attenuated FSK-stimulated I_{sc} responses by 78 %.

Table 2–5 Composition of low Cl^- Ringer's Solution. NaCl was replaced with equi-molar Na-gluconate in low Cl^- Ringer's solution. Once prepared, low Cl^- Ringer's solution was aerated with a 95 % O_2, 5 % CO_2 mix to achieve a pH of 7.4 and 285 ± 5 mOsms.

Component	Concentration (mM)
Na^+	140
K^+	5.2
Ca^{2+}	1.2
Mg^{2+}	0.8
Cl^-	4.8
HCO_3^-	25
$H_2PO_4^-$	2.4
D-glucose	10
Gluconate	115

2-3.1.3 Basolateral K^+ currents

Basolateral Ca^{2+}-induced K^+ currents (KCNN4) were measured as previously described (Kirk and Dawson, 1983). Monolayers of T_{84} cells were mounted in Ussing chambers and were apically permeabilised using the ionophore, amphotericin B (50 μM). After baseline I_{sc} had stabilised over 30 minutes K^+ was driven from the apical to the basolateral compartment by the imposition of a K^+ gradient (123.2–5.2 mM), created by addition of a high K^+ Ringer's solution (Table 2–6) to the apical reservoir. The Na^+/K^+-ATPase-specific inhibitor, ouabain (100 μM), was added basolaterally to remove any contribution of Na^+/K^+-ATPase activity to I_{sc} responses. Under these conditions changes in I_{sc} are wholly reflective of changes in basolateral K^+ currents through KCNN4.

Table 2–6 Composition of high K^+ Ringer's solution. NaCl was substituted with K^+-gluconate in high K^+ Ringer's solution. Once prepared, high K^+ Ringer's solution was aerated with a 95 % O_2, 5 % CO_2 mix to achieve a pH of 7.4 and an osmolarity of 285 ± 5 mOsms.

Component	Concentration (mM)
Na^+	25
K^+	123.2
Ca^{2+}	1.2
Mg^{2+}	0.8
Cl^-	4.8
HCO_3^-	25
$H_2PO_4^-$	2.4
D-glucose	10
Gluconate	115

2-3.1.4 Na^+/K^+-ATPase activity

Na^+/K^+-ATPase activity was measured by a method based on previously published protocols (DuVall *et al.*, 1998; Gomes and Soares-Da-Silva, 2002; Lam *et al.*, 2003). Monolayers of T_{84} cells were mounted in Ussing chambers and bathed bilaterally in low sodium Ringer's solution (Table 2–7). The monolayers were apically permeabilised by the ionophore, amphotericin B (50 μM). Following permeabilisation, the monolayers were allowed to re-equilibrate prior to stimulation with basolateral CCh (100 μM). Under these conditions changes in I_{sc} are wholly reflective of electrogenic transport by the Na^+/K^+-ATPase.

Table 2–7 Composition of low Na^+ Ringer's Solution. NaCl was substituted with equimolar N-methyl-D-glucamine (NMDG)-Cl^- In the low Na^+ Ringer's solution. Once prepared, low Na^+ Ringer's solution was aerated with a 95 % O_2, 5 % CO_2 mix to achieve a pH of 7.4 and an osmolarity of 285 ± 5 mOsms.

Component	Concentration (mM)
Na^+	25
K^+	5.2
Ca^{2+}	1.2
Mg^{2+}	0.8
Cl^-	119.8
HCO_3^-	25
$H_2PO_4^-$	2.4
D-glucose	10
$NMDG^+$	115

2-3.2 Intestinal tissue

All intestinal tissues were transported to the laboratory in ice-cold physiological Ringer's solution(s), the specific type of which dependent on the transporter to be investigated. Animal tissues with the exception of murine jejunum were microscopically stripped of underlying muscle layers. Murine tissues were mounted on inserts with an aperture of 0.3 cm^2, whereas rat tissues were mounted on larger inserts with an aperture of 0.5 cm^2.

2-3.2.1 Colonic epithelial Cl^- secretion

The large intestine was transported on ice to the laboratory in Ringer's solution (Table 2–3). All experiments were performed on distal colon which was distinguished from proximal colon by the lack of striation distinct to the proximal colon. The mesenteric fat and blood vessels were trimmed from the colon. The colon was then cut longitudinally along the mesenteric boarder and luminal contents were removed and the colon was washed in ice-cold Ringer's solution. The colonic tissue was then microscopically dissected, separating the epithelium from the underlying muscle layers. The colon was then cut laterally into 2–3 sections. Tissues were then mounted on inserts, and bathed in Ringer's solution (Table 2–3) in Ussing chambers at 37°C. Tissues were equilibrated for 25 minutes during which time PD, I_{sc}, and conductance (G) were recorded. Once the I_{sc} had stabilised, amiloride (100 μM) was added to the apical bath to inhibit Na^+ absorption by ENaC, thereby removing any possible contribution of apical Na^+ absorption to the observed current. Ca^+-activated Cl^- secretion was then stimulated by the basolateral addition of CCh (100 μM), and once the I_{sc} had returned to pre-stimulated levels, FSK (10 μM) was added to the apical bath to stimulate cAMP-activated Cl^- secretion. Bumetanide (100 μM) was added at the end of each experiment to the basolateral bath to inhibit NKCC1 activity, and thus provide a measure of the contribution of Cl^- secretion to observed I_{sc} responses.

2-3.2.2 SGLT-1 activity

Studies of SGLT-1 mediated absorption in mouse intestine were carried out using a protocol modified from previously published studies (Grubb, 1995). The small intestine was transported on ice to the laboratory in mannitol Ringer's solution (Table 2–8). This solution lacked D-glucose so as to maintain glucose transporters in a quiescent state. To identify the jejunum, the Ligament of Treitz was first identified, with the jejunum beginning approximately 4 cm distal to this and extending distally for approximately 10 cm. The mesenteric fat and blood vessels were trimmed away and the jejunum was cut longitudinally and then laterally into several sections. Unlike colonic tissue, jejunal tissue was mounted unstripped of underlying muscle layers. This was due to the abundance of lymphoidic Peyer's patches in jejunum which add to the fragility of the tissue and create technical difficulties for stripping away the muscle layers. SGLT-1 is known to be expressed apically in murine jejunum, therefore mannitol-containing Ringer's solution (5 mM) was added to the apical bath (Table 2–8), and D-glucose-containing Ringer's solution (5 mM) to the basolateral bath (Table 2–9). The concentrations of the carbohydrates used were adapted from a previously published protocol (Grubb, 1995). Tissues were allowed to equilibrate for 25 minutes to allow the I_{sc} to stabilise. Bumetanide (100 μM) was added to the basolateral bath to inhibit NKCC1 and thus any contribution of Cl^- secretion to observed currents. Amiloride was not routinely added to jejunal preparations since initial investigations revealed there was no observable ENaC-mediated current in these tissues. Na^+ absorption by SGLT-1 was stimulated by the addition of D-glucose (25 mM) to the apical bath. Mannitol (25 mM) was simultaneously added to the basolateral bath to maintain equi-osmolarity. The D-glucose-stimulated SGLT-1 current recorded was attenuated by the SGLT-specific inhibitor, phloridzin (1 mM).

Table 2–8 Composition of mannitol-containing Ringer's solution. Mannitol-containing Ringer's solution lacks D-glucose which is substituted with 5 mM mannitol. Once prepared, mannitol-containing Ringer's solution was aerated with a 95 % O_2, 5 % CO_2 mix to achieve a pH of 7.4 and an osmolarity of 285 ± 5 mOsms

Component	Concentration (mM)
Na^+	140
K^+	5.2
Ca^{2+}	1.2
Mg^{2+}	0.8
Cl^-	119.8
HCO_3^-	25
$H_2PO_4^-$	2.4
Mannitol	5

Table 2–9 Composition of D-glucose-containing Ringer's solution. D-glucose-containing Ringer's solution has less D-glucose (5 mM) than normal Ringer's solution (10 mM) (**Table 2–3**). Once prepared, 5 mM D-glucose Ringer's solution was aerated with a 95 % O_2, 5 % CO_2 mix to achieve a pH of 7.4 and an osmolarity of 285 ± 5 mOsms.

Component	Concentration (mM)
Na^+	140
K^+	5.2
Ca^{2+}	1.2
Mg^{2+}	0.8
Cl^-	119.8
HCO_3^-	25
$H_2PO_4^-$	2.4
D-glucose	5

2–3.2.3 ENaC activity

Na^+ absorption by ENaC was recorded from rat rectal tissue using a protocol modified from previously published studies (Inagaki *et al.*, 2004). Anatomically, the rectum of the rat is located in the pelvic cavity, behind the pelvis. Surrounding fat and muscle tissues were removed before excision of the rectum, which extends approximately 3 cm proximal from the anus. The tissue was isolated and transported to the laboratory in ice-cold Ringer's solution (Table 2–3). The tissue was microscopically stripped of underlying muscle layers and the mucosa was then mounted in Ussing chambers. The tissue was equilibrated in Ringer's solution for 25 minutes prior to addition of amiloride (10 μM) to the apical bath to inhibit ENaC activity.

2-4 Preparation of protein lysates from animal tissue

Segments of tissue were isolated from animals that has been treated with DMOG or vehicle control. The segments were cleaned of luminal debris using ice-cold Ringer's solution (Table 2-3) and were then snap-frozen in liquid nitrogen. Tissues were then stored at -80°C until required. Segments of tissue were ground to a fine powder in liquid nitrogen using a pestle and mortar kept on dry ice. The ground tissue was then weighed and NP-40 lysis buffer (Table 2-10) was added in a ratio of 1 g tissue: 5 ml lysis buffer. Samples were immediately vortexed and incubated on ice for 45 minutes, with intermittent vortexing every 10 minutes. Samples were then centrifuged at 10,621 x g for 20 minutes at 4°C. The supernatant was retained and analysed for protein content (Section 2–6). Protein content of each sample was then normalised using lysis buffer as a diluent. Samples were then separated by sodium dodecyl sulphate polyacrylamide gel electrophoresis (SDS-PAGE) (Section 2-7), and proteins were detected by western blotting.

2-5 Preparation of protein lysates from cells

T_{84} cells were cultured for protein extraction as described in **Section 2-2**. Following treatment, monolayers were washed twice in ice-cold 1 x phosphate buffered saline (PBS). Cells were then lysed *in situ* using Nonidet P40 (NP40) lysis buffer containing protease and phosphatase inhibitors (Table 2-10) for 45 minutes at 2–8°C. Lysed cells were scraped from inserts and were sonicated (3 x 10 second pulses) to solubilise membrane proteins. Sonicated lysates were centrifuged at 15,294 x g for 10 minutes at 4°C. The supernatant was retained and analysed for protein content (Section 2–6).

2-6 Analysis of protein content

The amount of protein in cell and tissue lysates was measured using the Lowry method (Lowry *et al.*, 1951). Using bovine serum albumin (BSA), a standard curve was prepared for each set of samples, an example of which is illustrated in Figure 2-3. A coefficient of determination (R^2), which is a statistical measure of how well the regression line approximates the real data points, was created from the standards. An R^2 of 1.0 indicates that the regression line perfectly fits the data. An R^2 of > 0.95 was determined to be the cut-off point, and any standard curves with R^2 values below this were repeated. Protein content was estimated from the standard curve using the equation: $y = mx + c$.

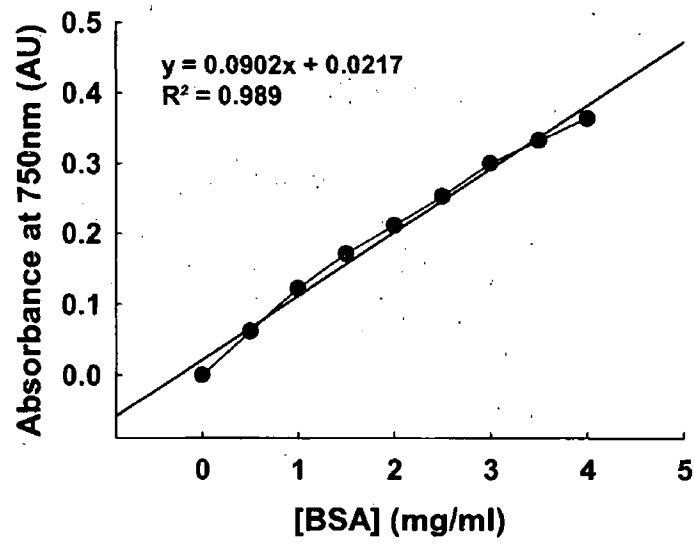

Figure 2-3 An example of a standard curve for protein determinations. Known concentrations of BSA (0–4 mg/ml) were prepared in lysis buffer. BSA standards and samples were incubated with Folin reagent for 20 minutes, and their absorbance was then measured at 750 nm. Protein concentrations in samples were calculated from the standard curve using the equation, $y = mx + c$.

2-7 Western blotting

Protein content of each sample was normalised using lysis buffer as a diluent. Samples were mixed with a half volume of 2 x loading buffer (Table 2-11) and then heated to either 37°C or 95°C to aid in the protein-denaturing process. Samples were then separated by SDS-PAGE using the appropriate percentage of acrylamide to separate proteins based on their size (Table 2-12). Separated proteins were transferred onto polyvinylidene difluoride (PVDF) membranes using a semi-dry electrophoretic transfer apparatus. Membranes were routinely blocked with appropriate blocking reagents (Table 2-13) for 1 hour with horizontal rotation prior to addition of the appropriate primary antibody diluted in the blocking reagent (Table 2-14). Following 2 washes in Tris buffered saline with 1 % tween (TBST), the secondary HRP-linked antibodies, diluted in the blocking reagents were routinely added for 1 hour with rotation at room temperature. Secondary antibody solutions were then removed and the membranes were washed a further 4 times. Immuno-reactive proteins were detected by enhanced chemiluminescence (ECL). Table 2-14 shows the transfer times used for each protein of interest, the blocking reagent used, the primary and secondary antibody concentrations used, and the optimum exposure time in ECL or ECL plus reagent.

Table 2-10 Composition of NP40 lysis buffer. NP40 is a non-ionic, non-denaturing detergent used to solubilise membrane proteins (Stephens, 1985). Phenylmethanesulfonyl fluoride (PMSF) is a serine and cysteine-protease inhibitor that also inhibits acetylcholinesterase, whereas sodium orthovanadate (Na_3VO_4) inhibits ATPase, alkaline phosphatase and tyrosine phosphatase (Turini *et al.*, 1969; Huyer *et al.*, 1997). Complete mini EDTA-free protease inhibitor tablets from Roche Diagnostics inhibit serine and cysteine proteases.

Component	Concentration
Nonidet P40	1 %
NaCl	150 mM
Tris base	50 mM
PMSF	0.1 mg/ml
Complete mini EDTA free protease inhibitor tablet	1 tablet / 10ml
Na_3VO_4	1 mM

Table 2-11 Composition of 2 x gel loading buffer. DL-Dithiothreitol (DTT) is used in sample loading buffers to reduce protein disulfide bonds prior to SDS-PAGE. Glycerol (5–10 %) increases the density of a sample so that the sample will layer at the bottom of the sample well. It also acts as a protein stabiliser and storage buffer component. SDS is a non-ionic detergent used to denature proteins and to confer them with a negative charge.

Component	Concentration
Tris HCl	50 mM
DTT	100 mM
Glycerol	40 %
SDS	4 %

Table 2-12 Polyacrylamide gels. Low percentage gels are recommended for the analysis of larger proteins and *vice versa*. The following protein molecular weights are approximate and were transcribed from Fermentas.com.

Recommended poly acrylamide gel (%)	Protein molecular weight range (kDa)
8	40 – 250
10	30 – 200
12	20 – 150

Table 2-13 Composition of blocking reagents for western blotting. Dried milk (Marvel) was used as a blocking reagent for most antibodies employed in these studies. However, for some antibodies more complex blocking reagents were used, such as goat serum for p-IκBα, as previously described (Taylor *et al.*, 1999).

Component	Concentration		
	Milk Blocker	Goat Blocker	BSA Blocker
Milk	5 %	-	-
Normal Goat serum	-	5 %	-
BSA	-	3 %	5 %
1 x TBST	+	-	+
NaCl	-	250 mM	-
Tween 20	-	0.02 %	-

Table 2-14 Parameters for western blot analysis of proteins. Conditions detailed below were optimised for use of antibodies with T_{84} cell lysates, with the exception of mHIF-1 α, which was optimised for lysates from murine intestine.

Protein	Protein size (kDa)	Lysate quantity (μg)	Incubation temperature (°C)	Transfer time (mins)	Blocking reagent	Primary antibody dilution	Primary antibody source	Cat. number	Developing reagent	Exposure time (mins)
ATP Synthase α	55	30	95	60	Milk	1/10,000	BD	612516	ECL $^+$	0.5
β-actin	42	30	37 / 95	any	any	1/20,000	Sigma	A5316	ECL $^+$	1
CFTR	168	40	37	90	Milk	1/800	Upstate	05-583	ECL $^+$	> 120
FIH-1	40	30	95	40	Milk	1/1000	Santa Cruz	sc-26219	ECL $^+$	0.5
HIF-1α	120	30	37	80	Milk	1/500	BD	610959	ECL $^+$	30
KCNN4	40	40	95	60	BSA	1/2000	Sigma	P4997	ECL $^+$	0.5
KCNQ1	75	30	37	80	Milk	1/400	Sigma	P5372	ECL $^+$	0.5
mHIF-1α	120	40	37	80	Goat	1/3000	Calbiochem	400080	ECL $^+$	0.5
MONaKA	65	30	95	65	Milk	1/3000	Santa Cruz	sc-100107	ECL $^+$	1
Na^+/K^+-ATPase α_1	112	30	37	80	Milk	1/10000	Abcam	ab7671	ECL	2
Na^+/K^+-ATPase β_1	35-55	30	37	45	Milk	1/3000	Abcam	ab8344	ECL $^+$	2
NKCC1	130	30	95	80	Milk	1/1000	Santa Cruz	sc-21545	ECL	4
phospho-IκBα	40	40	95	40	Goat	1/1000	Upstate	9246	ECL $^+$	12
PKC ζ	80	30	95	60	Milk	1/2000	Upstate	22080	ECL	0.5

2-8 Cell surface biotinylation.

The surface expression of Na^+/K^+-ATPase α_1 was analysed by employing a biotinylation technique adapted from previously published studies (Del Castillo *et al.*, 2005; Liu *et al.*, 2002). T_{84} cells were cultured for protein extraction, as described in Section 2-2. Following DMOG (1 mM; 24 hours) treatment, monolayers were washed thrice in ice-cold PBS. Biotinylation buffer was prepared fresh for each experiment as 1 mg/ml sulfo- N-hydroxysuccinimide (NHS)-biotin in PBS. The biotinylation buffer was added to the basolateral side of T_{84} monolayers on ice for 15 minutes with horizontal rotation, during which time biotin binds to amine groups of extracellular proteins. Due to the short half-life of sulfo-NHS-biotin at alkaline pH, the biotinylation buffer was replaced with a second fresh aliquot for a further 15 minutes with rotation. The reaction was stopped by addition of glycine (100 mM), the amine groups of which bind to and quench unbound biotin. Cells were then lysed in NP40 lysis buffer (Table 2-10) for 30 minutes at 2–8°C. Cell lysates were prepared and centrifuged (14,000 x g; 6 minutes; 4°C). Protein content of the supernatant was determined and 500 μg of protein was incubated with vertical rotation overnight at 2–8°C in the presence of 40 μL streptavidin-agarose beads, which bind strongly to biotin-protein complexes. The following day the beads were centrifuged, washed thrice in lysis buffer to remove any unbound proteins, and mixed with 2 x loading buffer (Table 2-11). Samples were heated (55°C; 30 minutes) and protein complexes were isolated from the beads by centrifuging through spin columns. Samples were prepared for SDS-PAGE, but were not boiled so as to prevent aggregation of Na^+/K^+-ATPase subunits that can occur through binding of the hydrophobic residues within their transmembrane domains (Yan *et al.*, 2004; Ura *et al.*, 1996; Donnet *et al.*, 2001). Proteins were then separated by SDS-PAGE and Na^+/K^+-ATPase α_1 was detected by western blotting (Section 2-7). Densitometric analysis of blots was performed and surface expressed Na^+/K^+-ATPase α_1 was calculated by the following equation:

$$\left\{ x = \frac{b}{(t/a)} \right\}$$

Where:

x = Na^+/K^+-ATPase α_1 surface expression

b = biotinylated Na^+/K^+-ATPase α_1

a = β-actin

t = total Na^+/K^+-ATPase α_1

2-9 Co-immunoprecipitation

T_{84} monolayers were grown on 4.2 cm^2 permeable supports as described in Section 2-2. Cells were lysed *in situ* by apical addition of NP40 lysis buffer (Table 2-10) for 30 minutes at 2–8°C. The cells were scraped from the inserts and the lysates centrifuged at 15,294 x g for 10 minutes at 4°C. The lysates were 'pre-cleared' to remove any non-specific antigen-antibody interactions by incubating the samples with donkey serum for 1 hour at 2–8°C with vertical rotation. The lysates were next incubated with protein-G sepharose beads for 1 hour with vertical rotation at 2–8°C to remove serum-bound antigens and any non-specific antibodies. These bead-lysate suspensions were then centrifuged at 14,000 x g for 10 minutes at 4°C. The supernatant was retained and further incubated with the relevant primary antibody for 1 hour at 2–8°C with vertical rotation. Protein-G bead suspension was then added to the antibody-antigen solution, and incubated at 2–8°C overnight with vertical rotation. On the second day the protein-G beads-antibody-protein complexes were added to spin columns and the supernatant was discarded. The beads were washed thrice with ice-cold NP40 lysis buffer. Aliquots of these washes were used to detect protein content to ensure optimal washing conditions, and no protein was detected even after 1 wash. The bound proteins were finally eluted. Proteins were then separated by SDS-PAGE and detected by western blotting (Section 2-7). The concentrations of the antibodies used to immunoprecipitate (IP) and immunoblot (IB) the protein of interest were determined from preliminary experiments (Figure 2-4), as were the pre-clearing steps and

number of washes employed to remove unbound proteins. Expression of β-actin was investigated since it should not co-IP with either Na^+/K^+-ATPase α_1, Na^+/K^+-ATPase β_1, or MONaKA, and therefore served as a negative control for these studies.

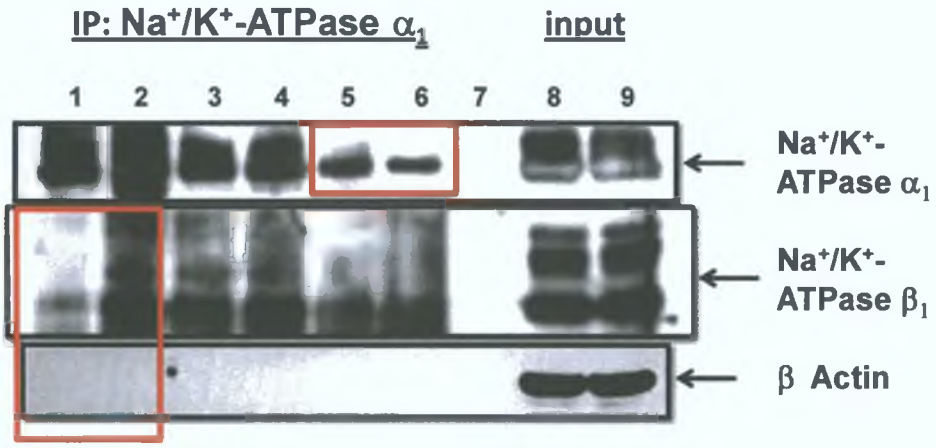

Figure 2-4 β-actin was absent from anti-Na^+/K^+-ATPase α_1 subunit immunoprecipitates. T_{84} cells were grown as monolayers on permeable supports until R_{te} stabilised at plateau levels. T_{84} cells were lysed and were immunoprecipitated using the following dilutions of Na^+/K^+-ATPase α_1 antibody: lanes 1 and 2, 1/250; lanes 3 and 4, 1/500; lanes 5 and 6, 1/1000. The red boxes highlight the optimum antibody dilutions for IP identified from these studies. Lane 7 was empty, whereas lanes 8 and 9 contained the total lysate, or input. β-actin was absent from the anti-Na^+/K^+-ATPase α_1 antibody immunoprecipitates in Lanes 1–6.

2-10 Intracellular pH measurements

The protocols for measurement of NKCC1 and NHE activities were adapted from those previously published (Heitzmann *et al.*, 2000; Reynolds *et al.*, 2007; Beltran *et al.*, 2008; Ramirez *et al.*, 2000). T_{84} cells were cultured on glass bottom petri dishes (1.54 cm^2) until they reached an optimal density of 70–90 %. The cells were treated as required and were washed twice with modified Krebs solution (37°C) (Table 2-15) prior to incubation with the pH-sensitive dye, 2'-7'-bis(carboxyethyl)-5(6)-carboxyfluorescein acetoxymethyl (BCECF-AM). BCECF-AM was re-constituted to a concentration of 5 μM in pluronic acid, which aids in the intracellular transport of the dye. BCECF is a pH-sensitive dye, and the acetoxymethyl (AM) ester derivative is membrane permeant, allowing bulk loading of cells. Once inside the cell, the lipophilic groups are cleaved by non-specific esterases, resulting in a charged form with 4–5 negative charges at physiological pH values of approximately 7.4 (Han and Burgess, 2010). Cells were loaded with the dye diluted in modified Krebs solution (Table 2-15) for 60 minutes at 37°C. The dye was removed and the cells were washed twice in modified Krebs solution, before being incubated in modified Krebs solution alone for a further 15 minutes in the dark at room temperature. The second incubation was necessary to facilitate leakage of dye from cells that could otherwise disrupt baseline readings during the experiments (Han and Burgess, 2010). Cells were mounted in a perfusion chamber on an epifluorescence Nikon microscope stage. Cells were incubated at room temperature in modified Krebs solution (Table 2-15) for several minutes before perfusion with NH_4 Krebs solution (Table 2-15). The initial rise in pH was due to NH_3 uptake via NKCC1 and the plateau phase acidification that follows is due to uptake of NH_4^+ by NKCC1 (Heitzmann *et al.*, 2000). The acid-load was then performed upon the removal of the NH_4-Krebs solution and perfusion with NMDG-Krebs solution (Table 2-15) for approximately 2 minutes to block the activity of NHEs and thus amplify the acidification. Under these conditions, acidification is due to the dissociation of H^+ from NH_4^+ to form $NH_3 + H^+$. Cells were perfused with

modified Krebs solution (Table 2-15) for the remainder of the experiment. pH recovery after the acid load is due to the extrusion of H^+ by NHEs, and thus represents the activity of NHEs. The ratio of BCECF-AM fluorescence with excitation at 505 or 450 nm (F 505/450) was measured every 3 seconds and images were captured with an intensified charge-coupled device (CCD) camera (ICCD200) and a MetaFluor imaging system. The pH recovery rate is expressed in arbitrary units (AU) and calculated as the change from t = 0 to t = 1, normalised to the value at t = 0 and represented by the following equation:

$$pH\ recovery\ rate\ (AU) = \frac{\Delta F_{490/440}\ t=1}{\Delta F_{490/440}\ t=0}$$

Where: a value of 1 = no recovery in pH,
a value of > 1 = a recovery in pH,
and a value < 1 = negative recovery in pH.

The solutions used for pH imaging are detailed in Table 2-15 and were adapted from previously published studies (Beltran *et al.*, 2008).

Table 2-15 Composition of Krebs solutions used for intracellular pH measurements. Once prepared, modified Krebs solutions and NMDG-Krebs solutions were brought to a pH of 7.4 and an osmolarity of 285 ± 5 mOsms. NH_4-Krebs solution was brought to a pH of 8.0 and an osmolarity of 285 ± 5 mOsms.

Compound	Concentration (mM)		
	Modified	NH_4	NMDG
KCl	5	5	5
NaCl	141	121	-
$CaCl_2$	1	1	1
$MgCl_2$	0.5	0.5	0.5
KH_2PO_4	0.4	0.4	0.4
$MgSO_4$	0.4	0.4	0.4
Na_2HPO_4	0.3	0.3	0.3
HEPES Na^+ salt	10	10	10
D-glucose	0.6	0.6	0.6
NH_4Cl	-	20	-
NMDG Cl	-	-	141

2-11 RNA isolation

T_{84} cells were cultured for RNA extraction as described in Section 2–2. Following treatment, monolayers were washed twice in ice-cold PBS. The cells were scraped from the inserts re-suspended in 1 ml ice-cold PBS and then centrifuged (600 x g; 3 minutes; 4°C). The supernatant was discarded and the cell pellet was snap frozen in liquid nitrogen and stored at -80°C. Total RNA was isolated using a Qiagen RNeasy Mini Kit. The RNA was then treated with DNase-I to digest and remove any genomic DNA contamination. RNA was quantified and reverse transcription reactions were performed using the purified and quantified RNA to create cDNA. A standard quantity of RNA was used for each reaction since it is technically difficult to quantify the resultant single-stranded cDNA. This is due to the presence of the single-stranded primers that interfere with the quantification of cDNA. RNA quality was determined using spectrophotometric methods. RNA has its absorption maximum at 260 nm and the ratio of absorbances at 260 and 280 nm was used to assess the purity of an RNA preparation, with proteins absorbing strongly at 280 nm. Pure RNA measured in water has an A260/A280 of 1.8–2.0. A secondary measure of RNA purity is the A260/230 ratio. Carbohydrates and phenols absorb at 230 nm, and thus an A260/230 ratio of 1.8 generally means that there are more of these contaminants in the sample. An example of the absorbances of purified RNA is shown in Table 2–16.

Table 2–16 Purified total RNA measured by spectrophotometric analysis. RNA quality was measured on a Nanodrop 8000. Of interest are the A260/280 and A260/230 ratios which are an indication of the purity of the RNA.

Sample ID	Conc.	Units	A260	A280	260/280	260/230
1	394.3	ng/ul	9.858	5.251	1.88	1.55
2	338.3	ng/ul	8.457	4.322	1.96	2.05
3	268.3	ng/ul	6.708	3.404	1.97	0.9
4	289.6	ng/ul	7.239	3.7	1.96	1.42
5	304.3	ng/ul	7.608	3.894	1.95	1.92
6	384.5	ng/ul	9.613	4.977	1.93	2.12

2-12 Primer design

Several of the primer sets employed in the current studies were obtained from previously published research (Table 2-1). Primer 3 primer design software was employed for genes for which no primer sequences had been previously published. The sequences obtained were cross referenced with the NCBI primer design Blast utility to ensure that there were no off-target amplicons. Primers were ordered from Invitrogen through Biosciences.

2-13 First strand cDNA synthesis, and PCR

The Improm II reverse transcriptase kit from Promega was used to perform the reverse transcription reaction. Once a cDNA library was created, amplification of the genes of interest was performed by semi-quantitative PCR and was performed using the primer sets shown in Table 2–17. It was assumed that reverse transcription occurred with equal efficiency in each reaction, and thus a standard volume of the newly synthesised cDNA was used for each PCR reaction. Amplicons were then separated and analysed by agarose gel electrophoresis. Negative controls were run in each set of primers for each experiment. The first negative control was for nucleic acid contamination (Negative Control). In the Negative Control an equal aliquot of water replaced RNA, and the RT reaction was run in parallel to the reactions containing RNA. PCR conditions were then optimised for each set of primers. Variables that were changed in order to optimise conditions were cycle number, annealing temperature, and elongation time. PCR was then performed using the optimised conditions, and samples were separated by agarose gel electrophoresis. Presence of a signal in the Negative Control indicated nucleic acid contamination of the reaction. The second control was that for genomic contamination (GC). In the GC control the reverse transcription reaction was performed without reverse transcriptase. PCR was then performed and samples were separated by agarose gel electrophoresis. Presence of a signal in

the GC control indicated genomic contamination of the reaction. Examples of these controls are shown in Figure 2–5.

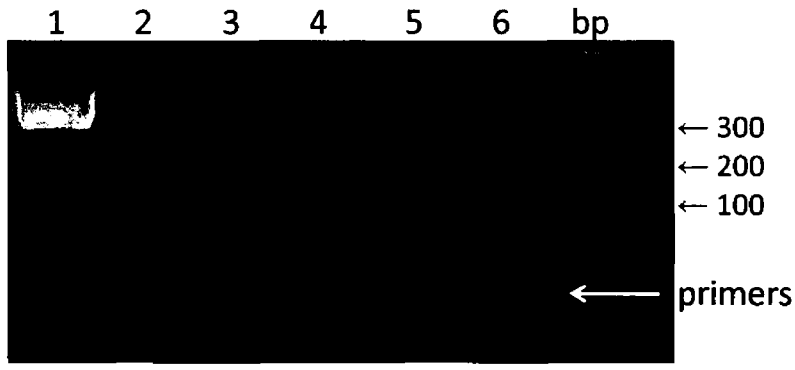

Figure 2-5 Genomic contamination and RNA contamination controls for PCR. In the Negative Control an equal aliquot of water replaced the RNA, and the reverse transcription reaction was run in parallel to the reactions containing RNA. PCR was then performed and samples were separated by agarose gel electrophoresis. Presence of signal in the Negative Control indicated nucleic acid contamination of the reaction. In the GC control the reverse transcription reaction was performed without reverse transcriptase. PCR was then performed and samples were separated by agarose gel electrophoresis. Lane 1 contains a cDNA sample of 18SrRNA amplified with 18SrRNA primers. Lane 2 is empty. Lanes 3 and 4 were loaded with the Negative Control sample, whereas lanes 5 and 6 were loaded with the GC control samples. In the experiment shown there were no bands in either the Negative Control or GC lanes, indicating no RNA or genomic contamination of the sample.

Table 2-17 Sequences of primers used to amplify cDNA and quantitatively compare mRNA expression. Primers were designed to contain approximately 50 % GC content.

Gene Target	Sense primer sequence 5'-3'	Antisense primer sequence 5'-3'	Amplicon size (bp)	Source
18SrRNA	GTCCCCCAACTTCTTAGAG	CACCTACGGAAACCTTGTTAC	421	-
CFTR	CCATCAGCCCCTCCGACAG	TACTAGCACATGGCAAGGGTTTTC	424	-
FIH-1	ACAGTGCCAGCACCCACAA	GCCCACAGTGTCATTGAGCG	188	(Metzen *et al.*, 2003)
FXYD3	CCTGGACCATTCCAGGAAAA	GGGACTTTGAGGCTTGTTGG	238	Primer 3
HIF-1α	CTCAAAGTCGGACAGCCTCA	CCCTGCAGTAGGTTTCTGCT	314	(Zhou *et al.*, 2006)
KCNN4	GCCGTGCGTGCAGGATTTAGG	GCCCGGCACCACGTCACCATAG	403	-
KCNQ1	CCAGGGCCGCGTCTACAA	AGAACACCAGCACGATC	272	-
MONaKA	CCAGCATCGAAGACTGACAA	CCCCAGATCCTGCTGAATTA	164	Primer 3
Na^+/K^+-ATPase α_1	TGTCCAGAATTGCAGGTCTTTG	TGCCCGCTTAAGAATAGGTAGGT	77	(Murphy *et al.*, 2004)
Na^+/K^+-ATPase β_1	ACCAATCTTACCATGGACACTGAA	ACCAATCTTACCATGGACACTGAA	80	(Murphy *et al.*, 2004)
NKCC1	ACAATGGCGAATGGTGACT	CATGGGGTTACTTTTTGGTTAC	518	-
PHD1	ACGGGCTCGGGTACGTAAG	CCCAGTTCTGATTCAGGTAATAGATACA	87	(Cioffi *et al.*, 2003)
PHD2	GACCTGATACGCCACTGTAACG	CCCGGATAACAAGCAACCAT	83	(Cioffi *et al.*, 2003)
PHD3	AACTGAATCTGCCCTCACTGAAG	AGAATTCAGGAACCGTTACTAAAATGA	82	(Cioffi *et al.*, 2003)

2-14 Intracellular Ca^{2+} imaging

T_{84} cells were cultured on glass coverslips until they reached an optimal density of 80 %. Cells were treated with DMOG (1 mM; 24 hours) and were then washed twice with physiological salt solution (PSS) (Table 2–18) at 37°C. Monolayers were then loaded with the Ca^{2+} binding dye Fura-2/AM (5 μM) in PSS at pH 7.4 for 30 minutes. Fura-2/AM was reconstituted in 0.01 % pluronic F-127 plus 0.1 % DMSO. Cells were then washed in PSS and mounted in a perfusion chamber on an epifluorescence Nikon microscope stage. Cells were incubated in room temperature PSS for 5 minutes before addition of CCh (100 μM). The ratio of Fura-2 fluorescence with excitation at 340 or 380 nm (F340/380) was measured every 3 seconds and images were captured with an intensified CCD camera (ICCD200) and the MetaFluor imaging system.

Table 2-18 Composition of physiological salt solution (PSS) for Ca^{2+} imaging. Once prepared the solution was adjusted to pH 7.4.

Compound	Concentration (mM)
NaCl	140
KCl	5
$CaCl_2$	1
D-glucose	10
HEPES-trimethylamine	10

2-15 cAMP assay

cAMP levels in T_{84} monolayers were measured using a commercially available kit, as per the manufacturers' instructions. The kit contains an enzyme-linked immunosorbent assay (ELISA) that uses a cAMP antibody to bind either cAMP in experimental samples or an alkaline phosphatase molecule bound to cAMP. Samples or standards, alkaline phosphatase conjugate, and antibody are simultaneously incubated at room temperature in a well coated with secondary antibody. Excess reagents are then washed away, substrate is added, and the resulting colour generated is spectrophotometrically analysed at 405 nm (Figure 2–6). The colour intensity is representative of the amount of alkaline phosphatase bound, which is inversely proportional to the amount of cAMP in the experimental sample.

T_{84} cells were cultured as described in Section 2–2. Following DMOG (1 mM; 24 hours) treatment, monolayers were stimulated with apical FSK (10 μM) for 5 minutes at 37°C, before being lysed on ice with HCl (100 mM) for 10–30 minutes. HCl also serves to inhibit endogenous phosphodiesterases, which hydrolyse cAMP to AMP, thus interfering with the assay. Monolayers were scraped and the lysates centrifuged (15,300 x g; 10 minutes; 4°C). Cell pellets were discarded and cAMP levels were detected in supernatants that were diluted 1:10 with assay buffer. Since basal levels of cAMP in T_{84} cells are low, samples were acetylated to increase the sensitivity of the assay. cAMP acetylation results in a molecule that more closely mimics that of the immunogenic conjugate, i.e. the compound against which the antibody was originally raised. Therefore, acetylated cAMP has a higher affinity for the cAMP antiserum and raises the sensitivity of the assay. cAMP levels were quantified from 2 separate standard curves for acetylated and non-acetylated cAMP. Results were expressed as pmol cAMP/mg protein.

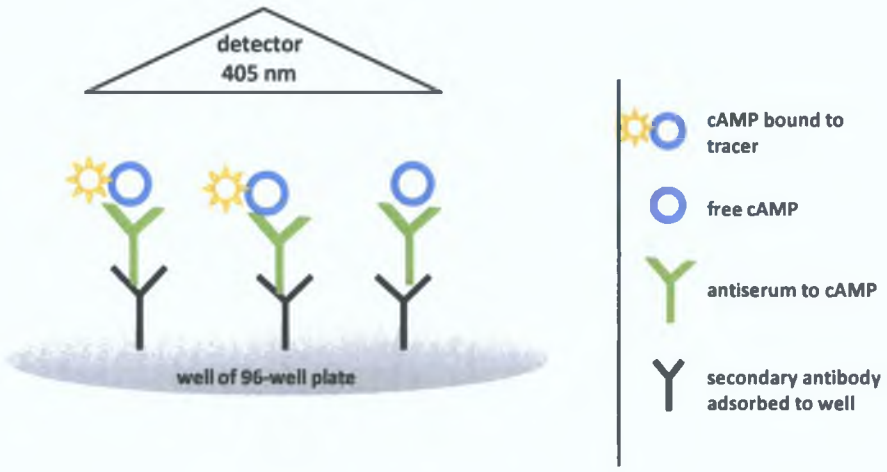

Figure 2-1 Schematic representation of the cAMP EIA. Antiserum, sample or standard, and cAMP-bound tracer were added simultaneously to the wells of a 96-well plate. Wells were washed, substrate was added, and the absorbance of the resulting colour was read at 405 nm.

2-16 Lactate dehydrogenase assay

The lactate dehydrogenase (LDH) assay was performed using a commercially available kit. LDH is an enzyme that interconverts pyruvate and lactate with the coincidental interconversion of NAD and NADH. LDH is a relatively stable enzyme in the cytosol, which is rapidly released from the cell upon damage to the plasma membrane. In the assay NAD gets reduced to NADH by LDH. NADH is then used to reduce a tetrazolium dye which forms a coloured compound upon reduction. Tetrazolium redox dyes scavenge electrons from oxidation/reduction reactions and are intracellularly reduced to brightly coloured formazan precipitates.

T_{84} cells were cultured as described in Section 2–2. Following DMOG (1 mM; 24 hours) treatment, culture medium from control and DMOG-treated cells was analysed for LDH release. A separate set of cells was incubated with lysis buffer at 37°C for 45 minutes, and the culture medium from these cells served as a positive control. Sterile serum-free culture medium was used as a negative control, the value of which was subtracted from sample readings. An equal volume (40 μl) of apical and basolateral media were combined and placed in the wells of a 96-well plate. Assay reagent was added to each well at a volume equal to twice that of medium sample used, and the reaction was incubated in the dark at room temperature for 25 minutes. The reaction was terminated upon the addition of 1/10 volume of HCl (1 M) (24 μl). The absorbance was then measured spectrophotometrically at 490 nm.

2-17 Serum alanine aminotransferase (ALT) measurement

Aminotransferases are enzymes which catalyse the reversible transformation of α-keto acids into amino acids by the transfer of amino groups. Alanine aminotransferase (ALT) is present in the cytosol of hepatocytes, and increased levels of ALT in the serum indicates a reduction in the integrity of hepatocyte plasma membrane. Thus, serum ALT was used in these experiments as a measure of liver toxicity in mice treated with DMOG. The reaction is based on the following principle: ALT in the presence of pyridoxal phosphate transfers the amino group of alanine to α-ketoglutarate to form pyruvate and glutamate. Pyruvate then enters an LDH-catalysed reaction with NADH to form lactate and NAD^+. Decreases in absorbance due to the consumption of NADH are measured at 340 nm and are proportional to ALT activity in the sample.

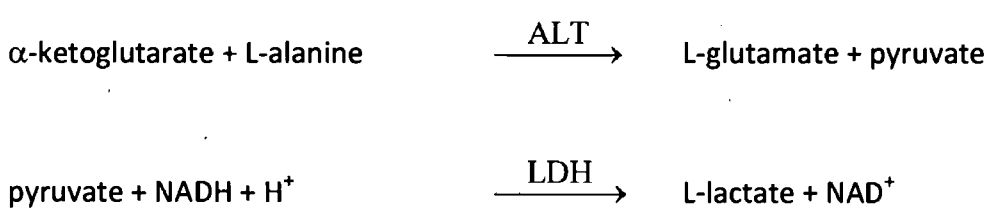

Blood was collected from mice and coagulated at room temperature for 20 minutes. Samples were then centrifuged (1200 x g; 15 minutes; 4°C), and the serum was retained for analysis. The ALT assay was performed using an Olympus Analyser and results were expressed as international units per litre (IU/L).

2-18 Serum creatinine measurement

Creatinine is a break-down product of creatine phosphate in muscle, and is usually produced at a fairly constant rate by the body. Creatinine is a spontaneously formed cyclic derivative of creatine and is filtered out of the blood by the kidneys. Deficient kidney filtration causes creatinine blood levels to rise. Thus, serum creatinine levels can be used to calculate creatinine clearance, which reflects the glomerular filtration rate and which, in turn, is a measure of renal function. The reaction is based on the following principle: Creatinine forms a yellow-orange coloured compound with picric acid in an alkaline medium. The rate of change in absorbance at 520/580 nm is proportional to the creatinine concentration in the sample.

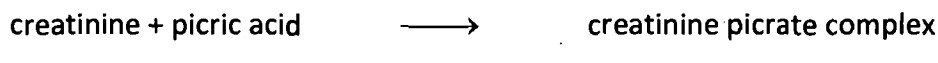

Blood was collected from mice and coagulated at room temperature for 20 minutes. Samples were then centrifuged (1200 x g; 15 minutes; 4 °C), and the serum was retained for analysis. The creatinine assay was performed using an Olympus Analyser and results are expressed mM per sample.

2-19 ATP assay

The ATP levels in T_{84} monolayers were measured using a commercially available kit as per the manufacturers' instructions. T_{84} cells were cultured as described in Section 2–2. Following treatment (DMOG 1 mM; 0–24 hours) cells were washed twice in ice-cold PBS. Cells cultured on 0.6 cm^2 inserts were then lysed on ice in 200 µl of hypotonic lysis buffer (Table 2-19), before being frozen *in situ* at -80°C until use. The assay uses recombinant luciferase to catalyze the following reaction:

$$\text{ATP} + \text{D-luciferin} + O_2 \rightarrow \text{oxyluciferin} + \text{AMP} + \text{PPi} + CO_2 + \text{light (560 nm)}$$

A 1/200 dilution of samples was made prior to analysis. An equal volume of diluted sample and substrate were mixed in a black 96-well plate and luminescence was detected. Protein content was also measured (Section 2–6) and results were expressed as nmol ATP per µg protein.

Table 2–19 Hypotonic Lysis Buffer

Component	Concentration
Tris base	100 mM
EDTA	2 mM
Acetic acid	As required to bring to pH 7.75

2-20 Meso scale discovery (MSD) assay

The MSD electro-chemiluminescence technology uses SULFO-TAG™ labels which emit light upon electrochemical stimulation at an electrode surface. The electrode is located at the base of the well of a 96-well plate. The antibody of interest (HIF-1α and HIF-2α) was purchased from MSD pre-adsorbed to the base of the well. The wells were blocked with 3 % Blocker A (MSD catalogue number R93AA-1) for 1 hour at room temperature. Wells were then washed x 3 with PBS + 0.05 % tween 20 (PBS-T). Lysate (25 μl) was then added to each well for 1 hour at room temperature with horizontal rotation. The wells were once again washed x 3 with PBS-T. Detection antibody (1 μg/ml labelled HIF-2α antibody + 10 nM labelled HIF-1α antibody in 1% Blocker A in PBS-T + 0.2 % IgG) was then added for 1 hour, and the plate was again washed x 3 in PBS-T. A detection buffer (Read buffer) which contains reactants that allow for amplification of the signal emitted by the labelled antibody was then added to the wells. A voltage was applied and the tags emit light to indicate the presence of substrate. The MSD assay platform utilises ruthenium (II) tris-bipyridine-(4-methylsulfone) [$Ru(bpy)_3$] that, once conjugated to the analyte, serves as the tracer in competitive assays. The $Ru(bpy)_3$-based tag undergoes a rapid redox reaction that emits light in the presence of an applied voltage. Only label bound in proximity of the electrode is detected and the plates are read at 620 nm in a Mesoscale Sector® Imager 2400 (Figure 2–7).

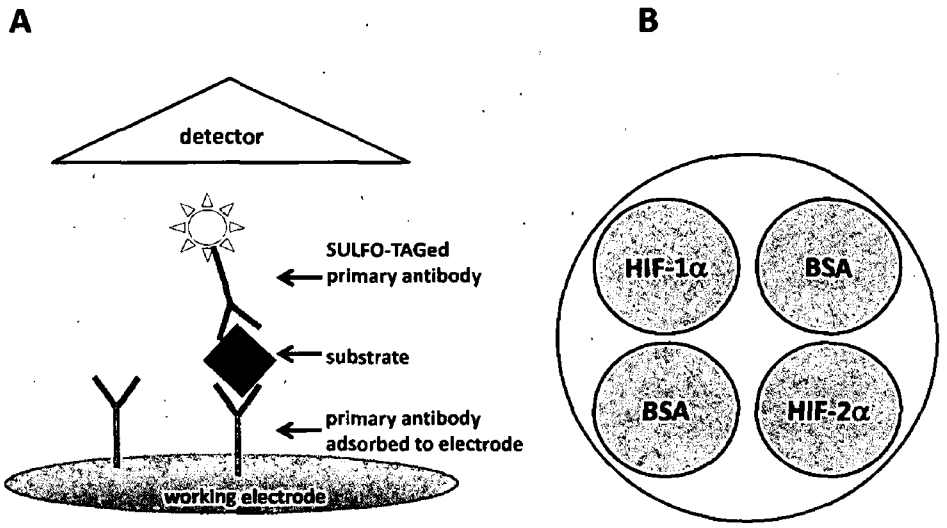

Figure 2–7 Schematic representation of meso scale discovery (MSD) assay.

A) Antibodies are adsorbed to the electrode, after which substrate binds. Labelled antibody is then loaded and light is emitted once an electrical current received from the electrode stimulates the tag. **B)** The format used in these experiments was the 96 well 4-spot format, from which multiple analytes can be measured from the same well. BSA was used as a loading control and standard curves were created with known concentrations of recombinant HIF-1α and HIF-2α.

2-21 siRNA

siRNAs are double stranded RNAs with 2 nucleotide-long 3' overhangs. Once they enter the cell they form a ribo-nuceloprotein complex called RNA induced silencing complex (RISC). RISC separates the double stranded siRNA, by argonaute 2 cleaving the sense strand. RISC and the antisense-strand then bind to the target sense strand mRNA. Slicer protein, part of RISC, then cleaves the target mRNA which is then degraded by the cell (Figure 2–8). siRNAs were purchased from Ambion. NeoFX transfection reagent was used to transfect cells as per the manufacturer's protocol. The optimum conditions for negative control transfection were 30 nM siRNA, using 4 % transfection reagent for 24

hours. This was assessed by analysis the FAM-labelled negative control siRNA by immunofluorescence as outlined in Section 2–23. The perinuclear staining indicative of successful transfection was present for 24 hours but had dissipated by 3 days.

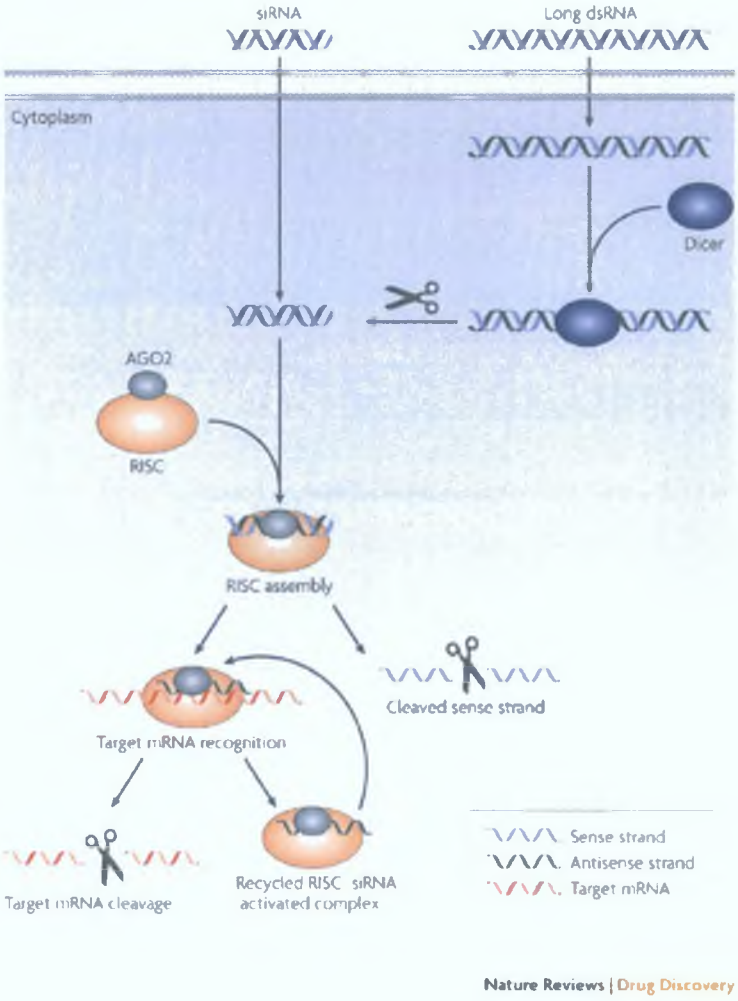

Figure 2-2 Mechanism of RNA interference and gene expression knockdown. siRNAs enter the cell and associate with RISC. The sense-strand of the siRNA is cleaved, and the RISC-siRNA anti-sense strand then binds to and cleaves target mRNA, thus silencing the target gene. This figure was adapted from (Whitehead *et al.*, 2009).

2-22 Crypt of Lieberkühn isolation

There are several methods by which colonic crypts may be isolated (Wildrick *et al.*, 1997). The approach employed in these studies used a combination of Ca^{2+} chelation and mechanical perturbation techniques. Colons from mice and rats were transported to the laboratory in ice-cold physiological solution (Table 2–3, Table 2–20). Human resected colonic tissue was transported to the lab from the Pathology Department at Beaumont hospital. This tissue was removed proximal to the resection margin and was determined by the pathologist to be normal. Tissues were cleaned of any debris using ice-cold Krebs Heinsleit solution (Table 2–20), and were then cut longitudinally and laterally into several pieces, and placed in crypt isolation buffer (Table 2–21) for 20 minutes at room temperature. The tissue was then vortexed vigorously for 1 minute to release the crypts, after which the tissue pieces were discarded. Crypts were then centrifuged at 600 x g at room temperature for 3 minutes. The supernatant was removed and the crypts were re-suspended in room temperature Krebs Heinsleit solution (Table 2–20), before centrifuging at 600 x g at room temperature for a further 3 minutes. The supernatant was again decanted, and the isolated crypts were re-suspended in 1 ml of PBS. Crypts were visualised at 40 x magnification under a light microscope to confirm isolation and integrity (Figure 2–9). Isolated crypts were then attached to chamber slides using Cell-Tak™ (Section 2–22), washed with PBS, and once again visualised to ensure attachment. The crypts were then fixed in 100 % ice-cold methanol for 20 minutes. Crypts were then stained as per the confocal microscopy protocol detailed in Section 2–23.

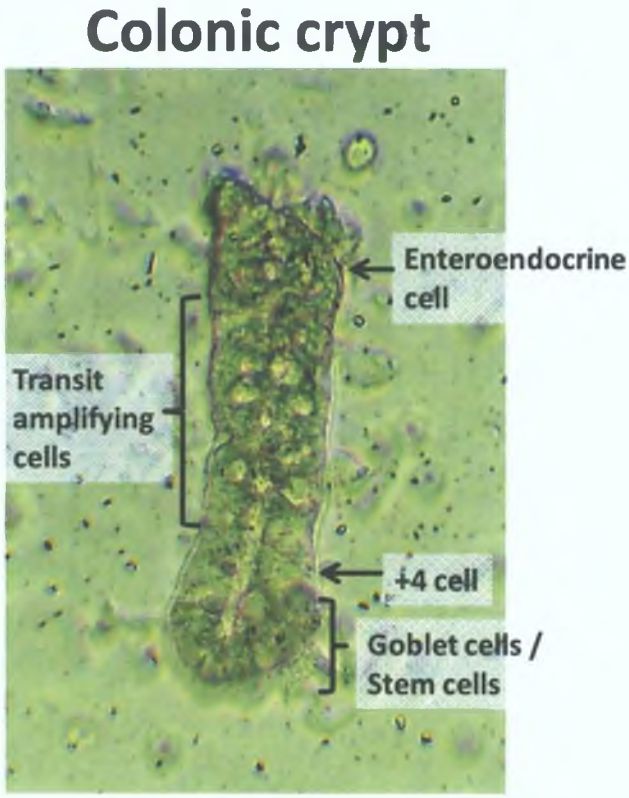

Figure 2–9 An isolated rat colonic crypt. Following isolation, colonic crypts were visualised using 40 x magnification under a light microscope. The different cell types indicated are approximate in location and were adapted from previously published studies (Barker *et al.*, 2009).

Table 2–20 Crypt isolation buffer. This buffer is Ca^{2+} and Mg^{2+}-free and contains Ca^{2+} chelators that serve to dislodge crypts from their basement membranes. Sorbitol and sucrose aid in the sedimentation of the crypts. DTT was used to dissolve mucus and was added freshly to the crypt isolation buffer each day as it is unstable in solution. The pH was adjusted to 7.4 by the addition of NaOH, and the osmolarity was 380 ± 5 mOsms.

Component	Concentration (mM)
NaCl	96
KCl	1.5
EDTA	27
Sorbitol	55
HEPES free acid	10
Tris base	10
Sucrose	44
DTT	1

Table 2–21 Krebs-Heinsleit solution. The Krebs-Heinsleit solution was adjusted to pH 7.4 by the addition of HCl and the osmolarity was recorded as 290 ± 5 mOsm.

Component	Concentration (mM)
NaCl	140
KCl	5
$MgCl_2.6H_2O$	1
$CaCl_2.2H_2O$	2
HEPES free acid	10
Tris base	10
D-glucose	10

2-23 Slide preparation with Cell-Tak™

Chamber slides were used to visualise isolated colonic crypts. However, the slides had to be first prepared with Cell-Tak™, a protein solution that immobilises cells and tissue. Each well of the chamber slide was coated with 200 µl of Cell-Tak™ solution (Table 2–22). Cell-Tak™ was allowed to adhere to the slides for at least 40 minutes before being aspirated. Wells were then washed thrice with de-ionised water, air dried, and stored at 2–8°C for 10–14 days until use.

Table 2–22 Cell-Tak™ preparation. Cell-Tak™ was prepared in order to add approximately 50 µg per chamber. The solution was prepared fresh and NaOH was only added immediately before use since Cell-Tak™ is unstable at basic pH ranges for long periods.

Component	Quantity (µl)
Cell-Tak™	6
NaOH (1 M)	3
$NaHCO_3$ (0.1 M; pH8)	191

2-24 Confocal microscopy.

Laser scanning confocal microscopy is a widely used technique, employed to visualise deep within specimens. It allows for the control of depth of field, the elimination of out-of-focus information, and the ability to collect serial optical sections from specimens whose thickness exceeds the immediate plane of focus. Light emitted from the laser passes through a pinhole aperture, and via a dichroic mirror, focuses a scanning point on the specimen. The fluorescence of the excited probe in the specimen is passed back through the dichroic mirror and focussed as a confocal point at the detector pinhole aperture. Any out of focus light is omitted from the image. Samples are scanned and pixel information is composed to form an image.

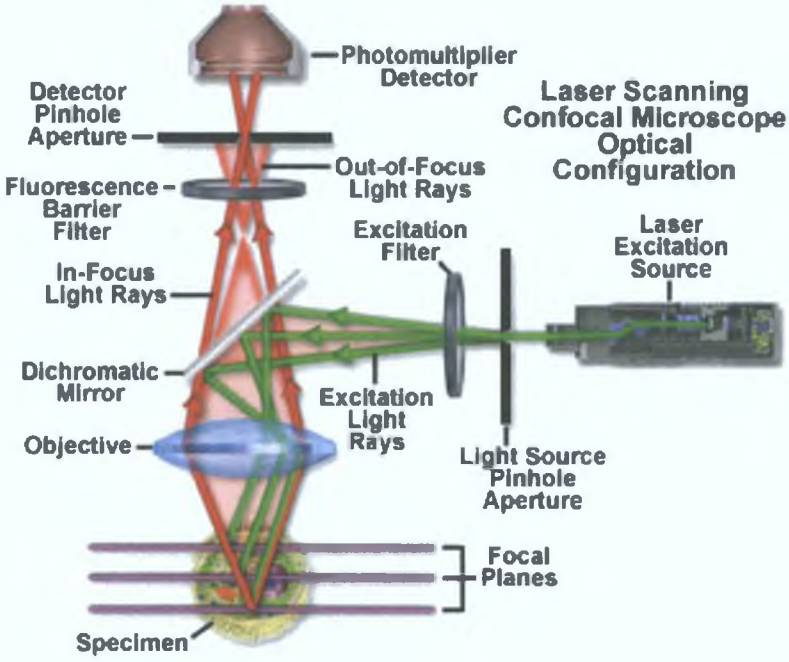

Figure 2–10 Schematic representation of a confocal laser scanning microscope. A confocal microscope is composed of multiple laser sources, a scan head with optical and electronic components, detectors, and a computer. This image was downloaded from the Carl-Zeiss Inc. website.

T_{84} cells for confocal imaging were grown on transparent permeable supports as described in Section 2–2. After treatment cells were washed thrice in ice-cold PBS. Both T_{84} cells and isolated colonic crypts (Section 2–21) were fixed on ice for 20 minutes with ice-cold methanol (100 %), washed thrice x 5 minutes, and permeabilised in Triton X-100 (0.4 %) for 3 minutes at room temperature. After a further 3 x 5 minute washes in PBS, non-specific binding was blocked with 10 % BSA in PBS for 15 minutes at room temperature. Cells or crypts were then incubated with the appropriate primary antibodies diluted in 5 % BSA in PBS for 2 hours at room temperature. Table 2–23 describes the optimal dilutions of antibodies used in these studies. Following 3 x 5 minute washes in PBS, cells or crypts were incubated with appropriate Alexa Fluor ® secondary antibodies, as detailed in Table 2–23, for 30 minutes in the dark at room temperature. Cells and crypts were washed a further 3 x 10 minutes in PBS. In the case of T_{84} cells, membranes were cut out of the hanging inserts and air dried, and mounted apical-side-up on glass slides. All preparations were then stained with hard-set Vectashield ® containing DAPI for nuclear detection. A cover-slip was gently placed over the sample and the slides were then dried in the dark at room temperature for at least 30 minutes, followed by overnight storage at 2–8°C. Confocal analyses were carried out using laser scanning microscopes (LSM) 710 and LSM 510 Zeiss microscopes. Negative controls for each of the Alexa Fluor ®-conjugated secondary antibodies used were incorporated into the experimental design, whereby confocal staining was performed in the absence of primary antibody (Figure 2–11). The capture settings of the microscope were then calibrated to this negative control, so that any signal could be confirmed to be due to binding of the primary antibody, and not due to non-specific binding of the secondary antibody, or auto-fluorescence.

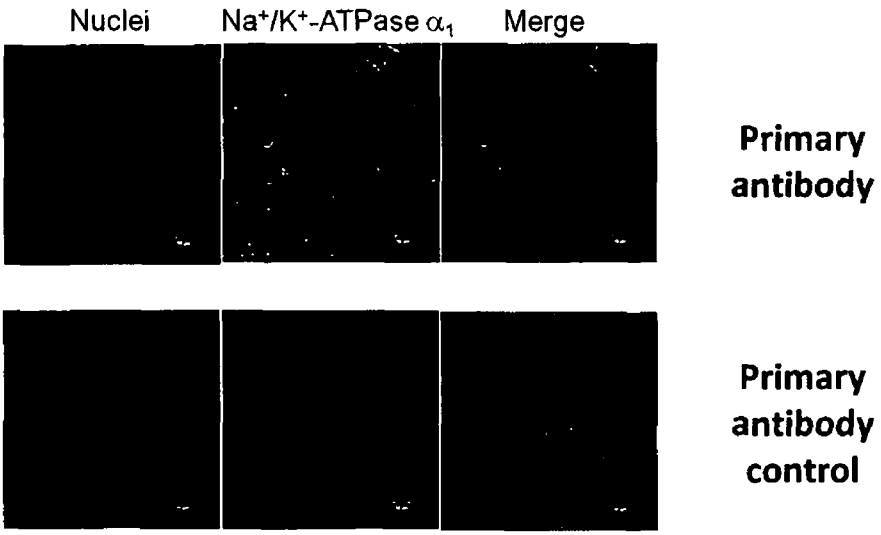

Figure 2–11 Antibody control for immunohistochemical studies. T_{84} cells were cultured as monolayers on permeable supports until R_{te} stabilised at plateau levels. Cells were washed in PBS, fixed in 100 % methanol, permeabilised with Triton X-100, and then treated with DAPI and anti-Na^+/K^+-ATPase α_1 antibodies, or BSA alone, followed by secondary rabbit anti-mouse Alexa Fluor 488. Pseudo-colours were assigned to the various fluorophores, with Na^+/K^+-ATPase α_1 being represented in green and nuclei in blue.

Table 2-3 Antibodies used for immunohistochemical studies. Conditions detailed below were optimised for use with T_{84} cells in the current studies.

Protein	Primary antibody source	Incubation time (mins)	Dilution factor	Secondary antibody source	Cat number	Species reactivity	Excitation λ (nm)	Emission λ (nm)	Incubation time (mins)	Dilution factor
F-actin	Sigma	120	1/2000	-	P1951	-	551	573	-	-
FIH-1	Santa Cruz	120	1/1000	Molecular Probes	A11079	rabbit anti goat Alexa 568	576	603	30	1/500
KCNQ1	Sigma	120	1/2000	Molecular Probes	A1108	goat anti rabbit Alexa 488	493	520	30	1/500
MONaKA	Santa Cruz	120	1/100	Molecular Probes	A11079	rabbit anti goat Alexa 568	576	603	30	1/500
Na^+/K^+-ATPase α_1	Abcam	120	1/400	Molecular Probes	A21204	rabbit anti mouse Alexa 488	493	520	30	1/500
Na^+/K^+-ATPase β_1	Abcam	120	1/400	Molecular Probes	A21204	rabbit anti mouse Alexa 488	493	520	30	1/500
NKCC1	Santa Cruz	120	1/500	Molecular Probes	A11078	rabbit anti goat Alexa 488	493	520	30	1/500

2-25 Statistical analysis.

All results are expressed as mean ± standard error of the mean (SEM) for a series of *n* experiments. Statistical analyses were performed using GraphPad Instat software, by paired t-test for comparisons of paired treatments between 2 groups, unpaired t-tests for comparisons of unpaired treatments between 2 groups, and one way ANOVA using Tukey multiple comparisons test for treatments of 3 groups or more. p values ≤ 0.05 were considered to be significant.

2-26 Materials.

Ambion, TX, USA: DNase I; Neo FX siRNA.

Antibodies: All antibody sources are indicated in Table 2–14 and Table 2–23.

BD Biosciences, NJ, USA: BD CELL-TAK™.

Calbiochem, Darmstadt, Germany: Bisindolylmaleimide I, BMS-345541.

Cayman, Frankfurt, Germany: DMOG.

FibroGen Inc., CA, USA: FG4497.

GE Healthcare, UK: PVDF membrane.

New England Biolabs, Inc., UK: 100bp DNA ladder, 1kb DNA ladder.

Pierce, IL, USA: Sulfo-NHS-biotin, spin columns.

Promega, WI, USA: Improm II reverse transcriptase kit; ENLITEN® ATP Assay.

Qiagen, Hilden, Germany: Qiagen RNeasy Mini Kit, RNA later.

Roche, Basel, Switzerland: Nonidet P40.

Sigma Aldrich, Wicklow, Ireland: All chemicals, kits and reagents, unless otherwise stated.

Thermo Scientific, IL, USA: *Lab-Tek™* Chamber Slide™ System, HyClone bovine calf serum, Restore™ western blot stripping buffer.

Tocris, Bristol, UK: H89, 4-phenylbutyrate.

Vector Laboratories, CA, USA: VECTASHIELD HardSet Mounting Medium with DAPI.

Chapter 3

Hydroxylases regulate intestinal epithelial ion transport

3-1 Introduction

One of the primary functions of the intestinal epithelium is to transport electrolytes and fluids across the epithelium. Intestinal fluid movement is driven by osmotic gradients that are, in turn, established by active ion transport across the epithelium. Fluid absorption normally predominates and is promoted by Na^+ absorption, while fluid secretion is driven by Cl^- secretion.

All epithelial transport, whether it is absorption or secretion, is highly dependent on the availability of O_2 for generation of cellular energy (Mandel and Balaban, 1981; Durand *et al.*, 1988; Carra *et al.*, 2011). HIF hydroxylases are the primary intracellular sensors of O_2 availability (Epstein *et al.*, 2001; Bruick and McKnight, 2001; Metzen and Ratcliffe, 2004). They are enzymatically active in the presence of sufficient α-ketoglutarate, Fe II, ascorbate, and O_2 which they use to hydroxylate target proteins. The 3 HIF prolyl hydroxylase enzymes (PHD1–3) and 1 HIF asparaginyl hydroxylase, known as Factor Inhibiting HIF (FIH-1), hydroxylate HIF-1α at prolines 402 and 564 and asparagine 803, respectively (Mahon *et al.*, 2001; Lando *et al.*, 2002a). Proline hydroxylation targets HIF-1α and HIF-2α for degradation via interaction with pVHL, whereas asparagine hydroxylation inhibits the binding of the p300/CBP transcriptional co-activator proteins to HIF-1α, thus inhibiting HIF-1 transcriptional activity.

Acute hypoxia has been shown to affect intestinal electrogenic transport, and although chronic hypobaric hypoxia is known to have whole-body physiological implications in those living at higher altitudes, there are few studies relating to the effects of chronic hypoxia in the intestine (Saravi *et al.*, 1996; Chinn and Hannon, 1969). Recent studies have implicated HIF-1 and HIF hydroxylases as being important regulators of intestinal epithelial barrier function. These studies have shown that increased HIF activation in the colon was protective against the onset of chemically-induced colitis in mouse models (Karhausen *et al.*, 2004; Cummins *et al.*, 2008; Robinson *et al.*, 2008). Our collaborators, and

others have shown that hydroxylase inhibition was protective against colitis, by inhibiting apoptosis associated with the onset of disease, and by activating HIF-1 and NFκB pathways (Robinson *et al.*, 2008; Cummins *et al.*, 2008). More recently our collaborators have identified that the anti-apoptotic effect of hydroxylase inhibition is PHD1-dependent (Tambuwala *et al.*, 2010). Both the HIF and NFκB pathways are associated with protective roles in intestinal epithelial cells, as shown using conditional intestinal epithelial cell knockout mice for HIF-1α and IKKβ, respectively (Karhausen *et al.*, 2004; Greten *et al.*, 2004; Chen *et al.*, 2003). PHD inhibition has been investigated in other systems for exploitation of its therapeutic potential and has been shown: A) to be protective against post-ischemic cardiac injury via induction of the unfolded protein response (UPR) (Natarajan *et al.*, 2009), B) to delay neuronal cell death caused by trophic factor deprivation (Lomb *et al.*, 2007), and C) to be beneficial in the treatment of anaemia (Muchnik and Kaplan, 2011). PHD inhibition has also been hypothesised to have beneficial effects in disease conditions, such as stroke (Ratan *et al.*, 2004).

With these previous studies in mind, we hypothesised that HIF-hydroxylases might also be useful targets for development of new therapies for intestinal disorders associated with dysregulated fluid and electrolyte transport. However, little was known of the role that hydroxylases play in the regulation of intestinal epithelial transport function.

3-2 Aim

Based on the hypothesis that HIF-hydroxylases may be important regulators of intestinal fluid and electrolyte transport, the main aim of this chapter was to investigate their potential role in regulating epithelial secretory function *in vitro* and *in vivo* (Cummins *et al.*, 2008; Robinson *et al.*, 2008).

More specifically, the primary aims of the chapter were:

1. To determine the effects of hydroxylase inhibition on intestinal epithelial Cl^- secretion in *in vitro* and *in vivo* models.
2. To test the efficacy of hydroxylase inhibitors in preventing diarrhoea *in vivo*.
3. To investigate the effects of hydroxylase inhibition on intestinal absorptive processes.

3-3 Results

3-3.1 HIF hydroxylase inhibition increases HIF-1α expression in T_{84} cells

Previous studies have shown that although individual PHD isoforms differ in the relative abundance of their mRNA, all 3 show a ubiquitous pattern of expression across various tissues. PHD2 has been found to be expressed in all tissues examined, PHD1 is expressed most highly in the testes, and PHD3 in the heart (Fong and Takeda, 2008; Lieb *et al.*, 2002; Willam *et al.*, 2006). As a starting point for these studies, expression of the HIF prolyl hydroxylase isoforms in T_{84} cells was examined. Using primer sequences modified from those previously published, mRNA expression of the 3 HIF prolyl hydroxylases (PHD1–3) was analysed by semi-quantitative RT-PCR (Demidenko *et al.*, 2005). In agreement with previous studies in mouse colonic epithelium, all three HIF PHDs were found to be expressed at the mRNA level in T_{84} cells (Figure 3–1) (Robinson *et al.*, 2008).

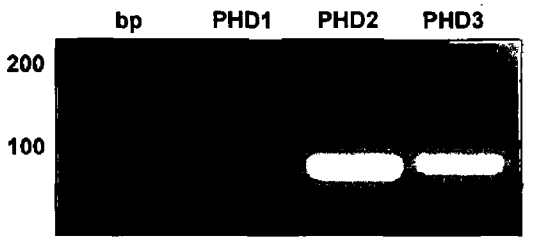

Figure 3–1 PHDs 1–3 are expressed in T_{84} colonic epithelial cells. T_{84} cells were grown on permeable supports until transepithelial electrical resistance (R_{te}) stabilised at plateau levels and total RNA was isolated. Analysis of the expression of the transcripts of PHDs 1–3 was performed by semi-quantitative reverse transcription polymerase chain reaction (RT-PCR).

In further studies the expression of PHD isoforms was also analysed following treatment of T_{84} cells with the hydroxylase inhibitor, DMOG. It was found that in line with previous findings, although PHD1 mRNA expression was unaltered by DMOG treatment (Figure 3–2 A), both PHD2 (Figure 3–2 B) and PHD3 (Figure 3–2 C) mRNA were increased (Epstein *et al.*, 2001; Berra *et al.*, 2003; Marxsen *et al.*, 2004). Interestingly, PHD3 appeared to be significantly downregulated at 3 hours, compared to 1 hour, but remained elevated thereafter.

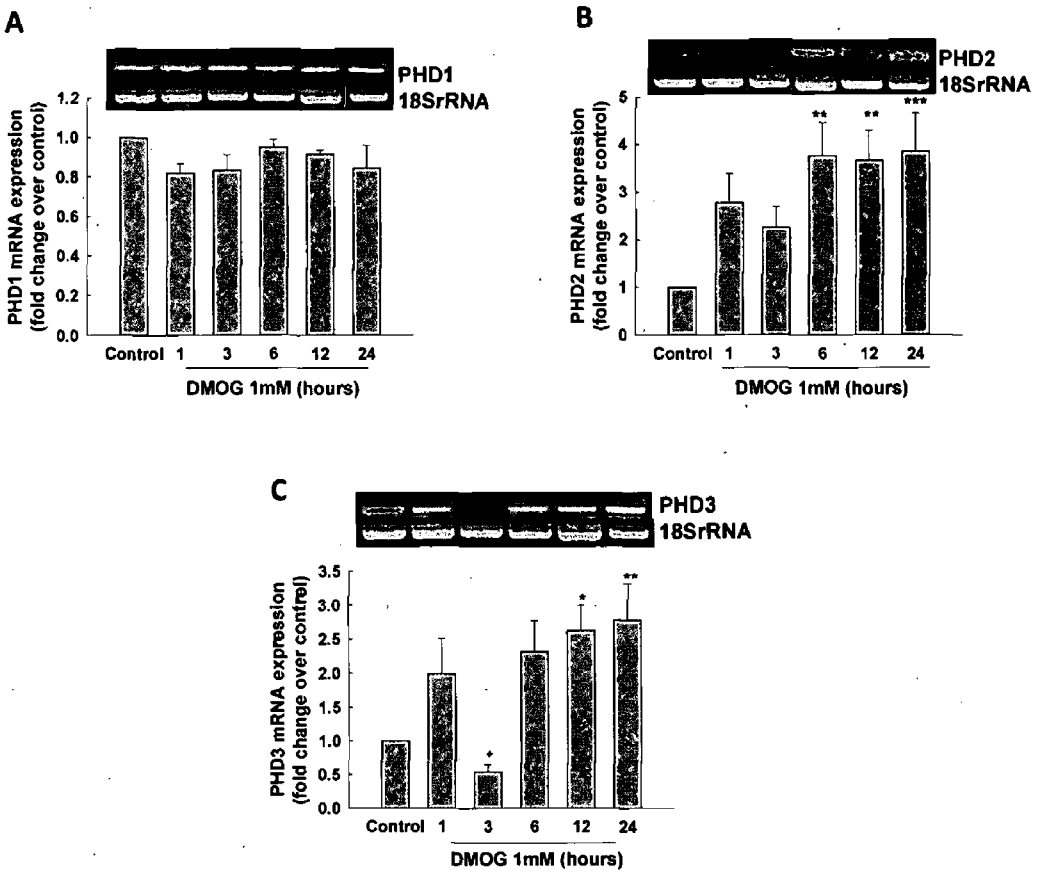

Figure 3–2 Hydroxylase inhibition increases PHD2 and PHD3 mRNA expression. T_{84} cells were grown on permeable supports until R_{te} stabilised at plateau levels. Cells were treated bilaterally with DMOG (1 mM) for various periods of time indicated above. Following this, total RNA was isolated and PHD mRNA expression was analysed by semi-quantitative RT-PCR. 18SrRNA was used as a loading control (n = 4–5; ANOVA; *$p \leq 0.05$, **$p \leq 0.01$, ***$p \leq 0.001$ compared to controls; + $p \leq 0.05$ compared to 1 hour time point).

The expression of the asparaginyl hydroxylase, FIH-1, was also investigated both at the mRNA and protein levels. Analysis of FIH-1 mRNA revealed that it is expressed in T_{84} cells but, in contrast to PHD2 and PHD3, its expression is not altered by hydroxylase inhibition (Figure 3–3 A). This was confirmed by analysis of FIH-1 protein levels in control and DMOG (1 mM; 24 hours)-treated cells (Figure 3–3 B).

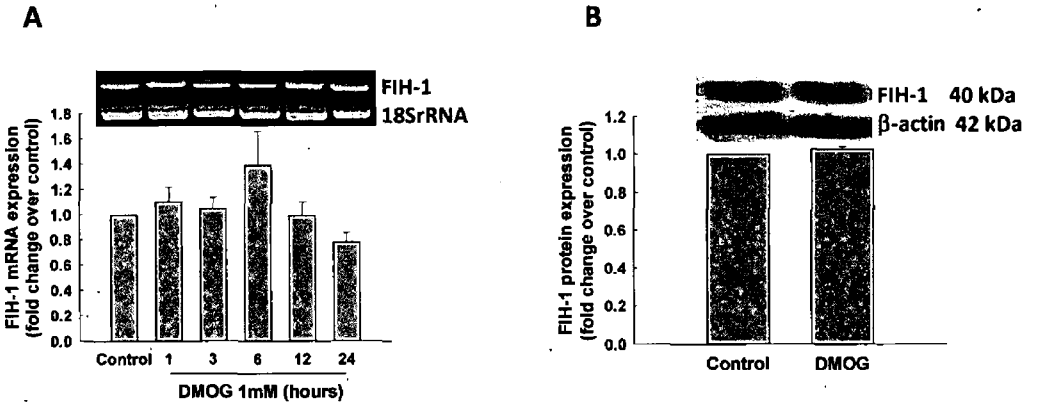

Figure 3–3 FIH-1 expression in T_{84} cells is not altered by hydroxylase inhibition. A) T_{84} cells were grown on permeable supports until R_{te} stabilised at plateau levels. Cells were treated bilaterally with DMOG (1 mM) for various periods of time indicated in panel **A**, and for 24 hours in panel **B**. Total RNA was isolated and FIH-1 mRNA expression was analysed by semi-quantitative RT-PCR. 18SrRNA was used as a loading control (n = 4). **B)** FIH-1 protein expression was analysed by western blot. β-actin was used as a loading control (n = 4).

Given their primary role in regulating cellular HIF-1α levels, it was expected that hydroxylase inhibition would increase HIF-1α expression in T_{84} cells. This was found to be the case with DMOG treatment increasing HIF-1α levels in a dose-

dependent manner as measured by western blotting (Figure 3–4). Conversely, mRNA expression of HIF-1α was significantly reduced after 24 hours treatment with DMOG (1 mM).

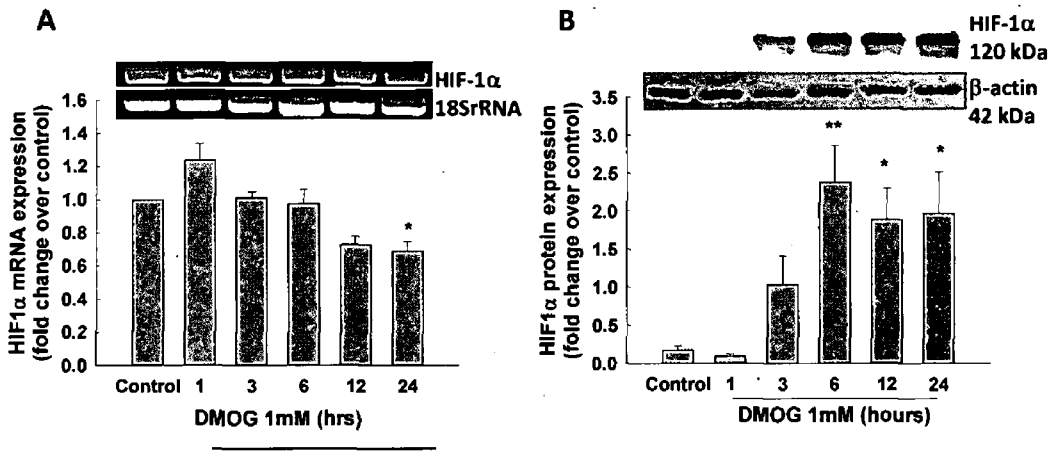

Figure 3–4 Hydroxylase inhibition increases HIF-1α protein expression, but decreases HIF-1α mRNA abundance. T_{84} cells were grown on permeable supports until R_{te} stabilised at plateau levels. Cells were treated bilaterally with DMOG (1 mM) for various periods of time indicated above, after which **A)** HIF-1α mRNA expression was measured by semi-quantitative RT-PCR. 18SrRNA was used as a loading control (n = 4; ANOVA, *$p \leq 0.05$ compared to control). **B)** HIF-1 α protein expression was measured by western blot. β-actin was used as a loading control (n = 4; ANOVA; *$p \leq 0.05$, **$p \leq 0.01$ compared to control).

HIF-α levels were also quantified in T_{84} cells using an MSD assay. T_{84} cells were cultured as monolayers on permeable supports, and were treated with DMOG (1 mM), at various concentrations, for 24 hours. Proteins were isolated, and HIF levels were quantified. Using this approach both HIF-1α and HIF-2α proteins were found to accumulate in T_{84} cells in response to DMOG-treatment, in a

concentration-dependent manner. HIF-1α protein levels were 560 ± 170 ng/ml in control cells, rising to 1194.4 ± 369.5 ng/ml following DMOG treatment, while HIF-2α protein levels were 43.4 ± 22.8 ng/ml in control cells, rising to 171.2 ± 21.5 ng/ml following DMOG treatment (Figure 3–5).

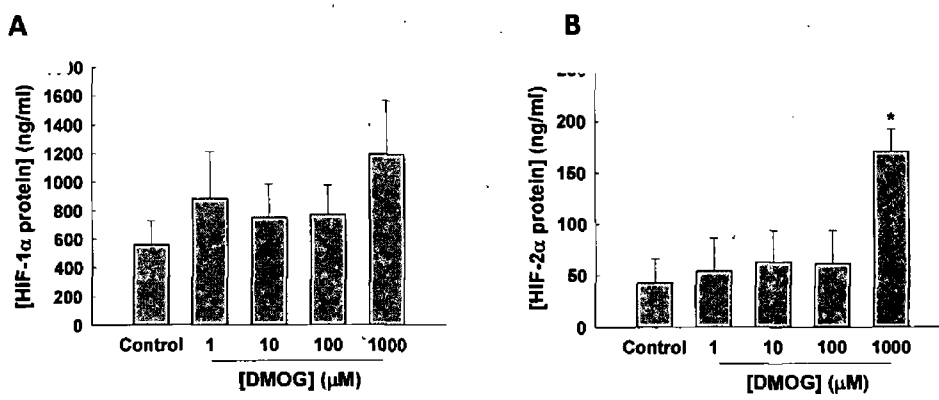

Figure 3–5 Hydroxylase inhibition by DMOG resulted in accumulation of HIF-1α and HIF-2α in T_{84} cells. T_{84} cells were grown as monolayers on permeable supports until R_{te} stabilised at plateau levels. Cells were treated bilaterally with various concentrations of DMOG in serum free medium for 24 hours, after which proteins were extracted. Concentrations of **A)** HIF-1α and **B)** HIF-2α were extrapolated from the standard curves generated for each (n = 4; ANOVA; * $p \leq 0.05$ compared to control).

Next, the possibility that DMOG may have toxic effects on T_{84} cells at the concentrations employed was examined. One of the characteristics of colonic epithelial cells is that they form electrically 'tight' monolayers. This tightness is referred to as the R_{te} and is generally high in healthy cells but is reduced in damaged cells. Thus, R_{te} can be used as a marker of epithelial cell viability. It was found that treatment of T_{84} cells with DMOG (1 mM) significantly increased R_{te} by 18.4 ± 7.1 % (n = 21 individual filters from 7 independent experiments;

paired t-test; * $p \leq 0.05$) indicating that it does not exert toxic effects on the cells (Figure 3–6 A). Another, more direct, measure of toxicity is the release of lactate dehydrogenase (LDH). In further experiments, cells were treated with DMOG (1 mM) for 3 and 24 hours, time points corresponding to when the antisecretory actions of the drug are initiated and are maximal, respectively (Figure 3–9 A). As seen in Figure 3–6 B, analysis of the culture medium in which the cells were grown, revealed that treatment with DMOG (1 mM) for either 3 or 24 hours did not cause an increase in LDH release compared to untreated control cells.

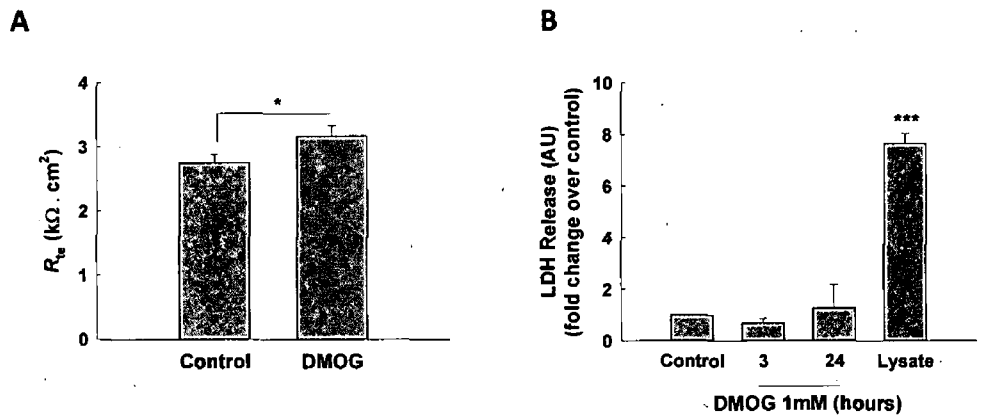

Figure 3–6 DMOG does not exert toxic actions on T_{84} cells. T_{84} cells were grown as monolayers on permeable supports until R_{te} stabilised at plateau levels. **A)** Cells were treated bilaterally with DMOG (1 mM) for 24 hours and subsequent R_{te} measurements were recorded using an epithelial voltohmeter, EVOM^2 (n = 21; * $p \leq 0.05$). **B)** Cells were treated bilaterally with DMOG (1 mM) for 3 or 24 hours. Lysate cells were treated with lysis buffer for a minimum of 30 minutes prior to analysis. An equal aliquot of apical and basolateral culture medium was taken, and LDH released into the culture medium was detected using a commercially-available assay (Section 2–16) (n = 3–6; ANOVA; *** $p \leq 0.001$ compared to control).

3-3.2 Hydroxylase inhibition attenuates Cl^- secretion across T_{84} cells

The effects of hydroxylase inhibition on epithelial secretory function were next examined. I_{sc} responses to CCh (100 μM) and FSK (10 μM) have previously been shown to be due to Cl^- secretion in T_{84} cells (Dharmsathaphorn and Pandol, 1986). It was found that treatment of T_{84} monolayers with DMOG (1 mM) for 24 hours exerted a profound antisecretory effect on the cells. When monolayers were mounted in Ussing chambers responses to the Ca^{2+}-dependent agonist, CCh (100 μM), and the cAMP-dependent agonist, FSK (10 μM) were reduced to 20.2 ± 2.6 % (n = 16; $p \leq 0.001$) and 38.8 ± 6.7 % (n = 16; $p \leq 0.001$) of those in control cells, respectively (Figure 3–7).

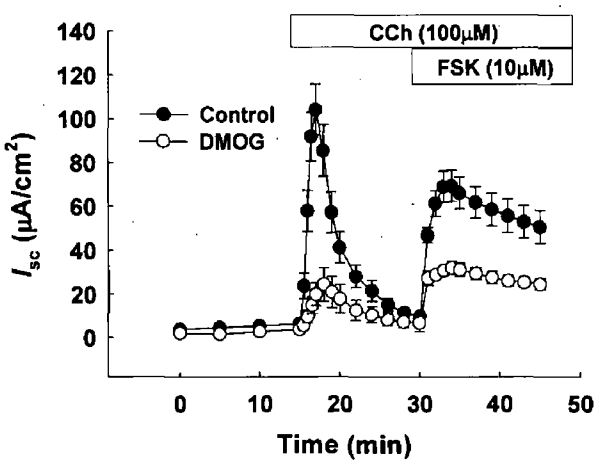

Figure 3–7 Hydroxylase inhibition attenuates Cl^- secretory responses in T_{84} cells. T_{84} cells were grown as monolayers on permeable supports until R_{te} stabilised at plateau levels. Cells were treated bilaterally with DMOG (1 mM) in serum-free medium for 24 hours. Cells were washed, mounted in Ussing chambers and bathed in Ringer's solution (Table 2–3). After an initial stabilisation period Cl^- secretory responses to CCh (100 μM) and FSK (10 μM) were measured as changes in I_{sc}.

Since DMSO was used as a vehicle for DMOG, in initial studies a 0.1 % solution of DMSO was routinely added to control cells. However, analysis of cells treated with vehicle (0.1 % DMSO) for 24 hours revealed no significant difference from those untreated, in secretory responses to CCh (100 μM) (128.99 ± 17.63 %) or FSK (10 μM) (86.79 ± 9.70 %) (n = 3–4).

Ca^{2+}-mediated Cl^- secretory responses in T_{84} cells stimulated by CCh occur following G protein-coupled receptor activation. Thus, in order to determine whether the antisecretory effect of DMOG on Ca^{2+}-mediated secretory responses occur at the level of receptor activation, thapsigargin (2 μM) was employed. Thapsigargin acts by inhibiting Ca^{2+} ATPase pumps on the sarcoplasmic and endoplasmic reticulum, thereby elevating intracellular Ca^{2+} in a receptor-independent fashion (Treiman *et al.*, 1998). As shown in Figure 3-8, thapsigargin-stimulated secretory responses were also significantly attenuated in DMOG-treated (1 mM; 24 hours) cells.

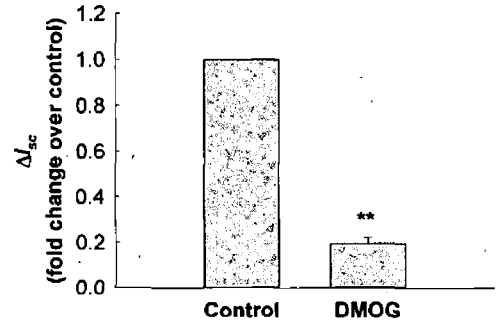

Figure 3–8 Hydroxylase inhibition attenuates thapsigargin-stimulated Cl^- secretory responses. T_{84} cells were grown as monolayers on permeable supports until R_{te} stabilised at plateau levels. T_{84} cells were treated bilaterally with DMOG (1 mM) in serum-free medium for 24 hours. Cells were then washed, mounted in Ussing chambers and bathed in Ringer's solution (Table 2–3). After an initial stabilisation period, Cl^- secretory responses to bilateral addition of thapsigargin (2 μM) were measured (n = 3; paired t-test; ** $p \leq 0.01$).

The effects of DMOG (1 mM) on agonist-induced secretory responses were time-dependent. When cells were treated with DMOG (1 mM) for several different time points, the antisecretory effects of DMOG on CCh (100 μM) and FSK (10 μM)-stimulated responses were found to be half maximal at approximately 8 hours (Figure 3–9 A). Effects of DMOG on Cl^- secretion were also found to be concentration-dependent. When cells were treated with DMOG for 24 hours, antisecretory effects were maximal at a concentration of 1 mM, the highest concentration employed (Figure 3–9 B).

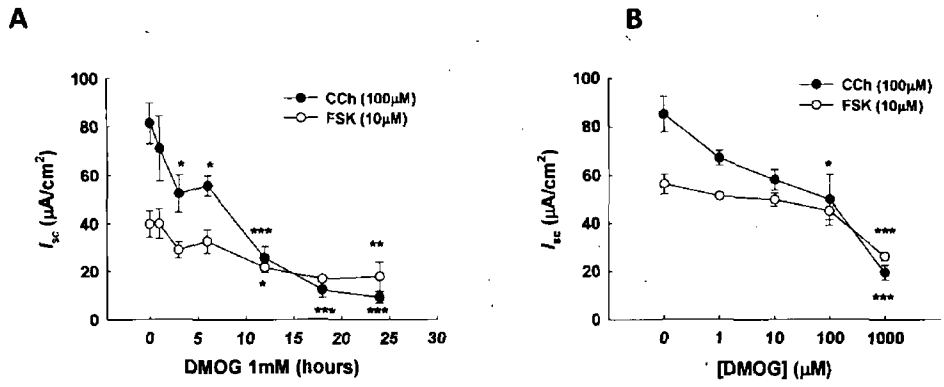

Figure 3–9 The antisecretory effects of hydroxylase inhibition in T_{84} cells are time- and concentration-dependent. T_{84} cells were grown as monolayers on permeable supports until R_{te} stabilised at plateau levels. **A)** Cells were treated bilaterally with DMOG (1 mM) in serum-free medium for various time points. Cells were then washed, mounted in Ussing chambers and bathed in Ringer's solution (Table 2–3). After an initial stabilisation period, Cl^- secretory responses to CCh (100 μM) and FSK (10 μM) were recorded (n = 3–8; ANOVA; * $p \leq 0.05$, ** $p \leq 0.01$, *** $p \leq 0.001$ compared to control). **B)** Cells were treated bilaterally with various concentrations of DMOG in serum-free medium for 24 hours, and subsequent Cl^- secretory responses to CCh (100 μM) and FSK (10 μM) were measured (n = 8; ANOVA; * $p \leq 0.05$, *** $p \leq 0.001$ compared to control).

3-3.3 DMOG does not alter secretagogue-induced generation of second messengers in T_{84} cells

There are many potential mechanisms by which DMOG could exert its antisecretory effects on the colonic epithelium. One possibility is that it alters the production of pro-secretory second messengers in the cell. Secretory responses in epithelial cells are stimulated by endogenous agonists, such as ACh and VIP, which act by increasing the abundance of intracellular second messengers, such as Ca^{2+} and cAMP. These effects can be mimicked by CCh and FSK, respectively. However, analysis of both basal and stimulated second messenger levels revealed that there were no alterations in the levels of either Ca^{2+} (Figure 3–10) or cAMP (Figure 3–11) in cells that were treated with DMOG (1 mM; 24 hours) compared to control cells.

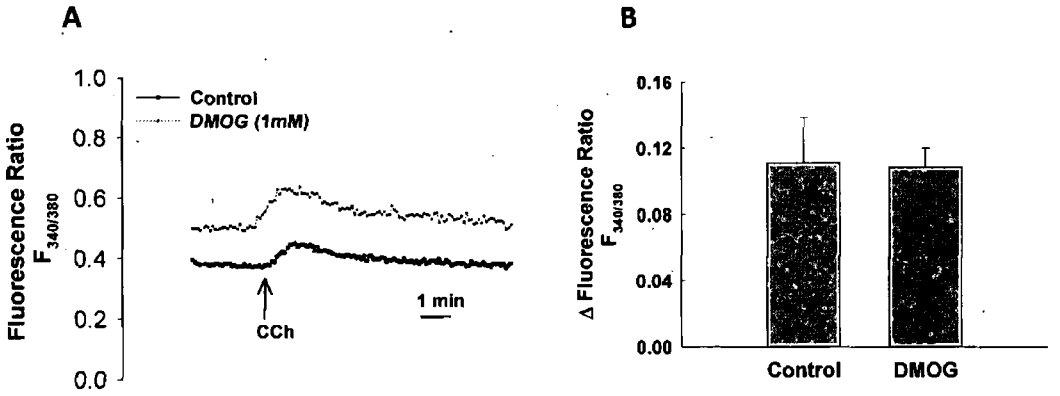

Figure 3–1 Hydroxylase inhibition does not alter CCh-stimulated Ca^{2+} mobilisation in T_{84} monolayers. T_{84} cells were cultured on glass cover slips and were treated with DMOG (1 mM) for 24 hours. Cells were then washed and loaded with the Ca^{2+}-sensitive dye Fura-2 AM. **A)** Ca^{2+} mobilisation was analysed by recording Fura-2 fluorescence at intervals of 3 seconds. Data are expressed as mean fluorescence ratio at 340 and 380 nm. **B)** Maximal changes in intracellular Ca^{2+} following stimulation with CCh (100 μM) were calculated as the maximal change in fluorescence ratio before and after agonist addition (n = 3).

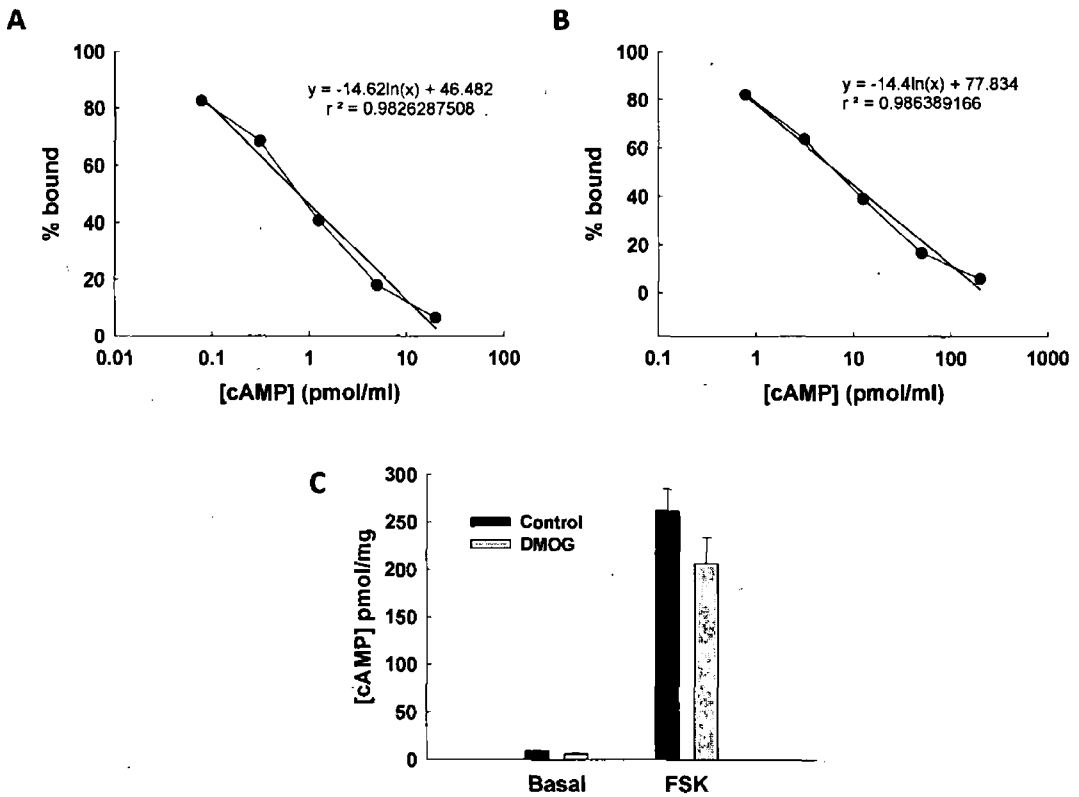

Figure 3–11 Intracellular cAMP levels are unaltered by hydroxylase inhibition. T_{84} cells were grown as monolayers on permeable supports until R_{te} stabilised at plateau levels. Cells were then treated bilaterally with DMOG (1 mM) for 24 hours. Cells were stimulated with apical FSK (10 μM) for 5 minutes, after which they were lysed in HCl (100 mM). cAMP levels were measured using a commercially available kit (Section 2–15). **A)** A standard curve was prepared for low concentrations of cAMP. **B)** A standard curve was prepared for higher concentrations of cAMP. **C)** Values are expressed as pmol cAMP per mg protein (n = 5).

3-3.4 Hydroxylase inhibition attenuates Cl^- secretion in *ex vivo* mouse colon and ameliorates allergic diarrhoea *in vivo*

Having shown that hydroxylase inhibition with DMOG exerts antisecretory actions in an *in vitro* culture model, these studies were next extended to a more physiological setting. A mouse model (C57BL/6) was chosen since this model has been successfully used by other researchers investigating the effects of HIF activation on the development of colitis. Mice were treated with DMOG (320 mg/kg) by IP injection. 24 hours later, the animals were sacrificed and their colons removed, stripped of underlying muscle layers, and mounted in Ussing chambers. Tissues were bathed in Ringer's solution (Table 2–3) and monitored for changes in I_{sc}. Each preparation was treated with apical amiloride (100 μM) prior to addition of secretagogues to prevent any contribution of ENaC to the observed I_{sc} responses. Responses to both CCh (100 μM) and FSK (10 μM) were significantly attenuated in DMOG-treated tissues (Figure 3–12). It is known that CFTR can conduct both Cl^- and HCO_3^-, therefore at the end of each experiment basolateral bumetanide (100 μM) was added to determine the Cl^--dependent portion of the I_{sc} response. Following inhibition of NKCC1, the remaining current was assumed to be predominantly apical HCO_3^- secretion, as previously reported in murine duodenum and rat colon (Clarke *et al.*, 2001; Schultheiss *et al.*, 1998).

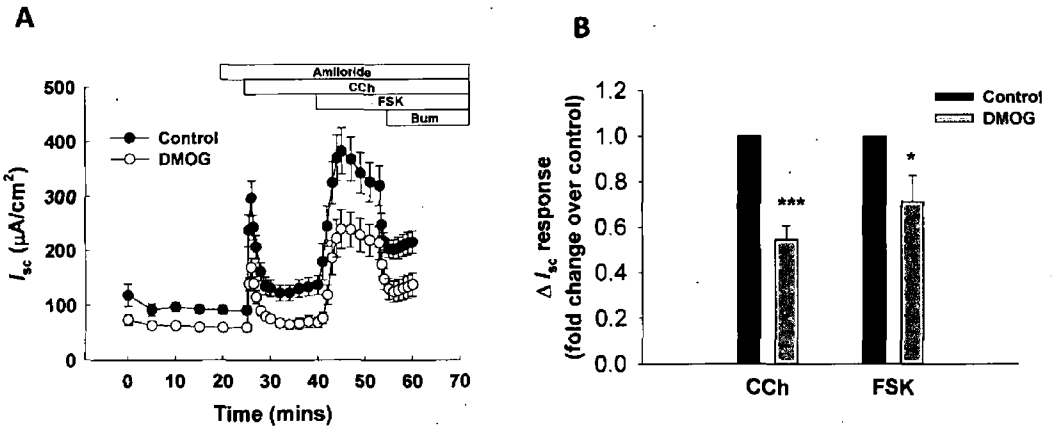

Figure 3–12 Hydroxylase inhibition exerts antisecretory effects in *ex vivo* mouse colon. Mice were treated with DMOG (320 mg/kg) or PBS by IP injection. After 24 hours, mice were sacrificed by cervical dislocation, and their colons removed. **A)** Colons were stripped of their muscularis layers by microdissection, mounted in Ussing chambers, and bathed in Ringer's solution (Table 2–3). Following a period of stabilisation, the epithelial sodium channel blocker, amiloride (100 μM), was added to the apical bath. Cl^- secretory responses were then stimulated with CCh (100 μM) and FSK (10 μM). Bumetanide (100 μM) was added basolaterally at the end of each experiment to confirm responses were largely due to Cl^- secretion. **B)** Maximal responses to CCh and FSK were plotted as fold change over control Δ I_{sc} responses (n = 11; paired t-tests; * $p \leq 0.05$, *** $p \leq 0.001$).

Having shown that hydroxylase inhibition exerts antisecretory effects in mouse colon, it was next investigated whether its effects could be translated into a pathophysiological model of diarrhoea. For these experiments an orally-induced allergic diarrhoea model was chosen, as was previously described (Brandt *et al.*, 2003). Mice were sensitised with ovalbumin (OVA) by IP injection twice, 2 weeks apart. Two weeks later, the animals were challenged orally with OVA 3 times per week and were monitored for stool output for 1 hour following oral administrations (Figure 3–13 A). Mice with profuse watery stool were recorded as being diarrhoea-positive. Mice were treated with IP DMOG (160 mg/kg) or PBS alone, 24 hours before each challenge with OVA. As seen in Figure 3–13 B, mice treated with DMOG had normal faecal pellet formation in the colon. The occurrence of diarrhoea is shown graphically in Figure 3–13 C. It was noted that after just 4 allergen challenges 100 % of mice sensitised to ovalbumin were diarrhoea-positive, whereas in those pretreated with DMOG, only 20 % displayed symptoms of diarrhoea.

A

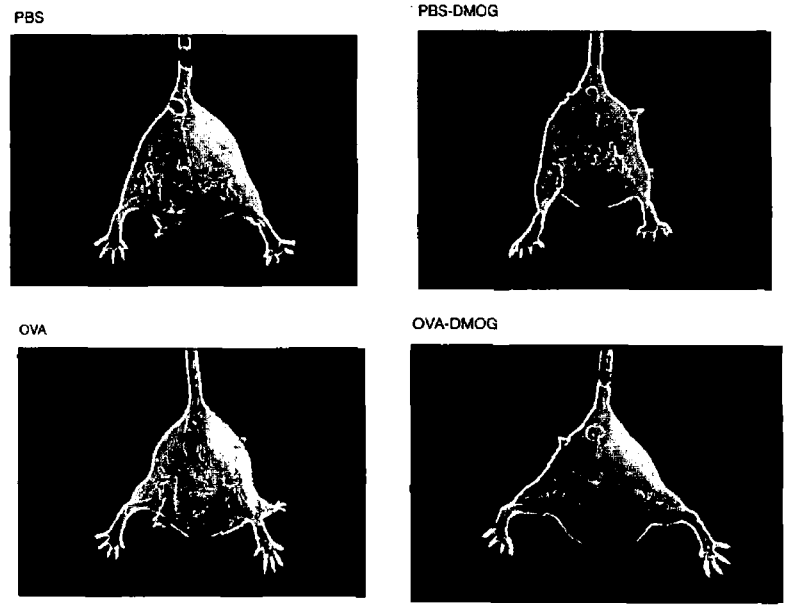

B

C

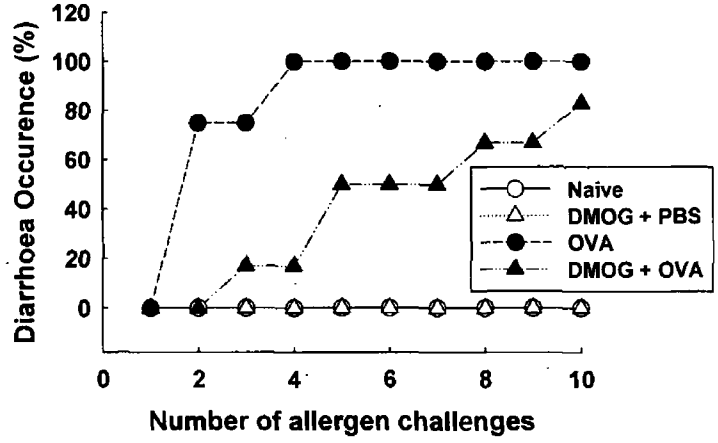

Figure 3–13 Hydroxylase inhibition ameliorates allergen-induced diarrhoea in a mouse model. Ovalbumin-sensitised mice were pre-treated with intraperitoneal DMOG (160 mg/kg) and after 24 hours were challenged by oral gavage with OVA (50 mg/mouse). Mice were treated with DMOG and OVA in this way every 2 days. **A)** Mice demonstrating profuse diarrhoea within 1 hour after OVA challenge were recorded as being diarrhoea-positive (n = 10). **B)** Colons of the mice were isolated and analysed for the presence of faecal pellet formation, indicated by the arrows. **C)** Graphical representation of the incidence of diarrhoea in the mice (n = 10).

The possibility that DMOG might exert toxic effects in the mice was also addressed by measuring serum markers of liver and kidney toxicity, ALT and creatinine, respectively. From the results of this analysis shown in Figure 3–14, it was clear that DMOG (160 mg/kg) did not exert toxic effects in either the liver or kidneys. This data was in concordance with our *in vitro* LDH data (*c.f.* Figure 3–6 B) showing that DMOG did not cause an increase in release of LDH from cultured colonic epithelial cells.

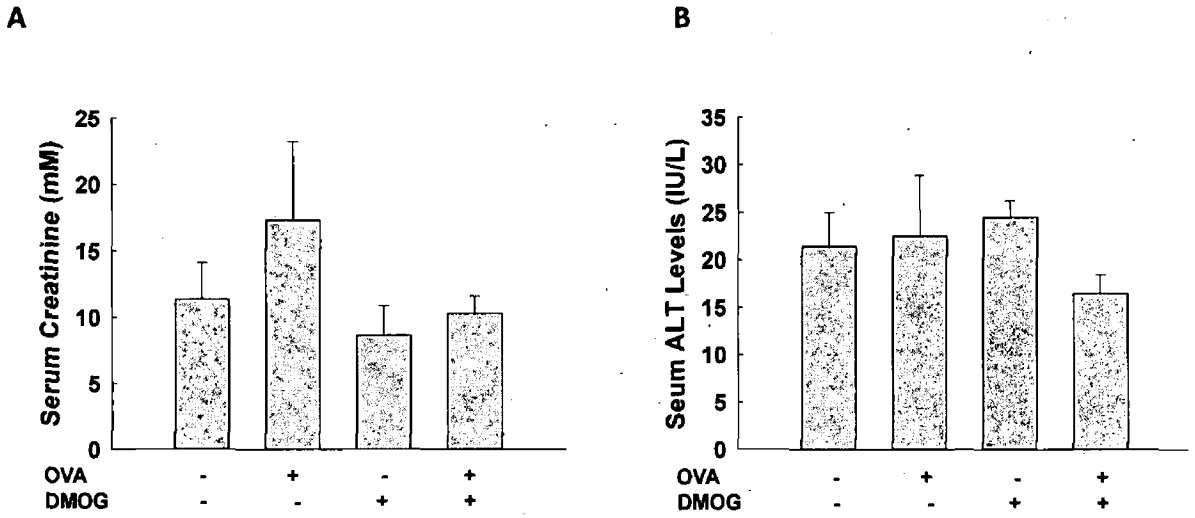

Figure 3–14 DMOG did not exert liver or kidney toxicity in mice. Mice were treated by IP injection with DMOG (160 mg/kg) for 24 hours. Blood was collected from the mice and was analysed for serum markers of kidney and liver toxicity (Sections 2–17 and 2–18). **A)** Renal toxicity was assessed by measurement of serum creatinine levels (n = 5). **B)** Hepatic toxicity was assessed by measurement of serum ALT levels and is expressed as international units per litre (IU/L) (n = 5).

In the *ex vivo* studies, mice were administered DMOG (320 mg/kg) by I.P injection using a dose that had previously been reported to increase the levels of mouse HIF-1α (mHIF-1α) in the intestine (Cummins *et al.*, 2008). However, we also carried out experiments to ensure that, at this concentration, DMOG was inhibiting hydroxylases, and in turn stabilising mHIF-1α. Indeed, it was found that there was robust accumulation of mHIF-1α following treatment with DMOG. The mHIF-1α antibody was raised in mice to detect human HIF-1α, and is cross reactive with mouse HIF-1α. It has been used previously to detect mHIF-1α (Cummins *et al.*, 2008). As a control for non-specific binding of the mouse HRP-linked secondary antibody, 2 lanes of whole tissue lysate were also run but were not exposed to primary HIF-1α antibody. It is clear from the blot that under the same exposure, there is little if any mHIF-1α present in these lanes (Figure 3–15).

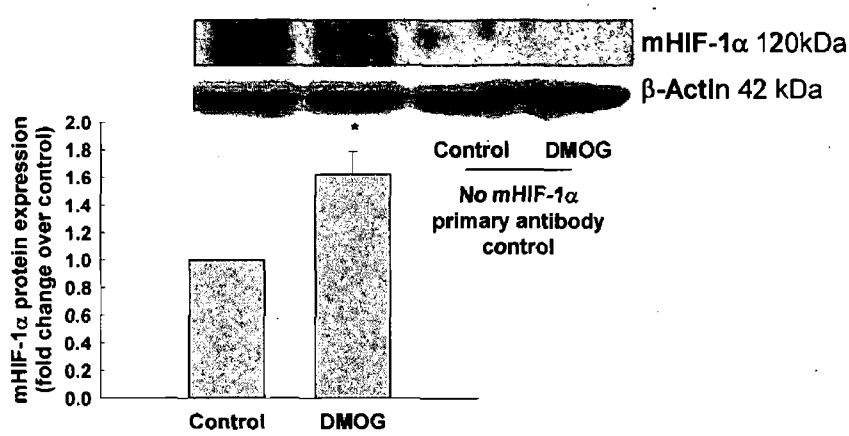

Figure 3–15 Hydroxylase inhibition stimulates accumulation of HIF-1α protein in mouse colonic tissue. Mice were treated with DMOG (320 mg/kg) by IP injection for 24 hours. Intestinal tissue was harvested and lysed. Proteins were then resolved by SDS-PAGE and probed with antibodies to mHIF-1α. The right-most 2 lanes were not treated with primary antibody. β-actin was used as a loading control (n = 4; paired t-test; * $p \leq 0.05$).

3-3.5 Hydroxylase inhibition attenuates ENaC activity in T_{84} cells

Having shown that hydroxylase inhibition exerts antisecretory actions on colonic epithelial cells, its effects on absorptive processes were next examined. T_{84} cells are a model of Cl^- secretion and do not express functional ENaC. However, a recent study (Iordache and Duszyk, 2007) has shown that short chain fatty acids can cause T_{84} cells to change their phenotype to that of an absorptive enterocyte. By treating the cells with 4-phenyl butyrate (4-PBA) (5 mM), T_{84} cells develop an amiloride-sensitive current. As shown in Figure 3–16, treatment of T_{84} cells with 4-PBA (5 mM) for 24 hours reliably induced an amiloride-sensitive current of 20.8 ± 0.5 μA/cm^2. Treatment of the cells with DMOG (1 mM; 24 hours) to inhibit hydroxylase activity significantly reduced this 4-PBA-induced basal current (n = 5; * $p \leq 0.05$).

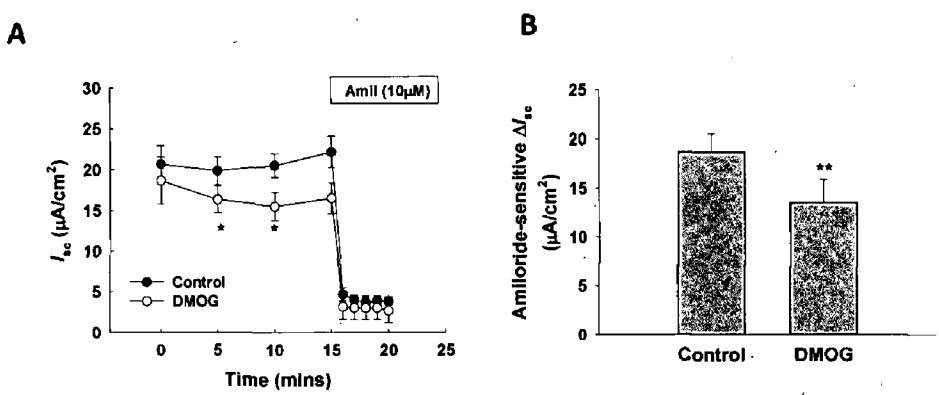

Figure 3–16 Hydroxylase inhibition attenuates ENaC-mediated Na^+ absorption in T_{84} cells. T_{84} cells were treated with 4-PBA (5 mM; 24 hours) to induce an amiloride-sensitive current. Cells were treated bilaterally with DMOG (1 mM; 24 hours) to inhibit hydroxylase activity. **A)** Cells were washed, mounted in Ussing chambers and amiloride (10 μM) was added to the apical compartment to inhibit Na^+ absorption through ENaC (n = 5; paired t tests; * $p \leq 0.05$ compared to control values of the same time point). **B)** Maximal amiloride-inhibited current was plotted as ΔI_{sc}. (n = 5; paired t test;** $p \leq 0.01$).

3-3.6 Hydroxylase inhibition attenuates ENaC activity in rat rectal tissue

Electrogenic Na^+ absorption through luminal ENaC is confined to the surface epithelium of the distal colon and it has been shown to contribute more to absorptive processes in humans and rats than it does in mice (Kunzelmann and Mall, 2002). Indeed, in C57BL/6 mice there was no detectable amiloride-sensitive current across stripped colonic tissue. Furthermore, pretreatment with DMOG (320 mg/kg) by IP injection for 24 hours did not alter the lack of sensitivity of these tissues to amiloride (Figure 3–17). The basal current shown in Figure 3–17 is composed of Cl^- and HCO_3^- secretion, and was significantly reduced in DMOG-treated tissues.

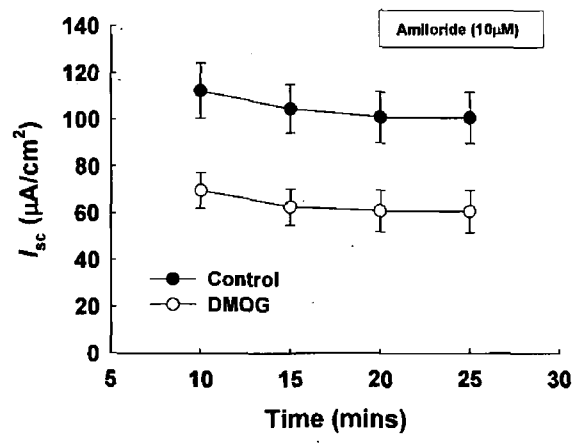

Figure 3–17 Hydroxylase inhibition did not induce or reduce an amiloride-sensitive current in the mouse colon. Mice were treated with DMOG (320 mg/kg) by IP injection for 24 hours. The colons were removed, washed in Ringer's solution, and mounted in Ussing chambers. Amiloride (10 μM) was added to the apical bath to inhibit Na^+ absorption through ENaC (n = 3–5).

In order to investigate the effects of hydroxylase inhibition on electrogenic Na^+ absorption in intact intestinal tissue, the rectum of male Sprague Dawley rats was employed. It was found that under control conditions, muscle-stripped sections of rat rectum exhibited a basal current of 40.79 ± 6.61 μA/cm^2. As previously reported this current was approximately 58 % sensitive to amiloride, indicating a large component is due to Na^+ absorption through ENaC (Inagaki *et al.*, 2004). In rats treated with DMOG (40 mg/kg by I.P injection, a concentration previously employed (Zhao *et al.*, 2010)) for 24 hours the amiloride-sensitive current was significantly lower, being 67 ± 13.3 % of that of controls (n = 6; ** $p \leq 0.01$) (Figure 3–18).

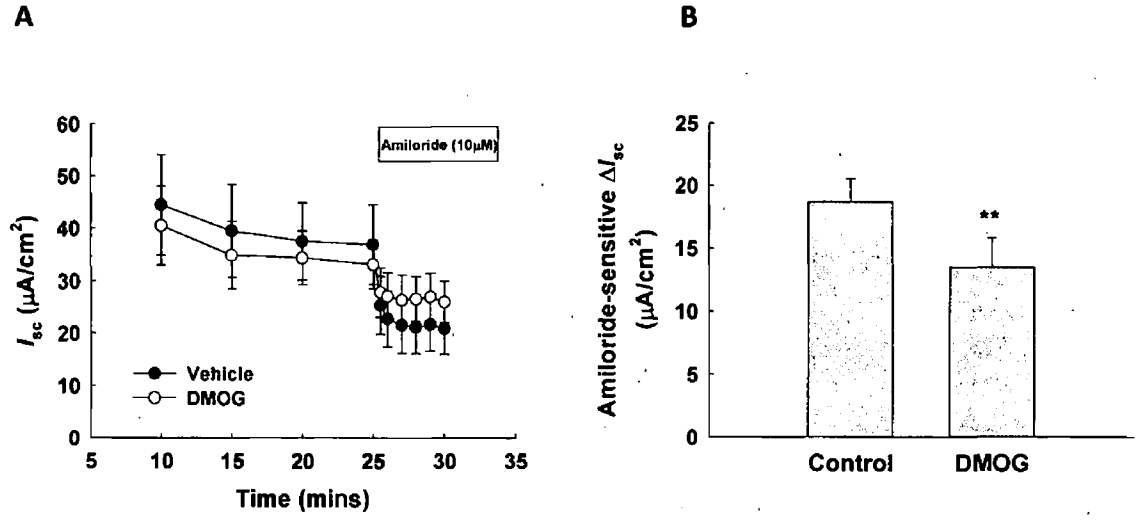

Figure 3–18. Hydroxylase inhibition attenuates Na^+ absorption through ENaC in rat rectum. Rats were treated by IP injection with DMOG (40 mg/kg) for 24 hours. **A)** Rats were sacrificed, their rectum removed, stripped of underlying muscle layers, and mounted in Ussing chambers for measurements of I_{sc}. After an initial stabilisation period, amiloride (10 μM) was added to the apical bath to inhibit Na^+ absorption through ENaC (n = 6). **B)** Maximal amiloride-sensitive current was plotted as ΔI_{sc} (n = 6; paired t test;** $p \leq 0.01$).

3-3.7 Jejunal SGLT-1 activity is unaltered by DMOG

SGLT-1 is an important transporter in the context of the jejunum (Wright *et al.*, 2011). It co-transports glucose and Na^+ from the lumen of the GI tract, with water following due to the osmotic gradients created. Mice were treated with DMOG (320 mg/kg by IP injection) for 24 hours, after which they were sacrificed and unstripped segments of jejunum were mounted in Ussing chambers. Jejunal tissues were then bathed mucosally in a mannitol-Ringer's solution (Table 2–8) and serosally in D-glucose-Ringer's solution (Table 2–9) in order to maintain apical SGLT-1 in a quiescent state. As shown in Figure 3–19 A, bumetanide (100 μM) was added to the serosal bath to inhibit Cl^- secretion into the apical compartment and thus prevent its contribution to the observed currents. SGLT-1 activity was stimulated by the mucosal addition of D-glucose (25 mM) and the SGLT-1 specific inhibitor, phloridzin (1 mM), was added after the D-glucose-stimulated current had peaked. Treatment of mice with DMOG did not alter the phloridzin-sensitive D-glucose-stimulated influx of Na^+ from the luminal compartment when compared to control tissues (Figure 3–19 B).

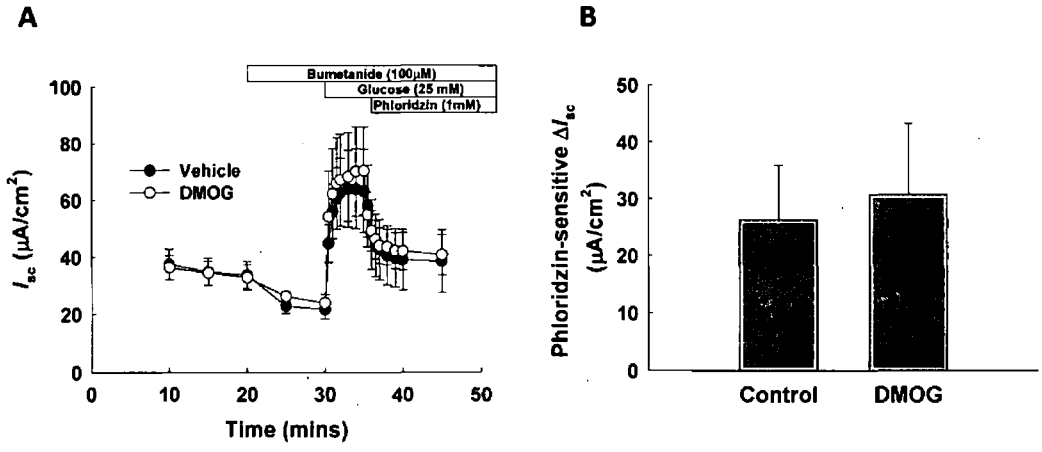

Figure 3–19 Jejunal SGLT-1 activity is unaltered by hydroxylase inhibition. A) Mice were treated with DMOG (320 mg/kg) by IP injection. 24 hours later, mice were sacrificed and their small intestine was removed. **A)** The jejunum was isolated, opened along the mesenteric boarder, rinsed in ice-cold mannitol-Ringer's solution (Table 2–8), and segments were mounted in Ussing chambers. The apical bath contained 5 mM mannitol-Ringer's solution, whereas the basolateral compartment contained 5 mM D-glucose-Ringer's (Table 2–9). The NKCC1 inhibitor, bumetanide (100 μM), was added to the basolateral bath, and SGLT-1 was stimulated by the addition of D-glucose apically (25 mM). SGLT-1 transport activity was inhibited by apical addition of phloridzin (1 mM). **B)** Maximal phloridzin-sensitive currents in control and DMOG-treated mice were plotted as ΔI_{sc} (n = 6).

3-3.8 Hydroxylase inhibition attenuates NHE activity in T_{84} cells

Having already investigated the activity of 2 of the primary Na^+ transporters, our attention next turned to the NHEs. NHE3 is responsible for the majority of Na^+ absorption in the intestine (Zachos *et al.*, 2005), therefore we wished to investigate the effect of hydroxylase inhibition on NHE activity in T_{84} cells. However, recent studies have shown that T_{84} cells do not express NHE3, but rather, they express NHE1 and NHE4 which are responsible for the maintenance of intracellular pH (Beltran *et al.*, 2008). We found that hydroxylase inhibition attenuated NHE activity in T_{84} cells, as demonstrated by their inability to return to steady-state pH following an acid-load (Figure 3–20).

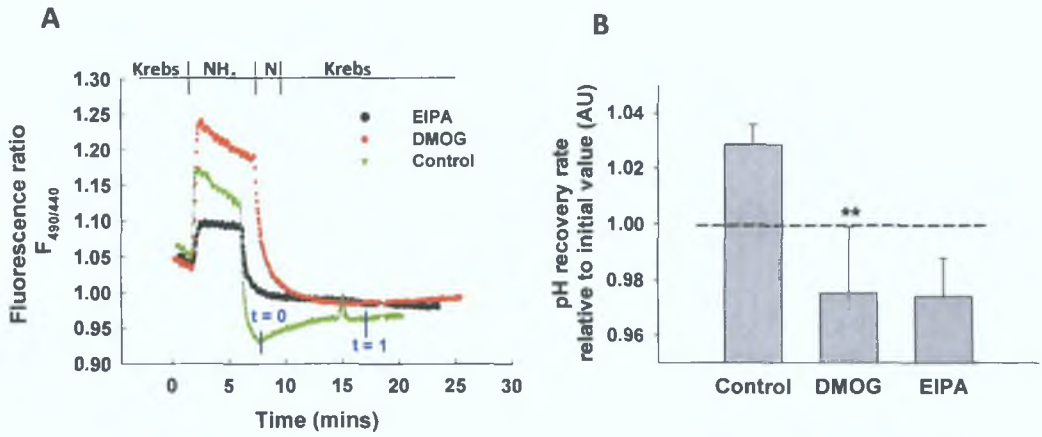

Figure 3–20 Hydroxylase inhibition attenuates NHE activity in T_{84} cells. T_{84} cells cultured on glass cover slips were treated with DMOG (1 mM; 24 hours). Cells were then washed and loaded with the pH-sensitive dye, BCECF/AM (5 μM; 60 minutes). **A)** Intracellular pH was analysed by recording BCECF fluorescence at intervals of 3 seconds. Cells were perfused with modified Krebs, followed by NH_4 Krebs, followed by NMDG-Cl^- Krebs (indicated by N), and finally returned to modified Krebs for the duration of the experiment (Table 2–15). Data are expressed as mean fluorescence ratio at 490 and 440 nm. **B)** NHE activity was recorded as the rate of change in pH back to steady state following an acid load which occurs following removal of NH_4 (n = 10; paired t-test; ** $p \leq 0.01$ compared to control) (*c.f.* Section 2–10). As a positive control, cells were treated with EIPA (25 μM) to inhibit NHE activity (n = 2).

Having shown that hydroxylase inhibition attenuates NHE activity, we next wished to investigate whether NHE inhibition, using the NHE-specific inhibitor EIPA, alters epithelial secretory responses. Since chronic exposure to hydroxylase inhibitors exerts antisecretory effects in T_{84} cells, we hypothesised that chronic exposure to the NHE inhibitor, EIPA, might have similar effects. However, we found that Cl^- secretory responses from T_{84} cells treated with EIPA

(25 μM; 24 hours; bilateral) alone were unaltered compared to controls (data not shown). Similarly, addition of EIPA (25 μM) bilaterally to control T_{84} cells in Ussing chambers was without effect on Cl^- secretion. However, co-treatment of T_{84} cells with EIPA (25 μM; 24 hours; bilateral) and DMOG (1 mM; 24 hours; bilateral), reversed the antisecretory effects of the hydroxylase inhibitor (Figure 3–21). This effect was not seen upon addition of EIPA (25 μM) to DMOG-treated cells in Ussing chambers.

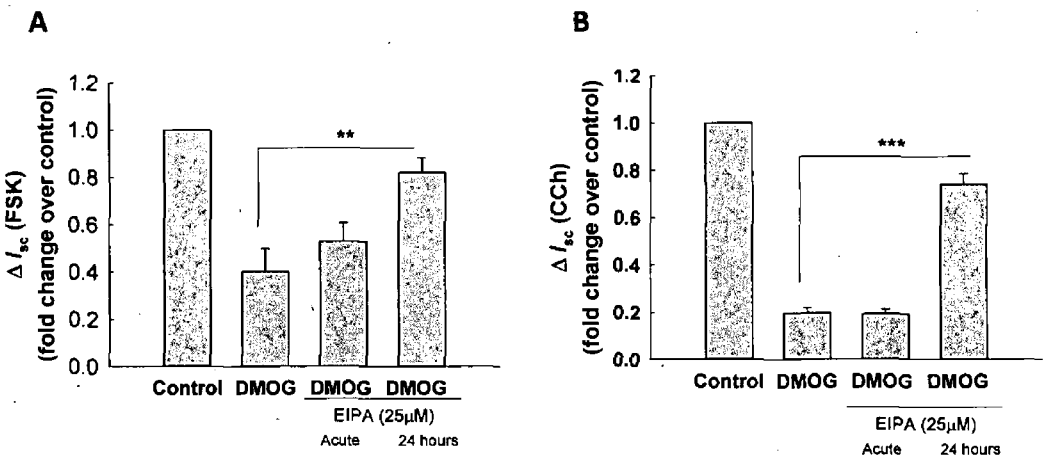

Figure 3-21 Chronic, but not acute, treatment of T_{84} cells with EIPA reversed the antisecretory effects of DMOG. T_{84} cells were grown as monolayers on permeable supports until R_{te} stabilised at plateau levels. Cells were treated bilaterally with DMOG (1 mM; 24 hours) in serum-free medium in the presence or absence of EIPA (25 μM; 24 hours). Cells were washed, mounted in Ussing chambers and bathed in Ringer's solution (Table 2-3). After an initial stabilisation period EIPA was added acutely to designated chambers. Cl^- secretory responses to **A)** FSK (10 μM) and **B)** CCh (100 μM) were measured (n = 3; ANOVA; ** $p \leq 0.01$, *** $p \leq 0.001$ compared to DMOG-only).

3-4 Discussion

In the present study we confirmed the expression of the HIF prolyl and asparaginyl hydroxylases in the T_{84} colonic epithelial cell model. Previous studies found that the expression of the HIF hydroxylases was regulated by induction of hypoxia, while in this study it was found that the expression of the hydroxylases was regulated by hydroxylase inhibitors, such as DMOG (Epstein *et al.*, 2001; Berra *et al.*, 2003; Marxsen *et al.*, 2004). While hydroxylase inhibition by DMOG and hypoxia are not one in the same, previous studies in a breast cancer cell line, MCF-7, have found there to be striking concordance between patterns of gene expression induced by hypoxia and by DMOG (Elvidge *et al.*, 2006). While many of these genes are HIF-1 or HIF-2-dependent, not all of the hypoxia or DMOG-regulated genes were targets of HIF, highlighting the importance of non-HIF targets of hydroxylases (Elvidge *et al.*, 2006). More recent studies have highlighted the sensitivity of the hydroxylases to varying levels of hypoxia versus hydroxylase inhibitors (Tian *et al.*, 2011b). For example, while proline hydroxylation is inhibited by 1 % hypoxia, asparagine hydroxylation is relatively insensitive to 1 % hypoxia, but is almost completely inhibited by DMOG. In agreement with other studies we found that hydroxylase inhibition caused a robust accumulation of HIF-1α and HIF-2α (Asikainen *et al.*, 2005). It was noted that HIF-1α mRNA expression was significantly reduced following treatment with DMOG. Interestingly, it has recently been shown by our collaborator's group that a negative feedback loop exists in which microRNA-155 induced by HIF-1α transcriptionally represses HIF-1α expression, thereby quenching the response (Bruning *et al.*, 2011). While the mRNA expression of PHD1 remained unaltered, PHD2 and PHD3 were transcriptionally upregulated in response to hydroxylase inhibition, potentially through the actions of HIF-1, as previously demonstrated (Marxsen *et al.*, 2004). Interestingly, PHD3 mRNA expression which was upregulated 1 hour after treatment with DMOG, was significantly reduced by 3 hours. This drop in PHD3 mRNA is coincident with the onset of the antisecretory effect of DMOG. With

this in mind one could speculate that PHD3 mediates the antisecretory effect of hydroxylase inhibition, with the discrepancy in the time course for mRNA expression and antisecretory actions being explained by the time it takes for PHD3 protein translation to occur. Further studies would be required to determine if this is indeed the case. FIH-1 expression remained unaltered at both the protein and mRNA levels, which was in accordance with previous studies showing FIH-1 is not regulated by hypoxia in human kidney cells (Schodel *et al.*, 2010).

The primary finding of this chapter is that hydroxylase inhibition by DMOG attenuates colonic epithelial responses to secretagogues (Figure 3–22). Upon stimulation with either the Ca^{2+} dependent secretagogue, CCh, or the cAMP dependent secretagogue, FSK, secretory responses were found to be significantly attenuated in DMOG-treated monolayers. The antisecretory effect of hydroxylase inhibition was recapitulated by the use of a more specific and potent inhibitor of PHDs, FG-4497, and these results are discussed in more detail in Chapter 4 of this thesis. The antisecretory effect of hydroxylase inhibition was slow in onset, occurring over several hours, and being half-maximal by approximately 8 hours after treatment. This slow onset of response suggests that alterations likely occur at the level of protein expression. The effects of hydroxylase inhibition by DMOG were also concentration-dependent, occurring at concentrations previously reported to inhibit PHDs and FIH-1 in other systems (Cummins *et al.*, 2008; Floyd *et al.*, 2007; Lando *et al.*, 2002b). Stabilisation of HIF-1α by hydroxylase inhibition temporally preceded the antisecretory effects, suggesting that DMOG may be exerting its antisecretory effects through altering HIF-1α expression. In support of this idea HIF-1 has previously been shown to transcriptionally down-regulate several of the transport proteins involved in the Cl^- secretory pathway (Zheng *et al.*, 2009; Ibla *et al.*, 2006). Acriflavine, an inhibitor of HIF-1α, was employed to investigate the role of HIF-1α in mediating the actions of DMOG, however acriflavine (5 μM) was found to be ineffective in attenuating the induction of the HIF-1 target,

PHD2. Acriflavine also had no effect on the antisecretory actions of DMOG. Thus, further studies would be required to determine if HIF-1 mediates the antisecretory effects of DMOG. Such studies could include the use of siRNAs to knock-down expression of HIF-1α.

Importantly, the anti-secretory effects of DMOG were not associated with cytotoxic actions in T_{84} cells, as evidenced by analysis of LDH release. In fact, R_{te}, a reliable measure of epithelial integrity was significantly increased following treatment of the cells with DMOG. This is supported by previous work showing that DMOG can exert anti-apoptotic effects in murine colonic epithelial cells, and therefore the drug may promote intestinal barrier function in this way (Cummins *et al.*, 2008). More recently our collaborators have identified that the mechanism by which PHD inhibition antagonises apoptosis is PHD1-dependent. In fact, histological analysis of the intestine of PHD1 knock-out mice showed an increase in epithelial cell density, which could have implications for intestinal transport function (Tambuwala *et al.*, 2010).

Pro-secretory second messenger production is stimulated by agonists, such as ACh and VIP, which bind to their cognate receptors, thereby raising levels of intracellular Ca^{2+} or cAMP, respectively. The current studies show that both Ca^{2+}- and cAMP-dependent Cl^- secretory responses are attenuated by hydroxylase inhibition. Reports of the effects of DMOG on intracellular second messenger levels are lacking, however, previous research in renal carcinoma cells showed that increased intracellular Ca^{2+} contributes to HIF-1α degradation, by a mechanism involving the calpain system (Zhou *et al.*, 2006). In the present study, DMOG caused a robust accumulation of HIF-1α, suggesting that Ca^{2+} levels were unaltered, which was indeed the case. In fact, neither agonist-induced release of intracellular Ca^{2+}, nor basal or stimulated levels of cAMP, were altered by treatment of T_{84} cells with DMOG. Furthermore, stimulation of cells with thapsigargin, an agent which increases intracellular Ca^{2+} levels in a

receptor-independent fashion, indicated that the antisecretory effect of DMOG on Ca^{2+}-stimulated responses occurs downstream of receptor activation.

Although T_{84} cells are an excellent tool for investigating mechanisms that regulate epithelial secretory function, they are ultimately a reductionist model, and findings may not be entirely translatable to *in vivo* situations. Thus, whether hydroxylase inhibition was also efficacious in inhibiting Cl^- secretion *in vivo* was investigated. A mouse model (C57BL/6) was employed since this model has been successfully used by other researchers for studying the effects of HIF-1 activation on the development of intestinal disease (Cummins *et al.*, 2008; Robinson *et al.*, 2008; Karhausen *et al.*, 2004). We found that similar to its effects in cultured colonic epithelial cells *in vitro*, hydroxylase inhibition in mice significantly reduced Cl^- secretory responses to both CCh and FSK across *ex vivo* colonic epithelium. The experiments carried out in mice were performed using a dose of DMOG previously reported to stabilise HIF-1α and to ameliorate colitis in mice, and which was found to increase cellular HIF-1α levels in the present study (Cummins *et al.*, 2008). Interestingly, there also appeared to be mHIF-1α present in control tissues, although this may not altogether be unexpected given the high turnover rate of HIF-1α and the presence of mild hypoxia in healthy colonic epithelium (Taylor and Colgan, 2007). However, the low levels of HIF-1α present suggest that it may not have a significant physiological role. Translation of these *ex vivo* findings into a pathophysiological model of diarrhoea was carried out using an allergic model of diarrhoea (Brandt *et al.*, 2003). Allergic diarrhoeas are associated with significant changes in I_{sc} and Cl^- secretion, and previous research has shown that OVA-induced diarrhoea is predominantly due to mast-cell stimulation of Cl^- secretion (Harari *et al.*, 1987; Perdue *et al.*, 1991). A lower dose of DMOG was required in these experiments based on experiments performed by our collaborators, which identified 160 mg/kg DMOG as being efficacious in ameliorating diarrhoeal disease. Strikingly, only 20 % of OVA-sensitised animals that were pre-treated with DMOG and then exposed to oral OVA were

diarrhoea-positive after 4 allergen challenges, whereas 100 % of animals treated with OVA-alone had diarrhoea. These data suggest that hydroxylase inhibition prevents secretory diarrhoea *in vivo* and could be of use in treatment of other diarrhoeal diseases, such as those associated with IBD, diarrhoea-predominant IBS, iatrogenic diarrhoeas such as those induced by chemotherapy, microscopic colitis, and bile acid malabsorption (Carter *et al.*, 2004; Maroun *et al.*, 2007; Oelkers *et al.*, 1997; Hofmann, 2009).

The intestine is predominantly an absorptive tissue, therefore investigation of potential therapies for diarrhoeal disease must include examination of their effects on absorptive processes. Fluid absorption follows Na^+ absorption by osmosis, therefore we first examined potential effects of DMOG on electrogenic Na^+ absorption. Since no cell culture models for ENaC-mediated absorption in the intestine exist, we adopted a previously employed approach (Iordache and Duszyk, 2007), where treatment of T_{84} colonic epithelial cells with the short chain fatty acid 4-PBA induces the expression of an amiloride-sensitive current. Following induction of active ENaC in T_{84} monolayers, inhibition of hydroxylases with DMOG caused a reduction in the basal ENaC current and by inference, a reduction in ENaC activity. Given that the mouse colon does not exhibit ENaC-mediated currents, our *in vitro* work was translated into a rat model, since it is known that the rectum of the rat exhibits a comparatively large amiloride-sensitive current (Inagaki *et al.*, 2004). In accordance with our *in vitro* work, at concentrations previously shown to inhibit hydroxylases in rats (Zhao *et al.*, 2010), DMOG caused a reduction in the amiloride-sensitive current in *ex vivo* rat rectum. The molecular mechanisms underlying this reduction remain to be elucidated, but may involve a reduction in the activity of the Na^+/K^+-ATPase, which is necessary for all transport processes in epithelial cells. This is discussed in more detail in Chapter 4 of this thesis. Hydroxylase inhibition specifically downregulated large intestinal ENaC activity, while small intestinal SGLT-1 activity remained unaltered. Contrary to this however, previous research has shown that acute hypoxia of 1 hour duration, inhibits SGLT-1 activity in rat

jejunum (Kles and Tappenden, 2002). However, these previous studies were conducted with supra-physiological levels of nutrients (120 mM). Since SGLT-1 is such an important transporter in the context of the jejunum, it is beneficial from the perspective of an antidiarrhoeal, that DMOG has no effect on its activity (Wright *et al.*, 2011). Finally, NHE activity in T_{84} cells was found to be attenuated by hydroxylase inhibition. We suspect that this is more likely to play a role in the regulation of intracellular pH (pH_i) as opposed to Na^+ absorption, since NHE3 has been reported to be absent from T_{84} cells (Beltran *et al.*, 2008). Interestingly, co-incubation of EIPA with DMOG reversed the antisecretory effect of DMOG. It has been reported that chronic hypoxia elevated pH_i by activating Na^+/H^+ exchange in pulmonary arterial smooth muscle cells and that this effect was inhibited by EIPA (Rios *et al.*, 2005). Although our results indicate an inhibition of NHE activity by DMOG, the possibility remains that hydroxylase inhibition alters steady-state pH_i, thereby attenuating Cl^- secretion. However, it should also be noted that EIPA-induced effects occurred only at doses >25 μM, which may indicate that this effect is due to non-specific actions of the inhibitor.

3-5 Summary

In summary these studies demonstrate a novel role for HIF hydroxylases in regulating intestinal epithelial ion transport *in vitro* and *in vivo*. Hydroxylase inhibition attenuates Cl^- secretion, an effect that *in vivo* would be expected to prevent fluid secretion into the intestine. These findings are important for our understanding of how epithelial transport function may be regulated in health and disease and suggest that hydroxylases, and their associated signalling mechanisms, may provide good targets for the development of new drugs to treat intestinal disorders associated with diarrhoea.

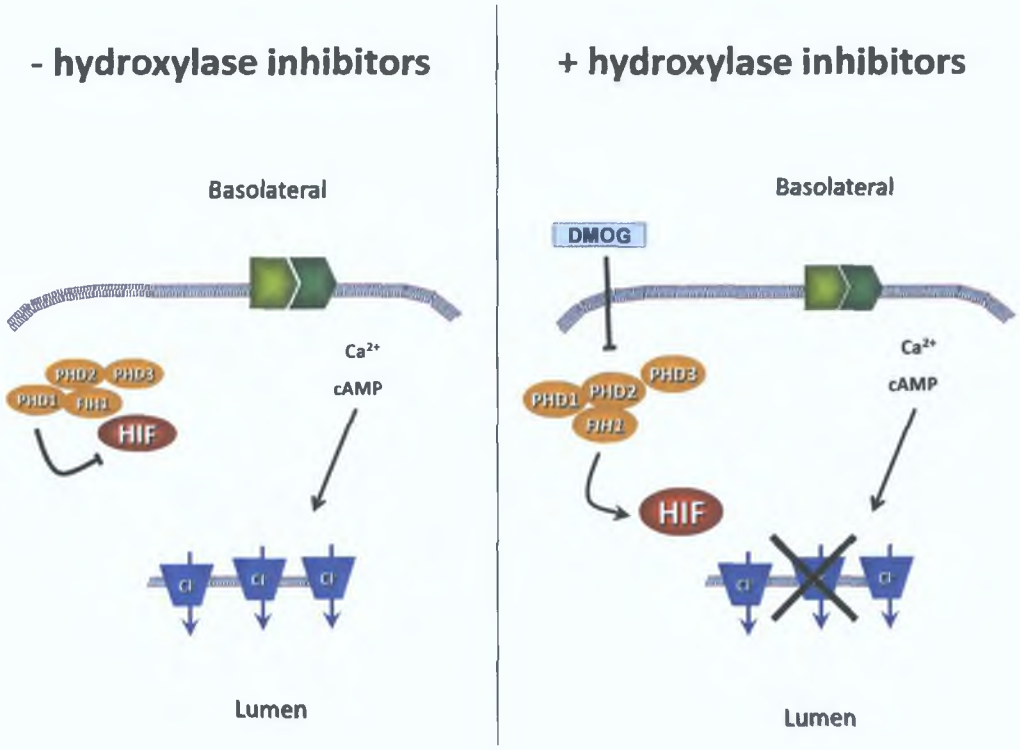

Figure 3–22 Hydroxylase inhibition attenuates colonic epithelial secretory function *in vitro* and *in vivo*. Upon treatment with the hydroxylase inhibitor, DMOG, the activity of HIF hydroxylases is blocked, leading to HIF-α stabilisation in the cell. Cl^- secretory responses to both Ca^{2+}- and cAMP-dependent agonists are significantly attenuated and this effect is not due to alterations in the abundance of these prosecretory second messengers. DMOG-induced inhibition of Cl^- secretion prevents fluid secretion into the intestinal lumen, thereby preventing diarrhoea.

Chapter 4

Hydroxylase inhibition attenuates epithelial Na^+/K^+-ATPase activity

4-1 Introduction

Fluid secretion in the intestine is driven by the luminal secretion of Cl^- from epithelial cells. The Cl^- secretory pathway is tightly regulated and is composed of several transport proteins that work in concert to drive Cl^- from the epithelium into the lumen of the gut. In the previous chapter we found that hydroxylase inhibition attenuated agonist-stimulated secretory responses across colonic epithelial cells. Thus, our data expand on previous studies which demonstrate that intestinal secretion can be regulated by hypoxia and its associated signalling mechanisms, including production of mitochondrial reactive oxygen species (ROS), reductions in ATP generation, and stimulation of HIF-1α and HIF-2α accumulation. Although mechanisms by which hypoxia regulates epithelial secretion are not well understood, previous studies suggest that hypoxic targets within epithelial cells can include transport proteins that comprise the Cl^- secretory pathway.

The driving force for apical Cl^- secretion and indeed, all epithelial electrolyte transport processes, is the basolaterally-located Na^+/K^+-ATPase (Skou, 1998; Kaplan, 2002). Several studies have shown the Na^+/K^+-ATPase to be regulated by hypoxia (Planes *et al.*, 1996; Mairbaurl *et al.*, 2002; Carpenter *et al.*, 2003; Dada *et al.*, 2003; Gusarova *et al.*, 2011). Initial studies indicated that hypoxia attenuated the activity of lung epithelial Na^+/K^+-ATPase, without altering its expression (Planes *et al.*, 1996; Carpenter *et al.*, 2003). The mechanisms involved are complex and involve mitochondrial ROS, which are produced during hypoxia, which activate Ca^{2+}/calmodulin-dependent kinase kinase β (CaMKKβ). Activated CaMKKβ then phosphorylates adenosine monophosphate-activated protein kinase (AMPK), which in turn phosphorylates PKC ζ (Gusarova *et al.*, 2011; Gusarova *et al.*, 2009). PKC ζ translocates to the plasma membrane where it phosphorylates Ser-18 on Na^+/K^+-ATPase α_1, culminating in clathrin-dependent pump endocytosis (Dada *et al.*, 2003; Chen *et al.*, 2006). This process was shown to require the ubiquitin-conjugating system and to be pVHL-

dependent, but interestingly was HIF-independent (Comellas *et al.*, 2006; Dada *et al.*, 2007; Zhou *et al.*, 2008). The aforementioned research was carried out in renal and alveolar epithelial cells, which are exposed to a pO_2 of approximately 20–50 torr and 100 torr (16 % O_2), respectively (Johannes *et al.*, 2006). These levels of O_2 are considerably higher than those to which intestinal epithelial cells are exposed, which when examined in the mouse, ranged from 58 torr in the stomach, to 3 torr in the colon (He *et al.*, 1999). Nevertheless, the fact that the mechanism of Na^+/K^+-ATPase inhibition by PKC ζ is conserved across renal and alveolar tissues, suggests that it may also be present in intestinal epithelia. Na^+/K^+-ATPase regulation is multifaceted, and thus has potential to be exploited for therapeutic intervention.

The activity of Na^+/K^+-ATPase pumps create an electrochemical driving force for entry of Na^+ through basolateral Na^+ K^+ $2Cl^-$ co-transporters (NKCC1). NKCC facilitates the entry of Na^+, K^+, and 2 Cl^- into epithelial cells and its function has been well characterised in the colon (Matthews *et al.*, 1992; Matthews *et al.*, 1994; D'Andrea *et al.*, 1996; Haas and Forbush, 2000; Del Castillo *et al.*, 2005). NKCC1 has been identified as the isoform expressed by human intestinal epithelium (Payne *et al.*, 1995). Although it is known to be regulated by hypoxia and specifically by HIF-1, there is still a paucity of studies on NKCC function under such conditions (Ibla *et al.*, 2006). However, since NKCC1 is a rate-limiting step in intestinal epithelial Cl^- secretion, it too is likely to be an important factor in the alterations of epithelial transport function that occur during hypoxia (Barrett and Keely, 2000).

K^+ ions that enter epithelial cells through NKCC1 are recycled through basolateral cAMP-activated K^+ channels, KCNQ1, and basolateral Ca^{2+}-activated K^+ channels KCNN4 (Schroeder *et al.*, 2000; Flores *et al.*, 2007). More recent research has also implicated apically located K^+ channels as being involved in luminal secretion of anions in the intestine (Nanda Kumar *et al.*, 2010). Recent studies have implicated AMPK as being important in regulation of KCNQ1 under

conditions of metabolic stress in kidney cells (Alzamora *et al.*, 2010). While it is possible that such effects may also occur in hypoxia, this has not been demonstrated in intestinal epithelial cells. However, since AMPK is not activated by hydroxylase inhibitors, it is unlikely to play a major role in mediating actions of DMOG described in the current studies (Emerling *et al.*, 2007). Research by other groups has shown that serum and glucocorticoid-responsive kinase-1 (SGK1) regulates KCNQ1/KCNE3 endocytosis (Seebohm *et al.*, 2007). SGK1 is known to be regulated by hypoxia in other systems (Aoyama *et al.*, 2005; Rusai *et al.*, 2009). Thus, previous studies suggest that KCNQ1 can be regulated under conditions of hypoxia, or by hydroxylase inhibitors, through activation of SGK1. However, studies on the role of hypoxia, or hydroxylase inhibitors, on KCNN4 function are scarce.

Cl^- accumulates in epithelial cells above its electrochemical equilibrium by its entry through NKCC1, and upon stimulation of the cells by agonists such as acetylcholine or VIP, accumulated Cl^- exits across the apical membrane (Figure 4-1). Luminal Cl^- exit is facilitated by Cl^- channels, such as cAMP-activated CFTR channels, and the more recently identified Ca^{2+}-activated apical Cl^- channel, TMEM16A (Ousingsawat *et al.*, 2009; Almaca *et al.*, 2009). Previous studies have indicated that hypoxia represses mRNA expression of CFTR in the intestine and other tissues, and further studies in the intestinal epithelium showed that this occurs by a HIF-1-dependent mechanism (Guimbellot *et al.*, 2008; Zheng *et al.*, 2009). In sinonasal respiratory epithelia, both CFTR and TMEM16A mRNA transcripts have been shown to be significantly attenuated in hypoxic cultures (Blount *et al.*, 2011). Thus, in light of the antisecretory actions of DMOG observed in the current studies, the effects of hydroxylase inhibition on Cl^- channel function warrants further investigation.

Each of the transport proteins that comprise the Cl^- secretory pathway has been the subject of extensive previous research and various protocols have been established by which their activities can be investigated in isolation. For

example, using simple modifications of the Ussing chamber/voltage clamp technique, the activity of several of these transport proteins can be measured as changes in I_{sc}. However, electrophysiological studies are only useful where the transport process under investigation results in a net charge moving across the epithelium. For electroneutral transporters, such as NKCC1, other techniques must be employed, such as rubidium flux assays or ratiometric imaging using fluorescent probes, such as BCECF (Reynolds *et al.*, 2007). In order to further our understanding of the antisecretory effects of hydroxylase inhibition in intestinal epithelial cells, we employed some of these techniques, along with biochemical and molecular approaches, to more closely analyse the effects of DMOG on the expression and activity of transport proteins involved in the secretory process.

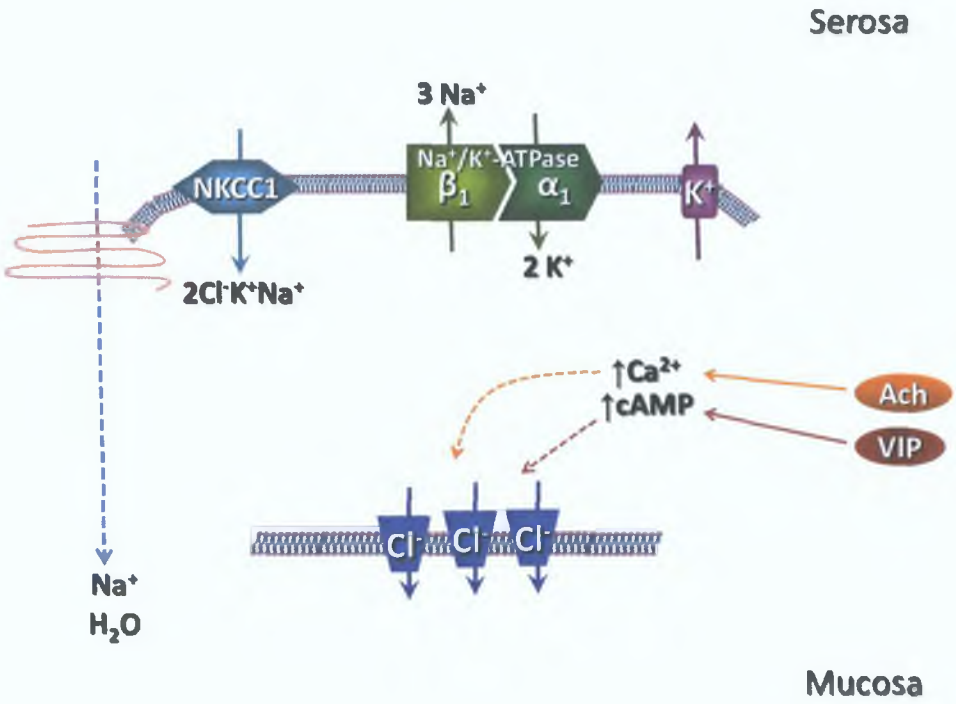

Figure 4-1 Schematic representation of the Cl^- secretory pathway in T_{84} cells. This rather simplistic representation of the Cl^- secretory pathway of T_{84} cells highlights the main types of transporters that contribute to Cl^- secretion in this model. The electrochemical driving force for Cl^- secretion is provided by the Na^+/K^+-ATPase on the basolateral membrane. The removal of 3 Na^+ from the cell against their electrochemical gradient creates a driving force for the entry of Na^+, K^+, and 2 Cl^- via basolateral NKCC1. Cl^- and K^+ accumulate within the cell, and upon stimulation by agonists such as ACh and VIP, which raise intracellular second messenger levels, basolateral K^+ channels and apical Cl^- channels open and luminal efflux of Cl^- occurs. The electrical gradient created by Cl^- efflux promotes paracellular Na^+ transport through tight junction pores and water follows passively by osmosis.

4-2 Aim

The overall goal of this chapter was to investigate the impact of hydroxylase inhibition on the activity and expression of individual transport proteins that constitute the Cl^- secretory pathway. Specifically, the aims of the chapter were to:

1. Identify alterations in transport protein activity and expression in response to hydroxylase inhibition.
2. Investigate molecular regulation of the Na^+/K^+-ATPase by hydroxylase inhibitors.
3. Investigate the potential involvement of HIF in the antisecretory effect of hydroxylase inhibitors.

4-3 Results

4-3.1 Hydroxylase inhibition attenuates CFTR expression

We first set out to investigate the effects of hydroxylase inhibition on the activity of apical CFTR channels. Using a previously established protocol (Rochwerger *et al.*, 1994), T_{84} cells were treated with DMOG (1 mM; 24 hours) and mounted in Ussing chambers. An apical to basolateral Cl^- gradient of 119.8–4.8 mM was established across the monolayers and the basolateral membranes were permeabilised by nystatin (100 μg/ml). Following stabilisation of the current, FSK (10 μM; apical) stimulated Cl^--currents were measured. Control Cl^- currents were inhibited 77.8 ± 2.3 % by the CFTR inhibitor, $CFTR_{inh172}$ (10 μM) (n = 6; *** $p \leq 0.001$), implying that the apical Cl^- current was predominantly CFTR-mediated. However, it was found that there was no difference in FSK-induced changes in current (ΔI_{sc}) when control and DMOG-treated cells were compared (Figure 4-2). $CFTR_{inh172}$ attenuated the current in DMOG-treated cells to a similar extent as that in control cells (78.6 ± 7.7 %; n = 3; $p \leq 0.001$), suggesting that Cl^- currents in DMOG-treated cells are also predominantly mediated by CFTR.

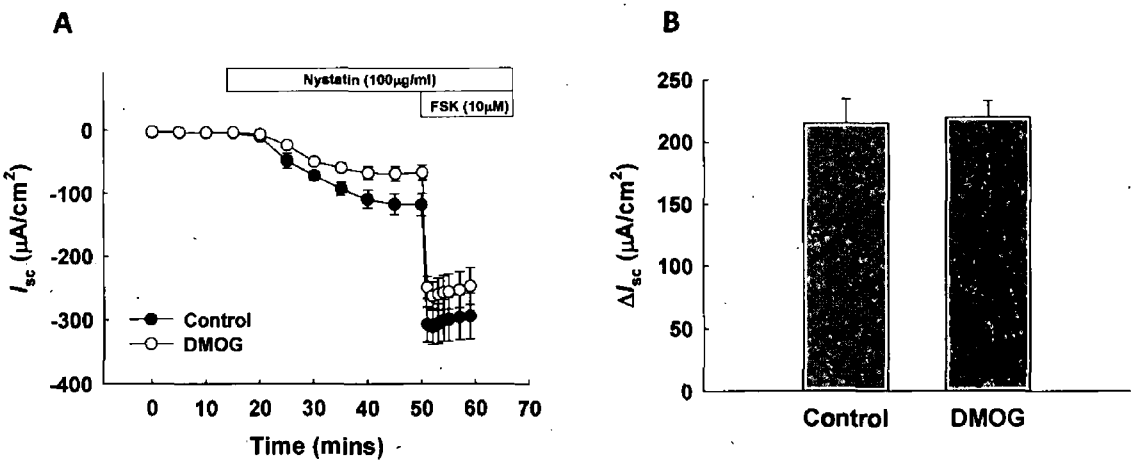

Figure 4-2 Hydroxylase inhibition does not alter apical Cl^- currents in T_{84} cells. T_{84} cells were grown as monolayers on permeable supports until R_{te} stabilised at plateau levels. Cells were treated bilaterally with DMOG (1 mM) in serum-free medium for 24 hours and were then washed and mounted in Ussing chambers. The apical chamber contained normal Ringer's solution (Table 2–3), whereas the basolateral chamber contained a low Cl^- solution, in which Cl^- was replaced with equimolar gluconate (Table 2–5). **A)** Following 30 minutes of permeabilisation by nystatin (100 µg/ml), FSK (10 µM) was added apically and changes in I_{sc} were measured. **B)** Maximal changes in current in control and DMOG-treated cells were plotted as ΔI_{sc} (n = 10).

To determine whether CFTR expression is altered in intestinal epithelial cells by inhibition of hydroxylases, cells were treated with DMOG (1 mM) for several time points up to 24 hours. After treatment, analysis of CFTR mRNA and protein was performed by semi-quantitative PCR and SDS-PAGE, respectively. We found that there was a dramatic reduction in both CFTR mRNA and protein expression following treatment with DMOG (Figure 4–3). This is consistent with previous work showing that HIF-1 transcriptionally represses CFTR (Zheng *et al.*, 2009).

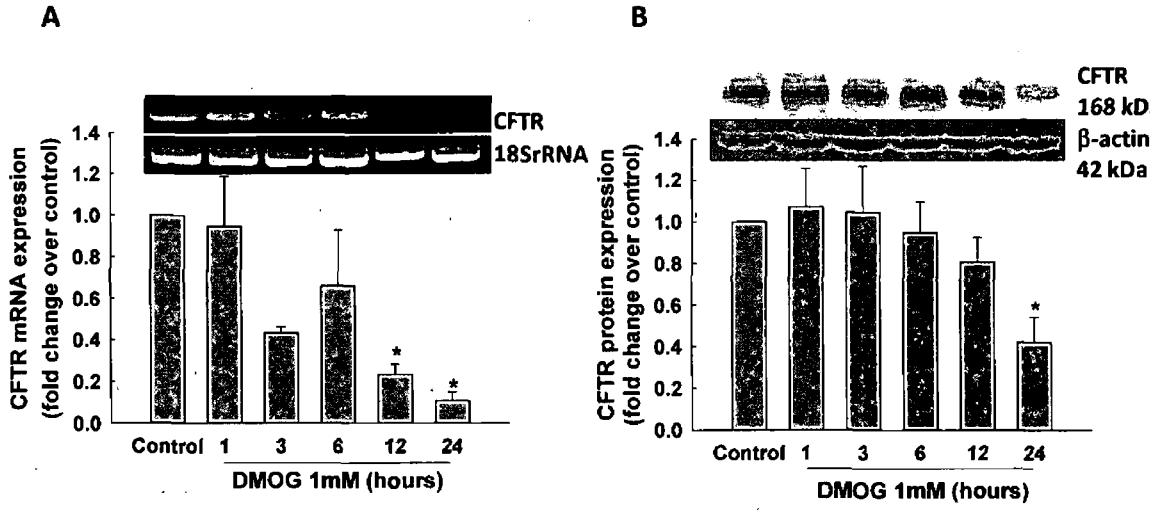

Figure 4–3 Hydroxylase inhibition attenuates CFTR expression in colonic epithelial cells. T_{84} cells were grown as monolayers on permeable supports until R_{te} stabilised at plateau levels. Cells were treated bilaterally with DMOG (1 mM) in serum-free medium for various times. **A)** mRNA was isolated from the cells and semi-quantitative PCR analysis was performed with primers specific for CFTR. 18SrRNA was used as a loading control (n = 4; ANOVA, * $p \leq 0.05$ compared to control). **B)** Total protein was isolated from cells and CFTR protein expression was measured by western blot. β-actin was used as a loading control (n = 5; ANOVA, * $p \leq 0.05$ compared to control).

The effects of hydroxylase inhibition on the recently identified Ca^{2+} activated Cl^- transporter TMEM16A were next investigated. TMEM16A has been implicated in facilitating Cl^- secretion across various epithelia in the GI tract, including the colon (Ousingsawat *et al.*, 2009; Almaca *et al.*, 2009). Recent research from our laboratory has implicated TMEM16A in mediating Ca^{2+} activated Cl^- currents from T_{84} cells (Mroz and Keely, 2011). However, analysis of TMEM16A mRNA expression revealed no significant change after treatment with DMOG (1 mM) over several time points (Figure 4–4).

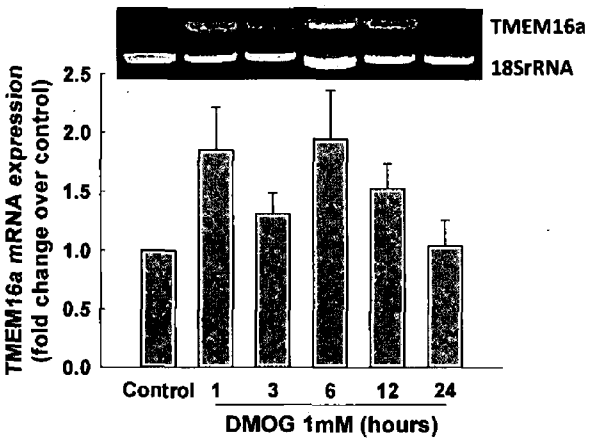

Figure 4–4 Hydroxylase inhibition does not significantly alter TMEM16A mRNA expression in colonic epithelial cells. T_{84} cells were cultured as monolayers on permeable supports until R_{te} stabilised at plateau levels. Cells were treated bilaterally with DMOG (1 mM) in serum-free medium for several time points up to 24 hours. Total RNA was isolated from the cells, cDNA was created using reverse transcriptase, and semi-quantitative RT-PCR analysis was performed with primers specific for TMEM16A. 18SrRNA was used as a loading control (n = 5).

4-3.2 Hydroxylase inhibition attenuates NKCC1 expression

NKCC1 has previously been shown to be transcriptionally repressed by HIF-1, therefore NKCC1 activity was next investigated (Ibla *et al.*, 2006). T_{84} cells were cultured on glass petri-dishes and were treated with DMOG (1 mM) for 24 hours. The cells were loaded with the pH sensitive dye BCECF and pH_i was analysed by recording BCECF fluorescence. Cells were then perfused with a solution containing NH_4Cl. Addition of NH_4^+ led to an initial alkalinisation, corresponding to NH_3 uptake. This was followed by an acidification, corresponding to NH_4^+ uptake. The plateau phase or rate of recovery following the acid load, is representative of the activity of the NKCC1 co-transporter transporting NH_4^+, a substrate for the co-transporter (Heitzmann *et al.*, 2000; Bachmann *et al.*, 2003). The rate of recovery in cells treated with DMOG was similar to that of controls (Figure 4–5).

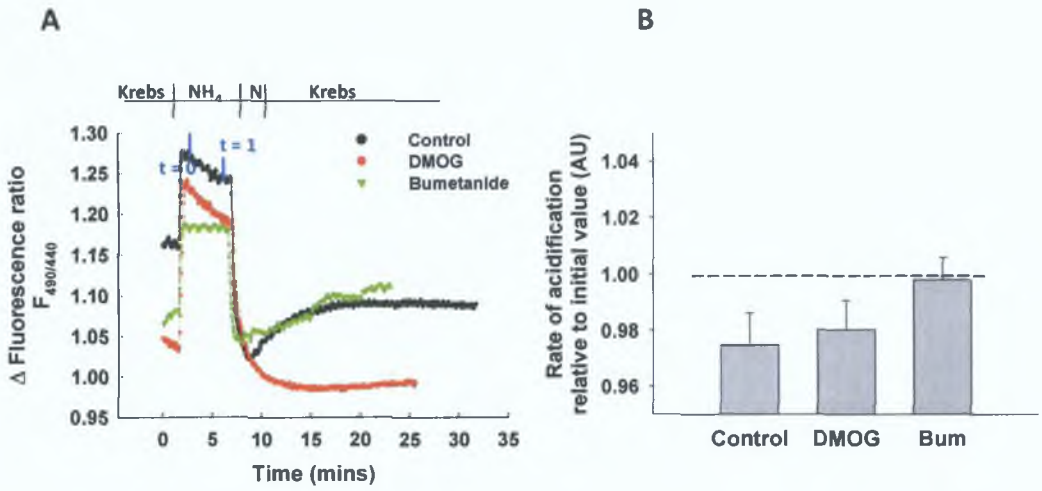

Figure 4-5 Hydroxylase inhibition does not alter NKCC1 activity in T_{84} cells. T_{84} cells were cultured on glass-bottomed petri-dishes until approximately 80 % confluent. Cells were treated with DMOG (1 mM; 24 hours) and then washed in modified Krebs solution (Table 2–15). Cells were loaded with BCECF-AM (5 μM; 60 minutes), washed, and were then incubated in modified Krebs solution for a further 15 minutes to facilitate any passive leakage of the dye. **A)** pH_i was analysed by recording BCECF fluorescence at intervals of 3 seconds. Cells were perfused with modified Krebs solution, NH_4-Krebs solution, or NMDG-Cl^- Krebs solution (indicated by N), and returned to modified Krebs solution for the remainder of the experiment. Data are expressed as mean fluorescence ratio at 490 and 440 nm. **B)** NKCC1 activity was recorded as the rate of change in pH_i during the acidification(from t = 0, to t = 1) (NH_4 uptake) stage (n = 3–10). Cells were treated with bumetanide (Bum) (100 μM) to inhibit NKCC1 activity.

The expression of NKCC1 mRNA and protein was next examined by semi-quantitative RT-PCR and western blotting, respectively. In agreement with published research showing that HIF-1 transcriptionally represses NKCC1, we found NKCC1 protein and mRNA expression to be significantly attenuated by hydroxylase inhibition following 24 hours treatment with DMOG (1 mM) (Figure 4–6) (Ibla *et al.*, 2006).

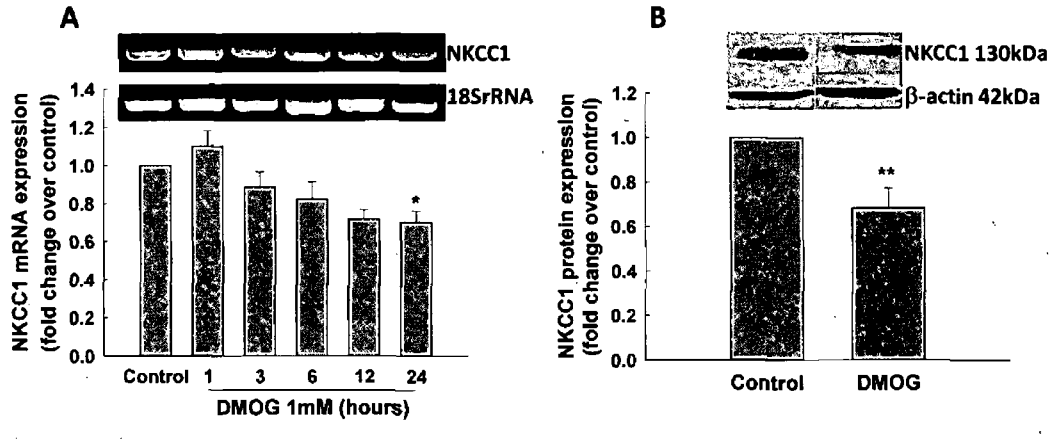

Figure 4–6 Hydroxylase inhibition attenuates NKCC1 expression in colonic epithelial cells T_{84} cells were cultured as monolayers on permeable supports until R_{te} stabilised at plateau levels. Cells were treated bilaterally with DMOG (1 mM) in serum-free medium for various periods of time. **A)** Total RNA was isolated from the cells and semi-quantitative PCR analysis was performed with primers specific for NKCC1. 18SrRNA was used as a loading control (n = 5; ANOVA; * $p \leq 0.05$ compared to control). **B)** Total protein was isolated from cells, and CFTR protein expression was measured by western blotting. β-actin was used as a loading control (n = 8; paired t-test; ** $p \leq 0.01$).

NKCC1 expression was further analysed by confocal microscopy. Cells were cultured on transparent permeable supports until R_{te} stabilised at plateau levels and were then treated with DMOG (1 mM) for 24 hours. Figure 4–7 shows that NKCC1 (green) is highly expressed on the basolateral side of T_{84} cells and that there appears to be no alteration in trafficking of the protein to the plasma membrane upon treatment with DMOG. Visualisation of the rhodamine-phalloidin-stained (red) actin collar around the apical membrane, and the basolateral nuclei stained with DAPI (blue) allows for orientation of the cells.

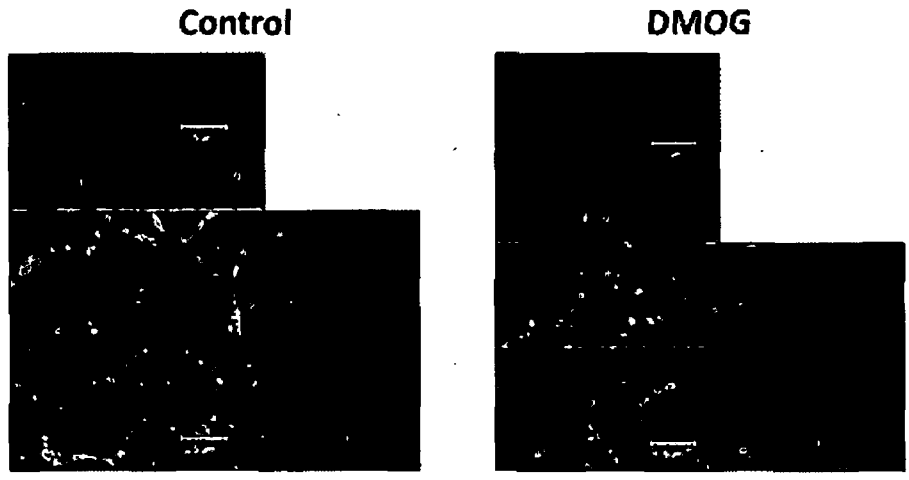

Figure 4–7 Hydroxylase inhibition does not alter NKCC1 membrane localisation in T_{84} cells. T_{84} cells were cultured as monolayers on permeable supports until R_{te} stabilised at plateau levels. Cells were treated bilaterally with DMOG (1 mM) in serum-free medium for 24 hours. Cells were then washed in PBS, fixed in 100 % methanol, permeabilised with Triton X-100, and stained with specific fluorophore-labelled antibodies as outlined in Section 2–24. Pseudo-colours were assigned to the various structures, with nuclei being represented in blue, f-actin in red and NKCC1 in green. Scale bars are 5 μm in length.

4-3.3 Hydroxylase inhibition does not affect basolateral K^+ channels, KCNN4 or KCNQ1

The basolateral K^+ channel involved in Ca^{2+}-activated Cl^- secretion across colonic epithelial cells has been previously identified as the intermediate conductance K^+ channel, KCNN4 (Flores *et al.*, 2007). The effect of hydroxylase inhibition on the activity of basolateral KCNN4 was next investigated using a previously established protocol (Kirk and Dawson, 1983). T_{84} cells were mounted in Ussing chambers and an apical to basolateral K^+ gradient of 123.2–5.2 mM was established across the epithelium. Apical membranes were then permeabilised with amphotericin B (50 μM) and after re-stabilisation of baseline current, basolateral K^+ currents were stimulated by addition of basolateral CCh (100 μM). We found that basal state K^+ currents were significantly increased in DMOG-treated cells, however, stimulated basolateral Ca^{2+}-activated K^+ currents were unaltered by hydroxylase inhibition (Figure 4–8).

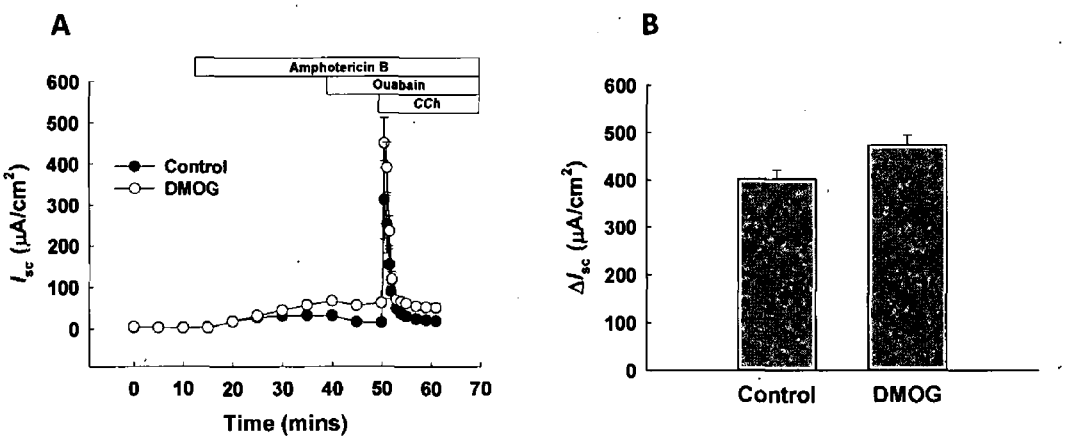

Figure 4–8 Hydroxylase inhibition does not alter Ca^{2+}-stimulated K^+ currents in T_{84} cells. T_{84} cells were cultured as monolayers on permeable supports until R_{te} stabilised at plateau levels. Cells were treated bilaterally with DMOG (1 mM) in serum-free medium for 24 hours, washed, and mounted in Ussing chambers. The apical Ringer's solution contained high [K^+] (Table 2–6), whereas the basolateral bath contained normal (low [K^+]) Ringer's solution (Table 2–3). **A)** After mounting in Ussing chambers, cells were allowed to equilibrate for 15 minutes, after which amphotericin B (50 μM) was added to the apical bath. After an additional 25 minutes, ouabain (100 μM) was added basolaterally to inhibit Na^+/K^+-ATPase activity. Basolateral CCh (100 μM) was then added to stimulate Ca^{2+}-activated K^+ channels in the basolateral membrane. **B)** Maximal changes in K^+ currents were plotted as ΔI_{sc} (n = 4).

In order to further analyse potential effects of hydroxylase inhibition on KCNN4, we investigated whether there was any change in the overall abundance of the transporter after treatment with DMOG. KCNN4 mRNA and protein expression were analysed by semi-quantitative RT-PCR and western blotting, respectively. Cells were treated with DMOG (1 mM) for several time points, and mRNA and proteins were isolated in the usual manner. As shown in Figure 4–9, there was no change in either mRNA or protein expression of KCNN4 following hydroxylase inhibition.

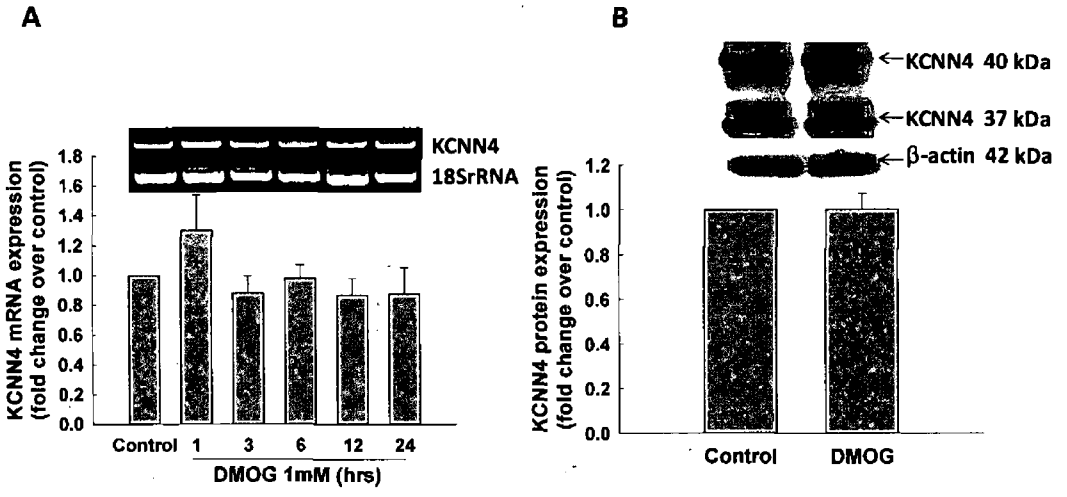

Figure 4–9 KCNN4 expression is unaltered by hydroxylase inhibition in T_{84} cells. T_{84} cells were cultured as monolayers on permeable supports until R_{te} stabilised at plateau levels. Cells were treated bilaterally with DMOG (1 mM) in serum-free medium for various periods of time. **A)** mRNA was isolated from the cells and semi-quantitative RT-PCR analysis was performed with primers specific for KCNN4. 18SrRNA was used as a loading control (n = 5). **B)** Total protein was isolated from cells, and KCNN4 (40 kDa) protein expression was measured by western blotting. β-actin was used as a loading control (n = 4).

As a logical progression of our studies, we next went on to investigate if hydroxylase inhibition alters the expression of the cAMP-regulated basolateral K^+ channel, KCNQ1. Hydroxylases were inhibited with DMOG (1 mM) for 24 hours and KCNQ1 expression was investigated at both the mRNA and protein levels by semi-quantitative RT-PCR and western blotting, respectively (Figure 4–10). It was found that there were no alterations in the expression of either KCNQ1 mRNA or protein in DMOG-treated cells.

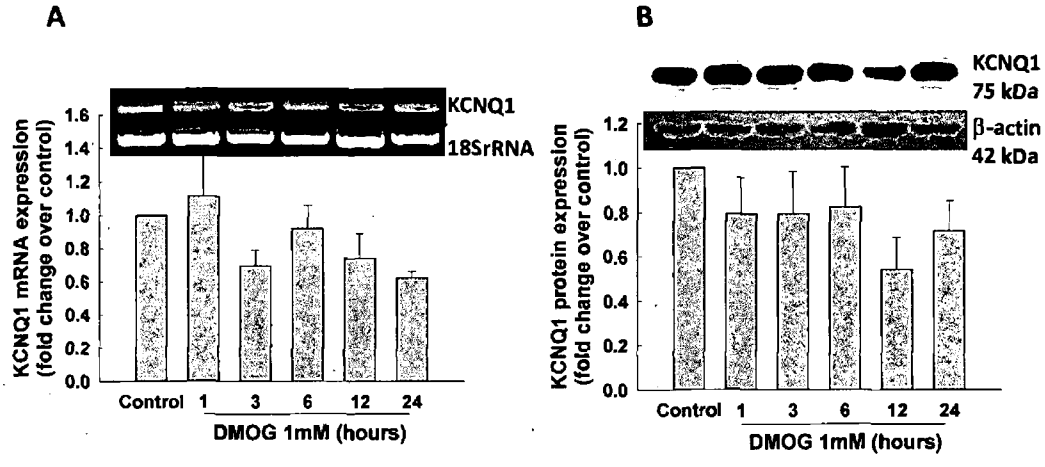

Figure 4–10 KCNQ1 expression is not altered by hydroxylase inhibition in T_{84} cells. T_{84} cells were cultured as monolayers on permeable supports until R_{te} stabilised at plateau levels. Cells were treated bilaterally with DMOG (1 mM) in serum-free medium for various periods of time. **A)** mRNA was isolated from the cells and semi-quantitative RT-PCR analysis was performed with primers specific for KCNQ1. 18SrRNA was used as a loading control (n = 4). **B)** Total protein was isolated from cells, and KCNQ1 protein expression was measured by western blot. β-actin was used as a loading control (n = 4).

KCNQ1 expression was further analysed by confocal microscopy. Cells were cultured on transparent permeable supports and were treated with DMOG (1 mM) for 24 hours. As shown in Figure 4–11, KCNQ1 (green) is highly expressed on the basolateral side of T_{84} cell monolayers. There was also quite an amount of cytosolic staining and some staining towards the apical membrane. Furthermore, we found that there was no alteration in the trafficking of KCNQ1 to the membrane in DMOG-treated cells. Visualisation of the rhodamine-phalloidin-stained (red) f-actin collar around the apical membrane allows for orientation of the cells. Although nuclei were also stained using DAPI, they were omitted from these images so that KCNQ1 expression could be fully appreciated.

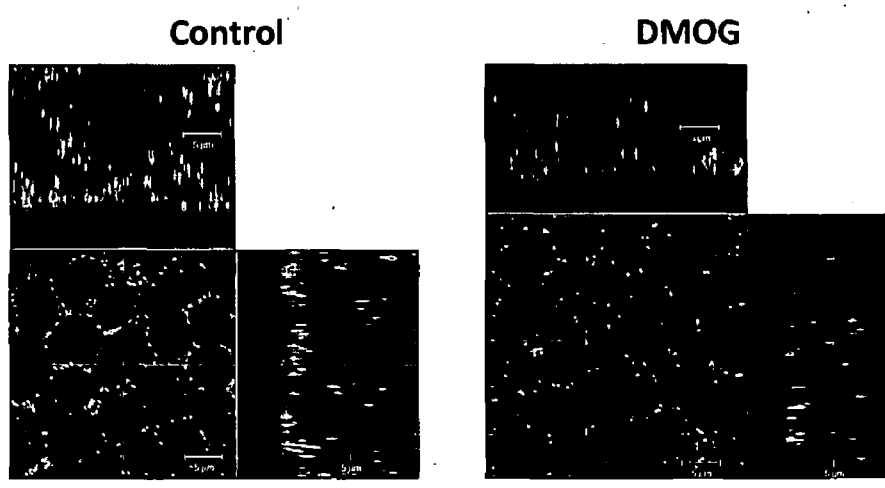

Figure 4–11 Hydroxylase inhibition does not alter KCNQ1 trafficking in T_{84} cells. T_{84} cells were cultured as monolayers on permeable supports until R_{te} stabilised at plateau levels. Cells were treated bilaterally with DMOG (1 mM) in serum-free medium for 24 hours. Cells were then washed in PBS, fixed in 100 % methanol, permeabilised with Triton X-100, and stained with specific fluorophore-labelled antibodies, as outlined in Section 2–24. Pseudo-colours were assigned to the various proteins, with f-actin being represented in red and KCNQ1 in green.

4-3.4 Hydroxylase inhibition attenuates Na^+/K^+-ATPase activity in colonic epithelial cells

Our attention next turned to investigating DMOG effects on the basolateral Na^+/K^+-ATPase. The Na^+/K^+-ATPase creates the electrochemical driving force for establishing the ionic gradients that drive ion transport across the epithelium. We used a well-established protocol to measure Na^+/K^+-ATPase pump activity (DuVall *et al.*, 1998; Gomes and Soares-Da-Silva, 2002; Lam *et al.*, 2003). However, preliminary experiments were first carried out to optimise this protocol, in order to more closely mimic physiological conditions under which the pump normally operates. To this end Na^+/K^+-ATPase activity was measured using 3 different concentrations of Na^+; 0, 25, and 140 mM. A correlation between $[Na^+]$ and Na^+/K^+-ATPase activity was observed (Figure 4–12). For subsequent experiments 25 mM Na^+ was employed, since this is more physiological than the 140 mM concentration employed in previous studies.

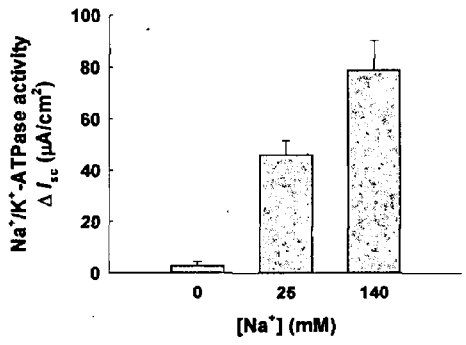

Figure 4–12 Na^+/K^+-ATPase activity is dependent on the concentration of Na^+ present in the buffering solution. T_{84} cells were cultured on permeable supports until R_{te} stabilised at plateau levels. Cells were then washed, mounted in Ussing chambers, and bathed in modified Ringer's solutions containing 0, 25, or 140 mM Na^+. Cells were apically permeabilised with amphotericin B (50 μM) and were then stimulated by the basolateral addition of CCh (100 μM). Maximal changes in current are plotted as ΔI_{sc} and expressed as $\mu A/cm^2$ (n = 3).

Using the conditions optimised in Figure 4-12, cells were next treated with DMOG (1 mM; 24 hours) and Na^+/K^+-ATPase activity was measured. Cells were mounted in Ussing chambers and apically permeabilised with amphotericin B (50 μM). Under basal conditions there was a significant reduction in the basal activity of the Na^+/K^+-ATPase in DMOG-treated cells (Figure 4-13 C). Similarly, hydroxylase inhibition significantly attenuated activity of the Na^+/K^+-ATPase in response to stimulation by CCh (100 μM) (Figure 4-13 A, B). Basolateral ouabain (100 μM) practically abolished pump activity (Figure 4-13 B).

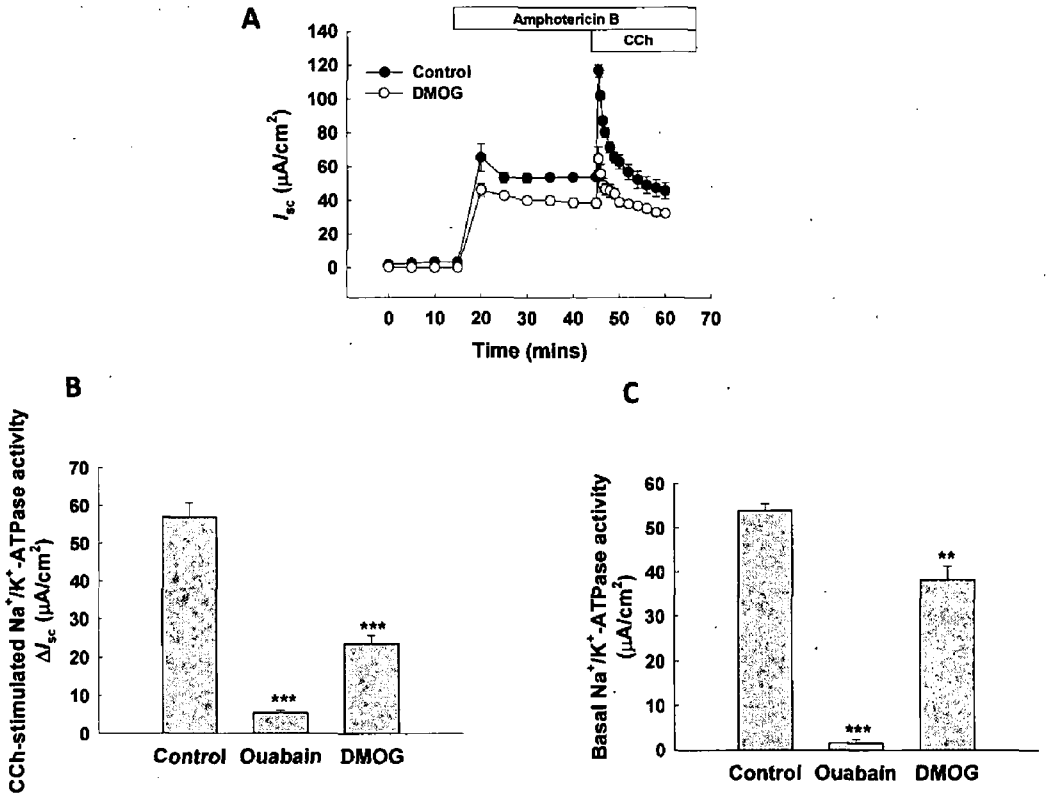

Figure 4–13 Hydroxylase inhibition attenuates Na^+/K^+-ATPase activity in T_{84} cells. T_{84} cells were cultured on permeable supports until R_{te} stabilised at plateau levels. Cells were treated with DMOG (1 mM; 24 hours), washed, mounted in Ussing chambers, and bathed in Ringer's solution containing 25 mM Na^+ (Table 2–7). **A)** Cells were apically permeabilised with amphotericin B (50 μM) for 30 minutes until the current had stabilised. Basolateral ouabain (100 μM) was added to negative control cells, and basolateral CCh (100 μM) was added to all cells to stimulate Na^+/K^+-ATPase activity. **B)** Maximal CCh-induced currents were plotted as ΔI_{sc} (n = 5; ANOVA; *** $p \leq 0.001$). **C)** Basal I_{sc} in control and DMOG-treated cells prior to addition of CCh was plotted as I_{sc} (n = 5; ANOVA; ** $p \leq 0.01$. *** $p \leq 0.001$).

Since the antisecretory effect of hydroxylase inhibition is slow in onset and occurs over several hours, we hypothesised that this effect is likely due to alterations in protein expression. Thus, Na^+/K^+-ATPase pump expression in the absence or presence of DMOG was next investigated in T_{84} cells. The catalytic Na^+/K^+-ATPase α_1 subunit was first investigated since this is the catalytic subunit that facilitates the transport of ions. However, we found that neither Na^+/K^+-ATPase α_1 subunit mRNA or protein expression were significantly altered by hydroxylase inhibition over a period of 24 hours (Figure 4–14).

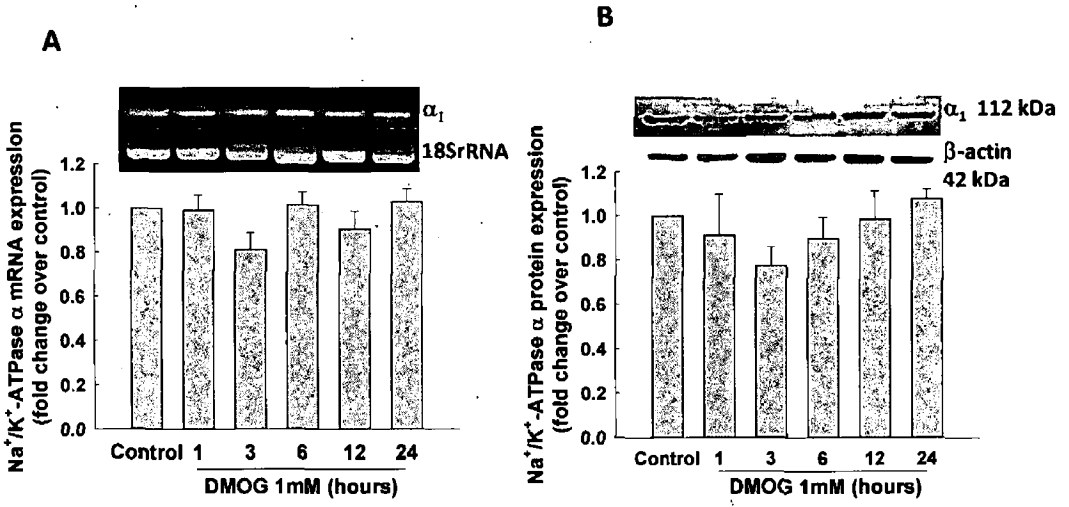

Figure 4–14 Hydroxylase inhibition does not alter Na^+/K^+-ATPase α_1 subunit expression in T_{84} cells. T_{84} cells were cultured as monolayers on permeable supports until R_{te} stabilised at plateau levels. Cells were treated bilaterally with DMOG (1 mM) in serum-free medium for various periods of time. **A)** mRNA was isolated from the cells and semi-quantitative RT-PCR analysis was performed with primers specific for the Na^+/K^+-ATPase α_1 subunit (labelled as α_1 in the upper panel). 18SrRNA was used as a loading control (n = 4). **B)** Total protein was isolated from cells, and Na^+/K^+-ATPase α_1 protein expression was measured by western blotting (labelled as α_1 in the upper panel). β-actin was used as a loading control (n = 4–7).

Since Na^+/K^+-ATPase α_1 subunit protein expression is unaltered by hydroxylase inhibition, we next examined the possibility that altered trafficking to be plasma membrane might be involved. To this end, we first employed an immunohistochemical approach. Cells were cultured on transparent permeable supports and treated with DMOG (1 mM) for 24 hours. As shown in Figure 4–15 Na^+/K^+-ATPase α_1 subunit is highly expressed on the basolateral side of T_{84} cells. However, using this approach we found that there was no alteration in membrane localisation of the Na^+/K^+-ATPase α_1 subunit in DMOG-treated cells.

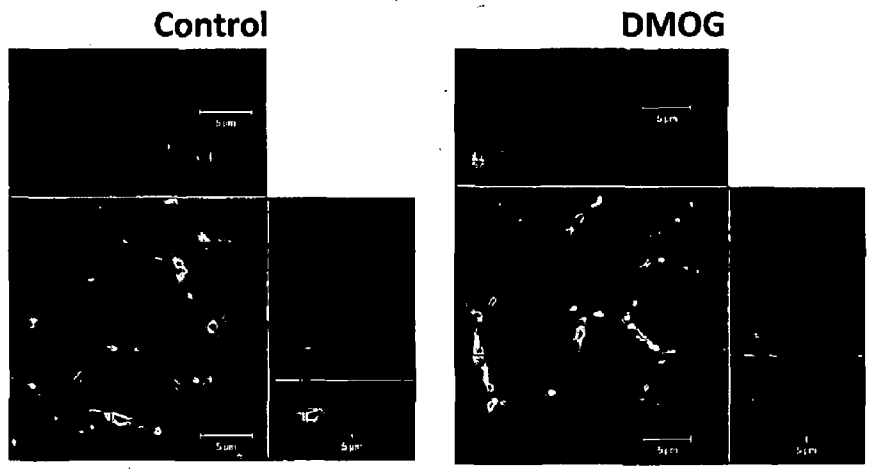

Figure 4–15 Hydroxylase inhibition does not alter Na^+/K^+-ATPase α_1 subunit membrane localisation in T_{84} cells. T_{84} cells were cultured as monolayers on permeable supports until R_{te} stabilised at plateau levels. Cells were treated bilaterally with DMOG (1 mM) in serum free medium for 24 hours. Cells were then washed in PBS, fixed in 100 % methanol, permeabilised with Triton X-100, and stained with specific fluorophore-labelled antibodies, as outlined in Section 2–3. Pseudo-colours were assigned to the various proteins, with the Na^+/K^+-ATPase α_1 subunit being represented in green. This image is representative of 4 similar experiments.

As an alternative approach, surface expression of the Na^+/K^+-ATPase α_1 subunit was next investigated by cell surface biotinylation. In agreement with our immunohistochemical findings, these experiments revealed there to be equal amounts of Na^+/K^+-ATPase α_1 subunit present in the basolateral membrane of control and DMOG-treated cells (Figure 4–16).

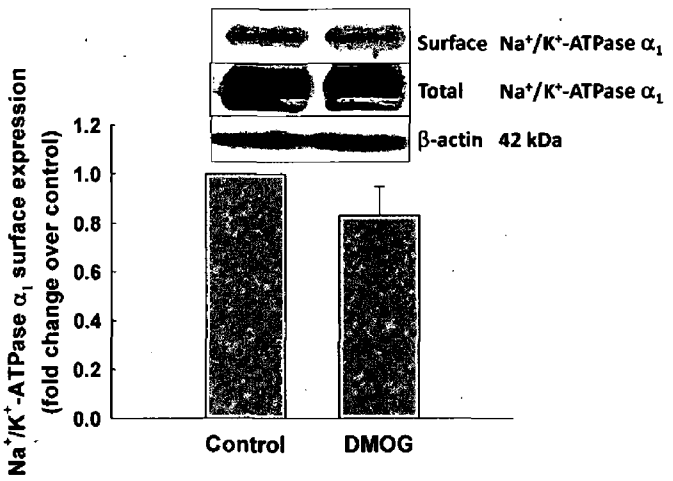

Figure 4–16 Hydroxylase inhibition does not alter surface expression of the Na^+/K^+-ATPase α_1 subunit in T_{84} cells. T_{84} cells were grown as monolayers on permeable supports until R_{te} stabilised at plateau levels. Cells were treated bilaterally with DMOG (1 mM) in serum-free medium for 24 hours. Cells were then biotinylated and lysed, and surface Na^+/K^+-ATPase α_1 subunit protein expression was expressed as a factor of total protein. Protein expression was measured by western blot. β-actin was used as a loading control (n = 4).

4-3.5 Hydroxylase inhibition does not alter ATP levels in T_{84} cells

As described above, the Cl^- secretory mechanism is a highly energy dependent process that derives its electrochemical driving force from Na^+/K^+-ATPase pump activity. Na^+/K^+-ATPase pumps are known to use large quantities of cellular ATP (Milligan and McBride, 1985). Interestingly, the catalytic subunit of ATP synthase, which is responsible for ATP synthesis, contains a putative prolyl hydroxylation motif, LXXLAP (Table 4–1). Therefore, with this in mind, we next investigated if alterations in ATP synthase or ATP generation might underlie the effects of DMOG on Na^+/K^+-ATPase pump activity.

Table 4–1 ATP synthase α amino acid sequence contains a putative prolyl hydroxylation motif.

HUMAN ATP synthase subunit α
MLSVRVAAAVVRALPRRAGLVSRNALGSSFIAARNFHASNTHLQKTGTAEMSSILEERILG ADTSVDLEETGRVLSIGDGIARVHGLRNVQAEEMVEFSSGLKGMSLNLEPDNVGVVVFG NDKLIKEGDIVKRTGAIVDVPVGEELLGRVVDALGNAIDGKGPIGSKTRRRVGLKAPGIIPRI SVREPMQTGIKAVDSLVPIGRGQRELIIGDRQTGKTSIAIDTIINQKRFNDGSDEKKKLYCIY VAIGQKRSTVAQLVKRLTDADAMKYTIVVSATASDAAP**LQYLAP**YSGCSMGEYFRDNGK HALIIYDDLSKQAVAYRQMSLLLRRPPGREAYPGDVFYLHSRLLERAAKMNDAFGGGSLTA LPVIETQAGDVSAYIPTNVISITDGQIFLETELFYKGIRPAINVGLSVSRVGSAAQTRAMKQV AGTMKLELAQYREVAAFAQFGSDLDAATQQLLSRGVRLTELLKQGQYSPMAIEEQVAVIY AGVRGYLDKLEPSKITKFENAFLSHVVSQHQALLGTIRADGKISEQSDAKLKEIVTNFLAGFE A

First, protein expression of the ATP synthase α subunit was investigated. T_{84} cells were treated with DMOG (1 mM) for different periods of time up to 24 hours. After cell lysis, proteins were resolved by SDS-PAGE, and probed for the ATP synthase α subunit by western blotting. It was found that protein expression of ATP synthase α was not significantly altered following hydroxylase inhibition with DMOG (Figure 4–17).

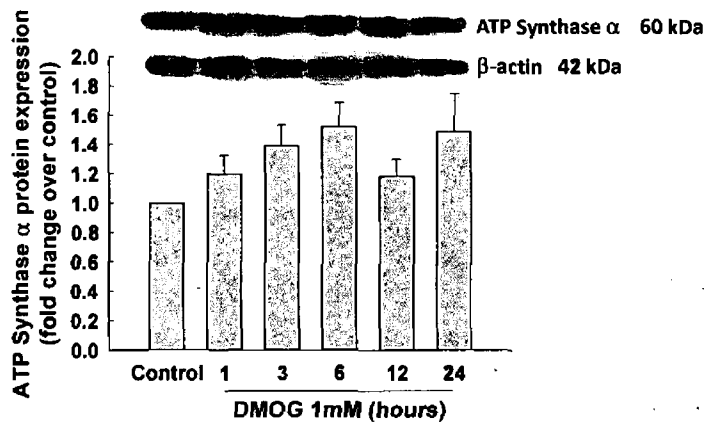

Figure 4–17 Hydroxylase inhibition does not alter ATP synthase α protein expression in T_{84} cells. T_{84} cells were cultured as monolayers on permeable supports until R_{te} stabilised at plateau levels. Cells were treated bilaterally with DMOG (1 mM) in serum-free medium for various periods of time. Cells were then lysed and ATP synthase α protein expression was analysed by western blotting. β–actin was used as a loading control (n = 4).

Hypoxia is known to reduce cellular ATP production due to a metabolic switch from oxidative phosphorylation to glycolysis (Semenza, 2007). Such effects can be detrimental if insufficient ATP is produced to meet the requirements of the cell. D-fructose has been shown to prevent hypoxic cell death in the liver by supplying ATP via glycolysis (Anundi *et al.*, 1987) Therefore, we carried out similar experiments to determine if supplementation of the culture medium with D-fructose altered the antisecretory effect of DMOG treatment in T_{84} cells. However, as shown in Figure 4–18, we found that pretreatment with D-fructose (20 mM) did not ameliorate the antisecretory effects of hydroxylase inhibition in T_{84} cells.

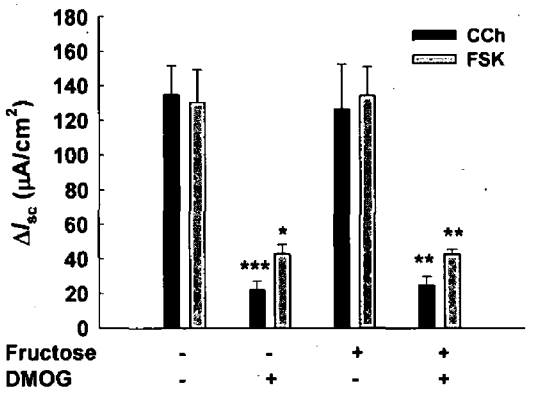

Figure 4–18 D-fructose does not ameliorate the antisecretory effects of hydroxylase inhibition in T_{84} cells. T_{84} cells were cultured as monolayers on permeable supports until R_{te} stabilised at plateau levels. 24 hours prior to treatment, cells were cultured in D-glucose-free, high D-fructose (20 mM), medium. Cells were then treated bilaterally with DMOG (1 mM) for 24 hours in serum-free medium containing D-fructose. Monolayers were washed, mounted in Ussing chambers and bathed in D-fructose Ringer's solution (Table 2–4). Subsequent secretory responses to CCh (100 μM) and FSK (10 μM) were recorded. Data are expressed as maximal changes in stimulated current (ΔI_{sc}) (n = 3, ANOVA; * $p \leq 0.05$; ** $p \leq 0.01$; *** $p \leq 0.001$ compared to respective controls).

Since Na^+/K^+-ATPase pumps use large quantities of cellular ATP, the ATP content of control and DMOG-treated cells was next investigated (Milligan and McBride, 1985). Using a commercially available kit, ATP levels of T_{84} cells treated with DMOG (1 mM) for 1, 3, or 24 hours were found to be no different to those of control cells. D-fructose treatment was also without effect on cellular ATP levels (Figure 4–19).

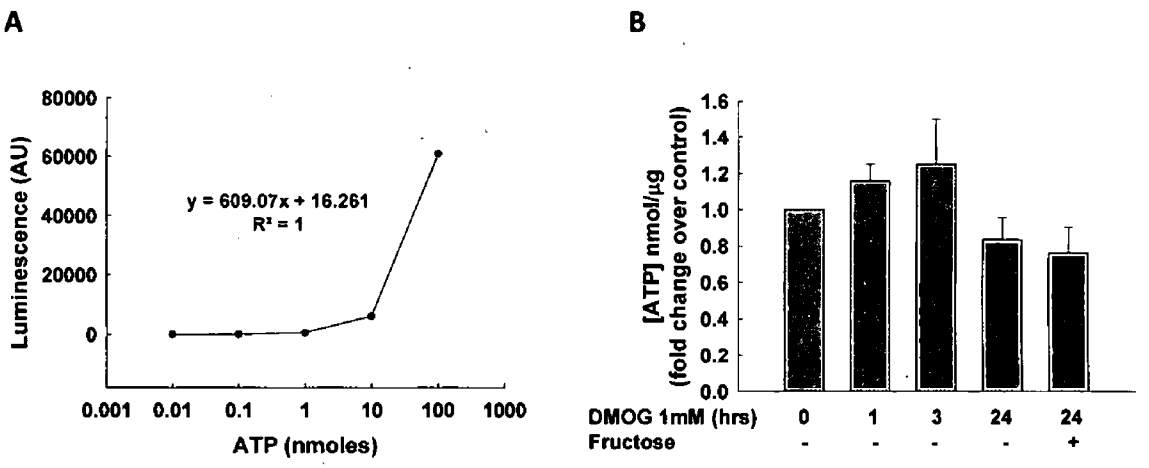

Figure 4-19 Hydroxylase inhibition does not alter ATP levels in T_{84} cells. T_{84} cells were grown as monolayers on permeable supports until R_{te} stabilised at plateau levels. Cells were treated bilaterally with DMOG (1 mM) in serum-free medium for 0, 1, 3, and 24 hours. D-fructose (20 mM) was substituted for D-glucose in one set of treatments. **A)** A standard curve of ATP concentration was generated using reagents supplied with the commercially available kit. **B)** Cells were lysed and the ATP content of DMOG- and D-fructose-treated cells was measured by extrapolation from the standard curve (n = 13).

4-3.6 The PHD inhibitor, FG-4497, exerts anti-secretory actions in T_{84} cells and inhibits Na^+/K^+-ATPase activity

FG-4497 is a hydroxylase inhibitor developed by FibroGen Inc. This small molecule inhibitor, specific for PHD enzymes, was previously disclosed in a patent filing, US20040254215A1. However, unlike DMOG, which is a pan-hydroxylase inhibitor, FG-4497 is reported to be specific for the HIF-prolyl hydroxylases. During the course of my PhD studies an opportunity to collaborate with FibroGen Inc. arose and we took this opportunity to employ FG-4497 to confirm our previous findings with DMOG. We first analysed the effects of FG-4497 on agonist-induced secretory responses and HIF-1α levels (Figure 4–20).

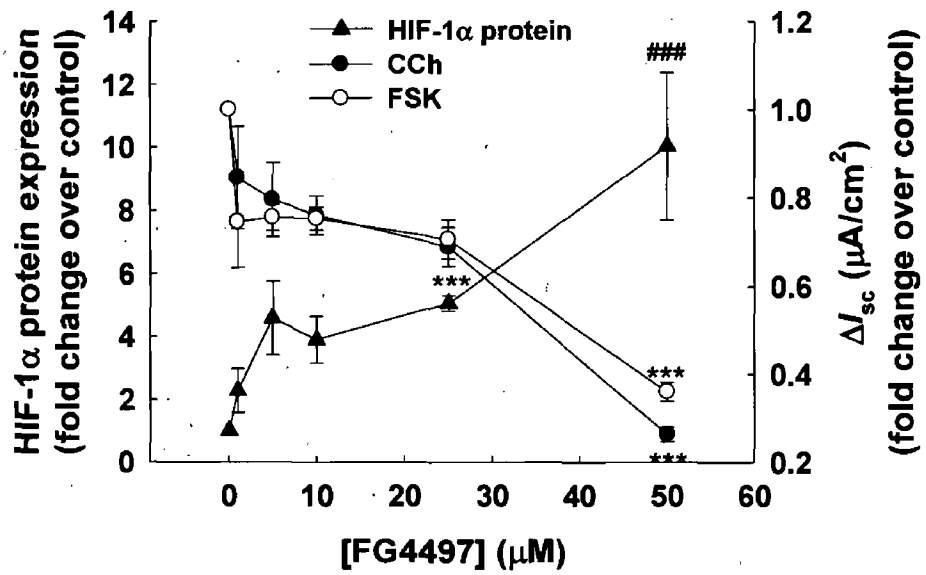

Figure 4–20 FG-4497 attenuates Cl^- secretion, and causes HIF-1α accumulation in a *concentration-dependent manner in T_{84} cells.* T_{84} cells were cultured as monolayers on permeable supports until R_{te} stabilised at plateau levels. Cells were treated bilaterally with various concentrations of FG-4497 for 24 hours. For protein expression analysis, cells were lysed and HIF-1α expression was measured by western blotting. β-actin was used as a loading control (n = 4; ANOVA, ### $p \leq 0.001$ compared to 0 μM FG4497). For electrophysiological experiments, cells were mounted in Ussing chambers, bathed in Ringer's solution (Table 2–3), and stimulated with basolateral CCh (100 μM), and apical FSK (10 μM) (n = 4; ANOVA, *** $p \leq 0.001$ compared to 0 μM FG4497).

In collaboration with FibroGen Inc. we also measured HIFα levels by an alternative approach using an MSD assay developed in their laboratories. T_{84} cells were cultured as monolayers on permeable supports, and were treated with FG-4497 at various concentrations for 24 hours. Hydroxylase inhibition by FG-4497 resulted in a robust accumulation of both HIFα isoforms. HIF-1α protein increased from 474.76 ± 149.84 ng/ml in controls to 1324.84 ± 397.96 ng/ml in FG-4497 (50 μM; 24 hours)-treated cells, while HIF-2α protein increased from 19.06 ± 8.21 ng/ml in controls to 167.41 ± 34.48 ng/ml in FG-4497-treated cells (Figure 4–21).

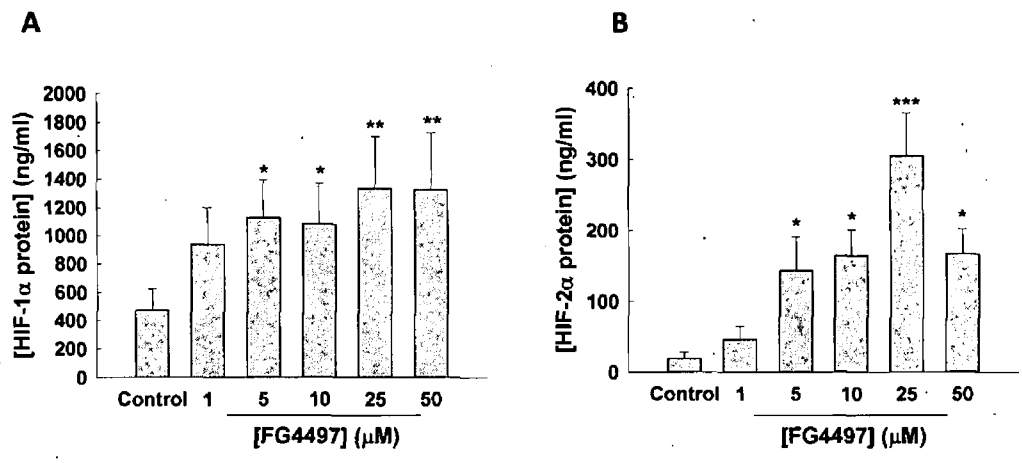

Figure 4–21 Hydroxylase inhibition by FG-4497 stimulated accumulation of HIF-1α and HIF-2α in T_{84} cells. T_{84} cells were grown as monolayers on permeable supports until R_{te} stabilised at plateau levels. Cells were treated bilaterally with various concentrations of FG-4497 in serum free medium for 24 hours. Proteins were extracted and MSD assays were performed (Section 2–19). Concentrations of **A)** HIF-1α and **B)** HIF-2α were extrapolated from standard curves generated (n = 4; ANOVA, * $p \leq 0.05$; ** $p \leq 0.01$; *** $p \leq 0.001$ compared to controls).

Using the experimental conditions optimised in Figure 4–12, cells were next treated with FG-4497 (50 μM; 24 hours) or DMOG (1 mM; 24 hours), and Na^+/K^+-ATPase activity was measured. Cells were mounted in Ussing chambers, apically permeabilised with amphotericin B (50 μM) and stimulated with basolateral CCh (100 μM). Similar to our previous observations with DMOG, we found that there was a significant attenuation of CCh-stimulated Na^+/K^+-ATPase activity in FG-4497-treated cells (Figure 4–22).

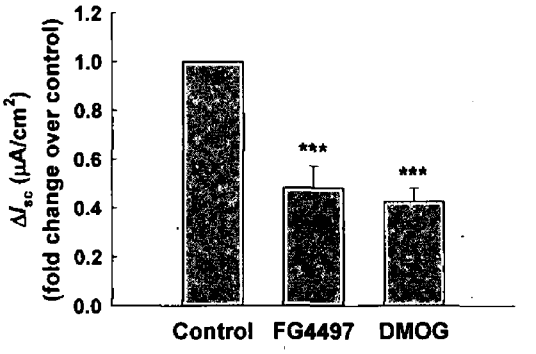

Figure 4–22 Na^+/K^+-ATPase activity is significantly attenuated in FG-4497-treated T_{84} cells. T_{84} cells were cultured on permeable supports until R_{te} stabilised at plateau levels. Cells were treated with FG-4497 (50 μM; 24 hours),or with DMOG (1 mM; 24 hours), washed, mounted in Ussing chambers, and bathed in Ringer's solution containing 25 mM Na^+ (Table 2-7). Cells were apically permeabilised with amphotericin B (50 μM) for 30 minutes. Basolateral CCh (100 μM) was then added to the cells to stimulate Na^+/K^+-ATPase activity. Maximal CCh-induced currents were plotted as ΔI_{sc} (n = 5–6; ANOVA; *** $p \leq 0.001$ compared to control).

4-3.7 $CoCl_2$ stabilises HIF-1α protein expression and attenuates Cl^- secretion independently of Na^+/K^+-ATPase activity

In order to further define the mechanisms by which hydroxylase inhibition might regulate epithelial secretory responses, we employed $CoCl_2$. $CoCl_2$ causes FIH-1-independent accumulation of HIF-1α (Tian *et al.*, 2011b), but also inhibits HIF-1α degradation in a different manner to DMOG and FG4497. $CoCl_2$ inhibits VHL-mediated degradation of HIF-1α by directly blocking the binding site of pVHL on HIF-1α (Yuan *et al.*, 2003). Co^{2+} is also known to deplete the cell of ascorbate, an essential cofactor for hydroxylase activity (Salnikow *et al.*, 2004). In initial experiments we set out to determine appropriate $CoCl_2$ concentrations to employ by examining its effects on LDH release and R_{te} as indices of toxicity. There was no increase in LDH release from T_{84} cells treated with $CoCl_2$ at concentrations as high as 1 mM (Figure 4-23 A). Similarly, after treatment with $CoCl_2$ at a concentration of 500μM, R_{te} did not significantly change compared to that of the cells prior to treatment (Figure 4-23 B).

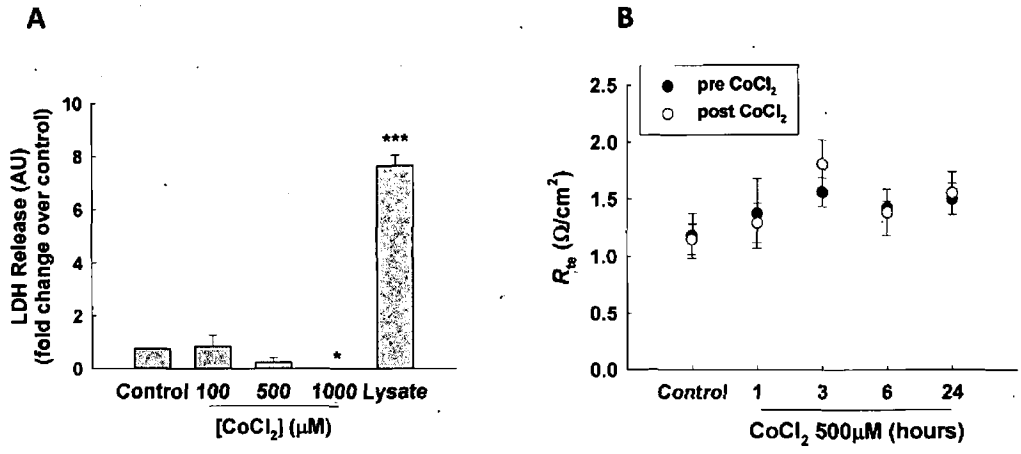

Figure 4–23 $CoCl_2$ does not exert toxic effects on T_{84} cells. T_{84} cells were cultured on permeable supports until R_{te} stabilised at plateau levels. **A)** Cells were treated bilaterally with varying concentrations of $CoCl_2$ for 24 hours. Lysate cells were treated with lysis buffer for a minimum of 30 minutes prior to analysis. An equal aliquot of apical and basolateral culture medium was taken and LDH released into the culture medium was measured using a commercially available kit (Section 2–16) (n = 3–6; ANOVA; * $p \leq 0.05$; *** $p \leq 0.001$ compared to control). **B)** Cells were treated bilaterally with $CoCl_2$ (500 μM) for defined periods of time and subsequent R_{te} measurements were recorded using an epithelial voltohmeter (n = 4)

We next examined the effects of $CoCl_2$ on HIF-1α protein expression in T_{84} cells. Cells were treated with various concentrations of $CoCl_2$ in order to determine an optimal concentration for $CoCl_2$ –induced HIF-1α stabilisation. As shown in Figure 4–24, HIF-1α robustly accumulates in T_{84} cells treated with 500 μM $CoCl_2$.

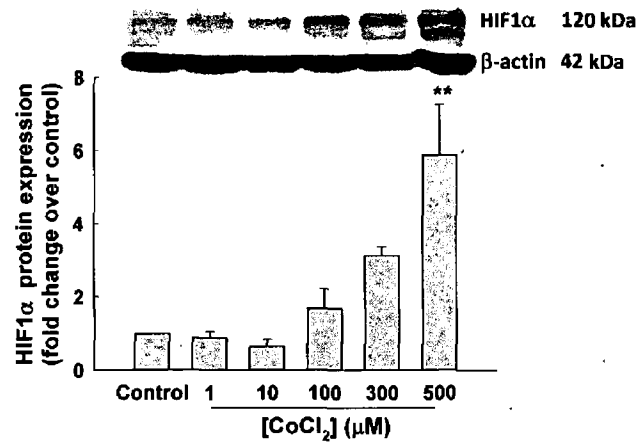

Figure 4–24 $CoCl_2$ stabilises HIF-1α protein expression in T_{84} cells. T_{84} cells were cultured on permeable supports until R_{te} stabilised at plateau levels. Cells were treated bilaterally with various concentrations of $CoCl_2$ in serum-free medium for 24 hours, after which HIF-1 α protein expression was measured by western blotting. β-actin was used as a loading control (n = 3; ANOVA, $^{**}p \leq 0.01$ compared to control).

The effects of $CoCl_2$ on epithelial secretory function were next examined. Similar to DMOG, it was found that treatment of T_{84} monolayers with $CoCl_2$ (500 μM) for 24 hours exerted a profound antisecretory effect on the cells. Secretory responses to CCh (100 μM) and FSK (10 μM) were attenuated to 51.63 ± 8.12 % (n = 4; ** $p \leq 0.01$) and 53.03 ± 8.43 % (n = 4; ** $p \leq 0.01$) of those in control cells, respectively (Figure 4–25).

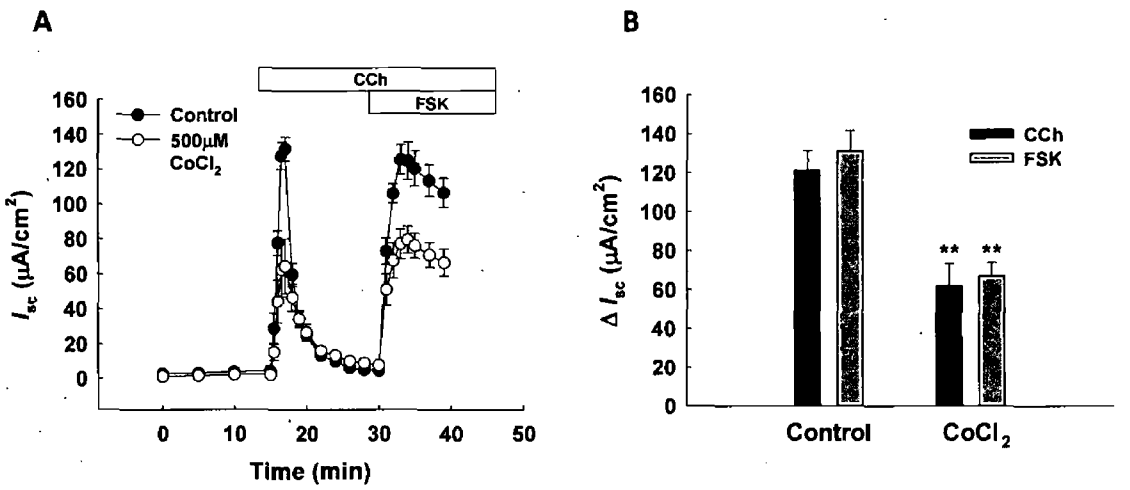

Figure 4–25 $CoCl_2$ attenuates agonist-induced Cl^- secretory responses in T_{84} cells. T_{84} cells were cultured on permeable supports until R_{te} stabilised at plateau levels. Cells were treated bilaterally with $CoCl_2$ (500 μM) in serum-free medium for 24 hours. Cells were then washed, mounted in Ussing chambers, bathed in Ringer's solution (Table 2–3), and subsequent Cl^- secretory responses to basolateral CCh (100 μM) and apical FSK (10 μM) were measured (n = 4; ANOVA; ** $p \leq 0.01$ compared to control). Panel **A** shows the time course of these experiments while Panel **B** shows maximal secretory responses, measured as ΔI_{sc}, to CCh and FSK in the absence or presence of $CoCl_2$.

In further experiments the effects of $CoCl_2$ on agonist-stimulated Cl^- secretion were found to be concentration-dependent. When cells were treated with $CoCl_2$ for 24 hours, antisecretory effects were maximal at a concentration of 500 μM (Figure 4–26 A). The effects of $CoCl_2$ (500 μM) were also time-dependent, being maximal at 24 hours for cAMP-mediated responses and between 6–24 hours for Ca^{2+}-dependent responses (Figure 4–26 B).

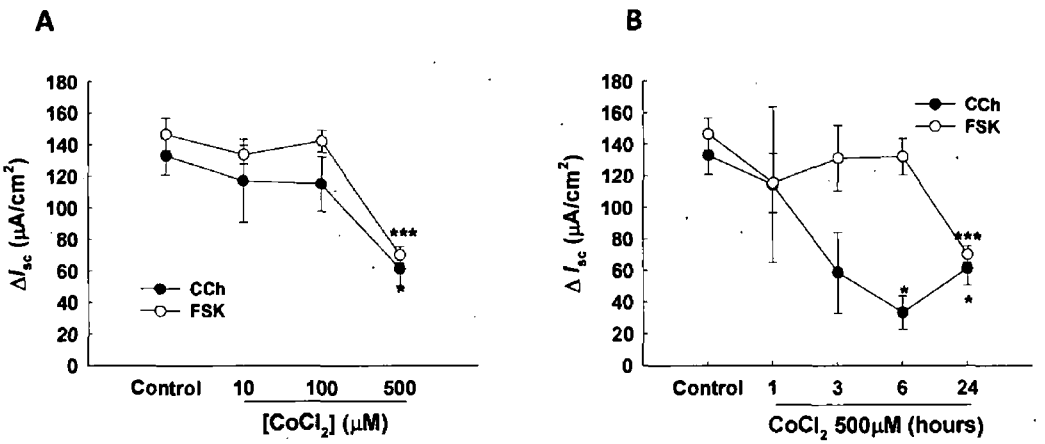

Figure 4–26 The antisecretory effect of $CoCl_2$ in T_{84} cells is time- and concentration-dependent. T_{84} cells were cultured on permeable supports until R_{te} stabilised at plateau levels. **A)** Cells were treated bilaterally with DMOG (1 mM) in serum-free medium for various time points. Cells were then washed, mounted in Ussing chambers, bathed in Ringer's solution (Table 2–3), and subsequent Cl^- secretory responses to basolateral CCh (100 μM) and apical FSK (10 μM) were measured (n = 4–8; ANOVA, * $p \leq 0.05$; *** $p \leq 0.001$ compared to control). **B)** Cells were treated bilaterally with $CoCl_2$ (500 μM) in serum-free medium for various times up to 24 hours before responses to basolateral CCh (100 μM) and apical FSK (10 μM) were measured in Ussing chambers (n = 4; ANOVA, * $p \leq 0.05$; *** $p \leq 0.001$ compared to control).

Potential mechanisms underlying the antisecretory effect of $CoCl_2$ in T_{84} cells were next investigated. Apical Cl^- currents, measured as previously described (Rochwerger *et al.*, 1994), were first investigated since $CoCl_2$ has previously been shown to inhibit Cl^- secretion in T_{84} cells (Taylor *et al.*, 1998). Apical Cl^- conductance was found to be significantly attenuated by $CoCl_2$ treatment (Figure 4–27 A). However, in direct contrast to our observations with DMOG, Na^+/K^+-ATPase activity was unaffected by treatment with $CoCl_2$ (Figure 4–27 B).

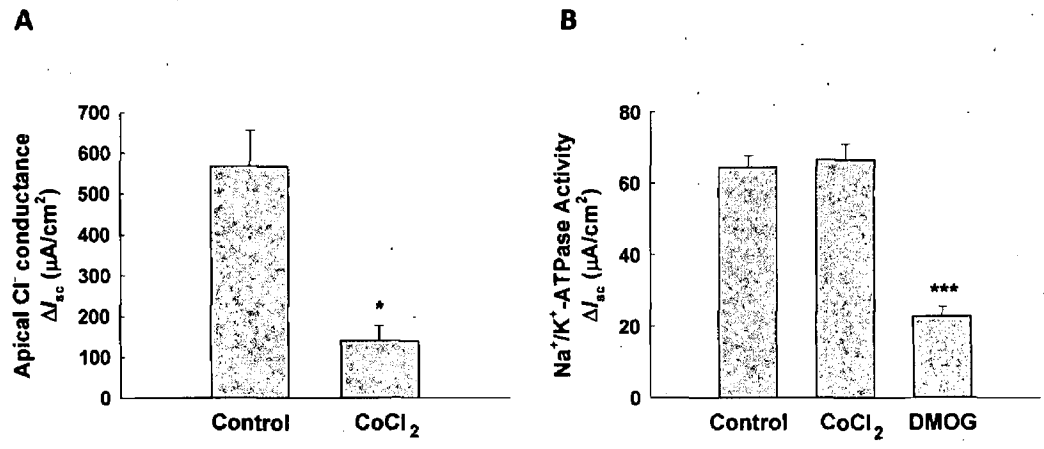

Figure 4–27 $CoCl_2$ attenuates apical Cl^- currents but not Na^+/K^+-ATPase activity in T_{84} cells. T_{84} cells were cultured as monolayers on permeable supports until R_{te} stabilised at plateau levels. Cells were treated bilaterally with $CoCl_2$ (500 μM) in serum-free medium for 24 hours. Cells were washed and mounted in Ussing chambers. **A)** For apical Cl^- conductance experiments the apical bath contained Ringer's solution (Table 2-3), whereas the basolateral bath contained a low [Cl^-] solution (Table 2-5). Cells were permeabilised by basolateral nystatin (100 μg/ml) after which apical FSK (10 μM) was added to stimulate Cl^- currents. Maximal changes in current were plotted as ΔI_{sc} (n = 3; unpaired t-test; * $p \leq 0.05$). **B)** For measurements of Na^+/K^+-ATPase activity, cells were bathed bilaterally in Ringer's solution containing 25 mM Na^+ (Table 2-7). Cells were apically permeabilised with amphotericin B (50 μM) after which basolateral CCh (100 μM) was added to stimulate Na^+/K^+-ATPase activity. Maximal changes in current were plotted as ΔI_{sc} (n = 3–6; ANOVA; *** $p \leq 0.001$ compared to control).

4-3.8 EIPA reverses the inhibitory effect of DMOG on Na^+/K^+-ATPase activity

Finally, having previously shown that chronic inhibition of NHEs by EIPA, in the presence of DMOG, reversed the antisecretory effect of DMOG, we wished to investigate whether this was due to a reversal of the inhibitory effect of DMOG on Na^+/K^+-ATPase activity. Indeed, chronic treatment of cells with EIPA (50 μM; 24 hours) in the presence of DMOG, reversed the inhibitory effects on Na^+/K^+-ATPase pump activity (Figure 4–28).

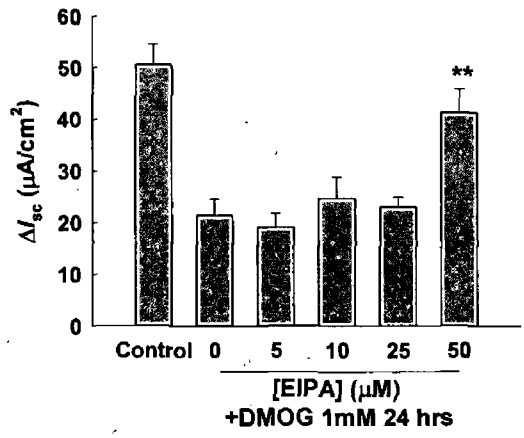

Figure 4–28 Chronic NHE inhibition by EIPA reverses inhibition of the Na^+/K^+-ATPase by DMOG. T_{84} cells were grown as monolayers on permeable supports until R_{te} stabilised at plateau levels. Cells were treated bilaterally with DMOG (1 mM; 24 hours) in serum free medium in the presence or absence of EIPA (5–50 μM; 24 hours). Cells were washed, mounted in Ussing chambers and bathed in low [Na^+] Ringer's solution (Table 2–7). After an initial stabilisation period EIPA was added to designated chambers. Cells were apically permeabilised with amphotericin B (50 μM) after which basolateral CCh (100 μM) was added to stimulate Na^+/K^+-ATPase activity. Maximal changes in current were plotted as ΔI_{sc} (n = 6; ANOVA, ** $p \leq 0.01$ compared to 0 μM EIPA).

4-4 Discussion

The main aim of this chapter was to identify specific transport proteins that may be targets of hydroxylase inhibitors in colonic epithelial cells and that could mediate their anti-secretory actions. Since previous studies have shown that CFTR may be a target of hydroxylase inhibition, we initiated these studies with experiments to study the effects of DMOG on CFTR function (Zheng *et al.*, 2009). Initially, the activity of CFTR was assessed using a modification of the Ussing chamber/voltage clamp technique (Rochwerger *et al.*, 1994). In these experiments the term apical Cl^- current was equated to CFTR activity based on the fact that the CFTR-specific inhibitor, $CFTR_{inh172}$, inhibited the apical Cl^- currents by approximately 78 % (Caci *et al.*, 2008). However, it was found that apical Cl^- currents in T_{84} cells treated with DMOG (1 mM) for 24 hours were no different to those of controls. These findings were initially perplexing since, consistent with previous reports, expression analysis of CFTR showed a robust down regulation in response to hydroxylase inhibition (Zheng *et al.*, 2009). One possible explanation for this was that DMOG might induce the expression of another type of apical Cl^- channel that compensates for loss of CFTR expression. However, this does not seem likely since it was found that, similar to its effects in control cells, $CFTR_{inh172}$ also attenuated apical Cl^- currents in DMOG-treated T_{84} cells by 78%. Furthermore, DMOG did not alter the expression of the Ca^{2+}-dependent Cl^- channel, TMEM16A, at least at the level of mRNA expression. However, an alternative explanation for these apparently conflicting data, that CFTR activity is unaffected while its expression is abated, could come from previous observations that only 20 % of normal CFTR expression is required to maintain cAMP-dependent secretory responses in epithelial cells (De Jonge, 2006). Thus, despite the impact of hydroxylase inhibition on CFTR expression, it does not seem likely that this is a predominant factor mediating attenuation of intestinal secretory responses by hydroxylase inhibition.

Having ruled out the potential involvement of altered apical Cl^- conductances in mediating antisecretory actions of hydroxylase inhibitors, we next turned our attention to basolateral K^+ channels. Recent studies have highlighted the role that K^+ channels play in luminal anion secretion in the intestine, while others have shown that they are important regulators of fluid homeostasis (Flores *et al.*, 2007; O'Mahony *et al.*, 2007). Isolation of basolateral K^+ conductances was achieved by modification of a previously published protocol (Kirk and Dawson, 1983). However, these experiments did not reveal any differences in K^+ currents stimulated by the Ca^{2+}-dependent secretagogue, CCh, between control and DMOG-treated cells. However, it should be noted that this protocol is somewhat limited for 2 main reasons. Firstly, it only allows for the isolation of K^+ conductances through basolateral KCNN4, and therefore potential effects on apical KCNN4 cannot be ruled out. It may be possible to investigate this in future studies by reversing the K^+ gradient and permeabilising the basolateral membrane. However, if such an action of hydroxylase inhibition on apical KCNN4 occurs, it is not likely to be as a consequence of altered protein expression, since the 37 kDa band that represents the apical isoform was unaltered following DMOG treatment. Secondly, this protocol only allows for isolation of Ca^{2+}-activated K^+ currents, whereas cAMP-activated currents through KCNQ1 are not detected in this activity assay. Potential effects of hydroxylase inhibition on KCNQ1 activity would require further analysis. Interestingly, we did observe a small, but significant, increase in the basal K^+ currents in DMOG-treated cells. This phenomenon could be explained by an increase in KCNQ1 activity, however, this hypothesis was not supported by any alterations in the expression of either KCNN4 or KCNQ1 at mRNA or protein levels.

We next turned our attention to studying a role for hydroxylases in regulating the Na^+/K^+-ATPase pump. The Na^+/K^+-ATPase pump consists of 2 subunits, a regulatory β subunit and a catalytic α subunit that pumps 3 Na^+ ions from the cell in exchange for 2 K^+ ions with each cycle of ATP cleavage (Skou, 1998;

Kaplan, 2002). The normal Ringer's solution which has been used throughout this thesis in unpermeabilised cells contains 140 mM Na^+. Such levels of Na^+ are normally used in studies of epithelial function, as they are similar to those present in the intestine *in vivo*. However, since intracellular [Na^+] is normally considerably lower (approximately 25 mM) than 140 mM, we speculated that at such high concentrations intracellular Na^+ would drive the Na^+/K^+-ATPase pump at its V_{max}, potentially masking any effects of hydroxylase inhibition. Thus, we employed a bathing solution which contained 25 mM Na^+. Upon measurement of Na^+/K^+-ATPase activity, it was found that hydroxylase inhibition significantly attenuated CCh-stimulated pump activity. Interestingly, basal pump activity was also significantly reduced in DMOG-treated cells. This suggests that the mechanisms underlying the antisecretory actions of hydroxylase inhibition affect the pump itself, and are not due to alterations in the signalling pathway that links the muscarinic M_3 receptor to pump activation.

The relatively slow kinetics for the onset of the antisecretory effects of hydroxylase inhibition suggest that alterations in expression of the Na^+/K^+-ATPase may be involved. However, this does not appear to be the case, since neither mRNA nor protein levels of the catalytic subunit were altered in DMOG-treated cells. Several studies suggest that Na^+/K^+-ATPase activity can also be regulated through altered trafficking of the α subunit to the cell membrane (Chow and Forte, 1995). However, examination of Na^+/K^+-ATPase α_1 subunit localisation by confocal microscopy and cell surface biotinylation revealed that this too was unaltered by hydroxylase inhibition.

As already mentioned, the Na^+/K^+-ATPase requires a significant quantity of cellular ATP for its functioning, and hypoxia is known to reduce mitochondrial ATP production, therefore limiting its availability for the pump (Milligan and McBride, 1985; Papandreou *et al.*, 2006). HIF also has the capacity to downregulate ATP synthesis in conditions of hypoxia, while MYC-associated factor X interactors (MXIs) have been shown to attenuate mitochondrial

biogenesis in response to HIF, and therefore cause ATP depletion (Semenza, 2007; Zhang *et al.*, 2007). Other research has shown that cellular damage and reductions in ATP levels that occur as a consequence of hypoxia/reperfusion injury, can be reversed by forcing the cell into glycolytic metabolism (Anundi *et al.*, 1987; Kim *et al.*, 2003). In this manner, D-fructose is taken up by the cell through apical GLUT5 transporters, thereby promoting an increase in glycolytic generation of ATP. Furthermore, ATP synthase, an important enzyme for production of cellular ATP, contains a putative prolyl hydroxylation motif in the catalytic α subunit which may have an impact on its expression or function.

Therefore, the question arose as to whether hydroxylase inhibition could attenuate the activity of the Na^+/K^+-ATPase by reducing cellular ATP levels. However, we found that hydroxylase inhibition by DMOG did not alter ATP levels in T_{84} cells. This may be accounted for by the fact that O_2 is not a limiting factor in the present studies, and therefore glycolysis is being promoted in aerobic conditions, as occurs with the Warburg effect (Warburg, 1956; Ferreira, 2010; Koppenol *et al.*, 2011). Our findings are consistent with a previous study showing that DMOG does not cause an increase in cellular ROS production, indicating no uncoupling of the electron transport chain and thus no reduction of mitochondrial ATP synthesis (Emerling *et al.*, 2007). Furthermore, another study showed that pretreatment of cardiomyocytes with DMOG preserved cellular ATP levels, even though O_2 consumption was reduced by approximately 85 % and ATP turnover rate was inhibited by 75 % (Sridharan *et al.*, 2008). Preservation of ATP levels was due to a shift in cellular metabolism, with ATP production from glycolysis increasing to 40 %. Such shifts can occur when the ratio of energy supply to demand decreases, as in chronic hypoxia, and cellular homeostatic mechanisms attempt to balance ATP production to utilization (Budinger *et al.*, 1996; Budinger *et al.*, 1998; Chandel *et al.*, 1997; Papandreou *et al.*, 2006; Wheaton and Chandel, 2011). Therefore, ATP concentration can remain relatively stable during hypoxia and it is therefore not the most sensitive index of cellular energy status. To promote the glycolytic pathway of ATP

synthesis, cells were cultured with D-fructose. However, we found that T_{84} cells cultured in D-fructose, with or without DMOG, exhibited no alterations in ATP content, nor was there a reversal of the antisecretory effect of hydroxylase inhibition. However, firm conclusions cannot yet be drawn from these experiments, since additional studies are required to investigate whether T_{84} cells even express functional GLUT5 transporters. Finally, we found by western blot analysis that expression of the ATP synthase α subunit, which contains a putative prolyl hydroxylation motif, is not altered by DMOG treatment, further supporting the idea that hydroxylase inhibition does not alter ATP levels in T_{84} cells.

As previously stated DMOG is a non-specific 4-prolyl hydroxylase inhibitor and is not specific for hydroxylases activated during hypoxia. Therefore, in collaboration with FibroGen Inc., we obtained the use of their proprietary compound, FG-4497, which blocks the active site of the HIF hydroxylases (Fraisl *et al.*, 2009). Importantly, for the current studies, we found that effects of hydroxylase inhibition with DMOG, which works by mimicking α-ketoglutarate, were recapitulated with FG-4497. Antisecretory effects of FG-4497 were slow in onset and were only present at relatively high concentrations, in excess of those which stabilise HIF-1α and HIF-2α. Furthermore, FG-4497, similar to DMOG, also potently inhibited Na^+/K^+-ATPase activity. Thus, our data suggest that the antisecretory effects of hydroxylase inhibitors are mediated by HIF-hydroxylases, but in a manner that is independent of HIF-1 activation.

In order to further define the mechanisms by which hydroxylase inhibition might regulate epithelial secretory responses, $CoCl_2$ was employed to stabilise HIF-α, by mechanisms distinct from those of DMOG and FG4497. $CoCl_2$ is well documented as a hypoxia mimetic and as a HIF-1α stabiliser, although little is known of the mechanism involved. Researchers investigating the molecular mechanisms of the $CoCl_2$-mediated stabilisation of HIF-1α have reported that $CoCl_2$ inhibits VHL-mediated degradation of HIF-1α by directly binding to the 2

PER-ARNT-SIM domains on the N-terminal region of HIF-1α, thus blocking the binding site for VHL on HIF-1α (Kanaya and Kamitani, 2003; Yuan *et al.*, 2003). More recent studies showed that Co^{2+} depleted cells of ascorbate, an essential cofactor of the HIF hydroxylases and it is now known that $CoCl_2$ causes the stabilisation of HIF-1α, but with no effect on FIH-1 activity (Salnikow *et al.*, 2004; Tian *et al.*, 2011b). In initial experiments, conditions with which to use $CoCl_2$ were optimised. While there was no increase in LDH release due to $CoCl_2$ treatment at any concentration tested, R_{te} was completely obliterated at a concentration of 1 mM, and therefore lower concentrations were employed for these studies. We found that $CoCl_2$ increased the accumulation of HIF-1α in a concentration-dependent manner at concentrations that were not toxic to the cells. We also found that not only does $CoCl_2$ attenuate cAMP-mediated Cl^- secretion in T_{84} cells, as previously shown (Taylor *et al.*, 1998), but it also attenuates Ca^{2+}-mediated Cl^- secretion. Further investigation into the mechanisms involved revealed that while apical Cl^- conductances were attenuated by $CoCl_2$, Na^+/K^+-ATPase activity was unaltered. This is in direct contrast to the mechanism elicited by DMOG, which inhibited Na^+/K^+-ATPase but not CFTR activity, suggesting that the antisecretory effects of hydroxylase inhibition by DMOG are likely to be FIH-1-dependent. However, further studies will be required to verify this.

Similar to its effects on CFTR, NKCC1 expression has previously been shown to be transcriptionally repressed by HIF-1 (Ibla *et al.*, 2006). In the current study we found that there was also a significant reduction in expression of NKCC1, both at the mRNA and protein levels, in response to treatment with DMOG. However, investigations into the activity of NKCC1 revealed no appreciable difference following hydroxylase inhibition. Previous studies have shown Cl^- secretion and NKCC1 expression to be more potently attenuated after longer periods of hypoxia (> 24 hours), therefore longer exposure to DMOG may yield similar results (Ibla *et al.*, 2006). The repression of NKCC1 may be an important factor in mediating the antisecretory effects of hydroxylase inhibition since

NKCC1 is the primary entry pathway for Cl^- ions into epithelial cells. Further experiments to investigate the activity and the expression of the co-transporter at later time points would be required to prove this.

4-5 Summary

In summary, our data suggest that the antisecretory effects of hydroxylase inhibition in intestinal epithelial cells occur, at least in part, through inhibition of Na^+/K^+-ATPase activity (Figure 4–29). The effects of hydroxylase inhibition appear to occur in a HIF-independent manner, and are likely to involve FIH-1. Furthermore, the mechanism by which hydroxylase inhibitors attenuate Na^+/K^+-ATPase activity does not appear to involve alterations in cellular ATP or localisation of the protein. Interestingly, previous studies show that there are multiple potential mechanisms by which Na^+/K^+-ATPase pump activity can be regulated without altering its membrane localisation. For example, FXYD proteins are membrane-associated proteins that can regulate pump activity without altering its surface expression (Garty and Karlish, 2006). Similarly, intracellular regulatory proteins, such as translationally-controlled tumour protein (TCTP) and sorting nexin 6 (SNX 6), are emerging as important regulators of Na^+/K^+-ATPase activity (Jung *et al.*, 2004; Yoon *et al.*, 2006). In the next section of this thesis a more detailed analysis of how hydroxylase inhibitors might regulate Na^+/K^+-ATPase activity to exert antisecretory actions on colonic epithelial cells was conducted.

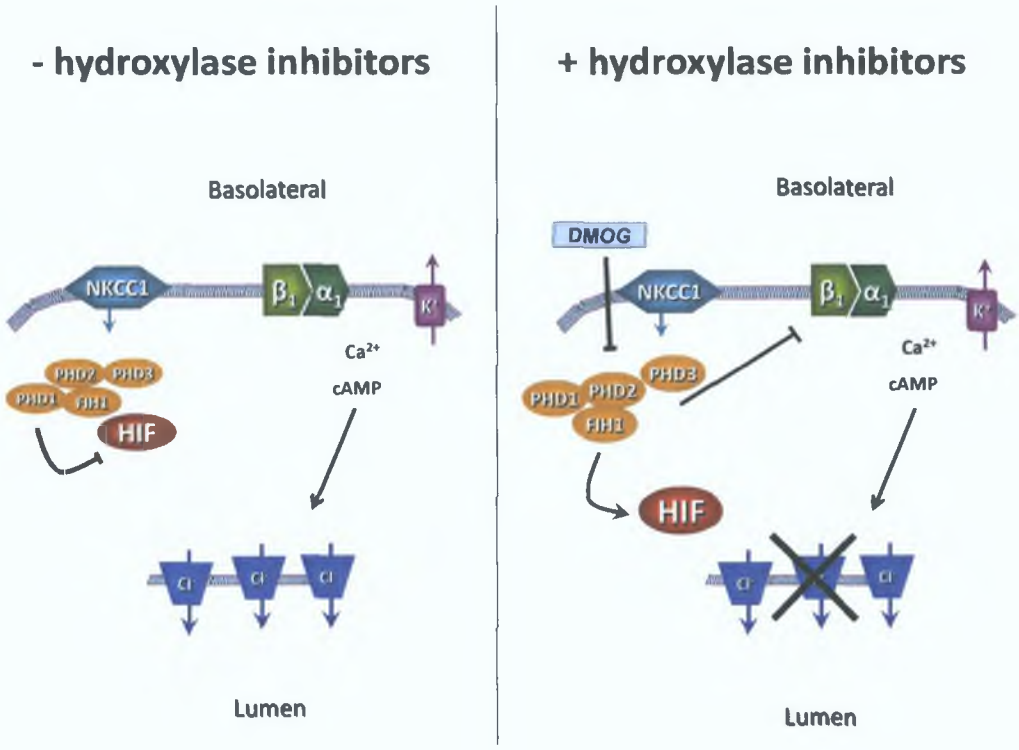

Figure 4-29 Hydroxylase inhibition specifically attenuates Na^+/K^+-ATPase activity in T_{84} cells. Hydroxylase inhibition attenuates luminal Cl^- secretion by a mechanism that involves attenuation of Na^+/K^+-ATPase activity, without altering expression of the pump at the basolateral cell surface. Although hydroxylase inhibitors reduce expression of apical CFTR channels, this does not appear to be a major contributing factor to their antisecretory actions. Our data suggest that the effects of hydroxylase inhibition are likely to occur in a HIF-independent, but FIH-1-dependent manner.

Chapter 5

Molecular mechanisms underlying hydroxylase regulation of Na^+/K^+-ATPase activity

5-1 Introduction

In the previous chapter we revealed a novel role for hydroxylases in regulating intestinal epithelial Na^+/K^+-ATPase activity, an effect that is likely to be important in mediating the antisecretory actions of hydroxylase inhibitors. When considering the use of such drugs as therapeutics, it is important to understand the molecular mechanisms involved. Thus, we next turned our attention to studying potential mechanisms by which hydroxylase inhibitors regulate Na^+/K^+-ATPase activity.

Na^+/K^+-ATPase pumps exist as heterodimers in the plasma membrane, with one α and one β subunit (Craig and Kyte, 1980). However, resolution of the crystal structure of the Na^+/K^+-ATPase in the recent past, also revealed the presence of Na^+/K^+-ATPase γ subunits in renal extracts (Morth *et al.*, 2007). Furthermore, additional studies show that Na^+/K^+-ATPase pumps exist as a complex of different subunits, allowing for tissue-specific regulation (Garty and Karlish, 2006; Yoon *et al.*, 2006). Thus, our knowledge of the structure of the Na^+/K^+-ATPase is constantly evolving, but remains incompletely understood. There are many mechanisms by which the Na^+/K^+-ATPase pump can be regulated, and some of these were investigated in Chapter 4 of this thesis. In our studies, we found that hydroxylase inhibition of pump activity was not due to alterations in its expression or localisation at the plasma membrane, nor was it due to an altered availability of ATP. However, another way by which hydroxylase inhibition could alter Na^+/K^+-ATPase function is by altering its interactions with regulatory proteins.

The field of molecular regulation of the Na^+/K^+-ATPase is very complex, a fact that is highlighted by the plethora of recently identified proteins that can associate with, and regulate, pump activity (Sweadner and Rael, 2000; Geering, 2006; Yoon *et al.*, 2006; Mao *et al.*, 2005; Gorokhova *et al.*, 2007). The proteins and molecules selected for investigation in this chapter were selected based on

published evidence of their involvement in pump regulation. For example, not only are endothelins known regulators of the Na^+/K^+-ATPase, they are also secreted from intestinal epithelial cells and are potently induced by hypoxia. Another example is FXYD3, which is known to be a negative regulator of the Na^+/K^+-ATPase and which is highly expressed in the colon. Several other proteins of interest are investigated in more detail throughout this chapter.

Endothelin (ET) 1, 2, and 3 are peptide hormones with potent vasoconstrictor properties which are synthesised and secreted predominantly by vascular endothelial cells (Rubanyi and Polokoff, 1994). One of the most potent inducers of ET-1 is hypoxia, and this is brought about by HIF-1 binding to the et-1 gene in conjunction with other transcription factors (Watanabe *et al.*, 1990; Tonnessen *et al.*, 1995; Yamashita *et al.*, 2001). More recent research has shown that hydroxylase inhibition by DMOG in rats can also induce ET-1 expression *in vivo* (Nagel *et al.*, 2011). ETs bind to ET receptors A (ETRA) and B (ETRB) and all 3 ETs and their receptors are expressed in the colonic epithelium (Takahashi *et al.*, 1990; Takizawa *et al.*, 2005; Kalabis *et al.*, 2008; Egidy *et al.*, 2000). Several studies have revealed that ET-1 exerts pro-secretory actions in humans and rats, with its actions being mediated by cyclo-oxygenase products and enteric nerves via activation of ETRA (Kuhn *et al.*, 1997; Moummi *et al.*, 1992; Kiyohara *et al.*, 1993). Interestingly, earlier studies conducted on renal tubular epithelial cells show that ET inhibits Na^+/K^+-ATPase activity, an effect that involves generation of prostaglandin E_2 (PGE_2) (Zeidel *et al.*, 1989). More recent studies demonstrate that activation of ETRB also inhibits Na^+/K^+-ATPase activity in renal proximal tubule cells (Liu *et al.*, 2009). Thus, since epithelial-derived ETs are known to have the capacity to acutely regulate Na^+/K^+-ATPase function, in the present studies their potential role in mediating the antisecretory actions of hydroxylase inhibition was investigated (Prasanna *et al.*, 2001; Liu *et al.*, 2009).

Another mechanism by which Na^+/K^+-ATPase pump activity can be downregulated in epithelial cells is by its sequestration into lipid rafts. Lipid

rafts are membrane microdomains that are rich in cholesterol and glycosphingolipids (Pike, 2009). They are of great interest in the context of this thesis for several reasons. First and foremost, lipid rafts are known to be regulated by hypoxia (Botto *et al.,* 2008). Secondly, hypoxia regulates cholesterol biosynthesis, an important component of lipid rafts (Nguyen *et al.*, 2007). Thirdly Na^+/K^+-ATPase function, membrane cholesterol, and caveolin-1 (an important constituent of caveolae), are inextricably linked at the molecular level (Chen *et al.*, 2009; Chen *et al.*, 2011; Cai *et al.*, 2008). Finally, as much as > 50 % of plasma membrane Na^+/K^+-ATPase can become sequestered into lipid rafts, where it is thought to function more as a signalling molecule than an ion transporter (Wang *et al.*, 2004). Interestingly, Na^+/K^+-ATPase movement to and from lipid rafts is dynamic, and upon cholesterol or caveolin depletion, some of this non-pumping Na^+/K^+-ATPase can return to the pumping pool (Liang *et al.*, 2007). Thus, sequestration into lipid rafts causes reduced activity of the pump without alterations in its cellular expression, a phenomenon that could explain the effects of hydroxylase inhibitors observed in the current studies. In its capacity as a signalling protein, the Na^+/K^+-ATPase has been shown to bind endogenous and exogenous cardiotonic steroids, such as ouabain, thereby evoking intracellular responses through interactions with downstream signalling proteins, such as Src (Liang *et al.*, 2006). Importantly, Src is also known to be a regulator of intestinal epithelial Cl^- secretion (Keely *et al.*, 2000). Therefore, we investigated if lipid rafts or Src family kinases might have a role to play in mediating the effects of hydroxylase inhibition on Na^+/K^+-ATPase activity.

Another possible mechanism by which hydroxylases might regulate epithelial secretory function could involve NFκB. NFκB is a known target of HIF-hydroxylases and has been shown to regulate transport proteins, specifically CFTR, expression in airway epithelial cells in response to interleukin-1β (Brouillard *et al.*, 2001) . Indeed, interleukin-1β itself has been shown to be upregulated in macrophages by HIF-dependent mechanisms (Imtiyaz *et al.*, 2010). Thus, a potential role for NFκB in DMOG-induced downregulation of Cl^-

secretion was investigated using BMS-345541, a highly selective inhibitor of IκB kinase (Burke *et al.*, 2003).

There is a multitude of intracellular signalling pathways involved in regulating epithelial Cl^- secretory responses, some of which directly regulate the activity of the Na^+/K^+-ATPase. One such signalling pathway protein is PKC, of which there are several isoforms, classified into different groups. The classical PKCs are α and βII; the novel PKCs consist of δ, ε, θ, and η; whereas the atypical PKCs are ζ and λ. PKC is a well characterised regulator of Cl^- secretion via its regulation of CFTR and NKCC1, amongst others (Song *et al.*, 2001; Matthews *et al.*, 1994). Interestingly, PKC ε has also been shown to regulate Cl^- secretion across T_{84} cells under conditions of chemically-induced ischemia, and as already mentioned in the introduction to Chapter 4, PKC ζ is a known regulator of Na^+/K^+-ATPase function (Yoo *et al.*, 2001). This PKC isoform translocates to the plasma membrane where it phosphorylates Ser-18 on Na^+/K^+-ATPase α_1, culminating in clathrin-dependent pump endocytosis (Dada *et al.*, 2003; Chen *et al.*, 2006). Another protein kinase, PKA, is known to be regulated by hypoxia (Beitner-Johnson *et al.*, 1998), and is an important regulator of epithelial Cl^- secretion, being best known for its role in regulating CFTR gating (Singh *et al.*, 1998; Forte *et al.*, 1992; Chappe *et al.*, 2005). Thus, we also investigated the potential involvement of PKC and PKA in mediating the antisecretory actions of hydroxylase inhibition.

In conditions of hypoxia, global transcriptional and translational processes are known to be dampened as a consequence of cellular energy conservation processes (Liu and Simon, 2004). Conversely the master regulator of hypoxia, HIF, becomes active during hypoxia and drives transcription of genes that aid in adaptive responses. Results from Chapter 4 indicated the antisecretory effects to be HIF-independent. However, given the profound transcriptionally-mediated effects of HIF during hypoxia, experiments were designed to more

conclusively explore the role of HIF in mediating the antisecretory effects of hydroxylase inhibition.

The Na^+/K^+-ATPase β subunit is one of the most important regulators of Na^+/K^+-ATPase activity since the pump has been shown to be inactive when it is absent (Horowitz *et al.*, 1990). The β subunit spans the membrane only once and is thought to be important for the correct insertion of the αβ heterodimer into the plasma membrane (Hasler *et al.*, 2001). More recent studies have shown that the polarised expression of Na^+/K^+-ATPase pumps in epithelia also depends on the association of β-subunits located in neighbouring cells, thus highlighting the importance of each of the pump subunits in regulating its transport properties (Shoshani *et al.*, 2005; Padilla-Benavides *et al.*, 2010).

As previously mentioned, the Na^+/K^+-ATPase exists as a protein complex with several subunits, such as the β subunit and the γ subunit (FXYD2) (Morth *et al.*, 2007). Another important family of proteins known to regulate Na^+/K^+-ATPase activity are the FXYD proteins. This family of 7 proteins are structurally characterised by an FXYD motif, 2 conserved glycines, and a serine residue (Sweadner and Rael, 2000). FXYD proteins are known to modify the transport properties of Na^+/K^+-ATPase pumps in a tissue-specific manner, without altering its expression (Delprat *et al.*, 2006; Geering, 2006). More recent research also suggests that they contribute to stabilisation of the pump at the membrane (Mishra *et al.*, 2011). Previous studies have implicated FXYD3 in regulation of Cl^- currents in Xenopus oocytes, although at the time it was not yet known to be a regulator of Na^+/K^+-ATPase activity (Morrison *et al.*, 1995). Subsequent studies have found FXYD3 to be highly expressed in the colon (Crambert *et al.*, 2005), and studies conducted on intestinal epithelial cells have shown that it negatively regulates Na^+/K^+-ATPase activity (Crambert *et al.*, 2005; Bibert *et al.*, 2009).

A relatively recently identified protein known as Modulator of Na^+/K^+-ATPase (MONaKA; PXK) is also of relevance to the current studies. This protein has been

shown to bind Na^+/K^+-ATPase β subunits and to negatively regulate pump activity (Mao *et al.*, 2005). MONaKA has been proposed by one group to be a functional sorting nexin that is important in regulating cellular function via its interaction with the actin cytoskeleton (Takeuchi *et al.*, 2010). Thus, we investigated if this protein might be involved in mediating the antisecretory effect of DMOG in colonic epithelial cells.

Finally, another possible mechanism by which hydroxylase inhibition downregulates secretory function involves FIH-1. Studies carried out in Chapter 4 showed that both DMOG and FG-4497 exert antisecretory actions at high concentrations, in excess of those required to stabilise HIF-1α. At such concentrations FIH-1 is also known to be inhibited, and in fact FIH-1 was found to be more sensitive to inhibition by DMOG than were the prolyl hydroxylases (Tian *et al.*, 2011b). Furthermore, FIH-1 is known to hydroxylate ankyrin repeat-containing proteins, including the cytoskeletal ankyrin family (Linke *et al.*, 2007; Cockman *et al.*, 2009; Yang *et al.*, 2011). The ankyrin repeat is one of the most common protein–protein interaction motifs found in nature and has been postulated as a molecular signal for protein recognition (Mosavi *et al.*, 2004; Li *et al.*, 2006). This is interesting considering the Na^+/K^+-ATPase α_1 subunit possesses 2 cytoplasmic ankyrin-binding domains, and that these ankyrin binding domains are important in the regulation of the pump via interactions with the spectrin cytoskeleton (Devarajan *et al.*, 1994; Zhang *et al.*, 1998; Woroniecki *et al.*, 2003). Thus, the possibility that FIH-1 mediates the effects of hydroxylase inhibition on Na^+/K^+-ATPase pump activity was further investigated in this chapter.

5-2 Aim

From the preceding Introduction it is clear that there are many potential mechanisms by which the activity of the Na^+/K^+-ATPase can be regulated. Therefore, the general aim of this chapter was to investigate molecular mechanisms underlying regulation of the Na^+/K^+-ATPase by hydroxylase inhibitors.

5-3 Results

As described in the introduction to this chapter, the Na^+/K^+-ATPase is an important protein that plays critical roles in regulating epithelial transport and signalling under the control of multiple intra- and extracellular factors, many of which can be altered in conditions of hypoxia. Thus, a rather broad approach was first taken to identify potential signalling mechanisms that underlie the effects of hydroxylase inhibition on Na^+/K^+-ATPase function.

5-3.1 The antisecretory effects of hydroxylase inhibition are not mediated by an acutely acting soluble factor

Endothelins, which can be potently induced under conditions of hypoxia, are secreted molecules known to have the capability to acutely regulate Na^+/K^+-ATPase activity. Therefore, the possibility that hydroxylase inhibition of pump activity is mediated by the release of a soluble factor, such as ET-1, was next investigated. Hydroxylases were inhibited in T_{84} cells by DMOG (1 mM; 24 hours). The apical and basolateral conditioned medium was then aspirated and applied to naive T_{84} cells for various periods of time ranging from 15 minutes to 1 hour. Although DMOG is still present in this conditioned medium, we would not expect to see direct effects of the inhibitor over such short periods of time, and any effects observed should be due to factors secreted into the medium. However, as shown in Figure 5–1, the application of conditioned medium to naive T_{84} cells had no impact on subsequent Cl^- secretory responses to either basolateral CCh (100 μM) or apical FSK (10 μM).

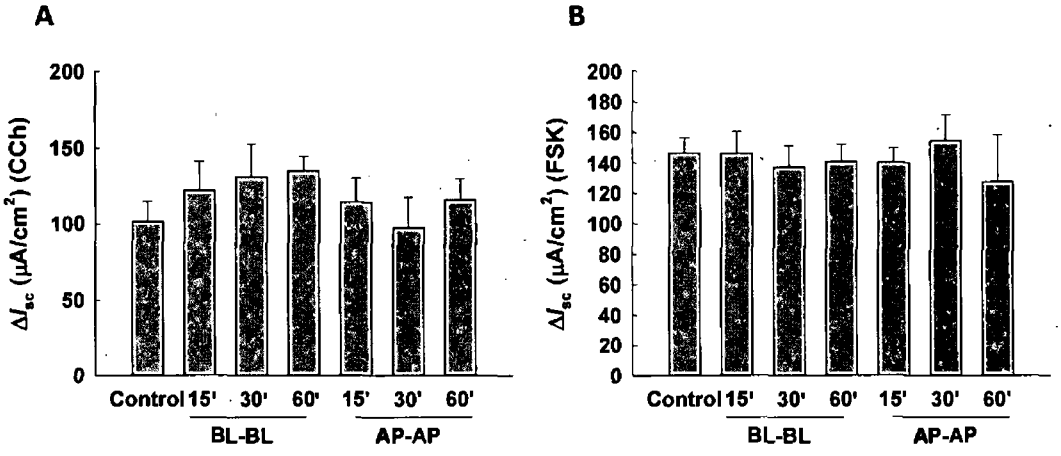

Figure 5–1 The antisecretory effects of hydroxylase inhibition are not mediated by an acutely acting soluble factor. T_{84} cells were cultured as monolayers on permeable supports until R_{te} stabilised at plateau levels. Cells were treated bilaterally with DMOG (1 mM) in serum-free medium for 24 hours. After 24 hours the conditioned medium from the apical side of DMOG-treated cells was aspirated and applied to the apical side of naive cells (AP-AP) for various periods of time from 15 to 60 minutes. Similarly, basolateral conditioned medium was applied to the basolateral side of naive cells (BL-BL). Naive T_{84} cells had been cultured in serum-free medium for 24 hours prior to treatment with conditioned medium. **A)** Maximal changes in current in response to basolateral CCh (100 μM) in control and treated cells were plotted as ΔI_{sc} (n = 3). **B)** Maximal changes in current in response to apical FSK (10 μM) in control and treated cells were plotted as ΔI_{sc} (n = 3).

5-3.2 Disruption of lipid rafts does not reverse Na^+/K^+-ATPase inhibition by hydroxylase inhibition

Na^+/K^+-ATPase pumps can become sequestered into lipid rafts under certain conditions, where it then acts as a signalling protein rather than an ion transporter. Thus, the effect of lipid raft disruption on Na^+/K^+-ATPase activity in DMOG-treated T_{84} cells was next investigated. As proof of principle that MβCD is working, cells were treated with MβCD alone, which should release sequestered Na^+/K^+-ATPase, and increase its activity. Pump activity was increased and was approaching significance in the presence of MβCD alone. However, it was found that basolateral treatment of the cells with MβCD with concentrations previously shown to deplete cholesterol in T_{84} cells (Wolf *et al.*, 2002), did not reverse the inhibitory effect of DMOG (Figure 5–2).

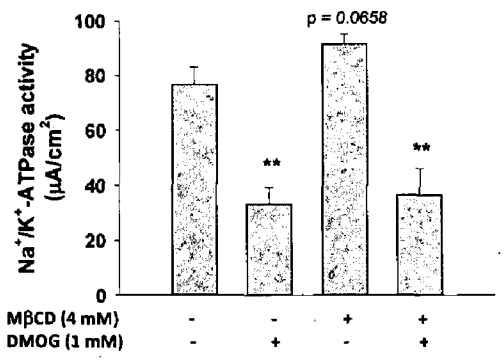

Figure 5–2 MβCD disruption of lipid rafts does not affect Na^+/K^+-ATPase activity in DMOG-treated T_{84} colonic epithelial cells. T_{84} cells were cultured as monolayers on permeable supports until R_{te} stabilised at plateau levels. Cells were treated bilaterally with DMOG (1 mM; 24 hours) in the presence or absence of basolateral MβCD (4 mM) for the final hour of DMOG treatment. Cells were washed, mounted in Ussing chambers, and bathed in Ringer's solution (Table 2-3). Maximal changes in current in response to basolateral CCh (100 μM) and apical FSK (10 μM) in control and treated cells were plotted as ΔI_{sc} (n = 3; ANOVA, ** $p \leq 0.01$, compared to untreated control).

5-3.3 Post-translational modifications facilitate antisecretory actions of hydroxylase inhibition

Having ruled out the involvement of lipid rafts or an acutely acting secreted autocrine factor, a broad investigation of the possible contributions of several different signalling pathways was next performed. NFκB is a known non-HIF target of hydroxylases that has been previously shown to have the capacity to regulate transport protein function (Cummins *et al.*, 2006; Brouillard *et al.*, 2001). Therefore, a potential role for NFκB activation in mediating hydroxylase effects on Na^+/K^+-ATPase activity was investigated. We employed BMS-345541 to pharmacologically inhibit NFκB, with experiments first being conducted to determine the efficacy of the inhibitor. Treatment of T_{84} cells with DMOG (1 mM; 30 minutes) caused phosphorylation of IκBα, as previously demonstrated, which was inhibited by BMS-345541 (Figure 5-3 A) (Cummins *et al.*, 2006). Basal levels of phosphorylated IκBα persisted in the presence of the inhibitor, which may be due to basal phosphorylation of the protein by other kinases, such as PKC (Steffan *et al.*, 1995). Next, T_{84} cells were cultured on permeable supports with BMS-345541 in the presence or absence of DMOG (1 mM) for 24 hours. Cells were then mounted in Ussing chambers and secretory responses to CCh (100 μM) and FSK (10 μM) were measured. We found that BMS-345541 had no effect on basal I_{sc} or R_{te}, nor did it ameliorate the antisecretory effect of hydroxylase inhibition (Figure 5–3 B).

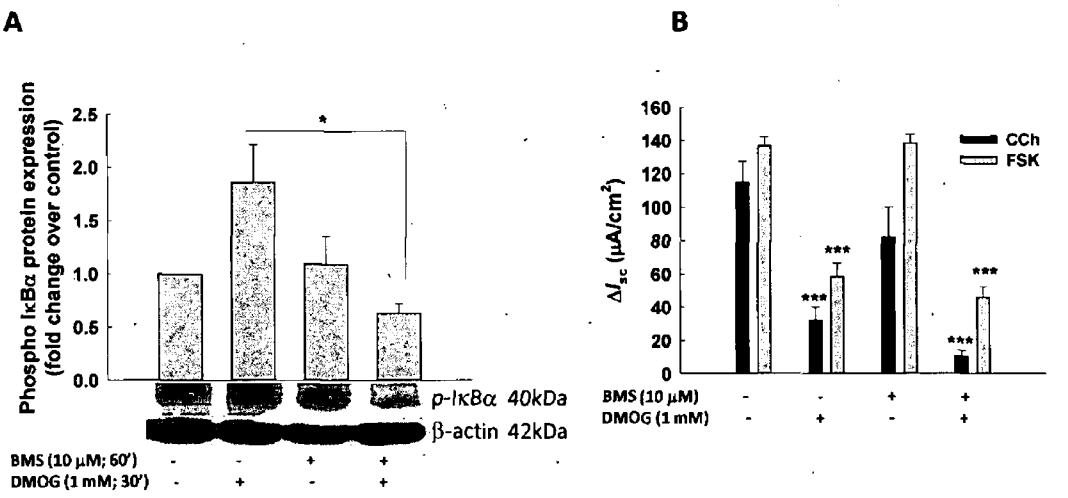

Figure 5–3 NFκB does not mediate the antisecretory effect of hydroxylase inhibition in T_{84} colonic epithelial cells. T_{84} cells were cultured as monolayers on permeable supports until R_{te} stabilised at plateau levels. **A)** Cells were treated with DMOG (1 mM; 30 minutes) to induce phosphorylation of IκBα. NFκB was inhibited by pretreatment of cells with BMS-345541 (10 μM) for 30 minutes prior to DMOG-treatment and then for the duration of DMOG-treatment. Cells were then lysed and proteins were separated by SDS-PAGE and analysed by western blotting for phopho-IκBα (n = 3; ANOVA; *** $p \leq 0.05$). **B)** Cells were treated bilaterally with DMOG (1 mM) in serum-free medium for 24 hours either in the absence or presence of BMS-345541. Cells were washed, mounted in Ussing chambers, and bathed in Ringer's solution (Table 2-3). Maximal changes in I_{sc} in response to basolateral CCh (100 μM) and apical FSK (10 μM) in control and treated cells were plotted as ΔI_{sc} (n = 5; ANOVA; *** $p \leq 0.001$, compared to respective controls).

Having shown that NFκB was not likely to be involved in mediating the antisecretory effect of hydroxylase inhibition, we next examined Src family kinases. These important signalling proteins are known to regulate epithelial transport function and can also be regulated in conditions of hypoxia (Keely *et al.*, 2000; Knock *et al.*, 2008). A potential role for Src family kinases was examined using PP2 (Hanke *et al.*, 1996). PP2 potentiated CCh (100 μM)-

stimulated responses to 191.51 ± 42.52 % of controls, but reduced FSK (10 μM)-stimulated responses to 64.62 ± 5.54 % of control similar to previous results (Keely *et al.*; 2000; Bertelsen *et al.*, 2002). Treatment with PP2 did not reverse the antisecretory effect of DMOG on Ca^{2+}-dependent responses. Interestingly, however, PP2 significantly attenuated the antisecretory effect of hydroxylase inhibition on cAMP-dependent responses. DMOG alone inhibited FSK-stimulated responses to 29.40 ± 2.92 % of those in controls. However, in the presence of both PP2 and DMOG, responses to FSK were 45.52 ± 5.15 % of controls (n = 5; ns compared to control) (Table 5–1). It is worth noting that the inhibition of FSK-stimulated current by DMOG in this set of experiments was greater than that initially reported and shown in Table 5–1. We attribute this variation to variation between experiments.

Similar to Src family kinases, PKC is a critical regulator of epithelial transport protein function. Therefore, we also examined its potential involvement in mediating the antisecretory actions of hydroxylase inhibition. A well-described general inhibitor of the classical and novel PKC isoforms, GF 109203X, was employed. However, it was found that 24 hours treatment with GF 109203X in the presence of DMOG did not significantly reverse the antisecretory effects of the hydroxylase inhibitor (Table 5–1).

PKA is also known to be an important regulator of epithelial Cl^- secretion (Singh *et al.*, 1998). However, upon its inhibition with the specific inhibitor, H89, there was no reversal of the antisecretory effect of hydroxylase inhibition (Table 5–1) (Davies *et al.*, 2000; Chijiwa *et al.*, 1990).

Finally, acriflavine (5 μM), which was employed as a HIF inhibitor was also without effect on the antisecretory actions of hydroxylase inhibition (Table 5–1) (Lee *et al.*, 2009).

Table 5–1 Pharmacological investigation of the involvement of various signalling pathways in mediating antisecretory actions of DMOG. T_{84} cells were cultured as monolayers on permeable supports until R_{te} stabilised at plateau levels. Cells were treated bilaterally with DMOG (1 mM; 24 hours) in the presence or absence of various pharmacological inhibitors (Table 2–2). Cells were washed, mounted in Ussing chambers, and bathed in *Ringer's solution* (Table 2-3). Cl^- secretory responses to basolateral CCh (100 μM) and apical FSK (10 μM) were then measured. Maximal responses to CCh and FSK are represented as % of respective control ΔI_{sc} responses analysed by ANOVA for each inhibitor.

Treatment	Target	Response to CCh (% of respective control)	Response to FSK (% of respective control)
DMOG	Prolyl-4 hydroxylases	20.2 ± 2.6 (n = 16; p ≤ 0.001)	38.8 ± 6.7% (n = 16; p ≤ 0.001)
GF Control	PKC	128.81 ± 20.88 (n = 3; ns)	105.33 ± 5.90 (n = 3; ns)
DMOG + GF		26.42 ± 1.54 (n = 3; p ≤ 0.001)	44.17 ± 1.22 (n = 3; p ≤ 0.001)
BMS-345541 Control	NFκB	76.32 ± 11.78 (n = 5; ns)	98.91 ± 5.07 (n = 5; ns)
DMOG + BMS-345541		11.81 ± 0.85 (n = 5; p ≤ 0.001)	32.05 ± 3.54 (n = 5; p ≤ 0.001)
PP2 Control	Src-family kinases	191.51 ± 42.52 (n = 4; p ≤ 0.05)	64.62 ± 5.53 (n = 4; ns)
DMOG + PP2		28.60 ± 5.96 (n = 4; p ≤ 0.001)	45.52 ± 5.15 (n = 4; ns)
Acriflavine Control	HIF	78.99 ± 6.02 (n = 6; ns)	80.78 ± 2.75 (n = 6; ns)
DMOG + Acriflavine		23.35 ± 3.22 (n = 6; p ≤ 0.001)	39.24 ± 6.41 (n = 6; p ≤ 0.01)
H89 Control	PKA	30.76 ± 3.18 (n = 4; p ≤ 0.001)	42.39 ± 1.71 (n = 4; p ≤ 0.001)
DMOG + H89		20.81 ± 3.27 (n = 4; p ≤ 0.001)	39.13 ± 2.93 (n = 4; p ≤ 0.001)

A potential role for new protein translation in mediating the antisecretory effect of hydroxylase inhibition was next investigated by use of the protein translation inhibitor, CHX. In order to verify the efficacy of CHX, experiments were first carried out in which HIF-1α protein expression was induced by treatment of T_{84} cells with DMOG (1 mM; 24 hours), in the presence or absence of various

concentrations of CHX (0–5 μM). CHX (5 μM) inhibited HIF-1α accumulation by 64 % compared to DMOG alone (n = 2) (Figure 5–4 A), similar to results previously obtained in T_{84} cells (McRoberts *et al.*, 1990). T_{84} cells were next cultured with CHX (5 μM) in the presence or absence of DMOG (1 mM; 24 hours). Cells were mounted in Ussing chambers and upon stimulation with basolateral CCh (100 μM) and apical FSK (10 μM), we found there to be no reversal of the antisecretory effect of hydroxylase inhibition (Figure 5–4 B).

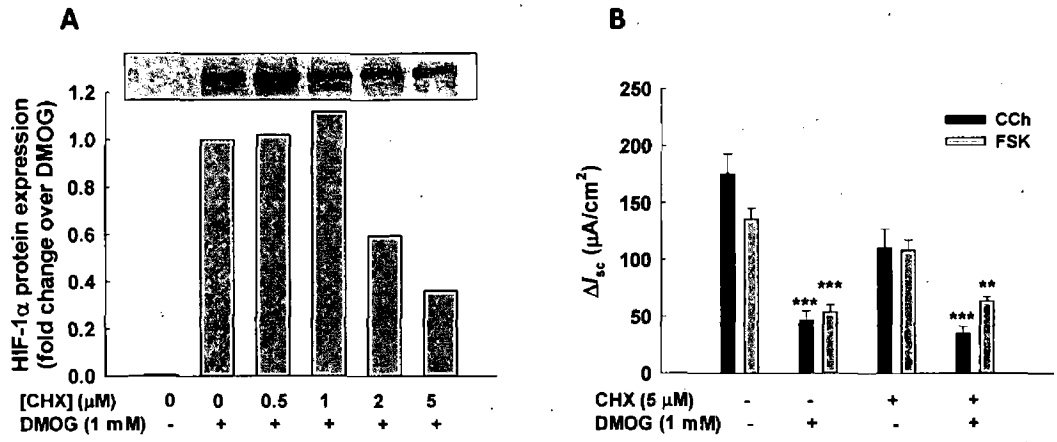

Figure 5–4 Cycloheximide does not alter the antisecretory effects of hydroxylase inhibition in T_{84} colonic epithelial cells. T_{84} cells were cultured as monolayers on permeable supports until R_{te} stabilised at plateau levels. **A)** Cells were treated bilaterally with DMOG (1 mM; 24 hours) to induce HIF-1α, in the presence or absence of CHX at various concentrations for 24 hours. Cells were lysed and proteins were separated by SDS-PAGE and HIF-1α was detected by western blot. β-actin was not used as a loading control in these experiments as its expression would also be expected to decrease due to CHX-treatment (n = 2). **B)** Cells were treated bilaterally with DMOG (1 mM; 24 hours) in the presence or absence of CHX (5 μM). Cells were washed, mounted in Ussing chambers, and bathed in Ringer's solution (Table 2–3). Maximal changes in current in response to basolateral CCh (100 μM) and apical FSK (10 μM) in control and treated cells were plotted as ΔI_{sc} (n = 4; ANOVA; * $p \leq 0.05$; *** $p \leq 0.001$, compared to their respective controls).

The potential involvement of gene transcription in mediating the antisecretory effect of hydroxylase inhibition was also investigated using the transcriptional inhibitor, AD. Again, to test the efficacy of AD, cells were first treated bilaterally with AD (250 ng/ml) for 24 hours and 18SrRNA mRNA expression was determined by semi-quantitative RT-PCR. These experiments showed that AD inhibited transcription of 18SrRNA to 61.51 ± 7.18 % of that in control cells (Figure 5–5 A). T_{84} cells were next cultured with AD (250 ng/ml) in the presence or absence of DMOG (1 mM; 24 hours), mounted in Ussing chambers and stimulated with basolateral CCh (100 μM) and apical FSK (10 μM). AD reduced both the Ca^{2+} and cAMP-mediated Cl^- secretory responses in control cells, but it was also clear that AD did not reverse the antisecretory effects of hydroxylase inhibition (Figure 5–5 B).

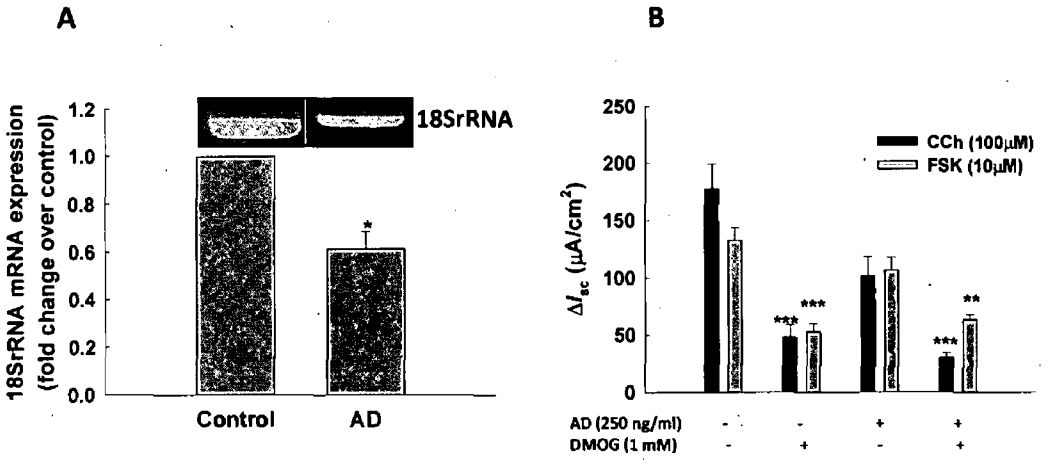

Figure 5–5 Actinomycin D does not attenuate the antisecretory effect of hydroxylase inhibition in T_{84} colonic epithelial cells. T_{84} cells were cultured as monolayers on permeable supports until R_{te} stabilised at plateau levels. **A)** Cells were treated bilaterally with AD (250 ng/ml) for 24 hours. Total RNA was isolated and mRNA expression of 18SrRNA was analysed by semi-quantitative RT-PCR (n = 4; paired t-test; ** $p \leq 0.05$). **B)** Cells were treated bilaterally with DMOG (1 mM) in serum-free medium for 24 hours in the presence or absence of AD (250 ng/ml). Cells were washed, mounted in Ussing chambers, and bathed in Ringer's solution (Table 2-3). Cl^- secretory responses were then stimulated with basolateral CCh (100 μM) and apical FSK (10 μM). Maximal responses to CCh and FSK were plotted as ΔI_{sc} responses (n = 6; ANOVA; ** $p \leq 0.01$; *** $p \leq 0.001$, compared to respective controls).

5-3.4 Na^+/K^+-ATPase β_1 protein expression is significantly increased by hydroxylase inhibition

Since it is insensitive to CHX and AD, our data suggested that the antisecretory effect of hydroxylase inhibition is likely mediated by a post-translational event. Thus, the expression of some known regulatory proteins of the Na^+/K^+-ATPase pump was next investigated. PKC ζ, as already discussed in the introduction to Chapter 4, was the first to be investigated. Hydroxylases were inhibited by DMOG (1 mM; 24 hours) and PKC ζ protein expression was investigated by western blotting (Figure 5–6). No changes in the abundance of PKC ζ in DMOG-treated cells were observed.

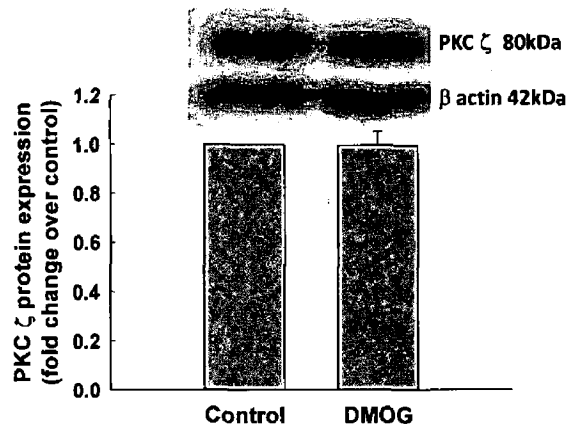

Figure 5–6 Hydroxylase inhibition does not alter PKC ζ expression in T_{84} colonic epithelial cells. T_{84} cells were cultured as monolayers on permeable supports until R_{te} stabilised at plateau levels. Cells were treated bilaterally with DMOG (1 mM) in serum-free medium for 24 hours. Cells were lysed, proteins were resolved by SDS-PAGE, and PKC ζ expression was analysed by western blotting. β-actin was used as a loading control (n = 4).

Another protein known the regulate Na^+/K^+-ATPase pump activity in colonic epithelial cells is FXYD3. Expression of this regulatory protein was also investigated at the mRNA level. Hydroxylases were again inhibited by DMOG (1 mM; 24 hours) and FXYD3 mRNA expression was investigated by semi-quantitative RT-PCR (Figure 5–7). However, there were no changes observed in FXYD3 mRNA expression in DMOG-treated cells.

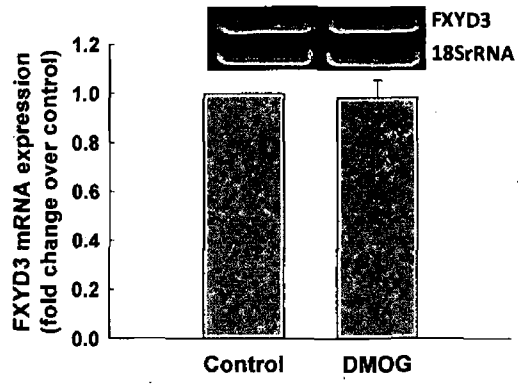

Figure 5–7 FXYD3 mRNA expression is not altered by hydroxylase inhibition in T_{84} colonic epithelial cells. T_{84} cells were cultured as monolayers on permeable supports until R_{te} stabilised at plateau levels. Cells were treated bilaterally with DMOG (1 mM) in serum-free medium for 24 hours. mRNA was isolated from the cells and semi-quantitative RT-PCR analysis was performed. 18SrRNA was used as a loading control (n = 5).

In further experiments, the expression of the regulatory subunit of the Na^+/K^+-ATPase heterodimer, Na^+/K^+-ATPase β_1, was also investigated. Hydroxylases were inhibited by DMOG (1 mM; 24 hours) and Na^+/K^+-ATPase β_1 expression was investigated at both the mRNA and protein levels by semi-quantitative RT-PCR and western blotting, respectively. Interestingly, we found that while there were no changes in mRNA expression (Figure 5–8 A), protein expression of the 35 kDa Na^+/K^+-ATPase β_1 subunit was significantly increased to 173.83 ± 17.27 % of that in control cells (Figure 5–8 B).

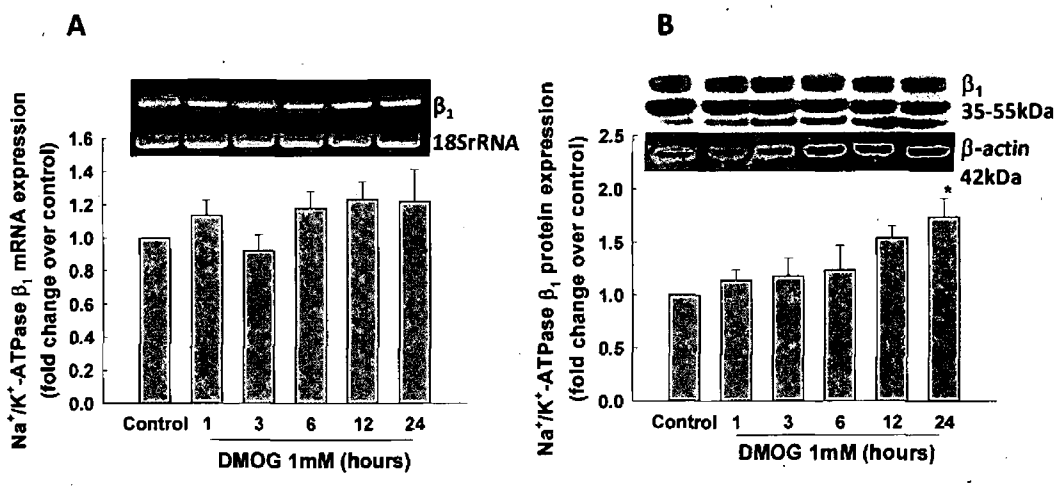

Figure 5–8 Na^+/K^+-ATPase β_1 protein expression is increased by hydroxylase inhibition in T_{84} colonic epithelial cells. T_{84} cells were cultured as monolayers on permeable supports until R_{te} stabilised at plateau levels. Cells were treated bilaterally with DMOG (1 mM) in serum-free medium for various periods of time. **A)** mRNA was isolated from the cells and semi-quantitative RT-PCR analysis was performed with primers specific for Na^+/K^+-ATPase β_1 (labelled as β_1 in the upper panel). 18SrRNA was used as a loading control (n = 5). **B)** Total protein was isolated from cells, and Na^+/K^+-ATPase β_1 protein expression was measured by western blotting (labelled as β_1 in the upper panel). β-actin was used as a loading control (n = 3; ANOVA; * $p \leq 0.05$ compared to control).

Having found that Na^+/K^+-ATPase β_1 subunit protein (35 kDa glycoprotein) expression is increased after treatment with DMOG, localisation of the protein at the plasma membrane in T_{84} cells was analysed by confocal microscopy. Cells were cultured on transparent permeable supports and treated with DMOG (1 mM; 24 hours). As shown in Figure 5–9, Na^+/K^+-ATPase β_1 is very specifically expressed basolaterally within one z-plane of T_{84} cells (indicated by arrows). In agreement with our western blot data, there also appeared to be an increase in the amount of Na^+/K^+-ATPase β_1 in the plasma membrane and cytosol of DMOG-treated cells.

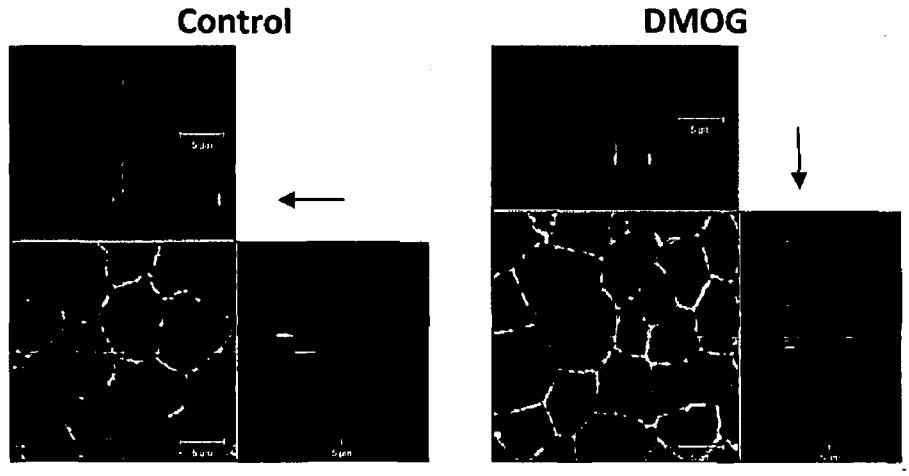

Figure 5–9 Na^+/K^+-ATPase β_1 expression in the plasma membrane is increased by hydroxylase inhibition in T_{84} colonic epithelial cells. T_{84} cells were cultured as monolayers on permeable supports until R_{te} stabilised at plateau levels. Cells were treated bilaterally with DMOG (1 mM) in serum-free medium for 24 hours. Cells were washed in PBS, fixed in 100 % methanol, permeabilised with Triton X-100, and stained with specific fluorophore-labelled antibodies as outlined in Section 2–23. Pseudo-colours were assigned to the various proteins where Na^+/K^+-ATPase β_1 is represented in green. This image is representative of 3 similar experiments.

5-3.5 MONaKA is expressed at the plasma membrane of intestinal epithelial cells, and is increased by hydroxylase inhibition

The results thus far show that while Na^+/K^+-ATPase pump activity is attenuated by hydroxylase inhibition, expression of the β_1 subunit of the protein is augmented. Thus, in the next series of experiments, the expression of MONaKA was investigated in T_{84} cells. MONaKA is known to be an Na^+/K^+-ATPase β_1-binding protein that attenuates pump activity (Mao *et al.*, 2005). Hydroxylases were inhibited by DMOG (1 mM) and after various periods of time MONaKA mRNA and protein expression were analysed. It was found that expression of MONaKA mRNA was significantly attenuated after 24 hours treatment with DMOG to 52.52 ± 6.32 % of that in control cells (Figure 5–10 A). However, in contrast, MONaKA protein expression was significantly increased following hydroxylase inhibition to 199.62 ± 25.92 % of that in controls (Figure 5–10 B).

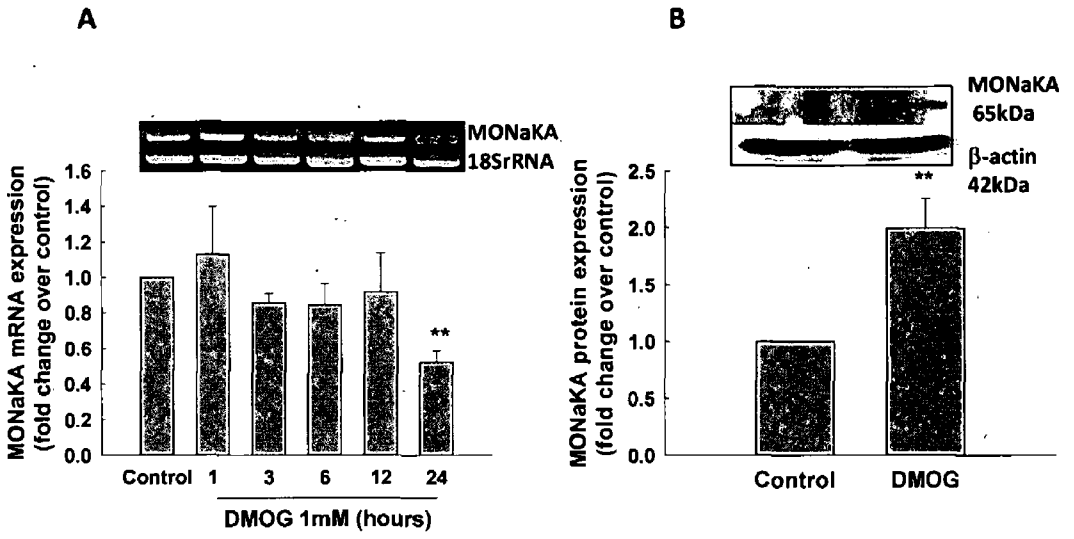

Figure 5–10 Hydroxylase inhibition attenuates MONaKA mRNA levels but increases MONaKA protein expression in T_{84} colonic epithelial cells. T_{84} cells were cultured as monolayers on permeable supports until R_{te} stabilised at plateau levels. **A)** Cells were treated bilaterally with DMOG (1 mM) in serum-free medium for various periods of time. mRNA was isolated from cells and semi-quantitative RT-PCR analysis was performed with primers specific for MONaKA. 18SrRNA was used as a loading control (n = 4; ** $p \leq 0.01$). **B)** Cells were treated bilaterally with DMOG (1 mM) in serum-free medium for 24 hours. Total protein was isolated from cells, and MONaKA protein expression was measured by western blotting. β-actin was used as a loading control (n = 14; ANOVA; ** $p \leq 0.01$ compared to control).

Since results from our previous experiments with CHX (Figure 5–4) suggest that the antisecretory effect of hydroxylase inhibition is independent of *de novo* protein synthesis, effects of CHX on MONaKA protein expression were also investigated. As shown in Figure 5–11, DMOG-induced expression of MONaKA was not altered in the presence of CHX and was 176.55 ± 18.13 % of that in untreated controls. This result of this experiment is somewhat limited however, by the omission of a CHX-only treated control with which to compare.

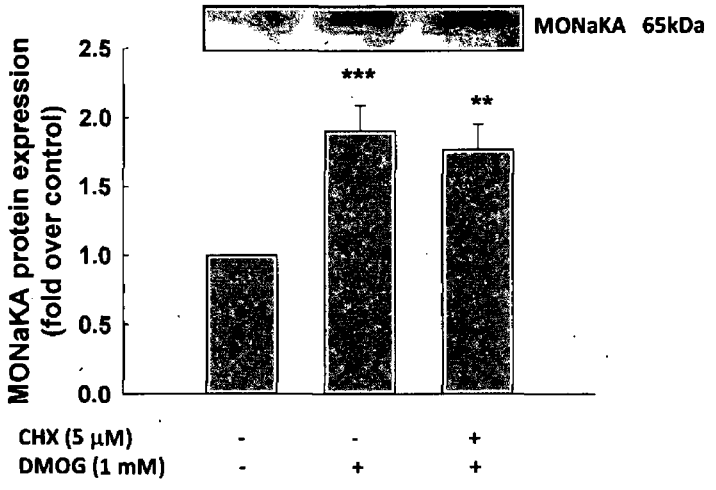

Figure 5–11 Hydroxylase inhibition increases MONaKA protein expression independently of *de novo* protein synthesis. T_{84} cells were cultured as monolayers on permeable supports until R_{te} stabilised at plateau levels. Cells were treated bilaterally with DMOG (1 mM; 24 hours) in the presence or absence of CHX (5 μM) for 24 hours. Cells were lysed, proteins were separated by SDS-PAGE, and MONaKA was detected by western blotting. β-actin was not used as a loading control in these experiments as its expression would be expected to decrease due to CHX-treatment (n = 6–20; ANOVA; ** $p \leq 0.01$; *** $p \leq 0.001$ compared to control).

Next, MONaKA localisation at the plasma membrane was investigated using an immunohistochemical approach. Cells were cultured on transparent permeable supports and were treated with DMOG (1 mM; 24 hours). As shown in Figure 5–12, and in agreement with previous reports (Mao *et al.*, 2005), MONaKA was found to be expressed in control cells, with predominant expression in the membrane, but also with expression in the cytosol. However, following hydroxylase inhibition by DMOG (1 mM; 24 hours), there was a dramatic translocation of MONaKA, specifically to the basolateral membrane (indicated by arrows).

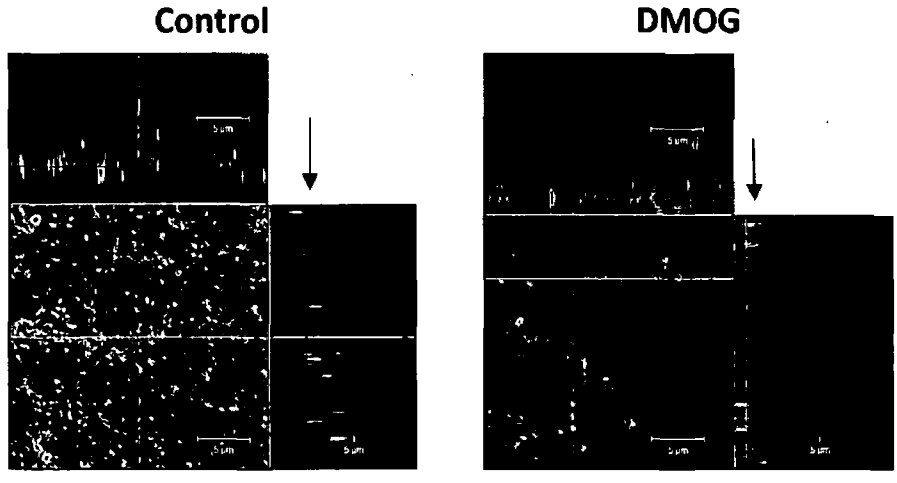

Figure 5–12 MONaKA expression in the basolateral membrane is increased by hydroxylase inhibition in T_{84} colonic epithelial cells. T_{84} cells were cultured as monolayers on permeable supports until R_{te} stabilised at plateau levels. Cells were treated bilaterally with DMOG (1 mM) in serum-free medium for 24 hours. Cells were washed in PBS, fixed in 100 % methanol, permeabilised with Triton X-100, and stained with specific fluorophore-labelled antibodies as outlined in Section 2-23. Pseudo-colours were assigned to the various proteins where MONaKA is represented in green. This image is representative of 3 similar experiments.

Since our data suggest that MONaKA and Na^+/K^+-ATPase β_1 subunits are both expressed basolaterally in T_{84} cells (Figures 5–9 and 5–12), the possibility that MONaKA may co-localise with the pump was next investigated using confocal microscopy. As shown in Figure 5–13, MONaKA has a more pronounced membrane expression following hydroxylase inhibition. However, co-localisation appears to be more specific with the Na^+/K^+-ATPase β_1 subunit, and is slightly offset with the Na^+/K^+-ATPase α_1 subunit.

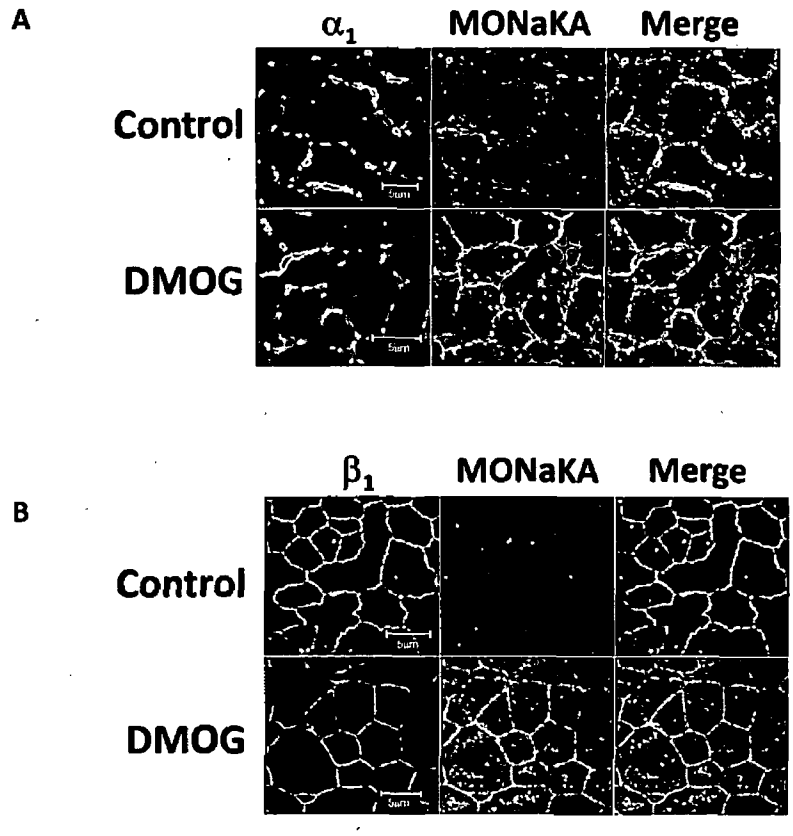

Figure 5–13 MONaKA co-localises with both the α_1 and β_1 subunit of the Na^+/K^+-ATPase pump in T_{84} cells. T_{84} cells were cultured as monolayers on permeable supports until R_{te} stabilised at plateau levels. Cells were treated bilaterally with DMOG (1 mM) in serum-free medium for 24 hours. Cells were washed in PBS, fixed in 100 % methanol, permeabilised with Triton X-100, and stained with specific fluorophore-labelled antibodies, as outlined in Section 2–23. Pseudo-colours were assigned to the various proteins where in **A)** Na^+/K^+-ATPase α_1 is represented in green and in **B)** Na^+/K^+-ATPase β_1 is represented in green. In both panels MONaKA is represented in magenta and the merge of the 2 colours is in white. This image is representative of 3 similar experiments. Scale bars are 5 μm in length.

While confocal images suggest that MONaKA co-localises with both the Na^+/K^+-ATPase α_1 and β_1 subunits, the spatial resolution of this approach is not sufficient the prove that protein-protein interactions are occurring. Thus, to further investigate potential interactions between MONaKA and the Na^+/K^+-ATPase, co-immunoprecipitations were carried out. As shown in Figure 5–14, MONaKA was found to co-immunoprecipitate with the Na^+/K^+-ATPase α_1 subunit. However, this experiment is somewhat limited by the omission of the IgG negative controls required to prove specificity of the protocol.

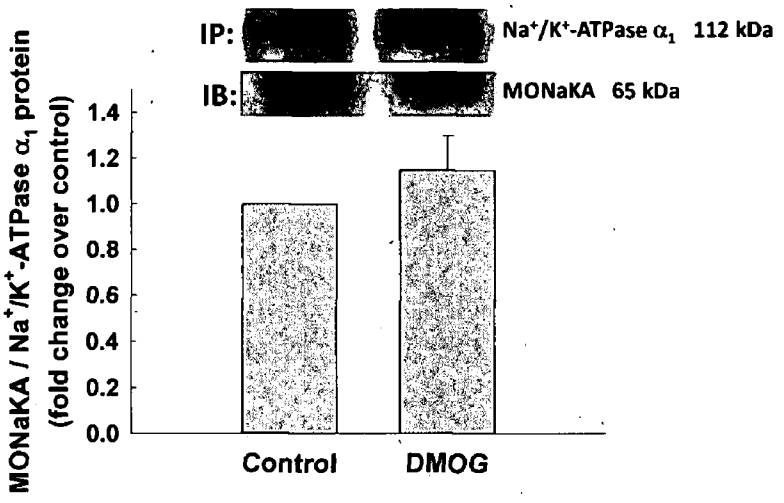

Figure 5–14 MONaKA co-immunoprecipitates with Na^+/K^+-ATPase α_1 subunit in T_{84} cells. T_{84} cells were cultured as monolayers on permeable supports until R_{te} stabilised at plateau levels. Cells were treated bilaterally with DMOG (1 mM) in serum-free medium for 24 hours and Na^+/K^+-ATPase α_1 subunits were immunoprecipitated (IP). Immunoprecipitates were washed thrice, and bound proteins were eluted using a low pH elution buffer. Proteins were resolved by SDS-PAGE, and MONaKA and Na^+/K^+-ATPase α_1 protein levels were measured by western blotting (IB) (n = 5).

Next, to confirm our findings from T_{84} cells, MONaKA localisation in isolated colonic crypts was also analysed using an immunohistochemical approach. Colonic crypts were isolated from mouse, rat, and human tissue, stained for MONaKA, and imaged by confocal microscopy. As shown in Figure 5–15 A–D, MONaKA (green) is highly expressed in crypts isolated from each species. Furthermore, it is clear from Figure 5–15 B, where the apical domain is labelled with a red actin collar, that MONaKA is predominantly localised to the basolateral membrane of crypt cells. Finally, but importantly, the pattern of expression of MONaKA appears to be conserved across the 3 species.

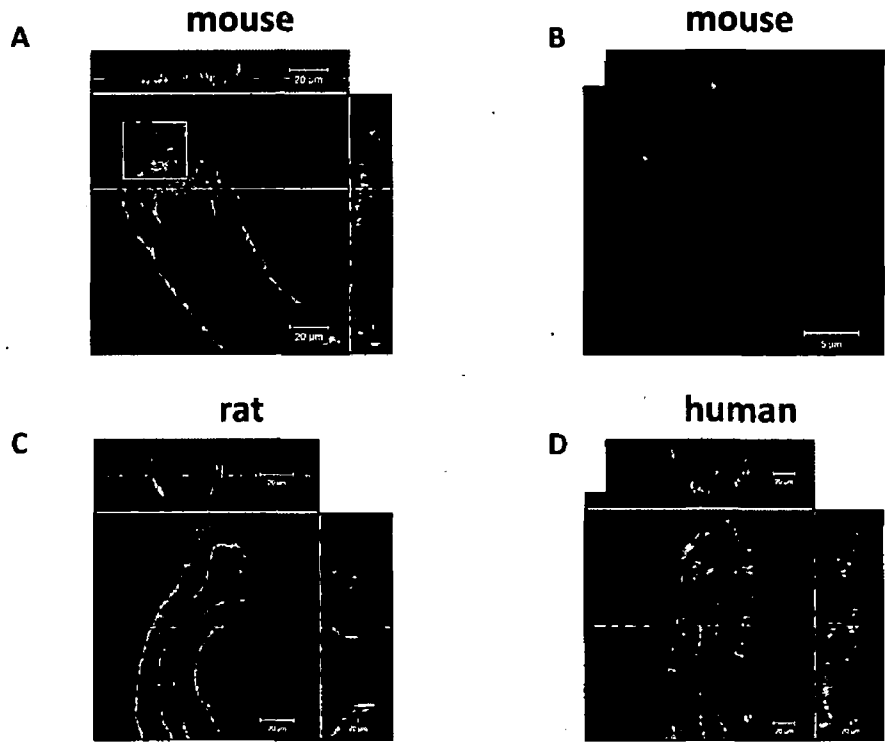

Figure 5–15 MONaKA is expressed basolaterally in mouse, rat, and human colonic crypts. Colonic tissue was isolated from vehicle-treated mice and rats, and human tissue was obtained from the Gastroenterology Department of Beaumont Hospital. Crypts were isolated using the protocol described in Section 2–21. Isolated crypts were then attached to chamber slides using Cell-Tak™ as described in Section 2–22. Crypts were washed in PBS, fixed in 100 % methanol, permeabilised with Triton X-100, and stained with specific fluorophore-labelled antibodies as outlined in Section 2–23. Pseudo-colours were assigned to the various structures, with nuclei being represented in blue, f-actin in red, and MONaKA in green (20 μm scale bars). Panel **B** shows the area defined by the square in panel **A** at higher magnification (5 μm scale bar).

Next, to further confirm *in vitro* observations in T_{84} cells, co-localisation of MONaKA and the Na^+/K^+-ATPase pump was investigated in human crypts, again using an immunocytochemical approach. As shown in Figure 5–16 A, MONaKA co-localises with the Na^+/K^+-ATPase α_1 subunit in the basolateral membrane (as indicated by arrow). The same was also found to be true for the Na^+/K^+-ATPase β_1 subunit as shown in Figure 5–16 B.

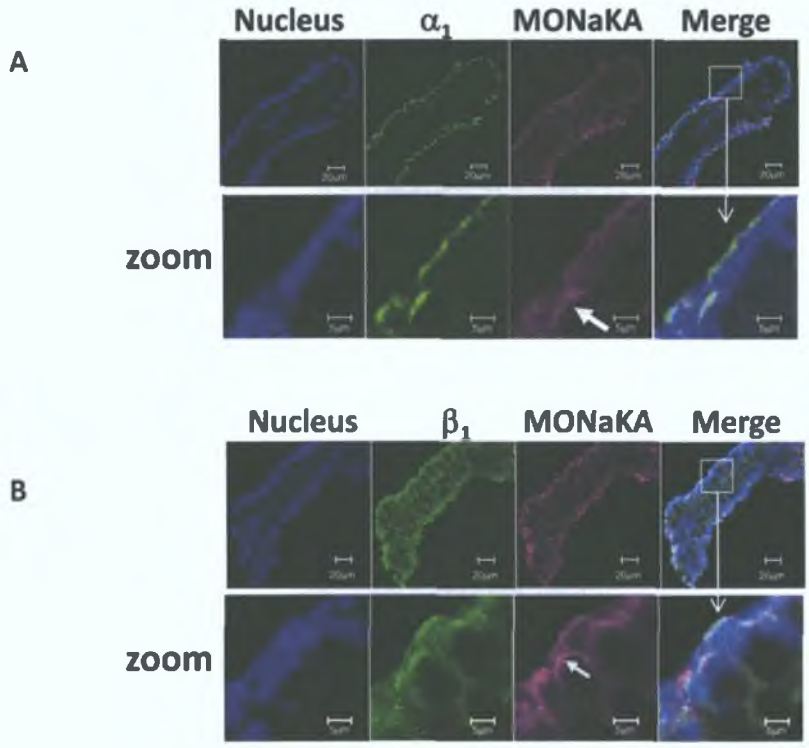

Figure 5–16 MONaKA co-localises with Na^+/K^+-ATPase α_1 and β_1 subunits in human crypts. Resected human colonic tissue was obtained from the Gastroenterology Department of Beaumont Hospital. Crypts were isolated (Section 2–21) and were attached to chamber slides using Cell-Tak™ (Section 2–22). Crypts were washed in PBS, fixed in 100 % methanol, permeabilised with Triton X-100, and stained with specific fluorophore-labelled antibodies, as outlined in Section 2–23. Pseudo-colours were assigned to the various markers. In panel **A)** Na^+/K^+-ATPase α_1 (labelled α_1) is represented in green and in panel **B)** Na^+/K^+-ATPase β_1 (labelled β_1) is represented in green (20 μm scale bars). In both panels, nuclei are stained with DAPI and are represented in blue, MONaKA is represented in magenta, and the merge is in white. The lower panels of both **A** and **B** show the areas defined by squares at higher magnification (5 μm scale bars).

Next, in order to directly investigate its role in regulating Na^+/K^+-ATPase function, a siRNA approach was attempted to knock down expression of MONaKA. Experiments were first carried out using 6-carboxyfluorescein (FAM)-labelled negative control siRNA to determine an appropriate transfection protocol for T_{84} cells. However, with the transient transfection methods employed, transfection efficiency was found to be very low. As shown in Figure 5–17 A, only 20 % of the cells displayed the expected perinuclear staining (indicated by arrow) of the FAM-labelled negative control siRNA, 24 hours following transfection. Using mRNA to quantify transfection efficiency, the manufacturers suggest that the siRNA should have an efficiency of 80 %. However, after 24 hours there was no knockdown of MONaKA mRNA as measured by semi-quantitative RT-PCR (data not shown). After 3 days (Figure 5–17 B) there was no distinct staining of the perinuclear space, although there was staining in the cytoplasm, and by 7 days (Figure 5–17 C) the FAM signal was very diffuse. We believe that at these later time points, the FAM reporter may be still present in the cells, but the siRNA has been degraded.

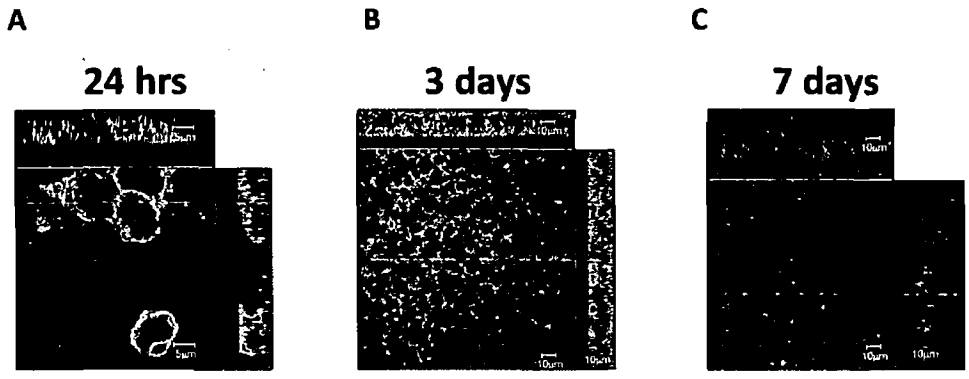

Figure 5–17 Transfection of T_{84} cells with FAM-labelled siRNA. T_{84} cells were trypsinised and transfected with FAM-labelled negative control siRNA (30 nM) with 0.4 % NeoFX transfection reagent from Ambion. Cells were cultured on permeable supports in serum-free medium for 24 hours post transfection. Cells were then stained with DAPI, and visualised by confocal microscopy. **A)** There was an approximately 20 % transfection efficiency after 24 hours (5 μm scale bar). **B)** Extra-nuclear cytoplasmic staining was present 3 days post-transfection (10 μm scale bar). **C)** Staining of the FAM-labelled negative control siRNA became very diffuse 7 days post-transfection (10 μm scale bar).

Similarly, attempts to use a siRNA approach to inhibit MONaKA expression in polarized T_{84} monolayers were not successful, and work to optimise conditions for siRNA transfection into T_{84} cell monolayers is continuing in the laboratory. Therefore, as an alternative, albeit indirect, approach to further investigate a potential role for MONaKA in mediating the antisecretory effects of hydroxylase inhibition, we investigated these effects after washout of DMOG from the culture medium. These experiments were carried out in order to temporally correlate changes in MONaKA expression with changes in Cl^- secretion. In these experiments, cells were treated with DMOG (1 mM; 24 hours) to inhibit hydroxylases, increase MONaKA protein expression, and attenuate Cl^- secretion. After 24 hours, the cells were washed of DMOG and then incubated for a further 24 hours in serum-free culture medium without the hydroxylase inhibitor. After this time, cells were mounted in Ussing chambers and secretory responses to CCh (100 μM) and FSK (10 μM) were measured. Although partially attenuated, the antisecretory effects of hydroxylase inhibition were still apparent 24 hours after removing DMOG from the culture medium (Figure 5–18 A). In similar experiments, expression of MONaKA was investigated using the same protocol for DMOG-treatment. As shown in Figure 5–18 B, 24 hours after removal of DMOG (wash), MONaKA expression remained elevated and was 216.87 ± 41.33 % of that in control cells. This indicates that MONaKA is a very stable protein *in vitro*. It is possible that its stability is promoted by its interaction with the Na^+/K^+-ATPase, or by some other post translational modification.

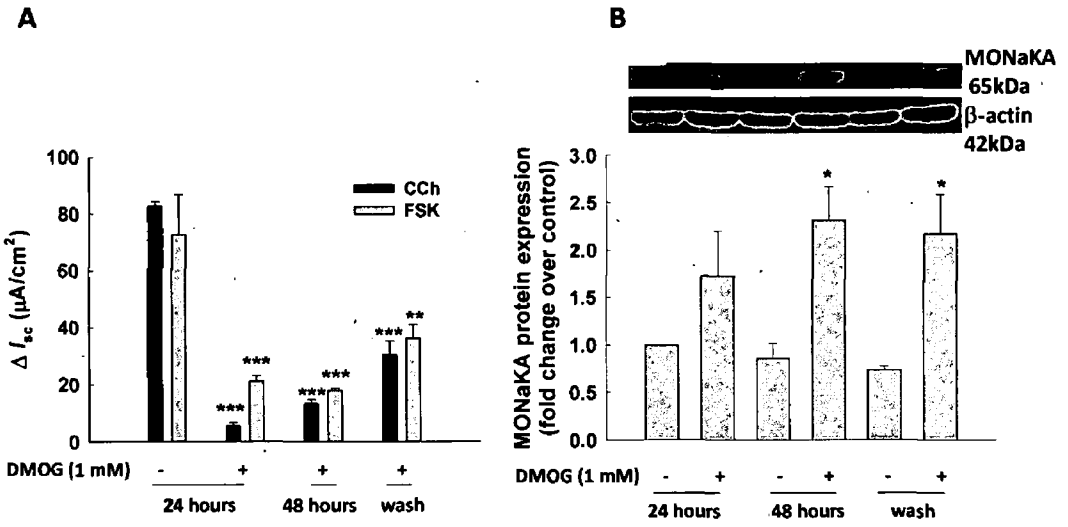

Figure 5–18 Antisecretory effects and increased MONaKA protein expression associated with hydroxylase inhibition are sustained after removal of inhibitor. T_{84} cells were cultured as monolayers on permeable supports until R_{te} stabilised at plateau levels. Cells were treated bilaterally with DMOG (1 mM) in serum-free medium for 24 hours, 48 hours, or for 24 hours in DMOG followed by a further 24 hours in serum-free medium without DMOG (indicated as 'wash' in panels A and B. **A)** Cells were mounted in Ussing chambers and stimulated with basolateral CCh (100 μM) and apical FSK (10 μM) (n = 3–4; ANOVA; ** $p \leq 0.01$; *** $p \leq 0.001$ compared to 24 hour no DMOG control). **B)** Cells were lysed, proteins resolved by SDS-PAGE, and MONaKA expression was analysed by western blotting. β-actin was used as a loading control (n = 4–5; ANOVA; * $p \leq 0.05$ compared to respective controls).

5-3.6 Hydroxylase inhibition increases membrane expression of FIH-1 and its association with Na^+/K^+-ATPase α_1

FIH-1 is known to hydroxylate ankyrin repeat domain-containing proteins and interestingly, the Na^+/K^+-ATPase α_1 subunit contains 2 ankyrin-binding domains, suggesting FIH-1 may have an ability to interact with the pump. Earlier in these studies, FIH-1 expression in response to hydroxylase inhibition was investigated (Figure 3–3) and was found to be unaltered at either the mRNA or protein level. Next, using an immunohistochemical approach, we investigated if FIH-1 localisation might be altered in response to DMOG treatment. Cells were cultured on transparent permeable supports and treated with DMOG (1 mM; 24 hours). As shown in Figure 5–19, FIH-1 is specifically expressed basolaterally in untreated T_{84} cells. Furthermore, there was a clear increase in the abundance of FIH-1 in the basolateral membrane of DMOG-treated cells. Interestingly, there also appeared to be a translocation of the protein in the z plane, from a relatively dispersed state in control cells (indicated by arrow) to a more distinct location in DMOG-treated cells (indicated by arrow).

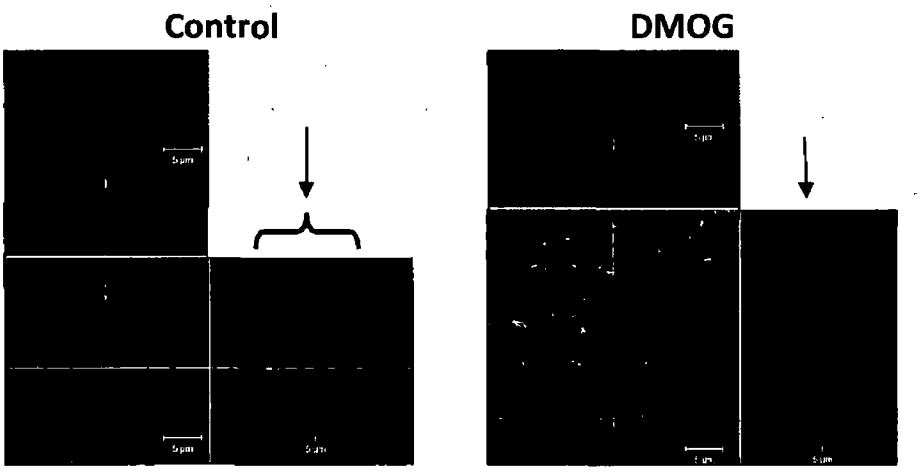

Figure 5–19 Hydroxylase inhibition increases FIH-1 expression in the basolateral membrane of T_{84} colonic epithelial cells. T_{84} cells were cultured as monolayers on permeable supports until R_{te} stabilised at plateau levels. Cells were treated bilaterally with DMOG (1 mM) in serum-free medium for 24 hours. Cells were washed in PBS, fixed in 100 % methanol, permeabilised with Triton X-100, and stained with specific fluorophore-labelled antibodies as outlined in Section 2–23. Pseudo-colours were assigned to the various proteins where FIH-1 is represented in magenta. This image is representative of 3 similar experiments.

Since FIH-1 appears to traffic to the membrane following hydroxylase inhibition, co-localisation of FIH-1 with the Na^+/K^+-ATPase subunits was next investigated in T_{84} cells and in human crypts by confocal microscopy. As shown in Figure 5–20 A there was a striking co-localisation of FIH-1 with the Na^+/K^+-ATPase α_1 subunit, displaying a more distinct membrane expression following hydroxylase inhibition. FIH-1 expression in human crypts appeared to be equally cytoplasmic and membranous (Figure 5–20 B).

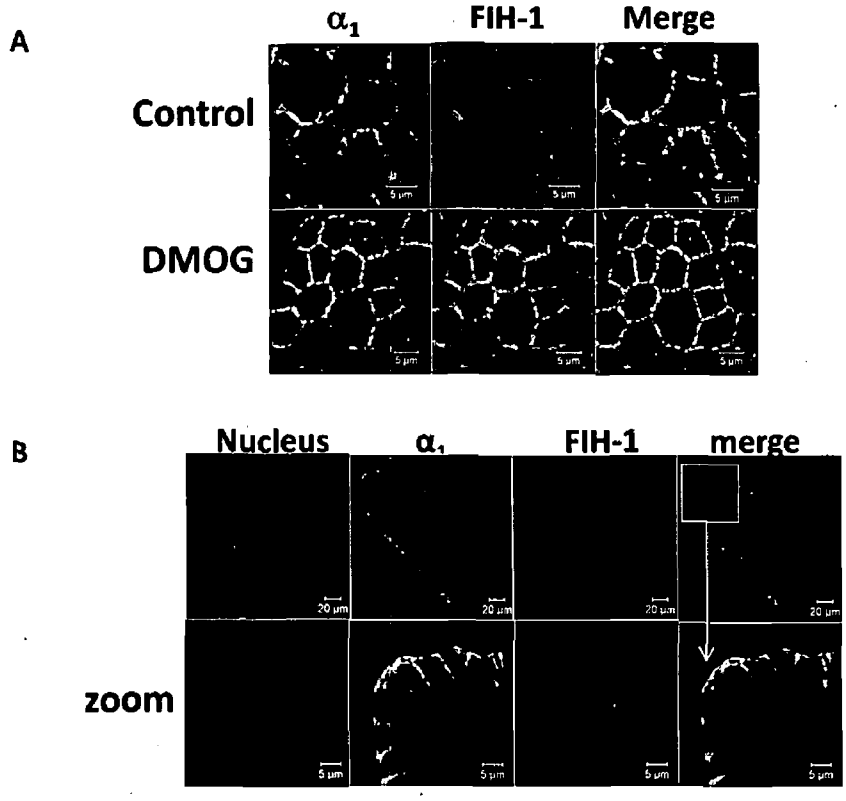

Figure 5–20 FIH-1 co-localises with the Na^+/K^+-ATPase α_1 subunit in T_{84} cells and human crypts. T_{84} cells were cultured as monolayers on permeable supports until R_{te} stabilised at plateau levels. Cells were treated bilaterally with DMOG (1 mM) in serum-free medium for 24 hours. Resected human colonic tissue was obtained from the Gastroenterology Department of Beaumont Hospital. Crypts were isolated (Section 2–21) and were then attached to chamber slides using Cell-Tak™ (Section 2-22). Cells and crypts were washed in PBS, fixed in 100 % methanol, permeabilised with Triton X-100, and stained with specific fluorophore-labelled antibodies, as outlined in Section 2–23. Pseudo-colours were assigned to the various proteins where Na^+/K^+-ATPase α_1 is represented in green. In both panels FIH-1 is in magenta and the merge is in white (5 μm scale bar in panels A and B zoom, and 20 μm in upper panel B). This image is representative of 3 similar experiments

To more directly demonstrate that that FIH-1 interacts with Na^+/K^+-ATPase pumps, co-immunoprecipitation experiments were carried out. Using this approach whereby Na^+/K^+-ATPase α_1 was immunoprecipitated, we found that there was increased levels of FIH-1 bound to Na^+/K^+-ATPase α_1 in DMOG-treated cells (Figure 5–21). However, this experiment is somewhat limited by the omission of the IgG negative controls required to prove specificity of the protocol.

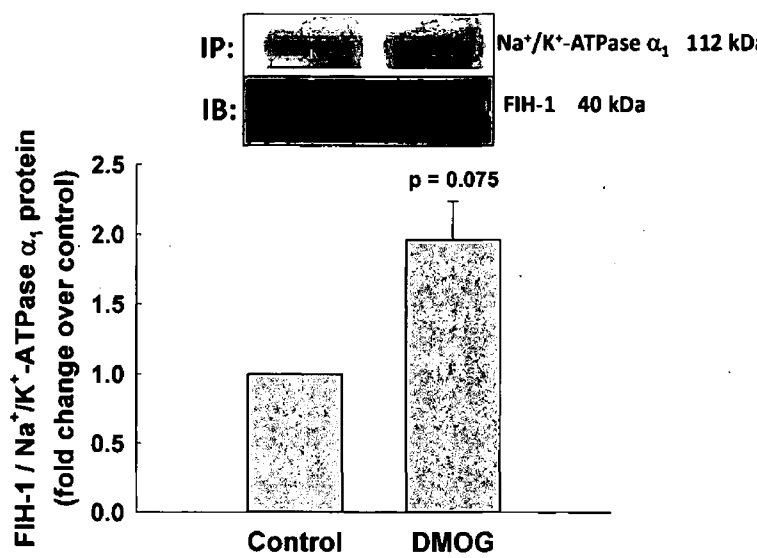

Figure 5–21 Hydroxylase inhibition increases FIH-1 binding to Na^+/K^+-ATPase α_1 subunits in T_{84} cells. T_{84} cells were cultured as monolayers on permeable supports until R_{te} stabilised at plateau levels. Cells were treated bilaterally with DMOG (1 mM) in serum-free medium for 24 hours and Na^+/K^+-ATPase α_1 subunits were immunoprecipitated (IP). Immunoprecipitates were washed thrice, and bound proteins were eluted using a low pH elution buffer. Proteins were resolved by SDS-PAGE and FIH-1 and Na^+/K^+-ATPase α_1 protein levels were measured by western blotting (IB) (n = 3; paired t-test; p = 0.075).

Finally, to explore whether FIH-1 interacts with MONaKA, preliminary co-immunoprecipitation experiments were carried out. Using this approach whereby MONaKA was immunoprecipitated, we found that there were increased levels of FIH-1 bound to MONaKA in DMOG-treated cells (Figure 5–22). However, this experiment is somewhat limited by the omission of the IgG negative controls required to prove specificity of the protocol.

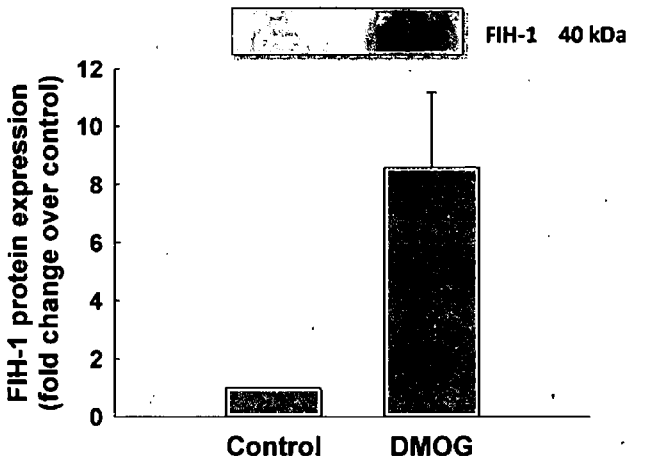

Figure 5–22 Hydroxylase inhibition increases FIH-1 binding to MONaKA in T_{84} cells. T_{84} cells were cultured as monolayers on permeable supports until R_{te} stabilised at plateau levels. Cells were treated bilaterally with DMOG (1 mM) in serum-free medium for 24 hours and MONaKA was immunoprecipitated. Immunoprecipitates were washed thrice, and bound proteins were eluted using a low pH elution buffer. Proteins were resolved by SDS-PAGE and FIH-1 protein expression was measured by western blotting (IB) (n = 3).

5-4 Discussion

Since our data from previous chapters suggested that hydroxylase inhibition does not alter membrane expression of the Na^+/K^+-ATPase or cellular ATP levels, in the current chapter we set out to investigate alternative mechanisms that do not involve altered pump expression or trafficking. Initially, we investigated the possibility that the effects of hydroxylase inhibition on Na^+/K^+-ATPase activity could be mediated by an epithelial-derived soluble factor, such as ET-1, acting in an autocrine fashion. Previous work has shown that ETs have the capacity to acutely regulate Na^+/K^+-ATPase function, via activation of ETB receptor, and subsequent increases in intracellular Ca^{2+} (Prasanna *et al.*, 2001; Liu *et al.*, 2009). There are various other endogenous molecules that are known to attenuate pump activity, such as cardiatonic steroids, and the hypoxia-stimulated hypothalamic inhibitory factor (Schoner and Scheiner-Bobis, 2005; De Angelis and Haupert, 1998), although whether these molecules can be synthesised by the intestinal epithelium is not known. If a secreted molecule, such as ET-1, was responsible for attenuating pump activity, then one would expect that conditioned medium from DMOG-treated cells should mimic the antisecretory effects of the drug. However, we did not find this to be the case, implying that secreted endothelins, or indeed other acutely acting soluble mediators, are not involved in mediating the effects of hydroxylase inhibition. In future studies the inclusion of a positive control for these experiments, such as stimulation of cells with ET-1 itself, and inclusion of protease inhibitors in the conditioned culture medium would bolster these results.

We also investigated the possibility that increased sequestration of the Na^+/K^+-ATPase into lipid rafts could mediate the effects of hydroxylase inhibition. Previous studies have shown that regulation of the pump in this manner attenuates its transporting function and promotes its role as a signalling protein through increased coupling to Src family kinases (Liang *et al.*, 2007). Thus, we investigated if chemical disruption of lipid rafts or inhibition of Src kinases could

reverse the antisecretory effects of DMOG-treatment. However, when MβCD was employed to disrupt lipid rafts in the basolateral plasma membrane, antisecretory actions of DMOG were unaltered. This suggests that sequestration into lipid rafts is not a factor underlying inhibition of Na^+/K^+-ATPase activity by hydroxylase inhibitors. However, this cannot be fully ruled out because, although the activity of the Na^+/K^+-ATPase was increased in MβCD-alone treated cells in what was the positive control for this experiment, it was approaching but did not quite reach statistical significance. Similarly, we know that activation of Src kinases contribute to the attenuation of Cl^- secretion, however, pharmacological inhibition of Src kinases with PP2 did not reverse the antisecretory effect of hydroxylase inhibition on Ca^{2+}-dependent secretory responses (Keely *et al.*, 2000). Interestingly however, upon Src inhibition with PP2, there was a partial reversal of the effect of DMOG on cAMP-dependent responses. These data may reflect a differential role for Src family kinases in mediating effects of hydroxylase inhibition on Ca^{2+} and cAMP-dependent secretory pathways. However, these data should be viewed cautiously since Src inhibition alone was noted to have profound effects on both Ca^{2+}- and cAMP-induced responses (Bertelsen *et al.*, 2002). A potential role for Src family kinases in mediating responses to hydroxylase inhibition could be further studied by investigating their phosphorylation and activation in response to DMOG treatment of colonic epithelial cells and by further investigating the effects of PP2 on DMOG-induced changes in transport protein function.

Several other signalling pathways were also investigated based on evidence indicating their potential for mediating the antisecretory effect of hydroxylase inhibition. PKC inhibition was found to be without effect on the antisecretory effects of DMOG. The PKC inhibitor, GF, has been reported to be a specific inhibitor of PKC that inhibits both classical and novel PKC isoforms (Toullec *et al.*, 1991; Roberts *et al.*, 2005). However, as with all chemical inhibitor data, one must be cautious in drawing conclusions, since other research has highlighted potential non-specific actions of the inhibitor (Alessi, 1997). PKA

inhibition was also without effect on the anti-secretory actions of DMOG. However, although H89 is widely used as an inhibitor of PKA, it also inhibits other pathways and therefore should not be used as the single source of evidence of PKA involvement (Murray, 2008; Lochner and Moolman, 2006). Finally, and as previously mentioned in Chapter 3, acriflavine was employed as a HIF inhibitor and was also found to be without effect on the antisecretory actions of DMOG. However, this result must also be treated with caution, since acriflavine was also without effect on DMOG-induced induction of the HIF-1-target, PHD2 (data not shown). This suggests that either HIF-1 was still transcriptionally active in the presence of acriflavine, or that PHD2 is under control of other transcription factors. Thus, our experiments using pharmacological inhibitors suggest that neither PKC, PKA, nor HIF are involved in mediating the antisecretory effects of hydroxylase inhibitors. However, these data should not be considered as conclusive since some of the inhibitors affected Cl^- secretion themselves, and further studies are required to definitively exclude these signalling pathways from mediating antisecretory actions of hydroxylase inhibition.

Further experiments were carried out to determine whether the inhibitory effect of hydroxylase inhibitors on Na^+/K^+-ATPase activity could be translationally or transcriptionally-mediated. However, we found that neither AD nor CHX, which are well-described inhibitors of transcription and translation respectively, attenuated the antisecretory effects of DMOG. This suggests that the effects of hydroxylase inhibition are likely to be post-translationally-mediated. Interestingly, previous reports on the regulation of transport protein function by HIF-1 show these actions to be transcriptionally-mediated (Ibla *et al.*, 2006; Zheng *et al.*, 2009). Therefore, the current data support the idea that HIF is not involved in mediating the antisecretory effects of hydroxylase inhibition. Furthermore, these findings suggest that post-translational modifications, such as altered interactions with regulatory proteins, or phosphorylation of the pump itself, may be involved.

To test the hypothesis that altered interactions with regulatory proteins might be involved, we first carried out some preliminary investigations to determine the expression of Na^+/K^+-ATPase-modifying proteins in colonic epithelial cells. It was found that neither FXYD3 nor PKC ζ expression was altered at either mRNA or protein levels, respectively. Of course, these proteins could be investigated in more depth by, for example, analysing their association with the Na^+/K^+-ATPase by co-immunoprecipitations or employing siRNA to inhibit their expression. Interestingly, although the mRNA expression of Na^+/K^+-ATPase β_1 subunit remained unaltered, Na^+/K^+-ATPase β_1 protein expression was significantly increased after 24 hours treatment with DMOG. Initially this result was perplexing, since the dogma has been that one Na^+/K^+-ATPase α subunit binds to one Na^+/K^+-ATPase β subunit, and in our previous studies we showed α_1 subunit expression to be unchanged by hydroxylase treatment. However, more recent studies investigating the ratio of Na^+/K^+-ATPase $\alpha : \beta$ subunits have shown that the α subunit can bind more than one β subunit, thereby offering an explanation for the observed increase in β_1, but not α_1 subunits (Clifford and Kaplan, 2008). Confocal analysis revealed that the Na^+/K^+-ATPase β_1 subunit appears to be specifically expressed within one z-plane in the basolateral membrane of T_{84} cells and that it co-localises with the Na^+/K^+-ATPase α_1 subunit. Immunohistochemical analysis showed a higher expression of Na^+/K^+-ATPase β_1 in the cytoplasm after treatment with DMOG, but it could not be conclusively determined as to whether there was a higher proportion of the β_1 subunit in the membrane. Analysis of the expression of the Na^+/K^+-ATPase β_1 subunit at the protein level yielded interesting results, with only the lower molecular weight (35 kDa) band showing increased expression in response to hydroxylase inhibition. However, increased expression of this unglycosylated form of the protein does not appear to affect activity of the pump, as demonstrated in previous studies using site-directed mutagenesis (Beggah *et al.*, 1997). Nor does glycosylation affect heterodimer formation or intracellular trafficking of the Na^+/K^+-ATPase (Tamkun and Fambrough, 1986). The

unglycosylated β_1 subunit is also associated with impairments in cell-cell junctions, decreased cell-cell contact, and increased migration, thereby causing an increase in paracellular permeability (Vagin *et al.*, 2007). However, our data do not support such a role for the β_1 subunit in colonic epithelial cells, since hydroxylase inhibition promoted, rather than attenuated, transepithelial resistance. Further studies are required to elucidate the precise role that the unglycosylated β_1 subunit plays in the antisecretory effects of hydroxylase inhibition, but one possibility could be that it interacts with another regulatory protein to alter Na^+/K^+-ATPase pump function.

A search of the literature for proteins that interact with the Na^+/K^+-ATPase β_1 subunit to negatively regulate pump activity yielded MONaKA as a potential candidate. MONaKA was originally discovered as a regulator of the Na^+/K^+-ATPase in astrocytes and has been shown to be expressed in other tissues. MONaKA contains a kinase domain, however it is thought to be inactive, thus it is currently unknown how MONaKA might regulate Na^+/K^+-ATPase activity. Studies by other groups present conflicting data regarding the expression profile of this protein. One study investigates expression of several splice forms and notes their absence from the heart (Zou *et al.*, 2005). However, a more recent study that investigated expression of one fragment of human MONaKA cDNA demonstrated its absence in the colon and presence in the heart (Takeuchi *et al.*, 2010). This is in contrast to data accessed on the Human Protein Atlas (www.humanproteinatlas.org) which shows that it is expressed in all GI tissues examined. The current studies revealed MONaKA to be expressed in colonic epithelial cells from a number of species, including humans. Furthermore, following hydroxylase inhibition its expression is increased almost 200 % of that in control cells. This effect appears to be independent of *de novo* protein synthesis as demonstrated by our findings with the inhibitor of translation, CHX. Interestingly, in contrast to its effects on protein expression, it was found that mRNA expression of MONaKA was significantly reduced after 24 hours treatment with DMOG. The mechanisms underlying these contrasting

actions at the mRNA and protein levels are as yet unknown, but it is possible that this represents a negative feedback loop. Indeed, future experiments involving a micro RNA screen of hydroxylase inhibitor-treated colonic epithelial cells could yield some interesting results and new lines of inquiry.

We also found that trafficking of MONaKA to the plasma membrane was increased in DMOG-treated cells. Confocal imaging revealed that MONaKA co-localised with Na^+/K^+-ATPase α_1 and β_1 subunits in human crypts. However, co-localisation in T_{84} cells was restricted to that of the β subunit. Co-immunoprecipitation experiments found MONaKA to associate with the Na^+/K^+-ATPase α_1 subunit, although these results require confirmation with an IgG negative control. In further experiments it was found that 24 hours following removal of hydroxylase inhibitors, MONaKA expression remained elevated, indicating that it is a very stable protein *in vitro*. It is possible that such stability is promoted by its interaction with the Na^+/K^+-ATPase or by some other post translational modifications.

Taken together the data presented here, along with what is already known regarding its inhibitory role in regulation of Na^+/K^+-ATPase pump activity, suggest that MONaKA plays an important role in mediating the antisecretory effects of hydroxylase inhibition in colonic epithelial cells. Furthermore, since we found that the pattern of expression of MONaKA in colonic crypts appears to be conserved across several species, our data underscore the likely importance of this protein in regulating intestinal secretory function. These data suggest that MONaKA might represent a target for the development of new anti-diarrhoeal therapies. However, the ubiquitous expression of the Na^+/K^+-ATPase and wide expression of MONaKA, would necessitate local intestinal targeting of a drug that targets MONaKA for the treatment of diarrhoea.

Our studies show that hydroxylase inhibition not only leads to increased association with MONaKA but also of the Na^+/K^+-ATPase $\beta1$ subunit with FIH-1.

Interestingly, as shown in Chapter 3, the asparaginyl hydroxylase is not regulated by hydroxylase inhibition at the mRNA or protein levels. However, analysis of its localisation within the cell before and after hydroxylase inhibition revealed that its expression at the membrane was increased upon treatment with DMOG and that it co-localised with the Na^+/K^+-ATPase α_1 subunit. How such interactions might regulate pump activity are as yet unknown, but one could speculate that similar to MONaKA, FIH-1 is a negative regulator of the pump and that, upon DMOG-treatment, it is released from other binding partners, e.g., HIF-1α, leaving it free to interact with the Na^+/K^+-ATPase (Mahon *et al.*, 2001). It has been shown that hydroxylation stabilises protein-protein interactions, therefore another possibility could be that via its ankyrin binding domain, the pump stably binds to a hydroxylated ankyrin partner, and that such an interaction facilitates its activity (Yang *et al.*, 2011). Such a mechanism has been previously shown to exist in the case of acetylated tubulin regulation of Na^+/K^+-ATPase activity (Casale *et al.*, 2003).

5-5 Summary

In summary, although there is still much work to be done, with the inclusion of more rigorous controls, the identification of MONaKA as a potential mediator of the antisecretory effects of hydroxylase inhibition in these studies is novel and intriguing. These data support existing evidence that the pump exists in a multimeric complex with several regulatory proteins, and suggest that both MONaKA and FIH are likely to have important roles to play in regulating pump activity in conditions of hypoxia (Figure 5-23). MONaKA is well known as a regulator of Na^+/K^+-ATPase pump function and our data suggest that it could act as a molecular switch that co-ordinates Na^+/K^+-ATPase pump activity with oxygen availability in epithelial cells. As such, MONaKA, and its associated regulatory proteins, represent good targets for the development of new anti-diarrhoeal drugs.

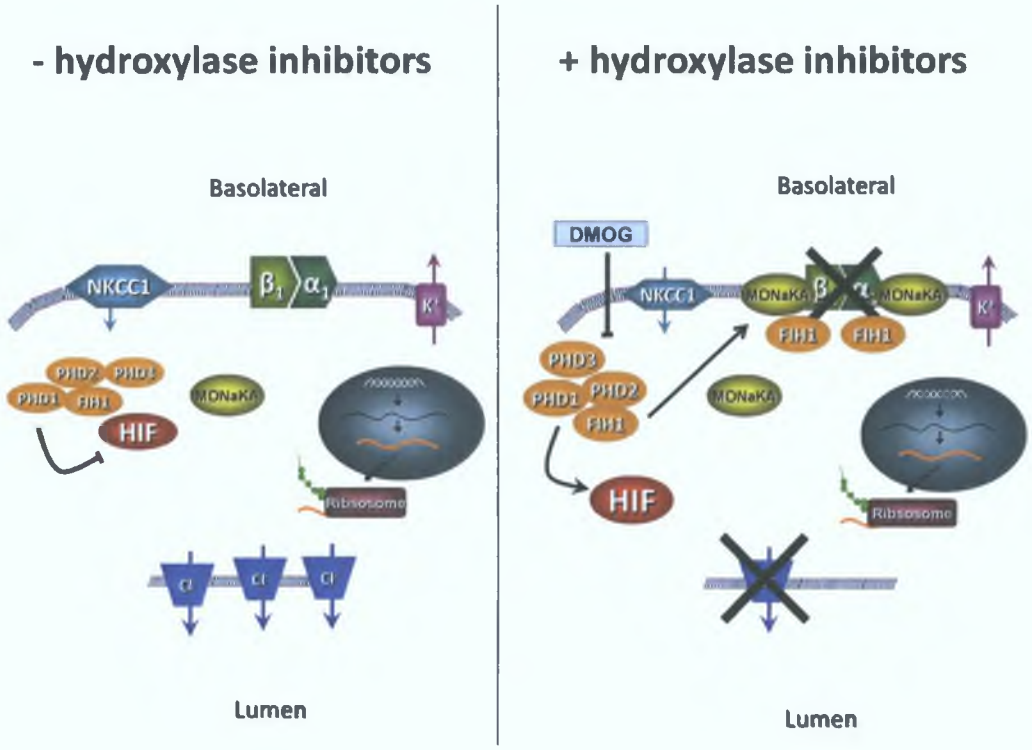

Figure 5–23 Hydroxylase inhibition stimulates the formation of a multimeric inhibitory complex at the Na^+/K^+-ATPase pump. Hydroxylase inhibition attenuates Cl^- secretion by reducing of the activity of the Na^+/K^+-ATPase. We propose that this occurs through the stabilisation of MONaKA protein, independent of transcription or translation. MONaKA then binds to the Na^+/K^+-ATPase at the plasma membrane where it forms a complex with FIH-1 and inhibits the activity of the Na^+/K^+-ATPase, thereby inhibiting epithelial secretory responses.

Chapter 6

General Discussion

HIF hydroxylases, which include FIH-1 and PHDs, are cellular oxygen sensors that serve as gatekeepers of the hypoxic response. They utilise O_2 as a co-substrate and couple the hydroxylation of HIF-1α to the oxidative decarboxylation of α-ketoglutarate and CO_2. They specifically hydroxylate target amino acids on HIF-1α and HIF-2α, IKK, and other proteins that contain consensus hydroxylation motifs. HIF hydroxylase regulation of cellular function is a rapidly expanding area of research as indicated by the number of publications on the topic in the recent past (Figure 1-4). One of the most prominent areas of HIF hydroxylase research is in the GI tract where research is particularly focussed on the role of HIF hydroxylases in the pathogenesis of inflammation (Robinson *et al.*, 2008; Cummins *et al.*, 2008; Tambuwala *et al.*, 2010; Hindryckx *et al.*, 2010; Hart *et al.*, 2011), and cancer (Xue *et al.*, 2010).

Cl^- secretion, an important physiological process in the intestine, is a highly energy-demanding process and depends on O_2 for the generation of cellular energy in the form of ATP (Mandel and Balaban, 1981; Durand *et al.*, 1988; Carra *et al.*, 2011). ATP is utilised by Na^+/K^+-ATPase pumps to create the electrochemical driving force for Cl^- secretion to occur. Previous studies have shown that hydroxylase inhibition ameliorates experimental colitis and prevents diarrhoea, thus this thesis was based on the overarching hypothesis that epithelial fluid and electrolyte transport may also be regulated by hydroxylase activity (Cummins *et al.*, 2008; Robinson *et al.*, 2008). The findings presented support this hypothesis by showing that hydroxylase inhibition significantly attenuates epithelial secretion both *in vitro* and *in vivo*. These findings make a significant contribution to our knowledge of the role of hydroxylases in intestinal physiology and suggest that these enzymes, and their associated signalling mechanisms, represent good targets for the development of new drugs to treat intestinal transport disorders. A schematic representation of our current understanding of how hydroxylase inhibition may downregulate epithelial secretion is shown in Figure 6-1.

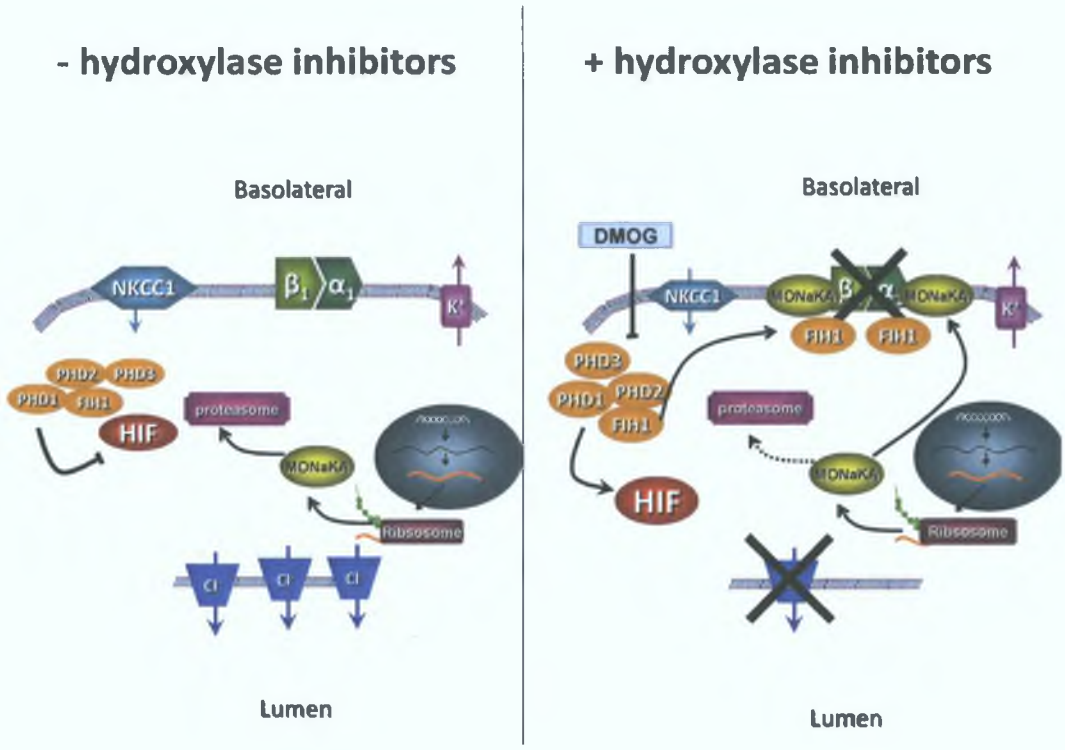

Figure 6-1 Hydroxylase inhibition attenuates colonic epithelial secretory function. Hydroxylase inhibition causes robust stabilisation of HIF-1α in colonic epithelia and also exerts profound antisecretory effects. Despite down-regulation of CFTR and NKCC1 expression, the activities of these transporters were unaltered by hydroxylase inhibition. Neither Ca^{2+} nor cAMP levels in the cells were altered by hydroxylase inhibition. However, hydroxylase inhibition reduced the activity of basolateral Na^+/K^+-ATPase pumps. Hydroxylase inhibition did not alter the expression of the catalytic Na^+/K^+-ATPase α_1 subunit, but caused an increase in the expression of the Na^+/K^+-ATPase β_1 subunit and MONaKA. We show that the anti-secretory phenomenon occurs independently of transcription or translation, and we propose that MONaKA stabilisation may occur by inhibition of its proteasomal degradation. MONaKA and the Na^+/K^+-ATPase α_1 subunit associate at the plasma membrane where they form a complex with FIH-1. This complex behaves as a molecular switch, that inhibits the activity of the Na^+/K^+-ATPase, thereby attenuating luminal Cl^- secretion.

Our investigations into regulation of ion transport by hydroxylase inhibition were initially focussed on the transport process of Cl^- secretion. *In vitro* studies revealed that hydroxylase inhibition by DMOG was potently anti-secretory, an

effect which was coincident with intracellular accumulation of HIF-1α and HIF-2α. Another inhibitor of HIF hydroxylases, FG-4497, which exerts its actions by directly blocking their active site, re-capitulated our findings with DMOG, re-affirming the role of HIF hydroxylases in mediating this antisecretory action. Intracellular second messengers which activate the Cl^- secretory pathway were not affected by hydroxylase inhibition which suggested that the antisecretory effect may be mediated by alterations in the transport proteins that constitute the Cl^- secretory pathway. However, to first give our *in vitro* findings some physiological relevance we carried out experiments to translate them into a mouse model. Similar to its effects in cultured epithelia, treatment of mice with DMOG significantly blunted agonist-stimulated colonic I_{sc} responses to CCh and FSK, which are known to be predominantly due to Cl^- secretion (Cuthbert *et al.*, 1994). Since previous studies have demonstrated that Cl^- secretion is the primary driving force underlying diarrhoea in anaphylactic models, we investigated the effect of hydroxylase inhibition in a mouse model of allergic diarrhoea (Perdue *et al.*, 1991; Brandt *et al.*, 2003). Diarrhoea in OVA-sensitised mice treated with DMOG was dramatically delayed and less severe compared to controls. These data clearly point to a potential role for drugs which target hydroxylase-dependent signalling mechanisms for treatment of diarrhoeal diseases.

While hydroxylase inhibition clearly exerts antisecretory actions in the colon, it is important to bear in mind that the intestine is primarily an absorptive organ. Approximately 9 litres of fluid enter the proximal small intestine each day and normally only approximately 200 ml are lost in the stool. With this in mind, when considering the development of new drugs for diarrhoea, their effects on absorptive processes must also be considered. SGLT-1 is one of the main pathways for intestinal fluid absorption and is also the primary transporter involved in oral rehydration therapy. Interestingly, we found that absorption through small intestinal SGLT1 was not affected by hydroxylase inhibition. Since most fluid absorption occurs in the small intestine, this is a very important

finding for consideration when using hydroxylase inhibitors for treatment of secretory diarrhoeas. In contrast with this, we found that the activity of another important intestinal epithelial Na^+ transporter, ENaC, was significantly reduced following treatment with DMOG. This could be a particularly important consideration for people with pseudohypoaldosteronism (PHA), where there is already urinary loss of Na^+ from the body (Kuhnle, 1997; Hummler and Horisberger, 1999). It has however, been suggested that under normal conditions there is a certain degree of redundancy in colonic ENaC function with regard to whole-body fluid and electrolyte homeostasis and therefore, specific targeting of hydroxylase inhibitors to the colon may be sufficient to overcome potential complications arising from renal effects of these drugs (Hummler and Horisberger, 1999).

NHEs are also important transport proteins that mediate absorption in the intestine and should also be considered when developing any new therapeutics that target epithelial transport function. Interestingly, it has been reported that chronic hypoxia elevated pH_i by activating Na^+/H^+ exchange in pulmonary arterial smooth muscle cells, an effect which was inhibited by exposure to EIPA (Rios *et al.*, 2005). Using fluorescent imaging techniques we were able to determine that the activity of NHEs was blunted by DMOG-treatment in T_{84} cells. However, the studies described here cannot discriminate which NHE isoform might be involved, therefore, it is difficult to draw detailed conclusions. This is further compounded by the fact that there is a lack of selective inhibitors available for the various NHE isoforms, and because NHE3 is not expressed in our T_{84} cell model of the colonic epithelium (Beltran *et al.*, 2008). NHE3 is expressed apically throughout the intestine and plays a major role in Na^+ absorption (Ikuma *et al.*, 1999; Zachos *et al.*, 2005; Schultheis *et al.*, 1998). Studies have shown that at high concentrations (>25 μM), EIPA inhibits NHE1 and 2, but also inhibits the EIPA-resistant NHE4 isoform (Beltran *et al.*, 2008). Since lower concentrations of EIPA (which inhibit NHE1 and 2, but not NHE4) did not affect Cl^- secretion, the reversal of the inhibitory effect of DMOG by

concentrations of EIPA > 25 μM suggest it is ah NHE4-mediated effect. NHE4 is expressed basolaterally in epithelia of several tissues and has been shown to be important in the regulation of intracellular pH (Pizzonia *et al.*, 1998; Beltran *et al.*, 2008). Given their important role in mediating fluid and electrolyte absorption in the intestine, the role of hydroxylase inhibitors in regulation of NHE function is a subject that requires further investigation. Future studies could investigate the expression of the various NHE isoforms in DMOG-treated cells, employ ^{22}Na isotopic flux assays for measurements of their activity, and siRNA approaches along with the use of more specific pharmacological inhibitors to elucidate the roles of individual isoforms.

Another intriguing aspect of NHE function that was not investigated in this study relates to its role in regulating inflammation. NHE inhibition has previously been shown to attenuate enterocyte inflammatory responses and to ameliorate the course of IBD in DSS-treated mice. This could have some bearing on previous findings by Cummins *et al* in the DSS model of colitis, where DMOG was shown to ameliorate colitis, attenuate apoptosis, and abrogate interleukin production (Cummins *et al.*, 2008). Previous studies have shown that NHE inhibition attenuates IL-8 production in endothelial and epithelial cells, while it inhibits apoptosis in colonic epithelial cells and other models (Nemeth *et al.*, 2002a; Nemeth *et al.*, 2002b; Rebillard *et al.*, 2007; Chakrabarti *et al.*, 1997). NHE-1 is expressed on the basolateral membrane of colonic epithelial cells and is thought to function in a house-keeping role by maintaining pH_i (Ikuma *et al.*, 1999). NHE1 and NHE3 are known to be induced in models of colitis, including TNBS-induced colitis (Khan *et al.*, 1998; Khan and Ali, 1999). Further studies have shown that inhibition of NHE1 ameliorates experimental colitis and reverses the colitis-induced reduction in contractility of colonic smooth muscle (Khan *et al.*, 2005). Interestingly, Robinson *et al* have shown that hydroxylase inhibition by FG-4497 in a TNBS-induced mouse model of colitis, enhanced fibroblast contraction in collagen gels (Robinson *et al.*, 2008). With this in mind, one could speculate that hydroxylase inhibition of NHE activity could be a

unifying mechanism that enhances contractility, attenuates interleukin production, and prevents apoptosis in colitis. Thus, further investigations of hydroxylase regulation of NHEs could yield some important results as to their roles in regulating both ion transport and inflammation.

In order to determine the mechanisms underlying the antisecretory effect of hydroxylase inhibition in intestinal epithelial cells, the activities of various components of the Cl^- secretory pathway were examined. No changes in apical CFTR currents following hydroxylase inhibition were observed. This was initially surprising, given that in agreement with previous studies, expression of CFTR was reduced in DMOG-treated cells (Zheng *et al.*, 2009). However, previous studies have shown that only small amounts of CFTR are required in the apical membrane for functionality which, in conjunction with studies of ion transport in the intestine of CF-mice, underscores the critical role that the channel plays in the lubrication of the intestinal lumen (De Jonge, 2006; Cuthbert *et al.*, 1994). In the current studies, an investigation of the effects of hydroxylase inhibition on expression of the Ca^{2+}-dependent Cl^- conductance, TMEM16A, indicated that there was a tendency towards an increase in expression of the protein at the mRNA level. Although this effect did not reach statistical significance in these studies, such a response *in vivo* could have important physiological significance where induction of Cl^- channels, such as TMEM16A, could be a mechanism to compensate for the repression of CFTR by HIF-1.

HIF-1α is a primary target of the HIF-hydroxylases and HIF-1 has previously been shown to be an important regulator of transport proteins that comprise the Cl^- secretory pathway (Ibla *et al.*, 2006; Zheng *et al.*, 2009). Since DMOG-induced stabilisation of HIF-1 was coincidental to the antisecretory actions of hydroxylase inhibition in the current studies, we carried out experiments to ascertain whether HIF-1 was involved in mediating this effect. Interestingly, we found that neither a HIF inhibitor (acriflavine) nor inhibition of transcription, or translation, reversed the antisecretory effects of hydroxylase inhibition. These

data suggest, therefore, that the antisecretory effects of hydroxylase inhibition occur by a HIF-independent mechanism. Furthermore, findings indicate that while $CoCl_2$ potently stabilised HIF, in contrast to DMOG it attenuated Cl^- secretion by inhibiting CFTR activity, without altering Na^+/K^+-ATPase activity. DMOG and $CoCl_2$ behave quite differently in terms of inhibition of HIF hydroxylases. $CoCl_2$ does not inhibit asparaginyl hydroxylation, whereas DMOG potently inhibits asparaginyl hydroxylation (Tian *et al.*, 2011b). This suggests that the antisecretory effects of DMOG may occur by a mechanism that involves inhibition of asparaginyl hydroxylation, but that is independent of HIF.

Since our data suggest that the antisecretory effect of hydroxylase inhibition is asparaginyl-hydroxylase-mediated, we explored the possibility that the asparaginyl hydroxylase, FIH-1, might be involved. Interestingly, FIH-1 translocated to the basolateral membrane where it bound to the Na^+/K^+-ATPase α_1 subunit following DMOG-treatment. This suggests that FIH-1 in conjunction with MONaKA and Na^+/K^+-ATPase β_1, binds the pump to form a negative regulatory complex. The role that FIH-1 plays in this complex is unknown but one could speculate that FIH-1 is a negative regulator of the pump and that, DMOG-treatment results in a dissociation from HIF-1α, leaving it free to interact with the Na^+/K^+-ATPase. It has been shown that hydroxylation stabilises protein-protein interactions, therefore another possibility could be that via its ankyrin binding domain, the pump stably binds to a hydroxylated ankyrin partner, and that such an interaction facilitates its activity (Yang *et al.*, 2011). Such a mechanism has been shown to exist as evidenced by regulation of the Na^+/K^+-ATPase pump by acetylated tubulin (Casale *et al.*, 2003).

While each of the transport proteins that comprise the Cl^- secretory pathway are interlinked and are dependent on each other for function, the activity of Na^+/K^+-ATPase pumps is the energy-dependent step of the process. Interestingly, although we found that hydroxylase inhibition dramatically attenuated activity of the pump, expression of the catalytic α_1 subunit remained

unaltered, as did levels of cellular ATP. This is in contrast to other research showing hypoxia attenuated pump expression as well as activity (Planes *et al.*, 1996; Mairbaurl *et al.*, 2002; Carpenter *et al.*, 2003; Dada *et al.*, 2003; Gusarova *et al.*, 2011). The mechanisms involved are complex and involve mitochondrial ROS, which is produced during hypoxia, but not by treatment with DMOG (Gusarova *et al.*, 2011; Emerling *et al.*, 2007). Therefore, we would not expect DMOG and hypoxia to have the same effects on the pump. We therefore investigated alternative mechanisms, and molecular regulation of the pump by proteins such as PKA, PKC, FXYD family members, Na^+/K^+-ATPase β_1, and MONaKA, amongst others. After an initial screen of these signalling pathways, an exploration of the expression of regulatory proteins was carried out, and the Na^+/K^+-ATPase β_1 subunit provided a target for further study. Hydroxylase inhibition caused an increase in Na^+/K^+-ATPase β_1 protein expression. Incidentally, increases in Na^+/K^+-ATPase β_1 subunit expression have been previously shown to enhance R_{te}. This is due to the n-glycan branching of the Na^+/K^+-ATPase β_1 subunit binding to other subunits on neighbouring cells, thereby increasing R_{te} (Vagin *et al.*, 2008). This might, at least in part, explain the increase in R_{te} we observed in response to hydroxylase inhibition in these studies. However, since the Na^+/K^+-ATPase β_1 subunit is known to facilitate pump activity, it seemed unlikely that increases in its expression would inhibit the pump after treatment with DMOG (Shoshani *et al.*, 2005; Padilla-Benavides *et al.*, 2010). Therefore, Na^+/K^+-ATPase β_1-interacting proteins that are known to inhibit pump activity were explored (Mao *et al.*, 2005; Gorokhova *et al.*, 2007). Investigation of one of these proteins, MONaKA, revealed it to be significantly upregulated by hydroxylase inhibition.

MONaKA exists as at least two splice variants, with the splicing conserved perfectly between mouse and human, suggesting that it serves an important function (Mao *et al.*, 2005). Following DMOG-treatment, MONaKA translocated to the basolateral membrane where interestingly, its expression is also conserved across mouse, rat, and human colonic crypts, again accentuating its

potential physiological importance in regulating basolateral transporters in intestinal epithelia. Although MONaKA protein expression was increased, mRNA expression was reduced by DMOG-treatment. This could be as a result of a post-translational modification of MONaKA leading to its stabilisation, or due to a negative feedback loop to regulate MONaKA expression, perhaps mediated by an miRNA-mediated mechanism. The importance of miRNA in mediating responses to hypoxia has recently been highlighted by our collaborators who showed regulation of HIF-1α by miRNA155 (Bruning *et al.*, 2011). Further studies to investigate the potential role for miRNAs in mediating hydroxylase actions on epithelial transport function are required.

In addition to MONaKA and the Na^+/K^+-ATPase β_1 subunit, there are several other proteins known to be important in regulating Na^+/K^+-ATPase pump expression, including TCTP, Na^+/K^+-ATPase-interacting (NKAIN), and FXYD family members. Due to time constraints, these proteins were not investigated in the current studies but do warrant some discussion. TCTP was initially identified as a protein that binds to the third cytoplasmic domain of Na^+/K^+-ATPase α_1, the expression of which was found to repress pump activity by a mechanism not yet fully understood (Jung *et al.*, 2004). Further research by the same group showed that another cytosolic protein, SNX6, reversed this repression by binding to, and sequestering, TCTP. However, there is a paucity of information on the physiological roles of TCTP and SNX6 in the intestine, and future studies into the effects of hydroxylase inhibition on their expression and association with the Na^+/K^+-ATPase pump could yield some interesting findings. FXYD family members are membrane-associated proteins that are known to modify the transport properties of Na^+/K^+-ATPase pumps in a tissue-specific manner, without altering its expression (Garty and Karlish, 2006; Delprat *et al.*, 2006; Geering, 2006). More recent research also suggests that they contribute to stabilisation of the pump at the membrane (Mishra *et al.*, 2011). Thus, this family of proteins could play an important role in mediating the effects of hydroxylases on pump activity in intestinal epithelial cells. Preliminary studies

showed that treatment of cells with DMOG did not alter FXYD3 mRNA. We cannot however, rule out the possibility that FXYD3 expression might be regulated by post-translational mechanisms and this could be a topic for future studies. FXYD5 is also a candidate for future research as its over-expression has been shown to increase pump activity in Xenopus oocytes (Lubarski *et al.*, 2005). Finally, NKAINs are of great relevance to the current studies as they have been recently identified as Na^+/K^+-ATPase β_1 interacting proteins that must also form complexes with MONaKA in order to be activated (Gorokhova *et al.*, 2007).

Overall, the data presented in this thesis provide important new insights into how intestinal fluid and electrolyte transport may be regulated in health and disease. The discovery that hydroxylases play a key role in the regulation of intestinal secretion suggests that under conditions of intestinal stress, such as hypoxia associated with inflammation or fibrosis, downregulation of Na^+/K^+-ATPase activity may serve as a physiological switch that attenuates epithelial transport processes, thereby conserving cellular energy. Under such conditions, reductions in ATP consumption by the pump may allow for the redistribution of cellular energy from costly transport processes into tissue restitution and repair. Such actions may, at least in part, underlie the protective effects of hydroxylase inhibitors observed in mouse models of IBD (Robinson *et al.*, 2008; Cummins *et al.*, 2008). In fact, decreased Na^+/K^+-ATPase activity has been recorded in the intestines of patients with IBD (Ejderhamn *et al.*, 1989). However, the current studies may have even more broad implications for our understanding of how intestinal physiology is regulated under normal conditions. Given the harsh environment in which the intestinal epithelium exists, between the richly perfused vasculature of the serosa and the anoxic lumen of the gut, O_2 levels are constantly fluctuating. These fluctuations are amplified by the dynamic nature of the splanchnic circulation, with post-prandial increases and exercise-associated decreases in blood flow (Musch *et al.*, 1987; Matheson *et al.*, 2000). Thus, a molecular switch, such as that potentially mediated by MONaKA/FIH-1, to regulate ATP consumption by the Na^+/K^+-ATPase would be beneficial in that it

could serve to co-ordinate epithelial transport with O_2 availability. For example, between meals, intestinal blood flow and O_2 availability are low and under these conditions, hydroxylases would be inactive. Under such conditions, we would expect Na^+/K^+-ATPase activity to be attenuated, thereby limiting energy expenditure on epithelial transport processes when they are not required. On the other hand, upon feeding, epithelial fluid and electrolyte secretion are required to provide a fluid environment for the mixing of food particles with digestive enzymes, and for lubrication of the food bolus as it moves through the lower intestine. Under these conditions, intestinal blood flow and O_2 availability increase, hydroxylases are activated, and pump activity increases, thereby allowing expenditure of cellular energy on transport processes. Our data suggest that MONaKA, the Na^+/K^+-ATPase β_1 subunit, and FIH-1 potentially play key roles in these processes by forming multimeric complexes with the Na^+/K^+-ATPase α_1 subunit in a hydroxylase-sensitive manner. It would be interesting to test this hypothesis in future studies by examining association of MONaKA and FIH-1 with the pump under fasting and non-fasting conditions.

In conclusion, from a clinical perspective our data suggest that by virtue of their ability to act as a molecular switch to regulate epithelial secretion, hydroxylases represent good targets for development of new anti-diarrhoeal drugs. However, our studies also reveal that the anti-diarrhoeal effects of hydroxylase inhibitors are mediated by inhibition of Na^+/K^+-ATPase activity, by a mechanism that likely involves MONaKA. Since these proteins are expressed throughout the body, there is the possibility that side effects may occur upon anti-diarrhoeal treatment with hydroxylase inhibitors. While it is encouraging that in our own *in vivo* studies we did not observe significant toxicity to DMOG at concentrations that prevent diarrhoea, future studies should focus on the potential for using targeted drug formulations to enhance the delivery of hydroxylase inhibitors to the intestine. Such technologies have received much attention and are already in use to treat a variety of intestinal disorders (Yang *et*

al., 2002; Haddish-Berhane *et al.*, 2007; Prakash and Malgorzata Urbanska, 2008).

Chapter 7

Bibliography.

AGRE, P., PRESTON, G. M., SMITH, B. L., JUNG, J. S., RAINA, S., MOON, C., GUGGINO, W. B. & NIELSEN, S. 1993. Aquaporin CHIP: the archetypal molecular water channel. *Am J Physiol,* 265, F463-76.

ALESSI, D. R. 1997. The protein kinase C inhibitors Ro 318220 and GF 109203X are equally potent inhibitors of MAPKAP kinase-1β (Rsk-2) and p70 S6 kinase. *FEBS Lett,* 402, 121-3.

ALMACA, J., TIAN, Y., ALDEHNI, F., OUSINGSAWAT, J., KONGSUPHOL, P., ROCK, J. R., HARFE, B. D., SCHREIBER, R. & KUNZELMANN, K. 2009. TMEM16 proteins produce volume-regulated chloride currents that are reduced in mice lacking TMEM16A. *J Biol Chem,* 284, 28571-8.

ALZAMORA, R., GONG, F., RONDANINO, C., LEE, J. K., SMOLAK, C., PASTOR-SOLER, N. M. & HALLOWS, K. R. 2010. AMP-activated protein kinase inhibits KCNQ1 channels through regulation of the ubiquitin ligase Nedd4-2 in renal epithelial cells. *Am J Physiol Renal Physiol,* 299, F1308-19.

AMASHEH, S., BARMEYER, C., KOCH, C. S., TAVALALI, S., MANKERTZ, J., EPPLE, H. J., GEHRING, M. M., FLORIAN, P., KROESEN, A. J., ZEITZ, M., FROMM, M. & SCHULZKE, J. D. 2004. Cytokine-dependent transcriptional down-regulation of epithelial sodium channel in ulcerative colitis. *Gastroenterology,* 126, 1711-20.

ANDERSON, J. M. & VAN ITALLIE, C. M. 2009. Physiology and function of the tight junction. *Cold Spring Harb Perspect Biol,* 1, a002584.

ANUNDI, I., KING, J., OWEN, D. A., SCHNEIDER, H., LEMASTERS, J. J. & THURMAN, R. G. 1987. Fructose prevents hypoxic cell death in liver. *Am J Physiol,* 253, G390-6.

AOYAMA, T., MATSUI, T., NOVIKOV, M., PARK, J., HEMMINGS, B. & ROSENZWEIG, A. 2005. Serum and glucocorticoid-responsive kinase-1 regulates cardiomyocyte survival and hypertrophic response. *Circulation,* 111, 1652-9.

APPELHOFF, R. J., TIAN, Y. M., RAVAL, R. R., TURLEY, H., HARRIS, A. L., PUGH, C. W., RATCLIFFE, P. J. & GLEADLE, J. M. 2004. Differential function of the prolyl hydroxylases PHD1, PHD2, and PHD3 in the regulation of hypoxia-inducible factor. *J Biol Chem,* 279, 38458-65.

ASIKAINEN, T. M., AHMAD, A., SCHNEIDER, B. K., HO, W. B., AREND, M., BRENNER, M., GUNZLER, V. & WHITE, C. W. 2005. Stimulation of HIF-1α, HIF-2α, and VEGF by prolyl 4-hydroxylase inhibition in human lung endothelial and epithelial cells. *Free Radic Biol Med,* 38, 1002-13.

BAADER, E., TSCHANK, G., BARINGHAUS, K. H., BURGHARD, H. & GUNZLER, V. 1994. Inhibition of prolyl 4-hydroxylase by oxalyl amino acid derivatives *in vitro,* in isolated microsomes and in embryonic chicken tissues. *Biochem J,* 300 (Pt 2), 525-30.

BACHMANN, O., WUCHNER, K., ROSSMANN, H., LEIPZIGER, J., OSIKOWSKA, B., COLLEDGE, W. H., RATCLIFF, R., EVANS, M. J., GREGOR, M. & SEIDLER, U. 2003. Expression and regulation of the Na^+-K^+-$2Cl^-$ cotransporter NKCC1 in the normal and CFTR-deficient murine colon. *J Physiol,* 549, 525-36.

BARKER, N., RIDGWAY, R. A., VAN ES, J. H., VAN DE WETERING, M., BEGTHEL, H., VAN DEN BORN, M., DANENBERG, E., CLARKE, A. R., SANSOM, O. J. &

CLEVERS, H. 2009. Crypt stem cells as the cells-of-origin of intestinal cancer. *Nature,* 457, 608-11.

BARMEYER, C., RAHNER, C., YANG, Y., SIGWORTH, F. J., BINDER, H. J. & RAJENDRAN, V. M. 2010. Cloning and identification of tissue-specific expression of KCNN4 splice variants in rat colon. *Am J Physiol Cell Physiol,* 299, C251-63.

BARRETT, K. E. 1991. Immune-related intestinal chloride secretion. III. Acute and chronic effects of mast cell mediators on chloride secretion by a human colonic epithelial cell line. *J Immunol,* 147, 959-64.

BARRETT, K. E., COHN, J. A., HUOTT, P. A., WASSERMAN, S. I. & DHARMSATHAPHORN, K. 1990. Immune-related intestinal chloride secretion. II. Effect of adenosine on T84 cell line. *Am J Physiol,* 258, C902-12.

BARRETT, K. E. & KEELY, S. J. 2000. Chloride secretion by the intestinal epithelium: molecular basis and regulatory aspects. *Annu Rev Physiol,* 62, 535-72.

BEGGAH, A. T., JAUNIN, P. & GEERING, K. 1997. Role of glycosylation and disulfide bond formation in the β subunit in the folding and functional expression of Na,K-ATPase. *J Biol Chem,* 272, 10318-26.

BEGUIN, P., BEGGAH, A. T., CHIBALIN, A. V., BURGENER-KAIRUZ, P., JAISSER, F., MATHEWS, P. M., ROSSIER, B. C., COTECCHIA, S. & GEERING, K. 1994. Phosphorylation of the Na,K-ATPase α-subunit by protein kinase A and C *in vitro* and in intact cells. Identification of a novel motif for PKC-mediated phosphorylation. *J Biol Chem,* 269, 24437-45.

BEITNER-JOHNSON, D., LEIBOLD, J. & MILLHORN, D. E. 1998. Hypoxia regulates the cAMP- and Ca^{2+}/calmodulin signaling systems in PC12 cells. *Biochem Biophys Res Commun,* 242, 61-6.

BELTRAN, A. R., RAMIREZ, M. A., CARRARO-LACROIX, L. R., HIRAKI, Y., REBOUCAS, N. A. & MALNIC, G. 2008. NHE1, NHE2, and NHE4 contribute to regulation of cell pH in T84 colon cancer cells. *Pflugers Arch,* 455, 799-810.

BERCHNER-PFANNSCHMIDT, U., TUG, S., TRINIDAD, B., OEHME, F., YAMAC, H., WOTZLAW, C., FLAMME, I. & FANDREY, J. 2008. Nuclear oxygen sensing: induction of endogenous prolyl-hydroxylase 2 activity by hypoxia and nitric oxide. *J Biol Chem,* 283, 31745-53.

BERGER, H. A., TRAVIS, S. M. & WELSH, M. J. 1993. Regulation of the cystic fibrosis transmembrane conductance regulator Cl^- channel by specific protein kinases and protein phosphatases. *J Biol Chem,* 268, 2037-47.

BERGLINDH, T. 1984. The mammalian gastric parietal cell *in vitro*. *Annu Rev Physiol,* 46, 377-92.

BERRA, E., BENIZRI, E., GINOUVES, A., VOLMAT, V., ROUX, D. & POUYSSEGUR, J. 2003. HIF prolyl-hydroxylase 2 is the key oxygen sensor setting low steady-state levels of HIF-1α in normoxia. *EMBO J,* 22, 4082-90.

BERSCHNEIDER, H. M., KNOWLES, M. R., AZIZKHAN, R. G., BOUCHER, R. C., TOBEY, N. A., ORLANDO, R. C. & POWELL, D. W. 1988. Altered intestinal chloride transport in cystic fibrosis. *FASEB J,* 2, 2625-9.

BERTELSEN, L. S., BARRETT, K. E. & KEELY, S. J. 2002. Src family kinases mediate cAMP-dependent Cl^- secretion in intestinal epithelial cells. *Gastroenterology,* 122, A140.

BIBERT, S., AEBISCHER, D., DESGRANGES, F., ROY, S., SCHAER, D., KHAROUBI-HESS, S., HORISBERGER, J. D. & GEERING, K. 2009. A link between FXYD3 (Mat-8)-mediated Na,K-ATPase regulation and differentiation of Caco-2 intestinal epithelial cells. *Mol Biol Cell,* 20, 1132-40.

BIJVELDS, M. J., BOT, A. G., ESCHER, J. C. & DE JONGE, H. R. 2009. Activation of intestinal Cl^- secretion by lubiprostone requires the cystic fibrosis transmembrane conductance regulator. *Gastroenterology,* 137, 976-85.

BLACK, J. W., DUNCAN, W. A., DURANT, C. J., GANELLIN, C. R. & PARSONS, E. M. 1972. Definition and antagonism of histamine H 2 -receptors. *Nature,* 236, 385-90.

BLOUNT, A., ZHANG, S., CHESTNUT, M., HIXON, B., SKINNER, D., SORSCHER, E. J. & WOODWORTH, B. A. 2011. Transepithelial ion transport is suppressed in hypoxic sinonasal epithelium. *Laryngoscope,* 121, 1929-34.

BOTTO, L., BERETTA, E., BULBARELLI, A., RIVOLTA, I., LETTIERO, B., LEONE, B. E., MISEROCCHI, G. & PALESTINI, P. 2008. Hypoxia-induced modifications in plasma membranes and lipid microdomains in A549 cells and primary human alveolar cells. *J Cell Biochem,* 105, 503-13.

BRADBURY, N. A. 1999. Intracellular CFTR: localization and function. *Physiol Rev,* 79, S175-91.

BRANDT, E. B., STRAIT, R. T., HERSHKO, D., WANG, Q., MUNTEL, E. E., SCRIBNER, T. A., ZIMMERMANN, N., FINKELMAN, F. D. & ROTHENBERG, M. E. 2003. Mast cells are required for experimental oral allergen-induced diarrhea. *J Clin Invest,* 112, 1666-77.

BRENNAN, K., OFFIAH, G., MCSHERRY, E. A. & HOPKINS, A. M. 2010. Tight junctions: a barrier to the initiation and progression of breast cancer? *J Biomed Biotechnol,* 2010, 460607.

BRETT, C. L., DONOWITZ, M. & RAO, R. 2005. Evolutionary origins of eukaryotic sodium/proton exchangers. *Am J Physiol Cell Physiol,* 288, C223-39.

BROUILLARD, F., BOUTHIER, M., LECLERC, T., CLEMENT, A., BAUDOUIN-LEGROS, M. & EDELMAN, A. 2001. NF-κB mediates up-regulation of CFTR gene expression in Calu-3 cells by interleukin-1β. *J Biol Chem,* 276, 9486-91.

BRUICK, R. K. & MCKNIGHT, S. L. 2001. A conserved family of prolyl-4-hydroxylases that modify HIF. *Science,* 294, 1337-40.

BRUNING, U., CERONE, L., NEUFELD, Z., FITZPATRICK, S. F., CHEONG, A., SCHOLZ, C. C., SIMPSON, D. A., LEONARD, M. O., TAMBUWALA, M. M., CUMMINS, E. P. & TAYLOR, C. T. 2011. MicroRNA-155 Promotes Resolution of Hypoxia-Inducible Factor-1α Activity During Prolonged Hypoxia. *Mol Cell Biol,* 19, 4087-96.

BUBIEN, J. K. 2010. Epithelial Na^+ channel (ENaC), hormones, and hypertension. *J Biol Chem,* 285, 23527-31.

BUCK, S. H. & BURCHER, E. 1985. The rat submaxillary gland contains predominantly P-type tachykinin binding sites. *Peptides,* 6, 1079-84.

BUDINGER, G. R., CHANDEL, N., SHAO, Z. H., LI, C. Q., MELMED, A., BECKER, L. B. & SCHUMACKER, P. T. 1996. Cellular energy utilization and supply during hypoxia in embryonic cardiac myocytes. *Am J Physiol,* 270, L44-53.

BUDINGER, G. R., DURANTEAU, J., CHANDEL, N. S. & SCHUMACKER, P. T. 1998. Hibernation during hypoxia in cardiomyocytes. Role of mitochondria as the O_2 sensor. *J Biol Chem,* 273, 3320-6.

BURKE, J. R., PATTOLI, M. A., GREGOR, K. R., BRASSIL, P. J., MACMASTER, J. F., MCINTYRE, K. W., YANG, X., IOTZOVA, V. S., CLARKE, W., STRNAD, J., QIU, Y. & ZUSI, F. C. 2003. BMS-345541 Is a Highly Selective Inhibitor of IκB Kinase That Binds at an Allosteric Site of the Enzyme and Blocks NF-κB-dependent Transcription in Mice. *J Biol Chem,* 278, 1450-6.

CACI, E., CAPUTO, A., HINZPETER, A., AROUS, N., FANEN, P., SONAWANE, N., VERKMAN, A. S., RAVAZZOLO, R., ZEGARRA-MORAN, O. & GALIETTA, L. J. 2008. Evidence for direct CFTR inhibition by $CFTR_{inh}$-172 based on Arg^{347} mutagenesis. *Biochem J,* 413, 135-42.

CAI, T., WANG, H., CHEN, Y., LIU, L., GUNNING, W. T., QUINTAS, L. E. & XIE, Z. J. 2008. Regulation of caveolin-1 membrane trafficking by the Na/K-ATPase. *J Cell Biol,* 182, 1153-69.

CARPENTER, T. C., SCHOMBERG, S., NICHOLS, C., STENMARK, K. R. & WEIL, J. V. 2003. Hypoxia reversibly inhibits epithelial sodium transport but does not inhibit lung ENaC or Na-K-ATPase expression. *Am J Physiol Lung Cell Mol Physiol,* 284, L77-83.

CARRA, G. E., IBANEZ, J. E. & SARAVI, F. D. 2011. Electrogenic transport, oxygen consumption, and sensitivity to acute hypoxia of human colonic epithelium. *Int J Colorectal Dis.*

CARTER, M. J., LOBO, A. J. & TRAVIS, S. P. 2004. Guidelines for the management of inflammatory bowel disease in adults. *Gut,* 53 Suppl 5, V1-16.

CARTWRIGHT, C. A., MCROBERTS, J. A., MANDEL, K. G. & DHARMSATHAPHORN, K. 1985. Synergistic action of cyclic adenosine monophosphate- and calcium-mediated chloride secretion in a colonic epithelial cell line. *J Clin Invest,* 76, 1837-42.

CASALE, C. H., PREVITALI, G. & BARRA, H. S. 2003. Involvement of acetylated tubulin in the regulation of Na^+,K^+ -ATPase activity in cultured astrocytes. *FEBS Lett,* 534, 115-8.

CHAKRABARTI, S., HOQUE, A. N. & KARMAZYN, M. 1997. A rapid ischemia-induced apoptosis in isolated rat hearts and its attenuation by the sodium-hydrogen exchange inhibitor HOE 642 (cariporide). *J Mol Cell Cardiol,* 29, 3169-74.

CHAMBREY, R., ACHARD, J. M. & WARNOCK, D. G. 1997. Heterologous expression of rat NHE4: a highly amiloride-resistant Na^+/H^+ exchanger isoform. *Am J Physiol,* 272, C90-8.

CHANDEL, N. S., BUDINGER, G. R., CHOE, S. H. & SCHUMACKER, P. T. 1997. Cellular respiration during hypoxia. Role of cytochrome oxidase as the oxygen sensor in hepatocytes. *J Biol Chem,* 272, 18808-16.

CHAPPE, V., IRVINE, T., LIAO, J., EVAGELIDIS, A. & HANRAHAN, J. W. 2005. Phosphorylation of CFTR by PKA promotes binding of the regulatory domain. *EMBO J,* 24, 2730-40.

CHEN, L. W., EGAN, L., LI, Z. W., GRETEN, F. R., KAGNOFF, M. F. & KARIN, M. 2003. The two faces of IKK and NF-κB inhibition: prevention of systemic inflammation but increased local injury following intestinal ischemia-reperfusion. *Nat Med,* 9, 575-81.

CHEN, Y., CAI, T., WANG, H., LI, Z., LOREAUX, E., LINGREL, J. B. & XIE, Z. 2009. Regulation of intracellular cholesterol distribution by Na/K-ATPase. *J Biol Chem,* 284, 14881-90.

CHEN, Y., LI, X., YE, Q., TIAN, J., JING, R. & XIE, Z. 2011. Regulation of α1 Na/K-ATPase expression by cholesterol. *J Biol Chem,* 286, 15517-24.

CHEN, Z., KRMAR, R. T., DADA, L., EFENDIEV, R., LEIBIGER, I. B., PEDEMONTE, C. H., KATZ, A. I., SZNAJDER, J. I. & BERTORELLO, A. M. 2006. Phosphorylation of adaptor protein-2 mu2 is essential for Na^+,K^+-ATPase endocytosis in response to either G protein-coupled receptor or reactive oxygen species. *Am J Respir Cell Mol Biol,* 35, 127-32.

CHENG, S. H., RICH, D. P., MARSHALL, J., GREGORY, R. J., WELSH, M. J. & SMITH, A. E. 1991. Phosphorylation of the R domain by cAMP-dependent protein kinase regulates the CFTR chloride channel. *Cell,* 66, 1027-36.

CHIJIWA, T., MISHIMA, A., HAGIWARA, M., SANO, M., HAYASHI, K., INOUE, T., NAITO, K., TOSHIOKA, T. & HIDAKA, H. 1990. Inhibition of forskolin-induced neurite outgrowth and protein phosphorylation by a newly synthesized selective inhibitor of cyclic AMP-dependent protein kinase, *N*-[2-(*p*-bromocinnamylamino)ethyl]-5-isoquinolinesulfonamide (H-89), of PC12D pheochromocytoma cells. *J Biol Chem,* 265, 5267-72.

CHINN, K. S. & HANNON, J. P. 1969. Efficiency of food utilization at high altitude. *Fed Proc,* 28, 944-7.

CHOW, D. C. & FORTE, J. G. 1995. Functional significance of the β-subunit for heterodimeric P-type ATPases. *J Exp Biol,* 198, 1-17.

CIOFFI, C. L., LIU, X. Q., KOSINSKI, P. A., GARAY, M. & BOWEN, B. R. 2003. Differential regulation of HIF-1 α prolyl-4-hydroxylase genes by hypoxia in human cardiovascular cells. *Biochem Biophys Res Commun,* 303, 947-53.

CITI, S., SABANAY, H., JAKES, R., GEIGER, B. & KENDRICK-JONES, J. 1988. Cingulin, a new peripheral component of tight junctions. *Nature,* 333, 272-6.

CLARKE, L. L., STIEN, X. & WALKER, N. M. 2001. Intestinal bicarbonate secretion in cystic fibrosis mice. *JOP,* 2, 263-7.

CLIFFORD, R. J. & KAPLAN, J. H. 2008. β-Subunit overexpression alters the stoicheometry of assembled Na-K-ATPase subunits in MDCK cells. *Am J Physiol Renal Physiol,* 295, F1314-23.

COCKMAN, M. E., LANCASTER, D. E., STOLZE, I. P., HEWITSON, K. S., MCDONOUGH, M. A., COLEMAN, M. L., COLES, C. H., YU, X., HAY, R. T., LEY, S. C., PUGH, C. W., OLDHAM, N. J., MASSON, N., SCHOFIELD, C. J. & RATCLIFFE, P. J. 2006. Posttranslational hydroxylation of ankyrin repeats in IκB proteins by the hypoxia-inducible factor (HIF) asparaginyl hydroxylase, factor inhibiting HIF (FIH). *Proc Natl Acad Sci U S A,* 103, 14767-72.

COCKMAN, M. E., WEBB, J. D. & RATCLIFFE, P. J. 2009. FIH-dependent asparaginyl hydroxylation of ankyrin repeat domain-containing proteins. *Ann N Y Acad Sci,* 1177, 9-18.

COLEMAN, M. L., MCDONOUGH, M. A., HEWITSON, K. S., COLES, C., MECINOVIC, J., EDELMANN, M., COOK, K. M., COCKMAN, M. E., LANCASTER, D. E., KESSLER, B. M., OLDHAM, N. J., RATCLIFFE, P. J. & SCHOFIELD, C. J. 2007. Asparaginyl hydroxylation of the Notch ankyrin repeat domain by factor inhibiting hypoxia-inducible factor. *J Biol Chem,* 282, 24027-38.

COMELLAS, A. P., DADA, L. A., LECUONA, E., PESCE, L. M., CHANDEL, N. S., QUESADA, N., BUDINGER, G. R., STROUS, G. J., CIECHANOVER, A. & SZNAJDER, J. I. 2006. Hypoxia-mediated degradation of Na,K-ATPase via mitochondrial reactive oxygen species and the ubiquitin-conjugating system. *Circ Res,* 98, 1314-22.

CORR, S. C., GAHAN, C. C. & HILL, C. 2008. M-cells: origin, morphology and role in mucosal immunity and microbial pathogenesis. *FEMS Immunol Med Microbiol,* 52, 2-12.

CRAIG, W. S. & KYTE, J. 1980. Stoichiometry and molecular weight of the minimum asymmetric unit of canine renal sodium and potassium ion-activated adenosine triphosphatase. *J Biol Chem,* 255, 6262-9.

CRAMBERT, G., LI, C., CLAEYS, D. & GEERING, K. 2005. FXYD3 (Mat-8), a new regulator of Na,K-ATPase. *Mol Biol Cell,* 16, 2363-71.

CUMMINS, E. P., BERRA, E., COMERFORD, K. M., GINOUVES, A., FITZGERALD, K. T., SEEBALLUCK, F., GODSON, C., NIELSEN, J. E., MOYNAGH, P., POUYSSEGUR, J. & TAYLOR, C. T. 2006. Prolyl hydroxylase-1 negatively regulates IκB kinase-β, giving insight into hypoxia-induced NFκB activity. *Proc Natl Acad Sci U S A,* 103, 18154-9.

CUMMINS, E. P., SEEBALLUCK, F., KEELY, S. J., MANGAN, N. E., CALLANAN, J. J., FALLON, P. G. & TAYLOR, C. T. 2008. The hydroxylase inhibitor dimethyloxalylglycine is protective in a murine model of colitis. *Gastroenterology,* 134, 156-65.

CUTHBERT, A. W., EGLEME, C., GREENWOOD, H., HICKMAN, M. E., KIRKLAND, S. C. & MACVINISH, L. J. 1987. Calcium- and cyclic AMP-dependent chloride secretion in human colonic epithelia. *Br J Pharmacol,* 91, 503-15.

CUTHBERT, A. W., MACVINISH, L. J., HICKMAN, M. E., RATCLIFF, R., COLLEDGE, W. H. & EVANS, M. J. 1994. Ion-transporting activity in the murine colonic epithelium of normal animals and animals with cystic fibrosis. *Pflugers Arch,* 428, 508-15.

D'ANDREA, L., LYTLE, C., MATTHEWS, J. B., HOFMAN, P., FORBUSH, B., 3RD & MADARA, J. L. 1996. Na:K:2Cl cotransporter (NKCC) of intestinal epithelial cells. Surface expression in response to cAMP. *J Biol Chem,* 271, 28969-76.

DADA, L. A., CHANDEL, N. S., RIDGE, K. M., PEDEMONTE, C., BERTORELLO, A. M. & SZNAJDER, J. I. 2003. Hypoxia-induced endocytosis of Na,K-ATPase in alveolar epithelial cells is mediated by mitochondrial reactive oxygen species and PKC-ζ. *J Clin Invest,* 111, 1057-64.

DADA, L. A., WELCH, L. C., ZHOU, G., BEN-SAADON, R., CIECHANOVER, A. & SZNAJDER, J. I. 2007. Phosphorylation and ubiquitination are necessary for Na,K-ATPase endocytosis during hypoxia. *Cell Signal,* 19, 1893-8.

DANIEL, H. 2004. Molecular and integrative physiology of intestinal peptide transport. *Annu Rev Physiol,* 66, 361-84.

DARMAN, R. B., FLEMMER, A. & FORBUSH, B. 2001. Modulation of ion transport by direct targeting of protein phosphatase type 1 to the Na-K-Cl cotransporter. *J Biol Chem,* 276, 34359-62.

DARWIN, C. 1871. *The descent of man, and selection in relation to sex. By Charles Darwin ... In two volumes...With illustrations,* London: John Murray.

DAVIES, S. P., REDDY, H., CAIVANO, M. & COHEN, P. 2000. Specificity and mechanism of action of some commonly used protein kinase inhibitors. *Biochem J,* 351, 95-105.

DE ANGELIS, C. & HAUPERT, G. T., JR. 1998. Hypoxia triggers release of an endogenous inhibitor of Na^+-K^+-ATPase from midbrain and adrenal. *Am J Physiol,* 274, F182-8.

DE JONGE, H., BIJVELDS, M., WILKE, M., BOT, A., JORNA, H., COLLEDGE, W., AND VERKADE, H. 2006. Intestinal and pancreatic biomarkers for CF. *Ped. Pulmonol. Suppl.,* 29, 148–149.

DEL CASTILLO, I. C., FEDOR-CHAIKEN, M., SONG, J. C., STARLINGER, V., YOO, J., MATLIN, K. S. & MATTHEWS, J. B. 2005. Dynamic regulation of Na^+-K^+-$2Cl^-$ cotransporter surface expression by PKC-ε in Cl^--secretory epithelia. *Am J Physiol Cell Physiol,* 289, C1332-42.

DELPRAT, B., BIBERT, S. & GEERING, K. 2006. [FXYD proteins: novel regulators of Na,K-ATPase]. *Med Sci (Paris),* 22, 633-8.

DEMIDENKO, Z. N., RAPISARDA, A., GARAYOA, M., GIANNAKAKOU, P., MELILLO, G. & BLAGOSKLONNY, M. V. 2005. Accumulation of hypoxia-inducible factor-1α is limited by transcription-dependent depletion. *Oncogene,* 24, 4829-38.

DEVARAJAN, P., SCARAMUZZINO, D. A. & MORROW, J. S. 1994. Ankyrin binds to two distinct cytoplasmic domains of Na,K-ATPase α subunit. *Proc Natl Acad Sci U S A,* 91, 2965-9.

DHARMSATHAPHORN, K., MANDEL, K. G., MASUI, H. & MCROBERTS, J. A. 1985. Vasoactive intestinal polypeptide-induced chloride secretion by a colonic epithelial cell line. Direct participation of a basolaterally localized Na^+,K^+,Cl^- cotransport system. *J Clin Invest,* 75, 462-71.

DHARMSATHAPHORN, K., MCROBERTS, J. A., MANDEL, K. G., TISDALE, L. D. & MASUI, H. 1984. A human colonic tumor cell line that maintains vectorial electrolyte transport. *Am J Physiol,* 246, G204-8.

DHARMSATHAPHORN, K. & PANDOL, S. J. 1986. Mechanism of chloride secretion induced by carbachol in a colonic epithelial cell line. *J Clin Invest,* 77, 348-54.

DIAKOV, A. & KORBMACHER, C. 2004. A novel pathway of epithelial sodium channel activation involves a serum- and glucocorticoid-inducible kinase

consensus motif in the C terminus of the channel's α-subunit. *J Biol Chem,* 279, 38134-42.

DONNET, C., ARYSTARKHOVA, E. & SWEADNER, K. J. 2001. Thermal denaturation of the Na,K-ATPase provides evidence for α-α oligomeric interaction and γ subunit association with the C-terminal domain. *J Biol Chem,* 276, 7357-65.

DONOWITZ, M., MOHAN, S., ZHU, C. X., CHEN, T. E., LIN, R., CHA, B., ZACHOS, N. C., MURTAZINA, R., SARKER, R. & LI, X. 2009. NHE3 regulatory complexes. *J Exp Biol,* 212, 1638-46.

DOWD, B. F. & FORBUSH, B. 2003. PASK (proline-alanine-rich STE20-related kinase), a regulatory kinase of the Na-K-Cl cotransporter (NKCC1). *J Biol Chem,* 278, 27347-53.

DUC, C., FARMAN, N., CANESSA, C. M., BONVALET, J. P. & ROSSIER, B. C. 1994. Cell-specific expression of epithelial sodium channel α, β, and γ subunits in aldosterone-responsive epithelia from the rat: localization by in situ hybridization and immunocytochemistry. *J Cell Biol,* 127, 1907-21.

DURAND, J., DURAND-ARCZYNSKA, W. & WANKMILLER, D. 1988. Coupling of active sodium transport to oxidative metabolism in the rabbit distal colon. *J Physiol,* 396, 55-64.

DUVALL, M. D., GUO, Y. & MATALON, S. 1998. Hydrogen peroxide inhibits cAMP-induced Cl^- secretion across colonic epithelial cells. *Am J Physiol,* 275, C1313-22.

EDELBLUM, K. L. & TURNER, J. R. 2009. The tight junction in inflammatory disease: communication breakdown. *Curr Opin Pharmacol,* 9, 715-20.

EDENHARDER, R. & KNAFLIC, T. 1981. Epimerization of chenodeoxycholic acid to ursodeoxycholic acid by human intestinal lecithinase-lipase-negative Clostridia. *J Lipid Res,* 22, 652-8.

EGIDY, G., JUILLERAT-JEANNERET, L., KORTH, P., BOSMAN, F. T. & PINET, F. 2000. The endothelin system in normal human colon. *Am J Physiol Gastrointest Liver Physiol,* 279, G211-22.

EISENHUT, M. 2006. Changes in ion transport in inflammatory disease. *J Inflamm (Lond),* 3, 5.

EJDERHAMN, J., FINKEL, Y. & STRANDVIK, B. 1989. Na,K-ATPase activity in rectal mucosa of children with ulcerative colitis and Crohn's disease. *Scand J Gastroenterol,* 24, 1121-5.

ELVIDGE, G. P., GLENNY, L., APPELHOFF, R. J., RATCLIFFE, P. J., RAGOUSSIS, J. & GLEADLE, J. M. 2006. Concordant regulation of gene expression by hypoxia and 2-oxoglutarate-dependent dioxygenase inhibition: the role of HIF-1α, HIF-2α, and other pathways. *J Biol Chem,* 281, 15215-26.

EMERLING, B. M., VIOLLET, B., TORMOS, K. V. & CHANDEL, N. S. 2007. Compound C inhibits hypoxic activation of HIF-1 independent of AMPK. *FEBS Lett,* 581, 5727-31.

EPPLE, H. J., AMASHEH, S., MANKERTZ, J., GOLTZ, M., SCHULZKE, J. D. & FROMM, M. 2000. Early aldosterone effect in distal colon by transcriptional regulation of ENaC subunits. *Am J Physiol Gastrointest Liver Physiol,* 278, G718-24.

EPSTEIN, A. C., GLEADLE, J. M., MCNEILL, L. A., HEWITSON, K. S., O'ROURKE, J., MOLE, D. R., MUKHERJI, M., METZEN, E., WILSON, M. I., DHANDA, A., TIAN, Y. M., MASSON, N., HAMILTON, D. L., JAAKKOLA, P., BARSTEAD, R., HODGKIN, J., MAXWELL, P. H., PUGH, C. W., SCHOFIELD, C. J. & RATCLIFFE, P. J. 2001. C. elegans EGL-9 and mammalian homologs define a family of dioxygenases that regulate HIF by prolyl hydroxylation. *Cell,* 107, 43-54.

FAMBROUGH, D. M., LEMAS, M. V., HAMRICK, M., EMERICK, M., RENAUD, K. J., INMAN, E. M., HWANG, B. & TAKEYASU, K. 1994. Analysis of subunit assembly of the Na-K-ATPase. *Am J Physiol,* 266, C579-89.

FANGER, C. M., GHANSHANI, S., LOGSDON, N. J., RAUER, H., KALMAN, K., ZHOU, J., BECKINGHAM, K., CHANDY, K. G., CAHALAN, M. D. & AIYAR, J. 1999. Calmodulin mediates calcium-dependent activation of the intermediate conductance KCa channel, IKCa1. *J Biol Chem,* 274, 5746-54.

FERAILLE, E., BEGUIN, P., CARRANZA, M. L., GONIN, S., ROUSSELOT, M., MARTIN, P. Y., FAVRE, H. & GEERING, K. 2000. Is phosphorylation of the α1 subunit at Ser-16 involved in the control of Na,K-ATPase activity by phorbol ester-activated protein kinase C? *Mol Biol Cell,* 11, 39-50.

FERREIRA, L. M. 2010. Cancer metabolism: the Warburg effect today. *Exp Mol Pathol,* 89, 372-80.

FIELD, M. 2003. Intestinal ion transport and the pathophysiology of diarrhea. *J Clin Invest,* 111, 931-43.

FIRSOV, D., GAUTSCHI, I., MERILLAT, A. M., ROSSIER, B. C. & SCHILD, L. 1998. The heterotetrameric architecture of the epithelial sodium channel (ENaC). *EMBO J,* 17, 344-52.

FLORES, C. A., MELVIN, J. E., FIGUEROA, C. D. & SEPULVEDA, F. V. 2007. Abolition of Ca^{2+}-mediated intestinal anion secretion and increased stool dehydration in mice lacking the intermediate conductance Ca^{2+}-dependent K^+ channel Kcnn4. *J Physiol,* 583, 705-17.

FLOYD, Z. E., KILROY, G., WU, X. & GIMBLE, J. M. 2007. Effects of prolyl hydroxylase inhibitors on adipogenesis and hypoxia inducible factor 1 α levels under normoxic conditions. *J Cell Biochem,* 101, 1545-57.

FONG, G. H. & TAKEDA, K. 2008. Role and regulation of prolyl hydroxylase domain proteins. *Cell Death Differ,* 15, 635-41.

FORTE, L. R., THORNE, P. K., EBER, S. L., KRAUSE, W. J., FREEMAN, R. H., FRANCIS, S. H. & CORBIN, J. D. 1992. Stimulation of intestinal Cl^- transport by heat-stable enterotoxin: activation of cAMP-dependent protein kinase by cGMP. *Am J Physiol,* 263, C607-15.

FRAISL, P., ARAGONES, J. & CARMELIET, P. 2009. Inhibition of oxygen sensors as a therapeutic strategy for ischaemic and inflammatory disease. *Nat Rev Drug Discov,* 8, 139-52.

FURUSE, M., HIRASE, T., ITOH, M., NAGAFUCHI, A., YONEMURA, S. & TSUKITA, S. 1993. Occludin: a novel integral membrane protein localizing at tight junctions. *J Cell Biol,* 123, 1777-88.

GARGOURI, Y., MOREAU, H. & VERGER, R. 1989. Gastric lipases: biochemical and physiological studies. *Biochim Biophys Acta,* 1006, 255-71.

GARTY, H. & KARLISH, S. J. 2006. Role of FXYD proteins in ion transport. *Annu Rev Physiol,* 68, 431-59.

GARTY, H. & PALMER, L. G. 1997. Epithelial sodium channels: function, structure, and regulation. *Physiol Rev,* 77, 359-96.

GEERING, K. 2006. FXYD proteins: new regulators of Na-K-ATPase. *Am J Physiol Renal Physiol,* 290, F241-50.

GEIBEL, J. P. 2005. Secretion and absorption by colonic crypts. *Annu Rev Physiol,* 67, 471-90.

GOMES, P. & SOARES-DA-SILVA, P. 2002. D_2-like receptor-mediated inhibition of Na^+-K^+-ATPase activity is dependent on the opening of K^+ channels. *Am J Physiol Renal Physiol,* 283, F114-23.

GOODMAN, B. E. 2010. Insights into digestion and absorption of major nutrients in humans. *Adv Physiol Educ,* 34, 44-53.

GOROKHOVA, S., BIBERT, S., GEERING, K. & HEINTZ, N. 2007. A novel family of transmembrane proteins interacting with β subunits of the Na,K-ATPase. *Hum Mol Genet,* 16, 2394-410.

GRETEN, F. R., ECKMANN, L., GRETEN, T. F., PARK, J. M., LI, Z. W., EGAN, L. J., KAGNOFF, M. F. & KARIN, M. 2004. IKKβ links inflammation and tumorigenesis in a mouse model of colitis-associated cancer. *Cell,* 118, 285-96.

GRUBB, B. R. 1995. Ion transport across the jejunum in normal and cystic fibrosis mice. *Am J Physiol,* 268, G505-13.

GUARNER, F. & MALAGELADA, J. R. 2003. Gut flora in health and disease. *Lancet,* 361, 512-9.

GUIMBELLOT, J. S., FORTENBERRY, J. A., SIEGAL, G. P., MOORE, B., WEN, H., VENGLARIK, C., CHEN, Y. F., OPARIL, S., SORSCHER, E. J. & HONG, J. S. 2008. Role of oxygen availability in CFTR expression and function. *Am J Respir Cell Mol Biol,* 39, 514-21.

GULLBERG, E. & SODERHOLM, J. D. 2006. Peyer's patches and M cells as potential sites of the inflammatory onset In Crohn's disease. *Ann N Y Acad Sci,* 1072, 218-32.

GUSAROVA, G. A., DADA, L. A., KELLY, A. M., BRODIE, C., WITTERS, L. A., CHANDEL, N. S. & SZNAJDER, J. I. 2009. α1-AMP-activated protein kinase regulates hypoxia-induced Na,K-ATPase endocytosis via direct phosphorylation of protein kinase C ζ. *Mol Cell Biol,* 29, 3455-64.

GUSAROVA, G. A., TREJO, H. E., DADA, L. A., BRIVA, A., WELCH, L. C., HAMANAKA, R. B., MUTLU, G. M., CHANDEL, N. S., PRAKRIYA, M. & SZNAJDER, J. I. 2011. Hypoxia Leads to Na,K-ATPase Downregulation via Ca^{2+} Release-Activated Ca^{2+} Channels and AMPK Activation. *Mol Cell Biol,* 31, 3546-56.

HAAS, M. & FORBUSH, B., 3RD 2000. The Na-K-Cl cotransporter of secretory epithelia. *Annu Rev Physiol,* 62, 515-34.

HADDISH-BERHANE, N., FARHADI, A., NYQUIST, C., HAGHIGHI, K. & KESHAVARZIAN, A. 2007. Biological variability and targeted delivery of therapeutics for inflammatory bowel diseases: an in silico approach. *Inflamm Allergy Drug Targets,* 6, 47-55.

HAERTEIS, S., KRUEGER, B., KORBMACHER, C. & RAUH, R. 2009. The δ-subunit of the epithelial sodium channel (ENaC) enhances channel activity and alters proteolytic ENaC activation. *J Biol Chem,* 284, 29024-40.

HAN, J. & BURGESS, K. 2010. Fluorescent indicators for intracellular pH. *Chem Rev,* 110, 2709-28.

HANKE, J. H., GARDNER, J. P., DOW, R. L., CHANGELIAN, P. S., BRISSETTE, W. H., WERINGER, E. J., POLLOK, B. A. & CONNELLY, P. A. 1996. Discovery of a novel, potent, and Src family-selective tyrosine kinase inhibitor. Study of Lck- and FynT-dependent T cell activation. *J Biol Chem,* 271, 695-701.

HARARI, Y., RUSSELL, D. A. & CASTRO, G. A. 1987. Anaphylaxis-mediated epithelial Cl^- secretion and parasite rejection in rat intestine. *J Immunol,* 138, 1250-5.

HART, M. L., GRENZ, A., GORZOLLA, I. C., SCHITTENHELM, J., DALTON, J. H. & ELTZSCHIG, H. K. 2011. Hypoxia-inducible factor-1α-dependent protection from intestinal ischemia/reperfusion injury involves ecto-5'-nucleotidase (CD73) and the A2B adenosine receptor. *J Immunol,* 186, 4367-74.

HARTZELL, C., PUTZIER, I. & ARREOLA, J. 2005. Calcium-activated chloride channels. *Annu Rev Physiol,* 67, 719-58.

HASLER, U., CRAMBERT, G., HORISBERGER, J. D. & GEERING, K. 2001. Structural and functional features of the transmembrane domain of the Na,K-ATPase β subunit revealed by tryptophan scanning. *J Biol Chem,* 276, 16356-64.

HATHAWAY, L. J. & KRAEHENBUHL, J. P. 2000. The role of M cells in mucosal immunity. *Cell Mol Life Sci,* 57, 323-32.

HE, G., SHANKAR, R. A., CHZHAN, M., SAMOUILOV, A., KUPPUSAMY, P. & ZWEIER, J. L. 1999. Noninvasive measurement of anatomic structure and intraluminal oxygenation in the gastrointestinal tract of living mice with spatial and spectral EPR imaging. *Proc Natl Acad Sci U S A,* 96, 4586-91.

HE, X. J., WU, X. Z., WELLNER, R. B. & BAUM, B. J. 1989. Muscarinic receptor regulation of Ca^{2+} mobilization in a human salivary cell line. *Pflugers Arch,* 413, 505-10.

HEITZMANN, D., WARTH, R., BLEICH, M., HENGER, A., NITSCHKE, R. & GREGER, R. 2000. Regulation of the $Na^+2Cl^-K^+$ cotransporter in isolated rat colon crypts. *Pflugers Arch,* 439, 378-84.

HINDRYCKX, P., DE VOS, M., JACQUES, P., FERDINANDE, L., PEETERS, H., OLIEVIER, K., BOGAERT, S., BRINKMAN, B., VANDENABEELE, P., ELEWAUT, D. & LAUKENS, D. 2010. Hydroxylase inhibition abrogates TNF-α-induced intestinal epithelial damage by hypoxia-inducible factor-1-dependent repression of FADD. *J Immunol,* 185, 6306-16.

HOFMANN, A. F. 2009. Bile acids: trying to understand their chemistry and biology with the hope of helping patients. *Hepatology,* 49, 1403-18.

HOGLUND, P., HAILA, S., SOCHA, J., TOMASZEWSKI, L., SAARIALHO-KERE, U., KARJALAINEN-LINDSBERG, M. L., AIROLA, K., HOLMBERG, C., DE LA CHAPELLE, A. & KERE, J. 1996. Mutations of the Down-regulated in

adenoma (DRA) gene cause congenital chloride diarrhoea. *Nat Genet,* 14, 316-9.

HOROWITZ, B., EAKLE, K. A., SCHEINER-BOBIS, G., RANDOLPH, G. R., CHEN, C. Y., HITZEMAN, R. A. & FARLEY, R. A. 1990. Synthesis and assembly of functional mammalian Na,K-ATPase in yeast. *J Biol Chem,* 265, 4189-92.

HUANG, J., ZHAO, Q., MOONEY, S. M. & LEE, F. S. 2002. Sequence determinants in hypoxia-inducible factor-1α for hydroxylation by the prolyl hydroxylases PHD1, PHD2, and PHD3. *J Biol Chem,* 277, 39792-800.

HUANG, L. E., GU, J., SCHAU, M. & BUNN, H. F. 1998. Regulation of hypoxia-inducible factor 1α is mediated by an O_2-dependent degradation domain via the ubiquitin-proteasome pathway. *Proc Natl Acad Sci U S A,* 95, 7987-92.

HUFLEJT, M. E., BLUM, R. A., MILLER, S. G., MOORE, H. P. & MACHEN, T. E. 1994. Regulated Cl transport, K and Cl permeability, and exocytosis in T84 cells. *J Clin Invest,* 93, 1900-10.

HUMMLER, E. & HORISBERGER, J. D. 1999. Genetic disorders of membrane transport. V. The epithelial sodium channel and its implication in human diseases. *Am J Physiol,* 276, G567-71.

HUYER, G., LIU, S., KELLY, J., MOFFAT, J., PAYETTE, P., KENNEDY, B., TSAPRAILIS, G., GRESSER, M. J. & RAMACHANDRAN, C. 1997. Mechanism of inhibition of protein-tyrosine phosphatases by vanadate and pervanadate. *J Biol Chem,* 272, 843-51.

IBLA, J. C., KHOURY, J., KONG, T., ROBINSON, A. & COLGAN, S. P. 2006. Transcriptional repression of Na-K-2Cl cotransporter NKCC1 by hypoxia-inducible factor-1. *Am J Physiol Cell Physiol,* 291, C282-9.

IKUMA, M., KASHGARIAN, M., BINDER, H. J. & RAJENDRAN, V. M. 1999. Differential regulation of NHE isoforms by sodium depletion in proximal and distal segments of rat colon. *Am J Physiol,* 276, G539-49.

IMTIYAZ, H. Z., WILLIAMS, E. P., HICKEY, M. M., PATEL, S. A., DURHAM, A. C., YUAN, L. J., HAMMOND, R., GIMOTTY, P. A., KEITH, B. & SIMON, M. C. 2010. Hypoxia-inducible factor 2α regulates macrophage function in mouse models of acute and tumor inflammation. *J Clin Invest,* 120, 2699-714.

INAGAKI, A., YAMAGUCHI, S. & ISHIKAWA, T. 2004. Amiloride-sensitive epithelial Na^+ channel currents in surface cells of rat rectal colon. *Am J Physiol Cell Physiol,* 286, C380-90.

IORDACHE, C. & DUSZYK, M. 2007. Sodium 4-phenylbutyrate upregulates ENaC and sodium absorption in T84 cells. *Exp Cell Res,* 313, 305-11.

IVAN, M., KONDO, K., YANG, H., KIM, W., VALIANDO, J., OHH, M., SALIC, A., ASARA, J. M., LANE, W. S. & KAELIN, W. G., JR. 2001. HIFα targeted for VHL-mediated destruction by proline hydroxylation: implications for O_2 sensing. *Science,* 292, 464-8.

JAAKKOLA, P., MOLE, D. R., TIAN, Y. M., WILSON, M. I., GIELBERT, J., GASKELL, S. J., KRIEGSHEIM, A., HEBESTREIT, H. F., MUKHERJI, M., SCHOFIELD, C. J., MAXWELL, P. H., PUGH, C. W. & RATCLIFFE, P. J. 2001. Targeting of HIF-α

to the von Hippel-Lindau ubiquitylation complex by O_2-regulated prolyl hydroxylation. *Science,* 292, 468-72.

JAEGER, L. A. & LAMAR, C. H. 1992. Immunolocalization of epidermal growth factor (EGF) and EGF receptors in the porcine upper gastrointestinal tract. *Am J Vet Res,* 53, 1685-92.

JOHANNES, T., MIK, E. G., NOHE, B., RAAT, N. J., UNERTL, K. E. & INCE, C. 2006. Influence of fluid resuscitation on renal microvascular PO_2 in a normotensive rat model of endotoxemia. *Crit Care,* 10, R88.

JOHNSON, L. R. 1994. *Physiology of the gastrointestinal tract,* New York N.Y., Raven Press.

JUNG, J., KIM, M., KIM, M. J., KIM, J., MOON, J., LIM, J. S. & LEE, K. 2004. Translationally controlled tumor protein interacts with the third cytoplasmic domain of Na,K-ATPase α subunit and inhibits the pump activity in HeLa cells. *J Biol Chem,* 279, 49868-75.

KACZMAREK, M. J. & ROSENMUND, H. 1977. The action of human pancreatic and salivary isoamylases on starch and glycogen. *Clin Chim Acta,* 79, 69-73.

KALABIS, J., LI, G., FUKUNAGA-KALABIS, M., RUSTGI, A. K. & HERLYN, M. 2008. Endothelin-3 stimulates survival of goblet cells in organotypic cultures of fetal human colonic epithelium. *Am J Physiol Gastrointest Liver Physiol,* 295, G1182-9.

KANAYA, K. & KAMITANI, T. 2003. pVHL-independent ubiquitination of HIF1α and its stabilization by cobalt ion. *Biochem Biophys Res Commun,* 306, 750-5.

KAPLAN, J. H. 2002. Biochemistry of Na,K-ATPase. *Annu Rev Biochem,* 71, 511-35.

KARHAUSEN, J., FURUTA, G. T., TOMASZEWSKI, J. E., JOHNSON, R. S., COLGAN, S. P. & HAASE, V. H. 2004. Epithelial hypoxia-inducible factor-1 is protective in murine experimental colitis. *J Clin Invest,* 114, 1098-106.

KEATING, N. & KEELY, S. J. 2009. Bile acids in regulation of intestinal physiology. *Curr Gastroenterol Rep,* 11, 375-82.

KEATING, N., MROZ, M. S., SCHARL, M. M., MARSH, C., FERGUSON, G., HOFMANN, A. F. & KEELY, S. J. 2009. Physiological concentrations of bile acids down-regulate agonist induced secretion in colonic epithelial cells. *J Cell Mol Med,* 13, 2293-303.

KEELY, S. J., CALANDRELLA, S. O. & BARRETT, K. E. 2000. Carbachol-stimulated transactivation of epidermal growth factor receptor and mitogen-activated protein kinase in T_{84} cells is mediated by intracellular Ca^{2+}, PYK-2, and $p60^{src}$. *J Biol Chem,* 275, 12619-25.

KELLY, L., MCDONOUGH, M. A., COLEMAN, M. L., RATCLIFFE, P. J. & SCHOFIELD, C. J. 2009a. Asparagine β-hydroxylation stabilizes the ankyrin repeat domain fold. *Mol Biosyst,* 5, 52-8.

KELLY, O. B., KEATING, N., SCHARL, M., KEAVENEY, K., MURRAY, F. E., HOFMANN, A. F. & KEELY, S. J. 2009b. Ursodeoxycholic Acid Exerts Antisecretory Actions On Colonic Epithelial Cells. *Gastroenterology,* 136, A-569.

KHAN, I., AL-AWADI, F. M. & ABUL, H. 1998. Colitis-induced changes in the expression of the Na^+/H^+ exchanger isoform NHE-1. *J Pharmacol Exp Ther,* 285, 869-75.

KHAN, I. & ALI, M. 1999. Altered expression of the Na^+/H^+ exchanger isoform-3 in experimental colitis: effect of garlic. *Mol Cell Biochem,* 200, 77-84.

KHAN, I., ORIOWO, M. A. & ANIM, J. T. 2005. Amelioration of experimental colitis by Na-H exchanger-1 inhibitor amiloride is associated with reversal of IL-1ss and ERK mitogen-activated protein kinase. *Scand J Gastroenterol,* 40, 578-85.

KIM, J. S., QIAN, T. & LEMASTERS, J. J. 2003. Mitochondrial permeability transition in the switch from necrotic to apoptotic cell death in ischemic rat hepatocytes. *Gastroenterology,* 124, 494-503.

KIRK, K. L. & DAWSON, D. C. 1983. Basolateral potassium channel in turtle colon. Evidence for single-file ion flow. *J Gen Physiol,* 82, 297-329.

KIYOHARA, T., OKUNO, M., NAKANISHI, T., SHINOMURA, Y. & MATSUZAWA, Y. 1993. Effect of endothelin 1 on ion transport in isolated rat colon. *Gastroenterology,* 104, 1328-36.

KLES, K. A. & TAPPENDEN, K. A. 2002. Hypoxia differentially regulates nutrient transport in rat jejunum regardless of luminal nutrient present. *Am J Physiol Gastrointest Liver Physiol,* 283, G1336-42.

KNOCK, G. A., SNETKOV, V. A., SHAIFTA, Y., DRNDARSKI, S., WARD, J. P. & AARONSON, P. I. 2008. Role of src-family kinases in hypoxic vasoconstriction of rat pulmonary artery. *Cardiovasc Res,* 80, 453-62.

KOPPENOL, W. H., BOUNDS, P. L. & DANG, C. V. 2011. Otto Warburg's contributions to current concepts of cancer metabolism. *Nat Rev Cancer,* 11, 325-37.

KUHN, M., FUCHS, M., BECK, F. X., MARTIN, S., JAHNE, J., KLEMPNAUER, J., KAEVER, V., RECHKEMMER, G. & FORSSMANN, W. G. 1997. Endothelin-1 potently stimulates chloride secretion and inhibits Na^+-glucose absorption in human intestine *in vitro. J Physiol,* 499 (Pt 2), 391-402.

KUHNLE, U. 1997. Pseudohypoaldosteronism: mutation found, problem solved? *Mol Cell Endocrinol,* 133, 77-80.

KUNZELMANN, K., HUBNER, M., SCHREIBER, R., LEVY-HOLZMAN, R., GARTY, H., BLEICH, M., WARTH, R., SLAVIK, M., VON HAHN, T. & GREGER, R. 2001. Cloning and function of the rat colonic epithelial K^+ channel KVLQT1. *J Membr Biol,* 179, 155-64.

KUNZELMANN, K. & MALL, M. 2002. Electrolyte transport in the mammalian colon: mechanisms and implications for disease. *Physiol Rev,* 82, 245-89.

LAM, R. S., APP, E. M., NAHIRNEY, D., SZKOTAK, A. J., VIEIRA-COELHO, M. A., KING, M. & DUSZYK, M. 2003. Regulation of Cl^- secretion by α_2-adrenergic receptors in mouse colonic epithelium. *J Physiol,* 548, 475-84.

LANDO, D., PEET, D. J., GORMAN, J. J., WHELAN, D. A., WHITELAW, M. L. & BRUICK, R. K. 2002a. FIH-1 is an asparaginyl hydroxylase enzyme that regulates the transcriptional activity of hypoxia-inducible factor. *Genes Dev,* 16, 1466-71.

LANDO, D., PEET, D. J., WHELAN, D. A., GORMAN, J. J. & WHITELAW, M. L. 2002b. Asparagine hydroxylation of the HIF transactivation domain a hypoxic switch. *Science,* 295, 858-61.

LARMONIER, C. B., LAUBITZ, D., THURSTON, R. D., BUCKNAM, A. L., HILL, F. M., MIDURA-KIELA, M., RAMALINGAM, R., KIELA, P. R. & GHISHAN, F. K. 2011. NHE3 modulates the severity of colitis in IL-10-deficient mice. *Am J Physiol Gastrointest Liver Physiol,* 300, G998-G1009.

LAURIN, M., EVERETT, M. L. & PARKER, W. 2011. The cecal appendix: one more immune component with a function disturbed by post-industrial culture. *Anat Rec (Hoboken),* 294, 567-79.

LEE, K., ZHANG, H., QIAN, D. Z., REY, S., LIU, J. O. & SEMENZA, G. L. 2009. Acriflavine inhibits HIF-1 dimerization, tumor growth, and vascularization. *Proc Natl Acad Sci U S A,* 106, 17910-5.

LEHRICH, R. W., ALLER, S. G., WEBSTER, P., MARINO, C. R. & FORREST, J. N., JR. 1998. Vasoactive intestinal peptide, forskolin, and genistein increase apical CFTR trafficking in the rectal gland of the spiny dogfish, Squalus acanthias. Acute regulation of CFTR trafficking in an intact epithelium. *J Clin Invest,* 101, 737-45.

LEPERCQ, P., GERARD, P., BEGUET, F., RAIBAUD, P., GRILL, J. P., RELANO, P., CAYUELA, C. & JUSTE, C. 2004. Epimerization of chenodeoxycholic acid to ursodeoxycholic acid by Clostridium baratii isolated from human feces. *FEMS Microbiol Lett,* 235, 65-72.

LI, J., MAHAJAN, A. & TSAI, M. D. 2006. Ankyrin repeat: a unique motif mediating protein-protein interactions. *Biochemistry,* 45, 15168-78.

LIANG, M., CAI, T., TIAN, J., QU, W. & XIE, Z. J. 2006. Functional characterization of Src-interacting Na/K-ATPase using RNA interference assay. *J Biol Chem,* 281, 19709-19.

LIANG, M., TIAN, J., LIU, L., PIERRE, S., LIU, J., SHAPIRO, J. & XIE, Z. J. 2007. Identification of a pool of non-pumping Na/K-ATPase. *J Biol Chem,* 282, 10585-93.

LIEB, M. E., MENZIES, K., MOSCHELLA, M. C., NI, R. & TAUBMAN, M. B. 2002. Mammalian EGLN genes have distinct patterns of mRNA expression and regulation. *Biochem Cell Biol,* 80, 421-6.

LINKE, S., HAMPTON-SMITH, R. J. & PEET, D. J. 2007. Characterization of ankyrin repeat-containing proteins as substrates of the asparaginyl hydroxylase factor inhibiting hypoxia-inducible transcription factor. *Methods Enzymol,* 435, 61-85.

LIU, J., PERIYASAMY, S. M., GUNNING, W., FEDOROVA, O. V., BAGROV, A. Y., MALHOTRA, D., XIE, Z. & SHAPIRO, J. I. 2002. Effects of cardiac glycosides on sodium pump expression and function in LLC-PK1 and MDCK cells. *Kidney Int,* 62, 2118-25.

LIU, L. & SIMON, M. C. 2004. Regulation of transcription and translation by hypoxia. *Cancer Biol Ther,* 3, 492-7.

LIU, Y., YANG, J., REN, H., HE, D., PASCUA, A., ARMANDO, M. I., YANG, C., ZHOU, L., FELDER, R. A., JOSE, P. A. & ZENG, C. 2009. Inhibitory effect of ETB receptor on Na^+-K^+ ATPase activity by extracellular Ca^{2+} entry and Ca^{2+}

release from the endoplasmic reticulum in renal proximal tubule cells. *Hypertens Res,* 32, 846-52.

LOCHNER, A. & MOOLMAN, J. A. 2006. The many faces of H89: a review. *Cardiovasc Drug Rev,* 24, 261-74.

LOMB, D. J., STRAUB, J. A. & FREEMAN, R. S. 2007. Prolyl hydroxylase inhibitors delay neuronal cell death caused by trophic factor deprivation. *J Neurochem,* 103, 1897-906.

LOWRY, O. H., ROSEBROUGH, N. J., FARR, A. L. & RANDALL, R. J. 1951. Protein measurement with the Folin phenol reagent. *J Biol Chem,* 193, 265-75.

LUBARSKI, I., PIHAKASKI-MAUNSBACH, K., KARLISH, S. J., MAUNSBACH, A. B. & GARTY, H. 2005. Interaction with the Na,K-ATPase and tissue distribution of FXYD5 (related to ion channel). *J Biol Chem,* 280, 37717-24.

LUKACS, G. L., SEGAL, G., KARTNER, N., GRINSTEIN, S. & ZHANG, F. 1997. Constitutive internalization of cystic fibrosis transmembrane conductance regulator occurs via clathrin-dependent endocytosis and is regulated by protein phosphorylation. *Biochem J,* 328 (Pt 2), 353-61.

LUTSENKO, S. & KAPLAN, J. H. 1995. Organization of P-type ATPases: significance of structural diversity. *Biochemistry,* 34, 15607-13.

MADARA, J. L. & DHARMSATHAPHORN, K. 1985. Occluding junction structure-function relationships in a cultured epithelial monolayer. *J Cell Biol,* 101, 2124-33.

MADARA, J. L. & PAPPENHEIMER, J. R. 1987. Structural basis for physiological regulation of paracellular pathways in intestinal epithelia. *J Membr Biol,* 100, 149-64.

MAHON, P. C., HIROTA, K. & SEMENZA, G. L. 2001. FIH-1: a novel protein that interacts with HIF-1α and VHL to mediate repression of HIF-1 transcriptional activity. *Genes Dev,* 15, 2675-86.

MAIRBAURL, H., MAYER, K., KIM, K. J., BOROK, Z., BARTSCH, P. & CRANDALL, E. D. 2002. Hypoxia decreases active Na transport across primary rat alveolar epithelial cell monolayers. *Am J Physiol Lung Cell Mol Physiol,* 282, L659-65.

MAKELA, S., KERE, J., HOLMBERG, C. & HOGLUND, P. 2002. SLC26A3 mutations in congenital chloride diarrhea. *Hum Mutat,* 20, 425-38.

MANDEL, L. J. & BALABAN, R. S. 1981. Stoichiometry and coupling of active transport to oxidative metabolism in epithelial tissues. *Am J Physiol,* 240, F357-71.

MAO, H., FERGUSON, T. S., CIBULSKY, S. M., HOLMQVIST, M., DING, C., FEI, H. & LEVITAN, I. B. 2005. MONaKA, a novel modulator of the plasma membrane Na,K-ATPase. *J Neurosci,* 25, 7934-43.

MAROUN, J. A., ANTHONY, L. B., BLAIS, N., BURKES, R., DOWDEN, S. D., DRANITSARIS, G., SAMSON, B., SHAH, A., THIRLWELL, M. P., VINCENT, M. D. & WONG, R. 2007. Prevention and management of chemotherapy-induced diarrhea in patients with colorectal cancer: a consensus statement by the Canadian Working Group on Chemotherapy-Induced Diarrhea. *Curr Oncol,* 14, 13-20.

MARXSEN, J. H., STENGEL, P., DOEGE, K., HEIKKINEN, P., JOKILEHTO, T., WAGNER, T., JELKMANN, W., JAAKKOLA, P. & METZEN, E. 2004. Hypoxia-

inducible factor-1 (HIF-1) promotes its degradation by induction of HIF-α-prolyl-4-hydroxylases. *Biochem J,* 381, 761-7.

MASEREEL, B., POCHET, L. & LAECKMANN, D. 2003. An overview of inhibitors of Na^+/H^+ exchanger. *Eur J Med Chem,* 38, 547-54.

MASSON, N., WILLAM, C., MAXWELL, P. H., PUGH, C. W. & RATCLIFFE, P. J. 2001. Independent function of two destruction domains in hypoxia-inducible factor-α chains activated by prolyl hydroxylation. *EMBO J,* 20, 5197-206.

MATHESON, P. J., WILSON, M. A. & GARRISON, R. N. 2000. Regulation of intestinal blood flow. *J Surg Res,* 93, 182-96.

MATTER, K. & BALDA, M. S. 2003. Signalling to and from tight junctions. *Nat Rev Mol Cell Biol,* 4, 225-36.

MATTHEWS, J. B., AWTREY, C. S. & MADARA, J. L. 1992. Microfilament-dependent activation of $Na^+/K^+/2Cl^-$ cotransport by cAMP in intestinal epithelial monolayers. *J Clin Invest,* 90, 1608-13.

MATTHEWS, J. B., SMITH, J. A., TALLY, K. J., AWTREY, C. S., NGUYEN, H., RICH, J. & MADARA, J. L. 1994. Na-K-2Cl cotransport in intestinal epithelial cells. Influence of chloride efflux and F-actin on regulation of cotransporter activity and bumetanide binding. *J Biol Chem,* 269, 15703-9.

MCCABE, J. 1912. *The Story of Evolution ... With 17 illustrations and 5 maps.* pp. xi. 340. Hutchinson & Co.: London.

MCNEILL, L. A., HEWITSON, K. S., GLEADLE, J. M., HORSFALL, L. E., OLDHAM, N. J., MAXWELL, P. H., PUGH, C. W., RATCLIFFE, P. J. & SCHOFIELD, C. J. 2002. The use of dioxygen by HIF prolyl hydroxylase (PHD1). *Bioorg Med Chem Lett,* 12, 1547-50.

MCROBERTS, J. A., ARANDA, R., RILEY, N. & KANG, H. 1990. Insulin regulates the paracellular permeability of cultured intestinal epithelial cell monolayers. *J Clin Invest,* 85, 1127-34.

MCSHERRY, E. A., BRENNAN, K., HUDSON, L., HILL, A. D. & HOPKINS, A. M. 2011. Breast cancer cell migration is regulated through junctional adhesion molecule-A-mediated activation of Rap1 GTPase. *Breast Cancer Res,* 13, R31.

MEINILD, A., KLAERKE, D. A., LOO, D. D., WRIGHT, E. M. & ZEUTHEN, T. 1998. The human Na^+-glucose cotransporter is a molecular water pump. *J Physiol,* 508 (Pt 1), 15-21.

METZEN, E., BERCHNER-PFANNSCHMIDT, U., STENGEL, P., MARXSEN, J. H., STOLZE, I., KLINGER, M., HUANG, W. Q., WOTZLAW, C., HELLWIG-BURGEL, T., JELKMANN, W., ACKER, H. & FANDREY, J. 2003. Intracellular localisation of human HIF-1 α hydroxylases: implications for oxygen sensing. *J Cell Sci,* 116, 1319-26.

METZEN, E. & RATCLIFFE, P. J. 2004. HIF hydroxylation and cellular oxygen sensing. *Biol Chem,* 385, 223-30.

MILLER, H., ZHANG, J., KUOLEE, R., PATEL, G. B. & CHEN, W. 2007. Intestinal M cells: the fallible sentinels? *World J Gastroenterol,* 13, 1477-86.

MILLIGAN, L. P. & MCBRIDE, B. W. 1985. Energy costs of ion pumping by animal tissues. *J Nutr,* 115, 1374-82.

MISHRA, N. K., PELEG, Y., CIRRI, E., BELOGUS, T., LIFSHITZ, Y., VOELKER, D. R., APELL, H. J., GARTY, H. & KARLISH, S. J. 2011. FXYD proteins stabilize

Na,K-ATPase: amplification of specific phosphatidylserine-protein interactions. *J Biol Chem,* 286, 9699-712.

MOFFETT, D. F., MOFFETT, S. B. & SCHAUF, C. L. 1993. *Human physiology : foundations & frontiers,* St Louis ; London, Mosby.

MOLE, D. R., SCHLEMMINGER, I., MCNEILL, L. A., HEWITSON, K. S., PUGH, C. W., RATCLIFFE, P. J. & SCHOFIELD, C. J. 2003. 2-oxoglutarate analogue inhibitors of HIF prolyl hydroxylase. *Bioorg Med Chem Lett,* 13, 2677-80.

MORRISON, B. W., MOORMAN, J. R., KOWDLEY, G. C., KOBAYASHI, Y. M., JONES, L. R. & LEDER, P. 1995. Mat-8, a novel phospholemman-like protein expressed in human breast tumors, induces a chloride conductance in Xenopus oocytes. *J Biol Chem,* 270, 2176-82.

MORTH, J. P., PEDERSEN, B. P., BUCH-PEDERSEN, M. J., ANDERSEN, J. P., VILSEN, B., PALMGREN, M. G. & NISSEN, P. 2011. A structural overview of the plasma membrane Na^+,K^+-ATPase and H^+-ATPase ion pumps. *Nat Rev Mol Cell Biol,* 12, 60-70.

MORTH, J. P., PEDERSEN, B. P., TOUSTRUP-JENSEN, M. S., SORENSEN, T. L., PETERSEN, J., ANDERSEN, J. P., VILSEN, B. & NISSEN, P. 2007. Crystal structure of the sodium-potassium pump. *Nature,* 450, 1043-9.

MOSAVI, L. K., CAMMETT, T. J., DESROSIERS, D. C. & PENG, Z. Y. 2004. The ankyrin repeat as molecular architecture for protein recognition. *Protein Sci,* 13, 1435-48.

MOUMMI, C., XIE, Y., KACHUR, J. F. & GAGINELLA, T. S. 1992. Endothelin-1 stimulates contraction and ion transport in the rat colon: different mechanisms of action. *J Pharmacol Exp Ther,* 262, 409-14.

MROZ, M. S. & KEELY, S. J. 2011. Epidermal Growth Factor Chronically Upregulates TMEM16A Expression in Colonic Epithelial Cells – Implications for Treatment of Cystic Fibrosis *Gastroenterology* 140, S-134.

MUCHNIK, E. & KAPLAN, J. 2011. HIF prolyl hydroxylase inhibitors for anemia. *Expert Opin Investig Drugs,* 20, 645-56.

MURAKAMI, H. & MASUI, H. 1980. Hormonal control of human colon carcinoma cell growth in serum-free medium. *Proc Natl Acad Sci U S A,* 77, 3464-8.

MUREK, M., KOPIC, S. & GEIBEL, J. 2010. Evidence for intestinal chloride secretion. *Exp Physiol,* 95, 471-8.

MURPHY, K. T., SNOW, R. J., PETERSEN, A. C., MURPHY, R. M., MOLLICA, J., LEE, J. S., GARNHAM, A. P., AUGHEY, R. J., LEPPIK, J. A., MEDVED, I., CAMERON-SMITH, D. & MCKENNA, M. J. 2004. Intense exercise up-regulates Na^+,K^+-ATPase isoform mRNA, but not protein expression in human skeletal muscle. *J Physiol,* 556, 507-19.

MURRAY, A. J. 2008. Pharmacological PKA inhibition: all may not be what it seems. *Sci Signal,* 1, re4.

MUSCH, T. I., FRIEDMAN, D. B., PITETTI, K. H., HAIDET, G. C., STRAY-GUNDERSEN, J., MITCHELL, J. H. & ORDWAY, G. A. 1987. Regional distribution of blood flow of dogs during graded dynamic exercise. *J Appl Physiol,* 63, 2269-77.

NAGEL, S., PAPADAKIS, M., CHEN, R., HOYTE, L. C., BROOKS, K. J., GALLICHAN, D., SIBSON, N. R., PUGH, C. & BUCHAN, A. M. 2011. Neuroprotection by

dimethyloxalylglycine following permanent and transient focal cerebral ischemia in rats. *J Cereb Blood Flow Metab,* 31, 132-43.

NAMKUNG, W., FINKBEINER, W. E. & VERKMAN, A. S. 2010. CFTR-adenylyl cyclase I association responsible for UTP activation of CFTR in well-differentiated primary human bronchial cell cultures. *Mol Biol Cell,* 21, 2639-48.

NANDA KUMAR, N. S., SINGH, S. K. & RAJENDRAN, V. M. 2010. Mucosal potassium efflux mediated via Kcnn4 channels provides the driving force for electrogenic anion secretion in colon. *Am J Physiol Gastrointest Liver Physiol,* 299, G707-14.

NATARAJAN, R., SALLOUM, F. N., FISHER, B. J., SMITHSON, L., ALMENARA, J. & FOWLER, A. A., 3RD 2009. Prolyl hydroxylase inhibition attenuates post-ischemic cardiac injury via induction of endoplasmic reticulum stress genes. *Vascul Pharmacol,* 51, 110-8.

NEMETH, Z. H., DEITCH, E. A., LU, Q., SZABO, C. & HASKO, G. 2002a. NHE blockade inhibits chemokine production and NF-κB activation in immunostimulated endothelial cells. *Am J Physiol Cell Physiol,* 283, C396-403.

NEMETH, Z. H., DEITCH, E. A., SZABO, C., MABLEY, J. G., PACHER, P., FEKETE, Z., HAUSER, C. J. & HASKO, G. 2002b. Na^+/H^+ exchanger blockade inhibits enterocyte inflammatory response and protects against colitis. *Am J Physiol Gastrointest Liver Physiol,* 283, G122-32.

NGUYEN, A. D., MCDONALD, J. G., BRUICK, R. K. & DEBOSE-BOYD, R. A. 2007. Hypoxia stimulates degradation of 3-hydroxy-3-methylglutaryl-coenzyme A reductase through accumulation of lanosterol and hypoxia-inducible factor-mediated induction of insigs. *J Biol Chem,* 282, 27436-46.

O'MAHONY, F., ALZAMORA, R., BETTS, V., LAPAIX, F., CARTER, D., IRNATEN, M. & HARVEY, B. J. 2007. Female gender-specific inhibition of KCNQ1 channels and chloride secretion by 17β-estradiol in rat distal colonic crypts. *J Biol Chem,* 282, 24563-73.

OELKERS, P., KIRBY, L. C., HEUBI, J. E. & DAWSON, P. A. 1997. Primary bile acid malabsorption caused by mutations in the ileal sodium-dependent bile acid transporter gene (SLC10A2). *J Clin Invest,* 99, 1880-7.

OGBI, M. & JOHNSON, J. A. 2006. Protein kinase Cε interacts with cytochrome c oxidase subunit IV and enhances cytochrome c oxidase activity in neonatal cardiac myocyte preconditioning. *Biochem J,* 393, 191-9.

OUSINGSAWAT, J., MARTINS, J. R., SCHREIBER, R., ROCK, J. R., HARFE, B. D. & KUNZELMANN, K. 2009. Loss of TMEM16A causes a defect in epithelial Ca^{2+}-dependent chloride transport. *J Biol Chem,* 284, 28698-703.

OUSINGSAWAT, J., MIRZA, M., TIAN, Y., ROUSSA, E., SCHREIBER, R., COOK, D. I. & KUNZELMANN, K. 2011. Rotavirus toxin NSP4 induces diarrhea by activation of TMEM16A and inhibition of Na^+ absorption. *Pflugers Arch,* 461, 579-89.

PADILLA-BENAVIDES, T., ROLDAN, M. L., LARRE, I., FLORES-BENITEZ, D., VILLEGAS-SEPULVEDA, N., CONTRERAS, R. G., CEREIJIDO, M. &

SHOSHANI, L. 2010. The polarized distribution of Na^+,K^+-ATPase: role of the interaction between β subunits. *Mol Biol Cell,* 21, 2217-25.

PAN, Y., MANSFIELD, K. D., BERTOZZI, C. C., RUDENKO, V., CHAN, D. A., GIACCIA, A. J. & SIMON, M. C. 2007. Multiple factors affecting cellular redox status and energy metabolism modulate hypoxia-inducible factor prolyl hydroxylase activity *in vivo* and *in vitro*. *Mol Cell Biol,* 27, 912-25.

PAPANDREOU, I., CAIRNS, R. A., FONTANA, L., LIM, A. L. & DENKO, N. C. 2006. HIF-1 mediates adaptation to hypoxia by actively downregulating mitochondrial oxygen consumption. *Cell Metab,* 3, 187-97.

PATEL, A. J. & HONORE, E. 2001. Molecular physiology of oxygen-sensitive potassium channels. *Eur Respir J,* 18, 221-7.

PAYNE, J. A., XU, J. C., HAAS, M., LYTLE, C. Y., WARD, D. & FORBUSH, B., 3RD 1995. Primary structure, functional expression, and chromosomal localization of the bumetanide-sensitive Na-K-Cl cotransporter in human colon. *J Biol Chem,* 270, 17977-85.

PEERS, C. & KEMP, P. J. 2001. Acute oxygen sensing: diverse but convergent mechanisms in airway and arterial chemoreceptors. *Respir Res,* 2, 145-9.

PERDUE, M. H., MASSON, S., WERSHIL, B. K. & GALLI, S. J. 1991. Role of mast cells in ion transport abnormalities associated with intestinal anaphylaxis. Correction of the diminished secretory response in genetically mast cell-deficient W/Wv mice by bone marrow transplantation. *J Clin Invest,* 87, 687-93.

PIECHOTTA, K., GARBARINI, N., ENGLAND, R. & DELPIRE, E. 2003. Characterization of the interaction of the stress kinase SPAK with the Na^+-K^+-2Cl- cotransporter in the nervous system: evidence for a scaffolding role of the kinase. *J Biol Chem,* 278, 52848-56.

PIKE, L. J. 2009. The challenge of lipid rafts. *J Lipid Res,* 50 Suppl, S323-8.

PIZZONIA, J. H., BIEMESDERFER, D., ABU-ALFA, A. K., WU, M. S., EXNER, M., ISENRING, P., IGARASHI, P. & ARONSON, P. S. 1998. Immunochemical characterization of Na^+/H^+ exchanger isoform NHE4. *Am J Physiol,* 275, F510-7.

PLANES, C., FRIEDLANDER, G., LOISEAU, A., AMIEL, C. & CLERICI, C. 1996. Inhibition of Na-K-ATPase activity after prolonged hypoxia in an alveolar epithelial cell line. *Am J Physiol,* 271, L70-8.

PRAKASH, S. & MALGORZATA URBANSKA, A. 2008. Colon-targeted delivery of live bacterial cell biotherapeutics including microencapsulated live bacterial cells. *Biologics,* 2, 355-78.

PRASANNA, G., DIBAS, A., HULET, C. & YORIO, T. 2001. Inhibition of Na^+/K^+-atpase by endothelin-1 in human nonpigmented ciliary epithelial cells. *J Pharmacol Exp Ther,* 296, 966-71.

PRINCE, L. S., WORKMAN, R. B., JR. & MARCHASE, R. B. 1994. Rapid endocytosis of the cystic fibrosis transmembrane conductance regulator chloride channel. *Proc Natl Acad Sci U S A,* 91, 5192-6.

PRINZ, C., KAJIMURA, M., SCOTT, D. R., MERCIER, F., HELANDER, H. F. & SACHS, G. 1993. Histamine secretion from rat enterochromaffinlike cells. *Gastroenterology,* 105, 449-61.

PROVENZANO, R., GOODKIN, D., KLAUS, S., LINDE, P., KAZAZI, F., LEE, T., NEFF, T. & YU, P. 2011. 253 Evaluation of FG-4592, a Novel Oral Hypoxia-Inducible Factor Prolyl Hydroxylase Inhibitor, to Treat Anemia in Hemodialysis Patients. *American Journal of Kidney Diseases,* 57, B80.

RAMIREZ, M. A., TORIANO, R., PARISI, M. & MALNIC, G. 2000. Control of cell pH in the T84 colon cell line. *J Membr Biol,* 177, 149-57.

RATAN, R. R., SIDDIQ, A., AMINOVA, L., LANGE, P. S., LANGLEY, B., AYOUB, I., GENSERT, J. & CHAVEZ, J. 2004. Translation of ischemic preconditioning to the patient: prolyl hydroxylase inhibition and hypoxia inducible factor-1 as novel targets for stroke therapy. *Stroke,* 35, 2687-9.

READ, N. W. 1983. Speculations on the role of motility in the pathogenesis and treatment of diarrhoea. *Scand J Gastroenterol Suppl,* 84, 45-63.

REBILLARD, A., TEKPLI, X., MEURETTE, O., SERGENT, O., LEMOIGNE-MULLER, G., VERNHET, L., GORRIA, M., CHEVANNE, M., CHRISTMANN, M., KAINA, B., COUNILLON, L., GULBINS, E., LAGADIC-GOSSMANN, D. & DIMANCHE-BOITREL, M. T. 2007. Cisplatin-induced apoptosis involves membrane fluidification via inhibition of NHE1 in human colon cancer cells. *Cancer Res,* 67, 7865-74.

REED, K. K. & WICKHAM, R. 2009. Review of the gastrointestinal tract: from macro to micro. *Semin Oncol Nurs,* 25, 3-14.

REYNOLDS, A., PARRIS, A., EVANS, L. A., LINDQVIST, S., SHARP, P., LEWIS, M., TIGHE, R. & WILLIAMS, M. R. 2007. Dynamic and differential regulation of NKCC1 by calcium and cAMP in the native human colonic epithelium. *J Physiol,* 582, 507-24.

RIORDAN, J. R., ROMMENS, J. M., KEREM, B., ALON, N., ROZMAHEL, R., GRZELCZAK, Z., ZIELENSKI, J., LOK, S., PLAVSIC, N., CHOU, J. L. & ET AL. 1989. Identification of the cystic fibrosis gene: cloning and characterization of complementary DNA. *Science,* 245, 1066-73.

RIOS, E. J., FALLON, M., WANG, J. & SHIMODA, L. A. 2005. Chronic hypoxia elevates intracellular pH and activates Na^+/H^+ exchange in pulmonary arterial smooth muscle cells. *Am J Physiol Lung Cell Mol Physiol,* 289, L867-74.

ROBERTS, N. A., HAWORTH, R. S. & AVKIRAN, M. 2005. Effects of bisindolylmaleimide PKC inhibitors on p90RSK activity *in vitro* and in adult ventricular myocytes. *Br J Pharmacol,* 145, 477-89.

ROBINSON, A., KEELY, S., KARHAUSEN, J., GERICH, M. E., FURUTA, G. T. & COLGAN, S. P. 2008. Mucosal protection by hypoxia-inducible factor prolyl hydroxylase inhibition. *Gastroenterology,* 134, 145-55.

ROCHWERGER, L., DHO, S., PARKER, L., FOSKETT, J. K. & BUCHWALD, M. 1994. Estrogen-dependent expression of the cystic fibrosis transmembrane regulator gene in a novel uterine epithelial cell line. *J Cell Sci,* 107 (Pt 9), 2439-48.

ROSS, F. A., RAFFERTY, J. N., DALLAS, M. L., OGUNBAYO, O., IKEMATSU, N., MCCLAFFERTY, H., TIAN, L., WIDMER, H., ROWE, I. C., WYATT, C. N., SHIPSTON, M. J., PEERS, C., HARDIE, D. G. & EVANS, A. M. 2011. Selective expression in carotid body type I cells of a single splice variant of the large conductance calcium- and voltage-activated potassium channel

confers regulation by AMP-activated protein kinase. *J Biol Chem,* 286, 11929-36.

ROSSIER, B. C., PRADERVAND, S., SCHILD, L. & HUMMLER, E. 2002. Epithelial sodium channel and the control of sodium balance: interaction between genetic and environmental factors. *Annu Rev Physiol,* 64, 877-97.

ROSSIER, B. C. & STUTTS, M. J. 2009. Activation of the epithelial sodium channel (ENaC) by serine proteases. *Annu Rev Physiol,* 71, 361-79.

RUBANYI, G. M. & POLOKOFF, M. A. 1994. Endothelins: molecular biology, biochemistry, pharmacology, physiology, and pathophysiology. *Pharmacol Rev,* 46, 325-415.

RUDOLPH, J. A., POCCIA, J. L. & COHEN, M. B. 2004. Cyclic AMP activation of the extracellular signal-regulated kinases 1 and 2: implications for intestinal cell survival through the transient inhibition of apoptosis. *J Biol Chem,* 279, 14828-34.

RUFO, P. A., MERLIN, D., RIEGLER, M., FERGUSON-MALTZMAN, M. H., DICKINSON, B. L., BRUGNARA, C., ALPER, S. L. & LENCER, W. I. 1997. The antifungal antibiotic, clotrimazole, inhibits chloride secretion by human intestinal T_{84} cells via blockade of distinct basolateral K^+ conductances. Demonstration of efficacy in intact rabbit colon and in an *in vivo* mouse model of cholera. *J Clin Invest,* 100, 3111-20.

RUSAI, K., WAGNER, B., ROOS, M., SCHMADERER, C., STROBL, M., BOINI, K. M., GRENZ, A., KUHL, D., HEEMANN, U., LANG, F. & LUTZ, J. 2009. The serum and glucocorticoid-regulated kinase 1 in hypoxic renal injury. *Cell Physiol Biochem,* 24, 577-84.

SAITOU, M., FURUSE, M., SASAKI, H., SCHULZKE, J. D., FROMM, M., TAKANO, H., NODA, T. & TSUKITA, S. 2000. Complex phenotype of mice lacking occludin, a component of tight junction strands. *Mol Biol Cell,* 11, 4131-42.

SALNIKOW, K., DONALD, S. P., BRUICK, R. K., ZHITKOVICH, A., PHANG, J. M. & KASPRZAK, K. S. 2004. Depletion of intracellular ascorbate by the carcinogenic metals nickel and cobalt results in the induction of hypoxic stress. *J Biol Chem,* 279, 40337-44.

SANDLE, G. I. 1989. Segmental heterogeneity of basal and aldosterone-induced electrogenic Na transport in human colon. *Pflugers Arch,* 414, 706-12.

SANDLE, G. I. 1998. Salt and water absorption in the human colon: a modern appraisal. *Gut,* 43, 294-9.

SANDLE, G. I., WILLS, N. K., ALLES, W. & BINDER, H. J. 1986. Electrophysiology of the human colon: evidence of segmental heterogeneity. *Gut,* 27, 999-1005.

SARAVI, F. D., SALDENA, T. A. & CINCUNEGUI, L. M. 1996. Colon epithelial electrical responses to acute hypoxia and reoxygenation *in vitro*. *Acta Gastroenterol Latinoam,* 26, 159-65.

SAVAGE, D. C. 1977. Microbial ecology of the gastrointestinal tract. *Annu Rev Microbiol,* 31, 107-33.

SCHEELE, G. A. 1980. Biosynthesis, segregation, and secretion of exportable proteins by the exocrine pancreas. *Am J Physiol,* 238, G467-77.

SCHNEIDER-POETSCH, T., JU, J., EYLER, D. E., DANG, Y., BHAT, S., MERRICK, W. C., GREEN, R., SHEN, B. & LIU, J. O. 2010. inhibition of eukaryotic translation elongation by cycloheximide and lactimidomycin. *Nat Chem Biol,* 6, 209-217.

SCHODEL, J., BOHR, D., KLANKE, B., SCHLEY, G., SCHLOTZER-SCHREHARDT, U., WARNECKE, C., KURTZ, A., AMANN, K., ECKARDT, K. U. & WILLAM, C. 2010. Factor inhibiting HIF limits the expression of hypoxia-inducible genes in podocytes and distal tubular cells. *Kidney Int,* 78, 857-67.

SCHONER, W. & SCHEINER-BOBIS, G. 2005. Endogenous cardiac glycosides: hormones using the sodium pump as signal transducer. *Semin Nephrol,* 25, 343-51.

SCHROEDER, B. C., WALDEGGER, S., FEHR, S., BLEICH, M., WARTH, R., GREGER, R. & JENTSCH, T. J. 2000. A constitutively open potassium channel formed by KCNQ1 and KCNE3. *Nature,* 403, 196-9.

SCHULTHEIS, P. J., CLARKE, L. L., MENETON, P., MILLER, M. L., SOLEIMANI, M., GAWENIS, L. R., RIDDLE, T. M., DUFFY, J. J., DOETSCHMAN, T., WANG, T., GIEBISCH, G., ARONSON, P. S., LORENZ, J. N. & SHULL, G. E. 1998. Renal and intestinal absorptive defects in mice lacking the NHE3 Na^+/H^+ exchanger. *Nat Genet,* 19, 282-5.

SCHULTHEISS, G., HORGER, S. & DIENER, M. 1998. The bumetanide-resistant part of forskolin-induced anion secretion in rat colon. *Acta Physiol Scand,* 164, 219-28.

SEAVILLEKLEIN, G., AMER, N., EVAGELIDIS, A., CHAPPE, F., IRVINE, T., HANRAHAN, J. W. & CHAPPE, V. 2008. PKC phosphorylation modulates PKA-dependent binding of the R domain to other domains of CFTR. *Am J Physiol Cell Physiol,* 295, C1366-75.

SEEBOHM, G., STRUTZ-SEEBOHM, N., BIRKIN, R., DELL, G., BUCCI, C., SPINOSA, M. R., BALTAEV, R., MACK, A. F., KORNIYCHUK, G., CHOUDHURY, A., MARKS, D., PAGANO, R. E., ATTALI, B., PFEUFER, A., KASS, R. S., SANGUINETTI, M. C., TAVARE, J. M. & LANG, F. 2007. Regulation of endocytic recycling of KCNQ1/KCNE1 potassium channels. *Circ Res,* 100, 686-92.

SEMENZA, G. L. 2007. Oxygen-dependent regulation of mitochondrial respiration by hypoxia-inducible factor 1. *Biochem J,* 405, 1-9.

SEMENZA, G. L. & WANG, G. L. 1992. A nuclear factor induced by hypoxia via *de novo* protein synthesis binds to the human erythropoietin gene enhancer at a site required for transcriptional activation. *Mol Cell Biol,* 12, 5447-54.

SHEN, L., WEBER, C. R., RALEIGH, D. R., YU, D. & TURNER, J. R. 2011. Tight junction pore and leak pathways: a dynamic duo. *Annu Rev Physiol,* 73, 283-309.

SHEPPARD, D. N. & WELSH, M. J. 1999. Structure and function of the CFTR chloride channel. *Physiol Rev,* 79, S23-45.

SHIP, J. A., PATTON, L. L. & WELLNER, R. B. 1990. Muscarinic regulation of potassium transport in a human submandibular epithelial cell line. *Am J Physiol,* 259, C340-8.

SHOSHANI, L., CONTRERAS, R. G., ROLDAN, M. L., MORENO, J., LAZARO, A., BALDA, M. S., MATTER, K. & CEREIJIDO, M. 2005. The polarized expression of Na^+,K^+-ATPase in epithelia depends on the association between β-subunits located in neighboring cells. *Mol Biol Cell,* **16,** 1071-81.

SINGH, A. K., TASKEN, K., WALKER, W., FRIZZELL, R. A., WATKINS, S. C., BRIDGES, R. J. & BRADBURY, N. A. 1998. Characterization of PKA isoforms and kinase-dependent activation of chloride secretion in T84 cells. *Am J Physiol,* 275, C562-70.

SKOU, J. C. 1998. Nobel Lecture. The identification of the sodium pump. *Biosci Rep,* **18,** 155-69.

SOBELL, H. M. 1985. Actinomycin and DNA transcription. *Proc Natl Acad Sci U S A,* 82, 5328-31.

SOHRABPOUR, A. A., MALEKZADEH, R. & KESHAVARZIAN, A. 2010. Current therapeutic approaches in inflammatory bowel disease. *Curr Pharm Des,* **16,** 3668-83.

SONG, J. C., HANSON, C. M., TSAI, V., FAROKHZAD, O. C., LOTZ, M. & MATTHEWS, J. B. 2001. Regulation of epithelial transport and barrier function by distinct protein kinase C isoforms. *Am J Physiol Cell Physiol,* 281, C649-61.

SRIDHARAN, V., GUICHARD, J., LI, C. Y., MUISE-HELMERICKS, R., BEESON, C. C. & WRIGHT, G. L. 2008. O_2-sensing signal cascade: clamping of O_2 respiration, reduced ATP utilization, and inducible fumarate respiration. *Am J Physiol Cell Physiol,* 295, C29-37.

STEFFAN, N. M., BREN, G. D., FRANTZ, B., TOCCI, M. J., O'NEILL, E. A. & PAYA, C. V. 1995. Regulation of IκBα phosphorylation by PKC- and Ca^{2+}-dependent signal transduction pathways. *J Immunol,* 155, 4685-91.

STEPHENS, R. E. 1985. Evidence for a tubulin-containing lipid-protein structural complex in ciliary membranes. *J Cell Biol,* 100, 1082-90.

STEVENSON, B. R., SILICIANO, J. D., MOOSEKER, M. S. & GOODENOUGH, D. A. 1986. Identification of ZO-1: a high molecular weight polypeptide associated with the tight junction (zonula occludens) in a variety of epithelia. *J Cell Biol,* 103, 755-66.

SULLIVAN, S., ALEX, P., DASSOPOULOS, T., ZACHOS, N. C., IACOBUZIO-DONAHUE, C., DONOWITZ, M., BRANT, S. R., CUFFARI, C., HARRIS, M. L., DATTA, L. W., CONKLIN, L., CHEN, Y. & LI, X. 2009. Downregulation of sodium transporters and NHERF proteins in IBD patients and mouse colitis models: potential contributors to IBD-associated diarrhea. *Inflamm Bowel Dis,* 15, 261-74.

SWEADNER, K. J. & RAEL, E. 2000. The FXYD gene family of small ion transport regulators or channels: cDNA sequence, protein signature sequence, and expression. *Genomics,* 68, 41-56.

TABCHARANI, J. A., CHANG, X. B., RIORDAN, J. R. & HANRAHAN, J. W. 1991. Phosphorylation-regulated Cl^- channel in CHO cells stably expressing the cystic fibrosis gene. *Nature,* 352, 628-31.

TAKAHASHI, H., YOSHIKA, M., KOMIYAMA, Y. & NISHIMURA, M. 2011. The central mechanism underlying hypertension: a review of the roles of

sodium ions, epithelial sodium channels, the renin-angiotensin-aldosterone system, oxidative stress and endogenous digitalis in the brain. *Hypertens Res,* PMID: 21814209

TAKAHASHI, K., JONES, P. M., KANSE, S. M., LAM, H. C., SPOKES, R. A., GHATEI, M. A. & BLOOM, S. R. 1990. Endothelin in the gastrointestinal tract. Presence of endothelinlike immunoreactivity, endothelin-1 messenger RNA, endothelin receptors, and pharmacological effect. *Gastroenterology,* 99, 1660-7.

TAKEUCHI, H., TAKEUCHI, T., GAO, J., CANTLEY, L. C. & HIRATA, M. 2010. Characterization of PXK as a protein involved in epidermal growth factor receptor trafficking. *Mol Cell Biol,* 30, 1689-702.

TAKIZAWA, S., UCHIDE, T., ADUR, J., KOZAKAI, T., KOTAKE-NARA, E., QUAN, J. & SAIDA, K. 2005. Differential expression of endothelin-2 along the mouse intestinal tract. *J Mol Endocrinol,* 35, 201-9.

TAMBUWALA, M. M., CUMMINS, E. P., LENIHAN, C. R., KISS, J., STAUCH, M., SCHOLZ, C. C., FRAISL, P., LASITSCHKA, F., MOLLENHAUER, M., SAUNDERS, S. P., MAXWELL, P. H., CARMELIET, P., FALLON, P. G., SCHNEIDER, M. & TAYLOR, C. T. 2010. Loss of prolyl hydroxylase-1 protects against colitis through reduced epithelial cell apoptosis and increased barrier function. *Gastroenterology,* 139, 2093-101.

TAMKUN, M. M. & FAMBROUGH, D. M. 1986. The Na^+ + K^+-ATPase of chick sensory neurons. Studies on biosynthesis and intracellular transport. *J Biol Chem,* 261, 1009-19.

TAYLOR, C. T. & COLGAN, S. P. 2007. Hypoxia and gastrointestinal disease. *J Mol Med (Berl),* 85, 1295-300.

TAYLOR, C. T., FUEKI, N., AGAH, A., HERSHBERG, R. M. & COLGAN, S. P. 1999. Critical role of cAMP response element binding protein expression in hypoxia-elicited induction of epithelial tumor necrosis factor-α. *J Biol Chem,* 274, 19447-54.

TAYLOR, C. T., LISCO, S. J., AWTREY, C. S. & COLGAN, S. P. 1998. Hypoxia inhibits cyclic nucleotide-stimulated epithelial ion transport: role for nucleotide cyclases as oxygen sensors. *J Pharmacol Exp Ther,* 284, 568-75.

TIAN, Y., KONGSUPHOL, P., HUG, M., OUSINGSAWAT, J., WITZGALL, R., SCHREIBER, R. & KUNZELMANN, K. 2011a. Calmodulin-dependent activation of the epithelial calcium-dependent chloride channel TMEM16A. *FASEB J,* 25, 1058-68.

TIAN, Y. M., YEOH, K. K., LEE, M. K., ERIKSSON, T., KESSLER, B. M., KRAMER, H. B., EDELMANN, M. J., WILLAM, C., PUGH, C. W., SCHOFIELD, C. J. & RATCLIFFE, P. J. 2011b. Differential sensitivity of hypoxia inducible factor hydroxylation sites to hypoxia and hydroxylase inhibitors. *J Biol Chem,* 286, 13041-51.

TONNESSEN, T., GIAID, A., SALEH, D., NAESS, P. A., YANAGISAWA, M. & CHRISTENSEN, G. 1995. Increased *in vivo* expression and production of endothelin-1 by porcine cardiomyocytes subjected to ischemia. *Circ Res,* 76, 767-72.

TOULLEC, D., PIANETTI, P., COSTE, H., BELLEVERGUE, P., GRAND-PERRET, T., AJAKANE, M., BAUDET, V., BOISSIN, P., BOURSIER, E., LORIOLLE, F. & ET

AL. 1991. The bisindolylmaleimide GF 109203X is a potent and selective inhibitor of protein kinase C. *J Biol Chem,* 266, 15771-81.

TOUMI, F., FRANKSON, M., WARD, J. B., KELLY, O. B., MROZ, M. S., BERTELSEN, L. S. & KEELY, S. J. 2011. Chronic regulation of colonic epithelial secretory function by activation of G protein-coupled receptors. *Neurogastroenterol Motil,* 23, 178-86, e43.

TREIMAN, M., CASPERSEN, C. & CHRISTENSEN, S. B. 1998. A tool coming of age: thapsigargin as an inhibitor of sarco-endoplasmic reticulum Ca^{2+}-ATPases. *Trends Pharmacol Sci,* 19, 131-5.

TSCHANK, G., BROCKS, D. G., ENGELBART, K., MOHR, J., BAADER, E., GUNZLER, V. & HANAUSKE-ABEL, H. M. 1991. Inhibition of prolyl hydroxylation and procollagen processing in chick-embryo calvaria by a derivative of pyridine-2,4-dicarboxylate. Characterization of the diethyl ester as a proinhibitor. *Biochem J,* 275 (Pt 2), 469-76.

TSUKITA, S., FURUSE, M. & ITOH, M. 2001. Multifunctional strands in tight junctions. *Nat Rev Mol Cell Biol,* 2, 285-93.

TURINI, P., KUROOKA, S., STEER, M., CORBASCIO, A. N. & SINGER, T. P. 1969. The action of phenylmethylsulfonyl fluoride on human acetylcholinesterase, chymotyrpsin and trypsin. *J Pharmacol Exp Ther,* 167, 98-104.

TURNER, J. T. & YU, H. 1991. Identification of functional receptors for vasoactive intestinal peptide and neurotensin in the human submandibular gland duct cell line, HSG-PA. *Regul Pept,* 36, 173-82.

URA, K., SOYANO, K., OMOTO, N., ADACHI, S. & YAMAUCHI, K. 1996. Localization of Na^+, K^+-ATPase in tissues of rabbit and teleosts using an antiserum directed against a partial sequence of the α-subunit. *Zoolog Sci,* 13, 219-27.

VAGIN, O., SACHS, G. & TOKHTAEVA, E. 2007. The roles of the Na,K-ATPase β_1 subunit in pump sorting and epithelial integrity. *J Bioenerg Biomembr,* 39, 367-72.

VAGIN, O., TOKHTAEVA, E., YAKUBOV, I., SHEVCHENKO, E. & SACHS, G. 2008. Inverse correlation between the extent of N-glycan branching and intercellular adhesion in epithelia. Contribution of the Na,K-ATPase β_1 subunit. *J Biol Chem,* 283, 2192-202.

VAN BERGE HENEGOUWEN, G. P. & HOFMANN, A. F. 1978. Nocturnal gallbladder storage and emptying in gallstone patients and healthy subjects. *Gastroenterology,* 75, 879-85.

VAN ITALLIE, C., RAHNER, C. & ANDERSON, J. M. 2001. Regulated expression of claudin-4 decreases paracellular conductance through a selective decrease in sodium permeability. *J Clin Invest,* 107, 1319-27.

VAN ITALLIE, C. M. & ANDERSON, J. M. 2004. The role of claudins in determining paracellular charge selectivity. *Proc Am Thorac Soc,* 1, 38-41.

WALSH, J. H. 1988. Peptides as regulators of gastric acid secretion. *Annu Rev Physiol,* 50, 41-63.

WANG, H., HAAS, M., LIANG, M., CAI, T., TIAN, J., LI, S. & XIE, Z. 2004. Ouabain assembles signaling cascades through the caveolar Na^+/K^+-ATPase. *J Biol Chem,* 279, 17250-9.

WARBURG, O. 1956. On the origin of cancer cells. *Science,* 123, 309-14.

WARDLAW, T., SALAMA, P., BROCKLEHURST, C., CHOPRA, M. & MASON, E. 2010. Diarrhoea: why children are still dying and what can be done. *Lancet,* 375, 870-2.

WASSERMAN, S. I., BARRETT, K. E., HUOTT, P. A., BEUERLEIN, G., KAGNOFF, M. F. & DHARMSATHAPHORN, K. 1988. Immune-related intestinal Cl^- secretion. I. Effect of histamine on the T_{84} cell line. *Am J Physiol,* 254, C53-62.

WATANABE, T., SUZUKI, N., SHIMAMOTO, N., FUJINO, M. & IMADA, A. 1990. Endothelin in myocardial infarction. *Nature,* 344, 114.

WATSON, A. J., DUCKWORTH, C. A., GUAN, Y. & MONTROSE, M. H. 2009. Mechanisms of epithelial cell shedding in the Mammalian intestine and maintenance of barrier function. *Ann N Y Acad Sci,* 1165, 135-42.

WEBER, C. R., RALEIGH, D. R., SU, L., SHEN, L., SULLIVAN, E. A., WANG, Y. & TURNER, J. R. 2010. Epithelial myosin light chain kinase activation induces mucosal interleukin-13 expression to alter tight junction ion selectivity. *J Biol Chem,* 285, 12037-46.

WEDENOJA, S., PEKANSAARI, E., HOGLUND, P., MAKELA, S., HOLMBERG, C. & KERE, J. 2011. Update on SLC26A3 mutations in congenital chloride diarrhea. *Hum Mutat,* 32, 715-22.

WEI, L., VANKEERBERGHEN, A., CUPPENS, H., CASSIMAN, J. J., DROOGMANS, G. & NILIUS, B. 2001. The C-terminal part of the R-domain, but not the PDZ binding motif, of CFTR is involved in interaction with Ca^{2+}-activated Cl^- channels. *Pflugers Arch,* 442, 280-5.

WHEATON, W. W. & CHANDEL, N. S. 2011. Hypoxia. 2. Hypoxia regulates cellular metabolism. *Am J Physiol Cell Physiol,* 300, C385-93.

WHITEHEAD, K. A., LANGER, R. & ANDERSON, D. G. 2009. Knocking down barriers: advances in siRNA delivery. *Nat Rev Drug Discov,* 8, 129-38.

WHO 1990. *The rational use of drugs in the management of acute diarrhoea in children,* World Health Organization, ISBN: 9241561424.

WHO 2005. The treatment of diarrhoea. A manual for physicians and other senior health workers, World Health Organization, ISBN: 9241593180.

WHO 2008. Global networks for surveillance of rotavirus gastroenteritis, 2001-2008. *Wkly Epidemiol Rec,* 83, 421-5.

WILDRICK, D. M., LOINTIER, P., NICHOLS, D. H., ROLL, R., QUINTANILLA, B. & BOMAN, B. M. 1997. Isolation of normal human colonic mucosa: comparison of methods. *In Vitro Cell Dev Biol Anim,* 33, 18-27.

WILLAM, C., MAXWELL, P. H., NICHOLS, L., LYGATE, C., TIAN, Y. M., BERNHARDT, W., WIESENER, M., RATCLIFFE, P. J., ECKARDT, K. U. & PUGH, C. W. 2006. HIF prolyl hydroxylases in the rat; organ distribution and changes in expression following hypoxia and coronary artery ligation. *J Mol Cell Cardiol,* 41, 68-77.

WILLS, N. K., REUSS, L. & LEWIS, S. A. 1996. *Epithelial transport : a guide to methods and experimental analysis,* London, Chapman & Hall.

WOLF, A. A., FUJINAGA, Y. & LENCER, W. I. 2002. Uncoupling of the cholera toxin-G_{M1} ganglioside receptor complex from endocytosis, retrograde

Golgi trafficking, and downstream signal transduction by depletion of membrane cholesterol. *J Biol Chem,* 277, 16249-56.

WORONIECKI, R., FERDINAND, J. R., MORROW, J. S. & DEVARAJAN, P. 2003. Dissociation of spectrin-ankyrin complex as a basis for loss of Na-K-ATPase polarity after ischemia. *Am J Physiol Renal Physiol,* 284, F358-64.

WORRELL, R. T., BEST, A., CRAWFORD, O. R., XU, J., SOLEIMANI, M. & MATTHEWS, J. B. 2005. Apical ammonium inhibition of cAMP-stimulated secretion in T_{84} cells is bicarbonate dependent. *Am J Physiol Gastrointest Liver Physiol,* 289, G768-78.

WORRELL, R. T. & FRIZZELL, R. A. 1991. CaMKII mediates stimulation of chloride conductance by calcium in T84 cells. *Am J Physiol,* 260, C877-82.

WRIGHT, E. M. & LOO, D. D. 2000. Coupling between Na^+, sugar, and water transport across the intestine. *Ann N Y Acad Sci,* 915, 54-66.

WRIGHT, E. M., LOO, D. D. & HIRAYAMA, B. A. 2011. Biology of human sodium glucose transporters. *Physiol Rev,* 91, 733-94.

WYATT, C. N., MUSTARD, K. J., PEARSON, S. A., DALLAS, M. L., ATKINSON, L., KUMAR, P., PEERS, C., HARDIE, D. G. & EVANS, A. M. 2007. AMP-activated protein kinase mediates carotid body excitation by hypoxia. *J Biol Chem,* 282, 8092-8.

XIE, W., KAETZEL, M. A., BRUZIK, K. S., DEDMAN, J. R., SHEARS, S. B. & NELSON, D. J. 1996. Inositol 3,4,5,6-tetrakisphosphate inhibits the calmodulin-dependent protein kinase II-activated chloride conductance in T84 colonic epithelial cells. *J Biol Chem,* 271, 14092-7.

XUE, J., LI, X., JIAO, S., WEI, Y., WU, G. & FANG, J. 2010. Prolyl hydroxylase-3 is down-regulated in colorectal cancer cells and inhibits IKKβ independent of hydroxylase activity. *Gastroenterology,* 138, 606-15.

YAMADA, T. & ALPERS, D. H. 2009. *Textbook of gastroenterology,* Chichester, West Sussex ; Hoboken, NJ, Blackwell Pub.

YAMASHITA, K., DISCHER, D. J., HU, J., BISHOPRIC, N. H. & WEBSTER, K. A. 2001. Molecular regulation of the endothelin-1 gene by hypoxia. Contributions of hypoxia-inducible factor-1, activator protein-1, GATA-2, AND p300/CBP. *J Biol Chem,* 276, 12645-53.

YAN, Y. B., WANG, Q., HE, H. W. & ZHOU, H. M. 2004. Protein thermal aggregation involves distinct regions: sequential events in the heat-induced unfolding and aggregation of hemoglobin. *Biophys J,* 86, 1682-90.

YANG, L., CHU, J. S. & FIX, J. A. 2002. Colon-specific drug delivery: new approaches and *in vitro/in vivo* evaluation. *Int J Pharm,* 235, 1-15.

YANG, M., GE, W., CHOWDHURY, R., CLARIDGE, T. D., KRAMER, H. B., SCHMIERER, B., MCDONOUGH, M. A., GONG, L., KESSLER, B. M., RATCLIFFE, P. J., COLEMAN, M. L. & SCHOFIELD, C. J. 2011. Asparagine and aspartate hydroxylation of the cytoskeletal ankyrin family is catalyzed by factor-inhibiting hypoxia-inducible factor. *J Biol Chem,* 286, 7648-60.

YEAMAN, C., GRINDSTAFF, K. K. & NELSON, W. J. 1999. New perspectives on mechanisms involved in generating epithelial cell polarity. *Physiol Rev,* 79, 73-98.

YOO, J., NICHOLS, A., SONG, J. C., MUN, E. C. & MATTHEWS, J. B. 2001. Protein kinase epsilon dampens the secretory response of model intestinal epithelia during ischemia. *Surgery,* 130, 310-8.

YOON, T., KIM, M. & LEE, K. 2006. Inhibition of Na,K-ATPase-suppressive activity of translationally controlled tumor protein by sorting nexin 6. *FEBS Lett,* 580, 3558-64.

YUAN, Y., HILLIARD, G., FERGUSON, T. & MILLHORN, D. E. 2003. Cobalt inhibits the interaction between hypoxia-inducible factor-α and von Hippel-Lindau protein by direct binding to hypoxia-inducible factor-α. *J Biol Chem,* 278, 15911-6.

ZACHOS, N. C., TSE, M. & DONOWITZ, M. 2005. Molecular physiology of intestinal Na^+/H^+ exchange. *Annu Rev Physiol,* 67, 411-43.

ZAHID, A. 2004. The vermiform appendix: not a useless organ. *J Coll Physicians Surg Pak,* 14, 256-8.

ZEIDEL, M. L., BRADY, H. R., KONE, B. C., GULLANS, S. R. & BRENNER, B. M. 1989. Endothelin, a peptide inhibitor of Na^+-K^+-ATPase in intact renaltubular epithelial cells. *Am J Physiol,* 257, C1101-7.

ZHANG, H., GAO, P., FUKUDA, R., KUMAR, G., KRISHNAMACHARY, B., ZELLER, K. I., DANG, C. V. & SEMENZA, G. L. 2007. HIF-1 inhibits mitochondrial biogenesis and cellular respiration in VHL-deficient renal cell carcinoma by repression of C-MYC activity. *Cancer Cell,* 11, 407-20.

ZHANG, N., FU, Z., LINKE, S., CHICHER, J., GORMAN, J. J., VISK, D., HADDAD, G. G., POELLINGER, L., PEET, D. J., POWELL, F. & JOHNSON, R. S. 2010. The asparaginyl hydroxylase factor inhibiting HIF-1α is an essential regulator of metabolism. *Cell Metab,* 11, 364-78.

ZHANG, Z., DEVARAJAN, P., DORFMAN, A. L. & MORROW, J. S. 1998. Structure of the ankyrin-binding domain of α-Na,K-ATPase. *J Biol Chem,* 273, 18681-4.

ZHAO, H. X., WANG, X. L., WANG, Y. H., WU, Y., LI, X. Y., LV, X. P., ZHAO, Z. Q., ZHAO, R. R. & LIU, H. R. 2010. Attenuation of myocardial injury by postconditioning: role of hypoxia inducible factor-1α. *Basic Res Cardiol,* 105, 109-18.

ZHENG, W., KUHLICKE, J., JACKEL, K., ELTZSCHIG, H. K., SINGH, A., SJOBLOM, M., RIEDERER, B., WEINHOLD, C., SEIDLER, U., COLGAN, S. P. & KARHAUSEN, J. 2009. Hypoxia inducible factor-1 (HIF-1)-mediated repression of cystic fibrosis transmembrane conductance regulator (CFTR) in the intestinal epithelium. *FASEB J,* 23, 204-13.

ZHENG, X., LINKE, S., DIAS, J. M., GRADIN, K., WALLIS, T. P., HAMILTON, B. R., GUSTAFSSON, M., RUAS, J. L., WILKINS, S., BILTON, R. L., BRISMAR, K., WHITELAW, M. L., PEREIRA, T., GORMAN, J. J., ERICSON, J., PEET, D. J., LENDAHL, U. & POELLINGER, L. 2008. Interaction with factor inhibiting HIF-1 defines an additional mode of cross-coupling between the Notch and hypoxia signaling pathways. *Proc Natl Acad Sci U S A,* 105, 3368-73.

ZHOU, G., DADA, L. A., CHANDEL, N. S., IWAI, K., LECUONA, E., CIECHANOVER, A. & SZNAJDER, J. I. 2008. Hypoxia-mediated Na-K-ATPase degradation requires von Hippel Lindau protein. *FASEB J,* 22, 1335-42.

ZHOU, J., KOHL, R., HERR, B., FRANK, R. & BRUNE, B. 2006. Calpain mediates a von Hippel-Lindau protein-independent destruction of hypoxia-inducible factor-1α. *Mol Biol Cell,* 17, 1549-58.

ZOU, X., QIU, G., CHEN, C., WU, M., HU, Y., ZHENG, H., LI, X., GU, S., JI, C. & MAO, Y. 2005. Expression pattern and subcellular localization of five splice isoforms of human PXK. *Int J Mol Med,* 16, 701-7.

List of Abbreviations

4-PBA	4 phenyl butyrate
ABC	adenosine tri-phosphate binding cassette
ACh	acetylcholine
AD	actinomycin D
ADP	adenosine di-phosphate
ADP	adenosine tri-phosphate
ALT	alanine aminotransferase
AMP	adenosine mono-phosphate
ARNT	aryl hydrocarbon receptor translocator
ATP	adenosine tri-phosphate
BCECF AM	2'-7'-bis(carboxyethyl)-5(6)-carboxyfluorescein acetoxymethyl
BSA	bovine serum albumin
CaCC	Ca^{2+} activated Cl^- channel
cAMP	cyclic adenosine monophosphate
CCD	charge-coupled device
CCh	carbamylcholine chloride
cDNA	complimentary deoxyribonucleic acid
CF	cystic fibrosis
CFTR	cystic fibrosis transmembrane conductance regulator
cGMP	cyclic guanosine monophosphate
CHX	cycloheximide
CLT	clotrimazole
DAPI	4',6-diamidino-2-phenylindole
DMOG	dimethyloxallylglycine
DMSO	dimethyl sulfoxide
DNA	deoxyribonucleic acid
DRA	down regulated in adenoma
DTT	dithiothriol

ECL	enterochromaffin like
EGF	epidermal growth factor
EIA	enzyme linked immunosorbent assay
EIPA	5-(N-Ethyl-N-isopropyl)amiloride
ENaC	epithelial sodium channel
ET	endothelin
FAM	6-carboxyfluorescein
FIH-1	factor inhibiting hypoxia inducible factor 1
FSK	forskolin
G	conductance
g	gravity
GF	GF 109203X
GI	gastrointestinal
GLUT	glucose transporters
H^+/K^+-ATPase	hydrogen potassium adenosine triphosphatase
H89	N-[2-[[3-(4-Bromophenyl)-2-propenyl]amino]ethyl]-5-isoquinolinesulfonamide dihydrochloride
HIF	hypoxia inducible factor
IBD	inflammatory bowel disease
IBS	irritable bowel syndrome
IKK	IκB kinase
IP	intraperitoneal
I_{sc}	short circuit current
IκBα	inhibitor of κ B
LDH	lactate dehydrogenase
LSM	laser scanning microscopes
MCE	methyl cellulose ester
miRNA	micro ribonucleic acid
MONaKA	modulator of Na^+/K^+-ATPase
MSD	meso scale discovery
MβCD	methyl b cyclodextrin

MβCD	methyl β cyclodextrin
Na^+/K^+-ATPase	sodium potassium adenosine triphosphatase
NAD	nicotinamide adenine dinucleotide
NFκB	nuclear factor κ B
NHE	sodium hydrogen exchanger
NHS	N-hydroxysuccinimide
NHERF	sodium hydrogen exchanger regulatory factor
NKAIN	sodium potassium adenosine triphosphatase interacting
NKCC1	sodium potassium chloride co transporter
NP-40	nonidet P40
OVA	ovalbumin
PAGE	polyacrylamide gel electrophoresis
PBS	phosphate buffered saline
PD	potential difference
PepT1	Peptide transporter 1
PET	Polyethylene Terephthalate
PHD	prolyl hydroxylase
PHI	prolyl hydroxylase inhibitors
PPi	$P_2O_7^{4-}$
PKA	cAMP-dependent protein kinase
PKC	protein kinase C
PMSF	phenylmethanesulfonyl fluoride
PP2	3-(4-chlorophenyl) 1-(1,1-dimethylethyl)-1H-pyrazolo[3,4-d]pyrimidin-4-amine
PSS	physiological salt solution
PVDF	polyvinylidene difluoride
pVHL	von Hippel-Lindau tumour suppressor protein
RISC	RNA induced silencing complex
RNA	ribonucleic acid
R_{te}	transepithelial resistance
RT-PCR	reverse transcriptase polymerase chain reaction

SDS	sodium dodecyl sulphate
SGK1	serum and glucocorticoid-responsive kinase-1
SGLT1	sodium glucose co-transporter 1
siRNA	short interfering ribonucleic acid
SNX	sorting nexin
TBST	tris buffered saline with tween (0.1 %)
TCTP	translationally-controlled tumour protein
TMEM16A	transmembrane protein 16A
UC	ulcerative colitis
VIP	vasoactive intestinal polypeptide
ZO-1	zonula occludens-1

Publications and Communications

Published manuscripts

1. WARD, J. B. J, LAWLER, K., AMU, S., TAYLOR, C. T., FALLON, P. G. & KEELY, S. J. 2011. Hydroxylase inhibition attenuates colonic epithelial secretory function and ameliorates experimental diarrhea. *FASEB J,* 25, 535-43.
2. TOUMI, F., FRANKSON, M., WARD, J. B., KELLY, O. B., MROZ, M. S., BERTELSEN, L. S. & KEELY, S. J. 2011. Chronic regulation of colonic epithelial secretory function by activation of G protein-coupled receptors. *Neurogastroenterol Motil,* 23, 178-86, e43.

Published abstracts

1. WARD, J. B., AMU, S., TAYLOR, C. T., FALLON, P. G. & KEELY, S. J. 2010. Hydroxylase Inhibition Attenuates Colonic Epithelial Secretory Function and Ameliorates Experimental Diarrhea. *Gastroenterology* 138, S-48.
2. WARD, J. B., TAYLOR, C. T. & KEELY, S. J. 2011b. Modifier of Na^+/K^+-ATPase; Upregulated by Hydroxylase Inhibition in Colonic Epithelial Cells: Implications for Epithelial Secretory Function. *Gastroenterology,* 140, S-659.
3. Keating N., Mroz M. S., Dunlevy. F., Ward J. B. J, Keely S. J. Farnesoid X-Receptor agonists inhibit colonic secretion in vitro and in vivo. Proceedings of Digestive Disease Week, New Orleans, 1st–5th May 2010. *Gastroenterology,* 138, S-589.

Manuscripts in preparation

1. WARD, J. B., TAYLOR, C. T. & KEELY, S. J. Review: Hypoxic Regulation of Intestinal Epithelial Cl^- Secretion. Target Journal: Physiological Reviews.

2. WARD, J. B., TAYLOR, C. T. & KEELY, S. J. Modifier of Na^+/K^+-ATPase; Upregulated by Hydroxylase Inhibition in Colonic Epithelial Cells: Implications for Epithelial Secretory Function. Target Journal: JBC
3. WARD, J. B., TAYLOR, C. T. & KEELY, S. J. HIF hydroxylases regulate electrogenic Na^+ absorption across colonic epithelium. Target Journal: AJP

Poster communications

1. WARD, J. B. J., Lawler, K., TAYLOR, C. T. & KEELY, S. J. Prolyl Hydroxylase inhibition down-Regulate Intestinal Epithelial Secretory Function. Hypoxia and Consequences: From Molecule to Malady, New York Academy of Sciences, March 2009.
2. WARD, J. B. J., Lawler, K., TAYLOR, C. T. & KEELY, S. J. Prolyl Hydroxylase Inhibition Attenuates Colonic Epithelial Secretory Function. Physiological Society "Epithelia & Membrane Transport" Themed Meeting, Newcastle University, September 2009.
3. WARD, J. B. J., AMU, S., TAYLOR, C. T. FALLON, P. G., & KEELY, S. J. Hydroxylase Inhibition Attenuates Colonic Epithelial Secretory Function and Ameliorates Experimental Diarrhoea. RCSI Research Day, April 2010.
4. WARD, J. B. J., AMU, S., TAYLOR, C. T. FALLON, P. G., & KEELY, S. J. O_2 Sensors Modulate Enterocyte Ion Transport and Suppress Allergen-Induced Diarrhoea. Physiological Society Main Meeting, Manchester, July 2010.
5. WARD, J. B. J., AMU, S., TAYLOR, C. T. FALLON, P. G., & KEELY, S. J. Hydroxylases Modulate Enterocyte Ion Transport and Suppress Allergen-Induced Diarrhoea. Gastrointestinal Response to Injury, Scottsdale, October 2010.
6. WARD, J. B. J., AMU, S., TAYLOR, C. T. FALLON, P. G., & KEELY, S. J. The Therapeutic Potential of Hydroxylase Inhibitors in Diarrhoeal Disease. Therapeutic aspects of hypoxia-dependent pathways, UCD, October 2010.

7. WARD, J. B. J., AMU, S., TAYLOR, C. T. FALLON, P. G., & KEELY, S. J. Modulator of Na^+/K^+-ATPase; a novel regulator of intestinal epithelial ion transport, regulated by hydroxylases. RCSI Research Day, April 2011.
8. WARD, J. B. J., TAYLOR, C. T. & KEELY, S. J. Modifier of Na^+/K^+-ATPase; upregulated by hydroxylase inhibition in colonic epithelial cells: implications for epithelial secretory function. Sheppard Prize, Beaumont Hospital, April 2011.
9. WARD, J. B. J., TAYLOR, C. T. & KEELY, S. J. Modifier of Na^+/K^+-ATPase; upregulated by hydroxylase inhibition in colonic epithelial cells: implications for epithelial secretory function. DDW, Chicago, May 2011.
10. WARD, J. B. J., TAYLOR, C. T. & KEELY, S. J. Prolyl hydroxylases regulate electrogenic sodium absorption across colonic epithelium. Physiological Society Main Meeting, Oxford, July 2011.
11. WARD, J. B. J., TAYLOR, C. T. & KEELY, S. J. Hydroxylases regulate epithelial modulator of Na^+/K^+ ATPase expression: implications for intestinal fluid and electrolyte transport function. FASEB SRC, Steamboat Springs, August 2011.

Oral communications

1. WARD, J. B. J., Lawler, K., TAYLOR, C. T. & KEELY, S. J. Prolyl Hydroxylase Inhibition Down Regulates Intestinal Epithelial Secretory Function. RCSI research Day, April 2009.
2. WARD, J. B. J., Lawler, K., TAYLOR, C. T. & KEELY, S. J. Prolyl Hydroxylase Inhibition Down Regulates Intestinal Epithelial Secretory Function. Sheppard Prize, Beaumont Hospital, April 2009.
3. WARD, J. B. J., Lawler, K., TAYLOR, C. T. & KEELY, S. J. Prolyl Hydroxylase inhibition Attenuates Intestinal Epithelial Secretory Function. RAMI, Section of Biomedical Sciences, Maynooth, June 2009
4. WARD, J. B. J., AMU, S., TAYLOR, C. T. FALLON, P. G., & KEELY, S. J. O_2 Sensors Modulate Enterocyte Ion Transport and Suppress Allergen-

Induced Diarrhoea. Physiological Society Main Meeting, Dublin, July 2009.

5. WARD, J. B. J., Lawler, K., TAYLOR, C. T. & KEELY, S. J. Prolyl Hydroxylase Inhibition Down Regulates Intestinal Epithelial Secretory Function. UEGF Teaching Activity on Basic Science, Cambridge, July 2009.
6. WARD, J. B. J., Lawler, K., TAYLOR, C. T. & KEELY, S. J. Hydroxylases Regulate Colonic Epithelial Secretory Function. IEPG, Kilkenny, October 2009.
7. WARD, J. B. J., Lawler, K., TAYLOR, C. T. & KEELY, S. J. Prolyl Hydroxylase Inhibition Down Regulates Intestinal Epithelial Secretory Function. Sheppard Prize, Beaumont Hospital, April 2010.
8. WARD, J. B. J., AMU, S., TAYLOR, C. T. FALLON, P. G., & KEELY, S. J. Hydroxylase Inhibition Attenuates Colonic Epithelial Secretory Function and Ameliorates Experimental Diarrhea. DDW, New Orleans, May 2010
9. WARD, J. B. J., TAYLOR, C. T. & KEELY, S. J. Hydroxylases regulate epithelial Modulator of Na^+/K^+ ATPase expression: Implications for intestinal fluid and electrolyte transport function. Physiological Society Main Meeting, Oxford, July 2011

Awards

1. Physiological Society Travel award to attend Physiological Society Epithelia and Membrane Transport Meeting, Newcastle, 2010
2. Physiological Society Travel award to attend Digestive Disease Week, New Orleans, 2010.
3. Physiological Society Travel award to attend Digestive Disease Week, Chicago, 2011.
4. United European Gastroenterology Federation Travel Award to attend United European Gastroenterology Federation workshop, Cambridge, 2009.

Acknowledgments

In the lab Chris Kindle one Christmas, I received a gift from an anonymous source, of a toy PacMan and Blinky. When wound up, they chased each other in circles, relentlessly, but never caught each other. The note attached to the gift made reference to the relationship between a student and their supervisor being somewhat like this. I think that I have been very fortunate to have Stephen as a supervisor. He has always encouraged our independence and ideas and has enthusiastically debated issues at length with us. Being a strong advocate of the promotion of our research at scientific meetings, Stephen has allowed me to become interested and aware of the "bigger picture"-which has been one of the most positive aspects of my Ph.D. But most of all it's his approachability and friendliness that has made the last 3 years a pleasure. Thanks a million, Stephen!

Our team became known as "Team Colon", glamour-less, but helpful for deterring people from long-term 'loans' of your possessions. The members of the team really made it a smooth transition back to academia and I'd especially like to give a buíochas mór do Magda, Orlaith, agus Niamh. I'd also like to thank everyone in MolMed, especially to Olive, who manages the lab so seamlessly, making it a pleasure to work there, whom I have never seen in a bad mood despite many Urgent requests, and who makes the best cakes!

I remember when I told my brother Daragh that I was going back to study for another 3 years, he told me I was crazy. He may have been right. Without all my family's support though, especially Mum and Dad, I would have given up a long time ago. Go raibh míle maith agaibh!

I think for people returning to education there is usually a catalyst or a spark that ignites such a desire. My best mate was really the catalyst behind me

undertaking this Ph.D. Muito obrigado Pun! I'm looking forward to our future collaborations mo chara!

Brian Harvey is the Director of the Molecular Medicine Laboratories here in Beaumont, and has instigated many thought-provoking conversations over the years, and has facilitated our work in the state-of-the-art laboratories, so thank you Brian.

I would also like to thank Cormac Taylor from UCD for affording me his expertise in the area hypoxia and for his support throughout this project.

I would like to acknowledge our collaborators who performed some experiments on our behalf.

1. Professor Padraic Fallon and Dr. Sylvie Amu of Trinity College Dublin performed the allergic model of diarrhoea (Figure 3-13).
2. Our colleagues in the Biochemistry Department of Beaumont Hospital performed the serum ALT and creatinine assays (Figure 3-14).
3. Our industrial collaborators FibroGen Inc. performed the MSD assay to quantify HIF-α levels (Figures 3-5 and 4-21).

Finally I would like to acknowledge Science Foundation Ireland for funding this research. Funding was awarded to S. J. Keely (Research Frontiers Project Award 08/RFP/BMT1327).

Appendix I